

**A NOVEL CONCEPT OF SERIES
CONNECTED MULTI-PHASE,
MULTI-MOTOR DRIVE SYSTEMS**

MARTIN JONES

**A thesis submitted in partial fulfilment of the requirements
of Liverpool John Moores University for the degree of
Doctor of Philosophy**

April 2005

**PUBLISHED PAPERS
NOT COPIED
AT THE REQUEST OF
THE UNIVERSITY**

ABSTRACT

There are many applications, such as paper mills, locomotive traction and machine tools, which require high performance control of more than one electric motor. These multi-motor drives are generally available in two configurations. The first one consists of a number of three-phase voltage source inverters (VSI) connected in parallel to a common DC link, each inverter feeding a three-phase AC motor. This configuration allows independent control of all machines by means of their own three-phase VSIs. The second method comprises one inverter, which feeds multiple parallel-connected three-phase motors. However, this configuration does not allow independent control of each motor and is suitable only for traction.

This thesis explores a novel concept for multi-motor drive systems, based on utilization of multi-phase machines and VSIs, and series connection of all the machines in the group. Application of a single multi-phase VSI in conjunction with multi-phase machines generates additional degrees of freedom. The research presented here utilises these additional degrees of freedom to control a number of machines independently within a novel multi-phase multi-machine drive. The concept is based on the fact that independent flux and torque control of any AC machine, regardless of the number of stator phases requires control of only two stator current components. This leaves the remaining current components free to control other machines within the group. It is shown that it is possible to connect the machines in such a way that what one machine sees as the flux/torque producing components the other machines see as non-flux/torque producing components, and vice versa. Therefore it is possible to connect in series a number of multi-phase machines and independently control each machine while supplying them from a single multi-phase inverter.

Different configurations of the multi-motor drive are possible depending on certain properties of the supply phase number. In general, higher the supply phase number is, higher the number of connectable machines is. However, some phase numbers are more favourable than others, as discussed in detail in the thesis. Simulation studies are provided for five, six, seven, nine, ten and fifteen phase configurations in order to verify the concept. It is shown that the concept is independent of the type of AC machines used and the only requirement is that they all have sinusoidal distributed magnetomotive force. Current control in both the stationary and rotating reference frames is considered and it is concluded that current control in the rotating reference frame requires compensation of the additional voltage drops caused by the series connection. Two possible methods of compensating for these voltage drops are suggested and verified by simulation.

Finally, a laboratory rig is described, which utilises two three-phase inverters connected in such a way as to form a single six-phase inverter. A six-phase two-motor drive comprising a symmetrical six-phase induction machine and a three-phase induction machine or a three-phase PMSM is investigated experimentally. An analysis of the performance of the two-motor drive is presented and it is shown that decoupled control of each machine is achieved.

Acknowledgements

There are many people who have supported me either academically or personally during the course of my studies. Although it would prove impossible to thank them all, I would like to take this opportunity to mention the following people with whom it has been my great privilege to work with over the past three years.

I would like to express my sincere gratitude to my Director of Studies, Professor Emil Levi, for his professional guidance and support throughout the course of the project and the presentation of this thesis.

Many thanks go to Dr S.N. Vuckosavic for his work designing and commissioning the experimental laboratory rig. I would also like to thank Mr Ron M^cgovern and Mr Brian Grey for their fabrication work.

On a more personal note, I would like to extend my heart felt thanks to all my family for there limitless support and to my partner Michelle for her patience, encouragement and love during the course of my studies.

Finally, I would like to thank my Mother, Sandra Jones, whose love strength of character and determination has always inspired me and to whom this work is dedicated.

CONTENTS

ABSTRACT	i
ACKNOWLEDGEMENTS	ii
CONTENTS	iii
LIST OF PRICIPAL SYMBOLS	x

Chapter 1 - Introduction

1.1	An overview of existing multi-machine drive systems	1
1.2	Proposed multi-machine system	2
1.3	Advantages and shortcomings of the proposed system	4
1.4	Research objectives and originality of the research	6
1.5	Organisation of the thesis	7

Chapter 2 – State of the art in multi-phase drives (literature review)

2.1	Historical background	10
2.2	Advantages of multi-phase machines	10
2.3	Modelling and control of multi-phase machines	14
2.4	Three-phase multi-motor drives	16
2.5	Summary	19

Chapter 3 – Modelling of multi-phase machines

3.1	Introduction	20
3.2	Phase domain model of an n -phase induction machine	20
3.3	Decoupling transformation	23
3.4	Application of the decoupling transformation onto the phase domain model	25
3.5	Application of the rotational transformation	28
3.6	Rotor flux oriented control of an n -phase current-fed induction machine	30
3.7	Summary	32

Chapter 4 – Series connections of n -phase machines

4.1	Introduction	34
4.2	Machine connectivity for a general n -phase case	34
4.3	Connectivity matrices and connection diagrams for machines with an odd number of phases	37
4.4	Connectivity matrices and connection diagrams for machines with an even number of phases	43
4.5	Machine connectivity related general considerations	47
	4.5.1 Odd number of phases	47
	4.5.2 Even number of phases	50
4.6	Summary	53

Chapter 5 – Simulation studies for odd phase numbers

5.1	Introduction	54
5.2	The five-phase single motor drive	54
	5.2.1 Phase domain model of a five-phase induction machine	54
	5.2.2 Simulation of a single five-phase induction machine (phase domain model)	58
	5.2.3 Simulation of indirect vector control of a current fed five-phase induction machine (torque mode) using phase-domain model	61
	5.2.4 Simulation of indirect vector control of a current fed five-phase induction machine (torque mode) using stationary reference frame model	63
5.3	The five-phase two-motor drive	63
	5.3.1 Simulation of series connection of two five-phase machines with phase transposition (phase-domain model)	66
	5.3.2 Series connection of two five-phase machines using stationary reference frame model	69
	5.3.3 Simulation of two five-phase induction machines using model in the stationary reference frame	72

5.3.4	Rotor flux oriented control of two series-connected five-phase induction machines with phase transposition (torque mode)	74
5.3.5	Simulation of series connection of two five-phase machines (torque mode) using phase domain model	76
5.3.6	Simulation of series connection of two five-phase machines (torque mode) using stationary reference frame model	77
5.3.7	Rotor flux oriented control of two series-connected five-phase induction machines (speed mode)	79
5.3.8	Simulation of series connection of two five-phase machines (speed mode)	80
5.4	The nine-phase four-motor drive	82
5.4.1	Simulation of rotor flux oriented control of three nine-phase machines and one three-phase induction machine connected in series (torque mode)	84
5.5	The fifteen-phase six-motor drive	86
5.5.1	Simulation of rotor flux oriented control of four fifteen-phase and two five-phase induction machines connected in series (torque mode)	87
5.6	Current cancellation	87
5.6.1	Simulation verification (five-phase case)	91
5.7	Summary	92

Chapter 6 – Simulation studies for even phase numbers

6.1	Introduction	95
6.2	The six-phase two-motor drive	96
6.2.1	Rotor flux oriented control of a six-phase and a three-phase induction machine connected in series with phase transposition	97
6.2.2	Simulation of rotor flux oriented control of a six-phase and a three-phase induction machine with phase transposition (torque mode)	98

6.3	The ten-phase four-motor drive	101
6.3.1	Simulation of rotor flux oriented control of two ten-phase and two five-phase induction machines connected in series with phase transposition (torque mode)	102
6.4	Current cancellation	104
6.4.1	Simulation verification (six-phase case)	106
6.5	Summary	107
Chapter 7 – Connection of different types of AC machines		
7.1	Introduction	109
7.2	Modelling of permanent magnet and synchronous reluctance machines	111
7.2.1	PMSM parameters	114
7.2.2	Syn-Rel parameters	114
7.3	Vector control of a PMSM and a Syn-Rel machine	115
7.3.1	Simulation of the seven-phase drive comprising an induction machine, a PMSM and a Syn-Rel machine (torque mode)	116
7.4	Summary	118
Chapter 8 – Current control in the synchronous reference frame		
8.1	Introduction	120
8.2	Phase domain modelling of the voltage-fed series-connected five-phase two-motor drive	122
8.2.1	Transformation of the two-motor five-phase series-connected model into the stationary reference frame	125
8.3	Phase domain modelling of the voltage-fed series-connected six-phase two-motor drive	127
8.3.1	Transformation of the two-motor six-phase series-connected machine model into the stationary reference frame	129
8.4	Vector control of a five-phase induction machine with current control in the synchronous reference frame	132

8.4.1	Tuning of the PI current controllers	134
8.4.2	Simulation of a five-phase vector controlled induction machine with current control in the synchronous reference frame	134
8.5	Series-connected five-phase two-motor drive with current control in the synchronous reference frame	136
8.5.1	Simulation of a vector controlled five-phase two-motor series-connected drive with current control in the synchronous reference frame	137
8.6	Feed-forward compensation of x-y voltage drops in the stationary reference frame	140
8.6.1	Simulation verification of the feed-forward method of x-y voltage drop compensation in the stationary reference frame for the five-phase and six-phase two-motor drives	143
8.7	Feed-forward compensation of x-y voltage drops in the synchronous reference frame	146
8.7.1	Simulation verification of the modified decoupling circuit method for the five-phase and six-phase two-motor drives	149
8.8	Summary	150

Chapter 9 – Quasi six-phase configurations

9.1	Introduction	153
9.2	Two-motor drive with two quasi six-phase machines	154
9.3	Two-motor drive with a quasi six-phase machine and a two-phase machine	158
9.4	Phase domain model of voltage-fed series-connected two-motor drive with two quasi six-phase machines	160
9.5	Phase domain model of voltage fed series-connected two-motor drive with a quasi six-phase machine and a two-phase machine	164
9.6	Current control techniques	165
9.6.1	Current control in the stationary reference frame	166

	9.6.2	Current control in the synchronous reference frame	166
9.7		Simulation verification	168
9.8		Current cancellation	172
	9.8.1	Two quasi six-phase machine configuration	172
	9.8.2	Two quasi six-phase machine alternative configuration	174
	9.8.3	Quasi six-phase\two-phase configuration	176
9.9		Summary	179
Chapter 10 – Experimental investigation			
10.1		Introduction	180
10.2		Description of the experimental rig	181
10.3		Details of the motors used in the experiments	184
10.4		Transient performance of a symmetrical six-phase induction motor	185
10.5		Experimental investigation of a series-connected two-motor six-phase drive system dynamics	189
	10.5.1	Six-phase motor transients	190
	10.5.2	Three-phase motor transients	196
10.6		Experimental investigation of dynamics of a two-motor drive using a three-phase permanent magnet synchronous machine	201
	10.6.1	Experimental results	202
10.7		Experimental investigation of steady-state operation	203
	10.7.1	Steady-state performance of symmetrical six-phase induction machine	208
	10.7.2	Steady-state performance of a two-motor six-phase drive	208
10.8		Summary	210
Chapter 11 – Conclusion			
11.1		Summary and conclusions	214
11.2		Future work	219
References			222

Appendix A Three-phase machine data	231
Appendix B Six-phase induction machine data	232
Appendix C Simulation data	236
Appendix D Publications from the thesis	237

List of principal symbols

v :	Voltage
i :	Current
ψ :	Flux linkage
R :	Resistance
L :	Inductance
M :	Magnetising inductance per phase
P :	Number of pole pairs
T_e :	Torque developed by the machine
T_L :	Load torque
J :	Inertia
p :	Differential operator
T_r :	Rotor time constant
$\omega, \omega_{11}, \omega_{22}$:	Rotational speed of the rotor with respect to the stator
ω_a :	Arbitrary rotational speed of the d-axis of the common reference frame
ω_r :	Rotational speed of the rotor flux space vector with respect to the stator
ω_{sl} :	Slip speed
$\omega_1, \omega_2, \omega_s$:	Supply angular frequency
$\theta_1, \theta_2, \theta_3$:	Instantaneous position of the magnetic axis of the rotor phase “a” with respect to the stationary magnetic axis of the stator phase “a”
θ_s :	Instantaneous angular position of the d-axis of the common reference frame with respect to the phase “a” magnetic axis of the stator
θ_r :	Instantaneous angular position of the d-axis of the common reference frame with respect to the phase “a” magnetic axis of the rotor

ϕ_r :	Instantaneous angular position of the rotor flux with respect to the phase “a” magnetic axis of the stator
ε :	Spatial angular coordinate along stator circumference
C :	Decoupling transformation matrix
D :	Rotational transformation matrix
α :	$2\pi/n$ (where n = number of phases)
K_p :	Proportional gain
T_i :	Integral time constant
σ :	Total leakage coefficient
e_{dq} :	Decoupling voltages

Superscripts

*	Reference (commanded value)
<i>INV</i>	Inverter

Subscripts

n :	Rated value
s :	Associated with stator winding
r :	Associated with rotor winding
l :	Associated with leakage
α, β :	Relates to variables after application of the decoupling transformation (includes stator variables in stationary common reference frame)
d, q :	Relates to variables after application of the decoupling and rotational transformations (includes rotor variables in stationary common reference frame)
$x-y$:	Relates to non flux/torque producing variables
*	Reference (commanded value)
$abc\dots$:	Associated with phase domain
1,2 :	Relates to machine number

General

_ : Underlined symbols are matrices except in sections 3.6, 8.6 and 8.7 where underlining identifies space vectors

CHAPTER 1

INTRODUCTION

1.1 An overview of existing multi-machine drive systems

A multi-machine drive is the one that consists of more than one motor. Such drives have numerous applications, for example in rolling mills, electric vehicles and locomotive traction [Belhadj et al (2001), Pena-Eguiluz et al (2001), Matsumoto et al (2001)]. Presently multi-machine drives are generally available in two configurations. The first one consists of a common DC link feeding a number of three-phase voltage source inverters (VSI) connected in parallel, each inverter feeding a three-phase AC machine (Fig. 1.1). The speed of each machine can be controlled independently using its own VSI and an appropriate control algorithm, as required in textile, paper or rolling mill industries.

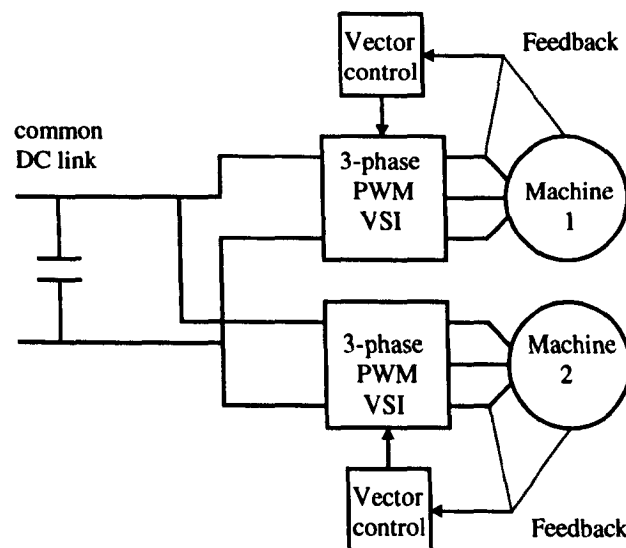


Fig. 1.1: Standard configuration of a multi-machine drive system (two machines).

The second method consists of one inverter, which feeds parallel-connected three-phase motors. In this structure motors have to be identical and operate under the same load torque and have exactly the same angular speed, which is a major disadvantage of this system [Belhadj et al (2001)]. However this system is useful in traction applications such as locomotives, coaches, ships and electric vehicles where it is used because of its compactness, lightness and economical advantages [Matsumoto et al

(2001)]. Control of the motors is achieved by either treating parallel connected three-phase motors as one large motor or the complete drive system is controlled by attaching the speed sensor to only one motor (which has to be properly chosen from the set of motors) [Kouno et al (2001)]. However, in this method unbalances of torque and current can make the system unstable [Kawai et al (2002)]. In locomotive traction applications this problem is overcome to a certain degree by virtue of the small differences in axle speeds and large vehicle masses resulting in slow acceleration speeds [Pena-Eguiluz et al 2001]. At present a method that will enable independent control of at least two AC machines, of the same or different type, while using only one three-phase VSI does not exist nor seems possible.

1.2 Proposed multi-machine system

In traditional electric machine applications a three-phase stator winding is normally selected, since the three-phase supply is readily available and the resulting cost is therefore the lowest. However, when an AC machine is supplied from an inverter, as the case is in the vast majority of variable speed drives, the need for a pre-defined number of phases on stator, such as three, disappears and other phase numbers can be chosen. AC machines with a phase number greater than three will be referred to in what follows as multi-phase machines.

It is not possible to connect in series a number of three-phase ($n=3$) machines, feed them via a single three-phase inverter and independently control the speed of each machine. However, application of a single multi-phase ($n>3$) VSI in conjunction with multi-phase machines ($n>3$), generates additional degrees of freedom. This allows series connection of a number of multi-phase machines with appropriate phase transposition between each machine, as discussed shortly (depending on certain connectivity rules to be explained later).

The most important property of a multi-phase machine (regardless of type) is that, when the modelling is completed, a new set of equations will be obtained in which only two components (d-q) will lead to stator to rotor coupling, while the rest do not give coupling [Klingshirn (1983), White and Woodson (1959)]. If the number of phases n is assumed to be an odd number, then for an n -phase machine there are, apart from the two components that yield stator to rotor coupling (d-q), one zero sequence component and

additional $(n-3)$ components or $(n-3)/2$ pairs of components (termed further on x-y components) that do not lead to stator to rotor coupling. Vector control enables independent control of flux and torque of an AC machine by means of two stator current components (one component pair) only (d-q). This leaves $(n-3)/2$ pairs of components as additional degrees of freedom. Hence, if it is possible to connect stator windings of $(n-1)/2$ machines (that are all in general n -phase) in such a way that what one machine sees as the d-q axis current components the other machines see as x-y current components, and vice versa, it would become possible to completely independently control speed (position, torque) of these $(n-1)/2$ machines while supplying the machines from a single voltage source inverter. In simple terms, and taking five-phase machines as an example, it is possible to independently realise vector control of two five-phase machines using a single five-phase voltage source inverter, provided that the stator windings of the two machines are connected in series and that an appropriate phase transposition is introduced so that the set of five-phase currents that produces rotating mmf in the first machine, does not produce rotating mmf in the second machine and vice versa. An alternative formulation of the reference frame theory of electric machines [Lipo (1984), Zhao and Lipo (1995)], based on the concept of an n -dimensional space for an n -phase machine, enables a rather simple explanation of the above described idea [Gataric (2000)]. Each pair of components appears in one plane of the n -dimensional space. Hence, what for the first machine are d-q components (and are used to perform the vector control of the first machine), appear for the second (and all the subsequent machines if $n>5$) as x-y components, what for the second machine are d-q components (and are used to perform the vector control of the second machine), appear for the first (and the third and so on, if applicable) as x-y components, and so on. The concept of the feeding of a set of n -phase machine stator windings connected in series from a single n -phase voltage source (inverter in practice) is illustrated in Fig. 1.2. Phase transposition blocks denote shift in connection of the phases 1,2, ... n of one machine to the phases 1,2, ... n of the other machine. For example, in the five-phase case there are two machines and phases 1,2,3,4,5 of the first machine are connected to phases 1,3,5,2,4, respectively, of the second machine [Gataric (2000)].

Multi-phase systems can be connected in star or in polygon and the supply can be either from an n -phase inverter or a set of n single-phase inverters [Ferraris and Lazzari (1983)]. If n is not a prime number, there are a number of possible star

connections with isolated neutrals and there are in general a number of possible polygon connections [Ferraris and Lazzari (1983)]. As far as this project is concerned, the only relevant connection is the star connection (in principle with a single neutral point) and the only relevant supply source is an n -phase voltage source inverter. Since vector control is under consideration here, an appropriate current control method for an n -phase inverter is required. The inverter is in general current controlled, with current control in either stationary reference frame (current fed machine) or rotating reference frame (voltage fed machine). Initially this project is restricted in scope to the simpler possibility of the two so that current fed AC machines are considered. This means that inverter current control is at all times exercised upon inverter phase currents. At a later stage, current control in the rotating reference frame will also be examined.

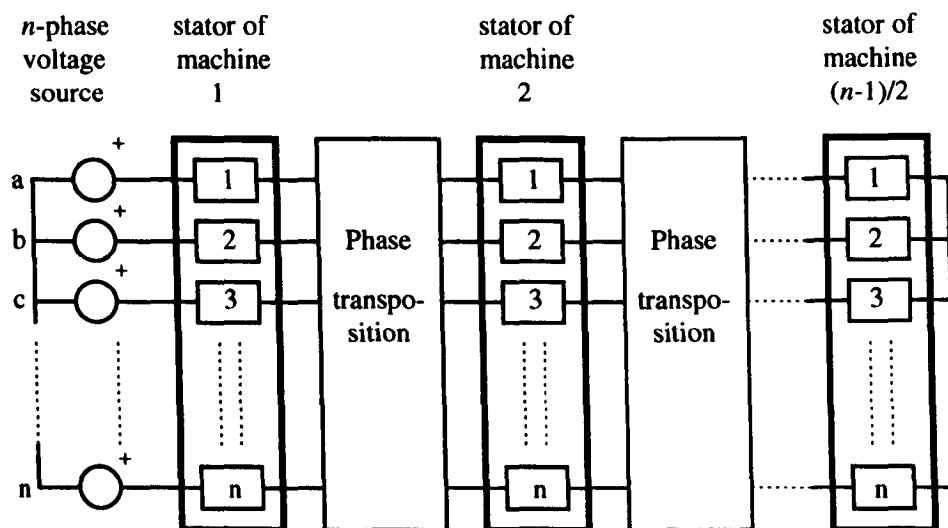


Fig. 1.2: Supply of $(n-1)/2$ machine stator windings, connected in series, from an n -phase voltage source inverter (odd phase number assumed).

1.3 Advantages and shortcomings of the proposed system

The principle novelty of the project is that a multi-drive system, of the form previously discussed, has never been realised in practice, anywhere in the world, for any number of phases. Furthermore, the only existing reference related to this concept [Gataric (2000)], utilised the concept of an n -dimensional space in the development and was restricted to the five-phase case with two induction motors connected in series. An entirely different approach is adopted here, based on general theory of electrical

machines. The underlying principles of operation of the system entirely rely on the correctness of the transformation theory of electric machines (according to which only two currents are required for control of any multi-phase machine). Some preliminary considerations of [Gataric (2000)] indicate that the proposed system is feasible for any number of phases equal to or greater than five, including even numbers. However, since the number of connectable machines is the same for any given odd phase number and the subsequent even number, the investigation in this project will initially concentrate on odd phase numbers. It is intended to investigate at first the whole spectrum of odd phase numbers (leaving aside the issue of how many phases can be realised in practice). The study will further be repeated for the whole spectrum of even phase numbers. Furthermore drives composed of different AC machine types will be looked at, since this approach to the multi-machine drive system appears to be entirely independent of the machine type.

The major advantage of the proposed system over the more traditional systems is that the overall number of inverter legs is reduced. In the five-phase case the number of inverter legs (or phases) reduces from six (for two three-phase machines) to five (for two five-phase machines). One leg (or two switches) less is therefore needed for the five-phase system. Higher the number of phases is, larger the reduction in the number of legs is (for example, an 11-phase system can supply five machines with 11 legs, while the supply of five three-phase machines asks for 15 legs; the saving in the number of legs is 4, or eight switches). Reduction in the number of switches means reduction in the protection and firing circuit components and, in general, improved reliability of the multi-motor drive due to the reduction of the overall number of components.

The proposed system preserves some of the important benefits of the existing multi-motor drive concept, based on independent VSI utilisation for each three-phase machine (Fig. 1.1), such as:

- The possibility of having within a multi-motor drive completely different machine types (induction motors, permanent magnet synchronous motors, synchronous reluctance motors, wound rotor synchronous motors). However, the multi-phase stator windings are now connected in series.
- The possibility of regenerative operation without the need for a controllable front-end rectifier. In the standard scheme power generated by one machine is returned to

the DC link and then supplied to another machine that operates as a motor. In the configuration that is to be developed here vector control of each machine is performed independently, so that at first the set of phase current references is created for each machine. Subsequent summation of current references for all machines (with appropriate phase transposition) leads to creation of inverter phase current references that automatically accounts for the power generated by one or more machines. The generated power is then used by other machine(s).

The proposed multi-motor drive concept offers some additional benefits over the existing approach, such as:

- Reduced number of semiconductor components and associated electronics.
- Since only one inverter is used, a multi-motor drive of this type is ideally suited to the application of a single DSP for independent vector control of all the machines in the system.

A rather obvious drawback of the proposed multi-drive system is that flow of non-torque/flux producing currents through a machine will cause additional losses. As the stator windings are connected in series, this is inevitable and is likely to reduce the overall efficiency of the system.

1.4 Research objectives and originality of the research

The principal objectives of the proposed project are:

1. *To carry out a comprehensive analytical study of the possibility of achieving independent control of a set of series-connected multi-phase electric machines, which are supplied from a single voltage source inverter, for various numbers of phases (odd and even). This part of the investigation will cover essentially all possible phase numbers, disregarding the physical viability of high phase numbers.*
2. *To examine the performance of a set of series-connected machines supplied from a single multi-phase source, by simulation, assuming ideal sinusoidal supply conditions.*
3. *To develop appropriate algorithms for vector control of a set of machines supplied from a single inverter and to examine the performance by simulation. The study will be related to the use of differing phase numbers (odd and even) and different types*

of AC machines within the multi-motor drive will be elaborated (induction, surface-mounted permanent magnet synchronous and synchronous reluctance machine). It will be assumed at this stage that inverter current control is executed in the stationary reference frame, so that the inverter supplied multi-motor drive system can be regarded as current-fed.

- 4. To examine the feasibility of using current control in the rotating reference frame for the realisation of a multi-phase series-connected multi-motor drive. Since this will result in a voltage-fed drive system, modelling, vector control and simulation will be significantly more involved than in the current-fed case.*
- 5. To compare the relative merits and shortcomings of the two principle methods of current control, discussed in 3 & 4.*
- 6. All the previously mentioned studies will be related to so-called true (symmetrical) multi-phase machines. Another study, related to the use of quasi (asymmetrical) multi-phase machines within the same type of drive system will be conducted as well, with the emphasis on quasi six-phase two-motor drives.*
- 7. To participate in realisation of an experimental rig that will incorporate multi-machine drive system[⊗] and to verify theoretical investigations experimentally. The rig will be capable of supplying at most four series-connected machines in the nine-phase configuration in speed sensed mode. It will be tested for the purposes of this thesis in the two-motor six-phase configuration. Both transient and steady-state operation will be investigated for various operating regimes.*

The original contributions of this thesis are contained in chapters 4 to 9.

1.5 Organisation of the thesis

Chapter 1 contains an overview of the proposed multi-phase multi-machine drive scheme. Existing multi-machine drive systems are described and the relative merits and downfalls of the proposed multi-phase multi-machine drive are highlighted. Finally, objectives and originality of the research are discussed.

[⊗] Experimental rig has been realised within the EPSRC project number GR/R64452/01, on which a post doctoral research associate and another PhD student are working.

Chapter 2 presents a literature review. Advantages of multi-phase machines over traditional three-phase machines are highlighted and issues relating to modelling and control of multi-phase machines are discussed. The state of the art in three-phase multi-motor drives is addressed.

Modelling of symmetrical multi-phase machines is explained in chapter 3, where both odd and even phase number machines are considered. Transformation of the phase domain model of an n -phase induction machine to the arbitrary reference frame is discussed and the resulting equations are given. The chapter concludes with indirect rotor flux oriented control of an n -phase induction machine and shows that the vector control algorithm is very similar to that of the standard three-phase machine.

Chapter 4 considers all possible configurations of series-connected symmetrical multi-phase machines. Connectivity matrices and connection diagrams for machines with either odd or even phase numbers are presented. General machine connectivity considerations for both odd and even phase number machines are discussed at the end of the chapter.

Chapter 5 contains simulation studies for selected odd phase number configurations. The chapter begins with modelling and simulation of a five-phase induction machine and verifies modelling of the machine in the rotor flux reference frame. Next, modelling and simulation of two series-connected five-phase machines are considered in both speed mode and torque mode of operation. The chapter moves on to consider the nine-phase scheme and the fifteen-phase scheme. Finally, current cancellation issues are addressed at the end of the chapter.

Chapter 6 contains simulation studies for selected even phase number configurations including the six-phase and the ten-phase schemes. Issues relating to the cancellation of inverter phase current references are considered at the end of the chapter.

The possibility of utilizing different types of AC machine in the multi-phase multi-machine drive is considered in chapter 7. It is shown, using mathematical models and simulation that the multi-phase multi-machine concept depends upon the sinusoidal distribution of the stator windings and is independent of the rotor structure of the machine. A seven-phase three-motor drive, consisting of an induction machine, permanent magnet synchronous machine and a synchronous reluctance machine, is verified by simulation.

The work presented thus far has only considered operation of the multi-phase multi-machine drive with current control performed in the stationary reference frame.

Chapter 8 looks at the situation when current control is performed in the synchronous reference frame, when the machines have to be considered as voltage fed. Simulations show that voltage drops created by the flow of x-y currents through the stator of each machine have to be compensated for. Two methods of x-y voltage drop compensation are proposed and verified by simulation. Simulation studies are conducted for both the five-phase and six-phase configurations.

Chapter 9 looks at various multi-machine configurations that apply when a quasi six-phase machine is employed. Two possible configurations are presented, one utilising two quasi six-phase machine and the other utilizing a quasi six-phase machine and a two-phase machine. Current control in the synchronous reference frame and the stationary reference frame are considered. The chapter concludes with an investigation of inverter phase current reference cancellation issues.

Chapter 10 is devoted to experimental investigations carried out using an experimental laboratory rig. The chapter begins with a description of the experimental rig and moves on to consider indirect rotor flux oriented control of a six-phase induction machine. An experimental investigation is undertaken in order to determine the dynamic performance of the drive. The chapter further addresses a six-phase two-motor drive comprising a six-phase induction motor and a three-phase induction motor connected in series. The dynamic performance of the drive is determined experimentally and results are presented. Connection of different types of AC machine is experimentally examined next. A six-phase induction motor and a three-phase PMSM are used to form a two-motor drive. Once again dynamic performance of the drive is investigated and experimental results are presented. Finally, steady-state results are presented for the single six-phase machine configuration and the two-motor drive scheme consisting of two induction machines.

Chapter 11 is the final chapter, and provides a summary of the thesis and the salient points from each chapter. Conclusions are made as to the viability of the series-connected multi-phase multi-motor drive and areas that require further research efforts are suggested.

CHAPTER 2

STATE OF THE ART IN MULTI-PHASE DRIVES (LITERATURE REVIEW)

2.1. Historical background

Since the beginning of last century electric power has been generated, transmitted and distributed using three phases. As a consequence the induction machine and all other AC machines were developed as three-phase devices and most variable speed induction motor drives are constructed by combining a three-phase motor with a three-phase inverter. While the number of phases feeding the input converter is governed by the utility supply, the inverter can be constructed to have as many output phases as required. In theory AC motors may be constructed with any number of phases. Motors with phase numbers greater than the traditional three possess certain advantages over their three-phase counterpart.

2.2. Advantages of multi-phase machines

Early interest in multi-phase machines was caused by the need to reduce torque pulsations developed by inverter-fed three-phase drives. Probably the first investigation into the use of a multi-phase machine within a variable speed electric drive was carried out by Ward and Härer (1969), when a five-phase induction motor, supplied from a five-phase ten-step voltage source inverter VSI was considered. It was found that the amplitude of the torque pulsation was reduced by a third and the frequency was increased. However the improvement was at the cost of severe distortion of the supply currents. Pavithran et al (1988) solved the problem by employing a pulse-width-modulated PWM VSI.

A six-phase induction machine (composed of two three-phase windings with isolated neutral points and shifted by 30 degrees in space and often called double star) was originally introduced because of the smoother torque. The supply may be coming from a six-phase VSI [Abbas et al (1984), Hadiouche et al (2000), Grochowalski

(2000), Monti et al (1995), Xu and Ye (1995), Nelson and Krause (1974), Abbas and Christen (1984)] or from a six-phase current source inverter (CSI) [Gopakumar et al (1984), Andresen and Bieniek (1980), Andresen and Bieniek (1981)]. With the advent of the PWM era the need to reduce the torque ripple by using multi-phase machines has become less important in the low to medium power range. However this advantage is still applicable in the high power range where the current limitations of semiconductor devices restrict the use of PWM [Xu and Ye (1995)].

Multi-phase drives possess some other important advantages compared to a three-phase motor drive. First of all, multi-phase machines offer significant advantages in high power applications. For the given motor power an increase in the number of phases enables reduction of the power per phase, which translates into a reduction of the power per inverter leg (that is, a semiconductor rating). Multi-phase machines are therefore often considered and applied in very high power applications. A six-phase (double star) 850 kW 6-pole field oriented controlled drive was developed by Camillis et al (2001) for use in an extruder pump in a polyethylene plant. In order to reduce the losses obtained when a 1400 kW permanent magnet synchronous generator is wound with a three-phase stator, a quasi nine-phase configuration is employed in Veen et al (1997). The nine-phase configuration is formed using three three-phase windings, supplied from three three-phase inverters. Zdenek (1986) describes a six-phase 25 MW synchronous motor drive for use in a turbo-compressor set. Steiner et al (2000) developed a special configuration of a nine-phase (triple star) induction motor drive for application in high power traction vehicles. A high power six-phase (double star) induction motor drive used in Adtranz locomotives is analysed by Mantero et al (1999). Other high power applications of multi-phase machines include a traction application of a two-level GTO inverter feeding a six-phase (double star) induction motor [Monti et al (1995)]. For use in automotive applications, Miller et al (2001) investigate the use of pole phase modulation (PPM) to allow extension of the constant power range of a nine-phase toroidal induction machine for an integrated starter-generator application. A five-phase permanent magnet 5 kW motor with square wave current excitation (BDCM) was developed for propulsion purposes in an electric vehicle by Chan et al (1994) because it possesses high power density, high efficiency and superior dynamic performance.

The ability of multi-phase drives to operate under fault conditions is the main reason for their use in applications such as locomotive traction [Steiner et al (2000), Mantero et al (1999)] and more electric aircraft [Mitcham and Cullen (2002)]. A

general multi-phase machine allows application of the parallel redundancy concept [Jahns (1980)] since it has n separate input terminals and continues to operate when only $(n-1)$ terminals or less are supplied. If one phase is open circuited, three-phase drives require a neutral line connected between the motor and the DC midpoint in order to allow the current in the remaining phases to be controlled to provide a rotating mmf. In multi-phase machines there exist additional degrees of freedom as a result of there being more phases. Thus the current combination required to produce a rotating mmf during fault conditions is no longer unique [Fu and Lipo (1994)]. Typical fault studies suggest that short circuit and open circuit are the most significant fault conditions. Jahns (1980) studied VSI and CSI fed machines for both types of fault conditions. It was found for the open circuit case that in VSI fed drives the drive compensates for the loss of current in one phase by increasing the current amplitudes in the remaining excited phases. However in the CSI fed case the current excitation does not permit the current in the remaining excited phases to change from the balanced excited values and so the performance of the machine was more seriously degraded. For the case where a six-phase machine was fed by a VSI the developed torque decreased by 10% and a 20% decrease was recorded for the case when the machine was fed via a CSI. It was shown by Jahns (1980) that the performance of the machine under fault conditions improved as the number of phases was increased. By controlling the remaining currents in multi-phase drives using a current regulated PWM inverter, it is possible to start and run the drive with loss of a phase (open circuited) without any reduction in torque [Fu and Lipo (1994), Toliyat (1998)]. The current required in the remaining phases was found by Fu and Lipo (1994) to decrease as the number of phases originally supplying the machine was increased. High power drives are particularly vulnerable to failures due to their high component count, which reduces the drive's mean-time-between failures [Jahns (1980)]. An increase in the number of phases supplying the machine results in a reduction in the power per phase compared to an equivalent three-phase machine. This means that the need for parallel or series stack switches in high power drives may not exist any more [Williamson and Smith (2001)], resulting in a lower component count and a less complex inverter structure. Thus improved reliability is anticipated for high power applications.

A potential benefit of multi-phase machines is that with an increase in the number of phases an increased torque per ampere for the same volume machine may be achieved [Toliyat et al (1998), Weh and Schroder (1985), Toliyat and Lipo (1994)].

Increased torque production can be achieved in multi-phase machines by virtue of higher harmonics other than the fundamental contributing towards torque production [Lyra and Lipo (2001), Xu et al (2001), Toliyat et al (1991), Kestelyn et al (2002), Hodge et al (2002)]. This is so since a three-phase machine can utilise only the fundamental component to develop torque, while a five-phase machine can utilise both the fundamental and the third harmonic components. By extension a seven-phase machine can be controlled to utilise the first, third and fifth harmonics for torque production [Xu et al (2001), Toliyat et al (1991)], while in a nine-phase machine it is possible to use injection of the third, the fifth and the seventh current harmonics [Coates et al (2001)]. This advantage stems from the fact that vector control of the machines' flux and torque, produced by the interaction of the fundamental field component and the fundamental stator current component, requires only two stator currents (d-q current components). In a multi-phase machine, with at least five phases or more, there are therefore additional degrees of freedom, which can be utilised to enhance the torque production through injection of higher order current harmonics. This is so since injection of any specific current harmonic requires again two current components, similar to the torque/flux production due to fundamental harmonic. In general, the possibility for an increase in torque density increases with the number of phases. However it appears that once when the number of phases reaches 15, further increase does not provide any further important advantage [Hodge et al (2002)]. It was reported by Xu et al (2001) that a 10% increase in torque is possible for a five-phase induction machine with concentrated windings. A synchronous reluctance machine with concentrated windings was investigated by Toliyat et al (1998), Toliyat et al (1992), Xu and Fu (2002), Shi et al (2001a) and a 10% increase in torque was reported. The research carried out thus far has not been confined to only five-phase machines. Lyra and Lipo (2001) considered a six-phase (double star) machine. The machine was reported to increase torque production by up to 40% compared to the equivalent three-phase machine. It was reported that the improvement in torque is due to two factors. First, by injecting the third harmonic current there is a reduction in the peak flux density of the air gap flux and so additional torque can be gained by increasing the fundamental flux component without saturating the machine. Secondly, the rotating field created by the third harmonic currents generates a small increase in torque.

Further advantages of multi-phase machines over the three-phase counterpart include reduction in stator and rotor losses [Williamson and Smith (2001)] and a

reduction in vibration and noise generated by the machine [Golubev and Ignatenko (2000)]. Recent surveys [Singh (2002), Jones and Levi (2002)] indicate an increasing interest in multi-phase machines within the scientific community. It has to be noted that some of the advantages of the multi-phase machines, which exist in the case of a single multi-phase motor drive, will not be applicable in the proposed multi-motor multi-phase system. For example, torque density cannot be increased in the manner previously discussed, since the existing degrees of freedom are to be used to control other machines in the group. Similarly, fault tolerance will be substantially reduced since all the available degrees of freedom are to be utilised for control of the machines in the system.

2.3 Modelling and control of multi-phase machines

The general theory of rotating machines, applied in analyses of three-phase machines, is also adequate for analysing multi-phase machines [White and Woodson (1959)]. The machines are modelled as a set of magnetically coupled coils. The flux linkage terms differ depending on the type of machine and the construction of the stator windings. For example, a six-phase stator can be constructed either with windings 60 degrees apart (true six-phase) or as in double star machines with two three-phase windings displaced by 30 degrees. Mathematical models have been developed for many different types of multi-phase machines both for the steady-state and the dynamic case. Transformation of machine equations from phase variable to d-q form is performed using either real or complex variable transformations. For example, d-q axis models for five-phase induction machines and synchronous reluctance machines are available in Ward and Härer (1969) and Toliyat et al (1992), respectively. Abbas et al (1984) modelled a double star induction machine, while the generalised case of a six-phase induction machine with an arbitrary displacement between the two sets of three-phase windings is given in Hadiouche et al (2000), Grochowalski (2000), Nelson and Krause (1974). Transformation of the phase variable model of multi-phase machines results in two components (d-q) contributing to torque and flux production, and $n-2$ components which do not contribute to torque production under the condition of sinusoidal mmf distribution [Klingshirn (1983), Zhao and Lipo (1995)]. Multi-phase machines can be modelled by considering an n -dimensional approach to the space vector theory [Gataric

(2000), Lipo (1984), Zhao and Lipo (1995), Kestelyn et al (2002)]. This method allows an n -phase machine to be modelled in n -dimensional space. Kestelyn et al (2002) demonstrated that a multi-phase machine is equivalent to a group of machines having smaller phase numbers and shows that a five-phase concentrated winding permanent magnet synchronous machine can be represented as a group of two two-phase and a single one-phase machine. Each phase of the machine is supplied by its own inverter (requiring 20 switches in total). It is on the basis of these transformed models that the methods of vector control for multi-phase machines are developed.

The well-known field oriented control (FOC) method, used to achieve high performance control of three-phase machines, can be extended to multi-phase machines. It has been shown by Nelson and Krause (1974) and Toliyat (1998) that multi-phase machine models can be transformed into a system of decoupled equations in orthogonal reference frames. The d-q axis reference frame currents contribute towards torque and flux production due to the fundamental of the mmf, whereas the remaining x-y components plus the zero sequence component(s) do not. This allows a simple extension of the rotor flux FOC principle in which the rotor flux linkage is maintained entirely in the d-axis, resulting in the q-axis component of rotor flux being maintained at zero. The electromagnetic torque equation is therefore reduced to the same form as that of a DC machine or a rotor flux oriented three-phase machine. Thus the electromagnetic torque and the rotor flux can be controlled independently by controlling the d and q components of stator current independently. Toliyat et al (2000) carried out the development of a vector control scheme for a five-phase synchronous reluctance machine. The strategy investigated was an indirect rotor flux oriented control technique using a space vector PWM strategy. Coates et al (2001) constructed a nine-phase four pole 5 kW synchronous reluctance drive under rotor flux oriented vector control. Rotor flux oriented control has been investigated for a five-phase induction and synchronous reluctance machine including third harmonic current injection by Xu et al (2001) and Shi et al (2001a), respectively, thus controlling both the fundamental and the third harmonic and resulting in a high performance drive with an increased torque. The other control method recently developed for high performance three-phase drives, direct torque control (DTC), is starting to be looked at in conjunction with multi-phase drives as well [Shi et al (2001b), Toliyat and Xu (2000)]. Shi et al (2001b) proposed DTC of a five-phase synchronous reluctance machine, while Toliyat and Xu (2000) analysed DTC of a five-phase induction machine.

The most frequently discussed multi-phase machines are either with five phases [Toliyat et al (1993), Favre et al (1993), Toliyat and Xu (2000)] or with six phases (double star) [Gopakumar et al (1993), Zhao and Lipo (1995), Petrov (1998), Lipo (1980), Fortuna and Palazzoli (1999)] (inclusive of those previously mentioned). One example of a seven-phase machine is given by Weh and Schroder (1985), while a nine-phase drive (with the winding composed of three three-phase windings) is discussed by Veen et al (1997) and Steiner et al (2000). Not surprisingly, a multi-phase induction motor is most frequently considered although multi-phase drives with permanent magnet synchronous machines, brushless DC machines, wound rotor synchronous motors and synchronous reluctance motors have all been described in literature.

The machine type is irrelevant in the context of the concept of the multi-machine system developed here and the research described in this thesis applies equally to multi-phase induction, synchronous reluctance, permanent magnet and wound rotor synchronous machines. The only requirements are that the supply is current controlled, since vector control will be ultimately applied and that the machine can be regarded as having sinusoidal distributed windings.

As discussed in chapter 1, the most important property of a multi-phase machine (regardless of type) is that, once the modelling is completed, a new set of equations will be obtained in which only two components will lead to stator to rotor coupling, while the rest do not give coupling. This is valid as long as only the fundamental harmonic of the mmf is under consideration. Modelling and transformation of multi-phase machines will be discussed next in chapter 3.

2.4 Three-phase multi-motor drives

As already noted multi-machine multi-inverter systems are present in many applications, such as textile and paper industries, rolling mills, robotics, electric vehicles and locomotive traction [Belhadj et al (2001)]. Multi-machine drives can be constructed and controlled in a number of ways. Matsumoto et al (2001) consider a single PWM VSI feeding parallel connected three-phase multiple induction motors for a locomotive traction application (Shinkansen, the fastest train in Japan). Stator flux oriented control is used in order to avoid over-magnetising the motor with the light load. The average value of the detected angular velocities of individual motors is used as the

value of the angular velocity for the control. Supply of two induction machines via a single VSI has advantages in terms of cost and size reduction; however the machines must be identical and equally loaded. If an incorrect electrical parameter estimation is made a mechanical perturbation will appear and will affect the system performance. Pena-Eguiluz et al (2001) compare the performance of two rotor flux observer strategies of a mean system controlled drive (mean system control consists of taking into account the necessary signals of both motors in order to recreate an imaginary mean motor). The two strategies under consideration involve the use of one rotor flux observer fed via the average of the two measured motor values and the use of two rotor flux observers taking the average of their outputs. The system consisting of two rotor flux observers was found to offer better performance. Kouno et al (2001) and Kawai et al (2002) examined a speed sensorless vector control method for parallel-connected induction machines fed via a single VSI. A rotor flux observer was used in order to eliminate the need for a flux sensor and an adaptive scheme for rotor speed is employed in order to eliminate the speed sensor. The system was found to operate satisfactorily for different ratings of each machine. Watanabe and Yamashita (2002) consider a speed sensorless system for use in a drive consisting of four induction motors supplied via a single three-phase VSI for a locomotive traction application. The method allowed for easier detection of wheel slippage based on the behaviour of motor currents.

Pena-Eguiluz et al (2002) examined different control structures for single inverter multi-motor three-phase drives utilising a rotor flux observer for each machine. Four different control structures were compared: mean drive control, which takes into account the necessary signals of both motors in order to calculate the average motor variables; switched master-slave drive control, which alternates between the estimated and measured signals for each machine every sampling period; mean drive control for dual motor, which averages the VSI reference signals obtained for both machines; and mean and differential drive control of the dual motor, which controls two different variables (torque and differential torque) by the d-axis regulation. The study found the mean drive control method to be the most effective under the adherence loss of one wheel.

Only one multi-motor three-phase system, fed by a single CSI is considered in literature [Ma et al (2001)]. The drive consists of a three-phase space vector modulated CSI feeding two three-phase induction machines connected in parallel. The drive creates two resonant modes due to parallel connection of filter capacitor and the motor.

A low frequency resonance due to the capacitor and magnetising inductance and a high frequency resonance due to the capacitor and the leakage inductance take place. The problem is solved using an active damping control system.

As mentioned previously, a quite different topology of the multi-drive system is the most common one. This system employs a number of three-phase machines each connected to its own VSI and fed via a common DC link, thus allowing for independent control of the speed and torque developed by each machine in the system. Belhadj et al (2001) considered both direct torque control (DTC) and field oriented control (FOC) strategies and found that they gave similar results in systems with mechanical coupling (i.e. connection of both machines to the same load) and systems without mechanical coupling (i.e. independent loads applied to each machine). It was concluded that the DTC scheme was advantageous because it offers a simpler realisation than FOC.

If a multi-motor system consists of m three-phase machines, this approach requires $3m$ inverter legs. Numerous topologies have been proposed for reducing the total number of inverter legs required in a multi-machine system [Lee et al (2001), Ledezma et al (2001), Jacobina et al (2002)]. The two solutions analysed in detail by Jacobina et al (2002) require only $2m$ and $2m+1$ inverter legs, respectively. However, both configurations lead to a substantial increase in the total harmonic distortion and reduced voltage capability. The authors conclude that the configuration with $2m+1$ legs offers a better performance than the configuration with $2m$ legs. Both are however inferior with respect to the standard solution with $3m$ legs. Klumper and Blaabjerg (2002) examined a multi-machine system fed via a two stage matrix converter and compared it to the standard solution with a separate VSI for each machine.

It can be concluded that a number of different topologies and control methods exist for the multi-machine three-phase drive system. However, none of the systems described in the literature allow independent control of machines fed via a single VSI. A potential solution, that is to be developed in this research, will be based on the utilisation of multi-phase machines. As noted, interest in multi-phase machines amongst the research community has been steadily increasing over the past few years due to the many advantages they offer over traditional three-phase machines. Advantages, such as fault tolerance, reduced power per phase, reduced torque ripple and reduced stator loss have led to their use in many high power and/or safety critical applications [Smith (2002)].

2.5 Summary

A literature review, provided in this chapter, has surveyed the state of the art in all the areas relevant for the research undertaken in the project. In particular, present realisations of three-phase multi-motor drives were reviewed and it was shown that independent control is not possible with a single inverter supply. The advantages of multi-phase machines over their three-phase counterpart were highlighted and the methods for a single multi-phase drive control were surveyed.

This research aims to develop a multi-phase multi-machine drive that allows for independent high performance control of each machine in the set, while using a single multi-phase inverter as the supply. In order to explain the concept of this system, mathematical modelling of an n -phase machine is elaborated next.

CHAPTER 3

MODELLING OF MULTI-PHASE MACHINES

3.1 Introduction

Mathematical modelling of n -phase induction machines in terms of phase variables is considered first. The resulting equations are highly coupled and contain time varying coefficients. For this reason a decoupling transformation is applied and it is shown that any n -phase machine can be considered in terms of flux and torque production as a two-phase machine. Next, a rotational transformation is applied resulting in a set of equations describing the n -phase induction machine in a common reference frame. Finally, equations describing a current-fed rotor flux oriented induction machine are derived.

3.2 Phase domain model of an n -phase induction machine

An n -phase symmetrical induction machine, such that the spatial displacement between any two mmfs produced by any two consecutive phases is $\alpha = 2\pi/n$, is under consideration. For the sake of generality both stator and rotor are assumed to be of n -phase structure. In arriving at a mathematical model of an n -phase machine the following standard simplifying assumptions were made:

- The mmf produced by a winding is sinusoidally distributed along the air gap circumference.
- The air gap is uniform.
- The B-H curve of the iron core is linear and so the main flux saturation can be neglected.
- Iron core losses are neglected.
- The winding resistances and inductances are constant.

It is also assumed that the rotor winding has been referred to stator winding, using winding transformation ratio. Stator and rotor voltage equilibrium and flux linkage equations can then be written as [White and Woodson (1959)]:

$$\begin{aligned}\underline{v}^s &= \underline{R}_s \underline{i}^s + \frac{d\underline{\psi}^s}{dt} \\ \underline{\psi}^s &= \underline{L}_s \underline{i}^s + \underline{L}_{sr} \underline{i}^r\end{aligned}\quad (3.1)$$

$$\begin{aligned}\underline{v}^r &= \underline{R}_r \underline{i}^r + \frac{d\underline{\psi}^r}{dt} \\ \underline{\psi}^r &= \underline{L}_r \underline{i}^r + \underline{L}_{rs} \underline{i}^s\end{aligned}\quad (3.2)$$

Let the phases of both stator and rotor be identified with numbers 1,2,3... n according to the spatial ordering of the windings along the circumference of the stator and rotor. The following definition of phase voltages, currents and flux linkages then applies to (3.1)-(3.2):

$$\begin{aligned}\underline{v}^s &= [v_{1s} \ v_{2s} \ v_{3s} \ \dots \ v_{ns}]^T \\ \underline{i}^s &= [i_{1s} \ i_{2s} \ i_{3s} \ \dots \ i_{ns}]^T \\ \underline{\psi}^s &= [\psi_{1s} \ \psi_{2s} \ \psi_{3s} \ \dots \ \psi_{ns}]^T\end{aligned}\quad (3.3)$$

$$\begin{aligned}\underline{v}^r &= [v_{1r} \ v_{2r} \ v_{3r} \ \dots \ v_{nr}]^T \\ \underline{i}^r &= [i_{1r} \ i_{2r} \ i_{3r} \ \dots \ i_{nr}]^T \\ \underline{\psi}^r &= [\psi_{1r} \ \psi_{2r} \ \psi_{3r} \ \dots \ \psi_{nr}]^T\end{aligned}\quad (3.4)$$

The matrices of stator and rotor inductances are given with ($\alpha = 2\pi/n$):

$$\underline{L}_s = \begin{bmatrix} L_{11s} & L_{12s} & L_{13s} & \dots & L_{1ns} \\ L_{21s} & L_{22s} & L_{23s} & \dots & L_{2ns} \\ L_{31s} & L_{32s} & L_{33s} & \dots & L_{3ns} \\ \dots & \dots & \dots & \dots & \dots \\ L_{n1s} & L_{n2s} & L_{n3s} & \dots & L_{nns} \end{bmatrix} = \begin{bmatrix} L_{1s} + M & M \cos \alpha & M \cos 2\alpha & \dots & M \cos(n-1)\alpha \\ M \cos(n-1)\alpha & L_{1s} + M & M \cos \alpha & \dots & M \cos(n-2)\alpha \\ M \cos(n-2)\alpha & M \cos(n-1)\alpha & L_{1s} + M & \dots & M \cos(n-3)\alpha \\ \dots & \dots & \dots & \dots & \dots \\ M \cos \alpha & M \cos 2\alpha & M \cos 3\alpha & \dots & L_{1s} + M \end{bmatrix}\quad (3.5)$$

$$\underline{L}_r = \begin{bmatrix} L_{11r} & L_{12r} & L_{13r} & \dots & L_{1nr} \\ L_{21r} & L_{22r} & L_{23r} & \dots & L_{2nr} \\ L_{31r} & L_{32r} & L_{33r} & \dots & L_{3nr} \\ \dots & \dots & \dots & \dots & \dots \\ L_{n1r} & L_{n2r} & L_{n3r} & \dots & L_{nnr} \end{bmatrix} = \begin{bmatrix} L_{1r} + M & M \cos \alpha & M \cos 2\alpha & \dots & M \cos(n-1)\alpha \\ M \cos(n-1)\alpha & L_{1r} + M & M \cos \alpha & \dots & M \cos(n-2)\alpha \\ M \cos(n-2)\alpha & M \cos(n-1)\alpha & L_{1r} + M & \dots & M \cos(n-3)\alpha \\ \dots & \dots & \dots & \dots & \dots \\ M \cos \alpha & M \cos 2\alpha & M \cos 3\alpha & \dots & L_{1r} + M \end{bmatrix}\quad (3.6)$$

Mutual inductances between stator and rotor windings are given with:

$$\underline{L}_{sr} = M \begin{bmatrix} \cos \theta & \cos(\theta + \alpha) & \cos(\theta + 2\alpha) & \dots & \cos(\theta + (n-1)\alpha) \\ \cos(\theta + (n-1)\alpha) & \cos \theta & \cos(\theta + \alpha) & \dots & \cos(\theta + (n-2)\alpha) \\ \cos(\theta + (n-2)\alpha) & \cos(\theta + (n-1)\alpha) & \cos \theta & \dots & \cos(\theta + (n-3)\alpha) \\ \dots & \dots & \dots & \dots & \dots \\ \cos(\theta + \alpha) & \cos(\theta + 2\alpha) & \cos(\theta + 3\alpha) & \dots & \cos \theta \end{bmatrix} \quad (3.7)$$

$$\underline{L}_{rs} = \underline{L}_{sr}^T$$

The angle θ denotes the instantaneous position of the magnetic axis of the rotor phase "a" with respect to the stationary magnetic axis of the stator phase "a" (i.e. the instantaneous position of the rotor with respect to stator). Stator and rotor resistance matrices are diagonal $n \times n$ matrices,

$$\begin{aligned} \underline{R}_s &= \text{diag}(R_s, R_s, R_s, \dots, R_s) \\ \underline{R}_r &= \text{diag}(R_r, R_r, R_r, \dots, R_r) \end{aligned} \quad (3.8)$$

Motor torque can be expressed in terms of phase variables as:

$$T_e = \frac{P}{2} \underline{i}^T \frac{d\underline{L}}{d\theta} \underline{i} = \frac{P}{2} \begin{bmatrix} \underline{i}^{sT} & \underline{i}^{rT} \end{bmatrix} \frac{d\underline{L}}{d\theta} \begin{bmatrix} \underline{i}^s \\ \underline{i}^r \end{bmatrix} \quad (3.9a)$$

where $\underline{L} = \begin{bmatrix} \underline{L}_s & \underline{L}_{sr} \\ \underline{L}_{rs} & \underline{L}_r \end{bmatrix}$. The torque equation can be further developed as follows:

$$T_e = \frac{P}{2} \begin{bmatrix} 0 & \underline{i}^{sT} \frac{d\underline{L}_{sr}}{d\theta} \\ \underline{i}^{rT} \frac{d\underline{L}_{rs}}{d\theta} & 0 \end{bmatrix} \begin{bmatrix} \underline{i}^s \\ \underline{i}^r \end{bmatrix} = \frac{P}{2} \left(\underline{i}^{sT} \frac{d\underline{L}_{sr}}{d\theta} \underline{i}^r + \underline{i}^{rT} \frac{d\underline{L}_{rs}}{d\theta} \underline{i}^s \right) \quad (3.9b)$$

As $\underline{i}^{rT} \frac{d\underline{L}_{rs}}{d\theta} \underline{i}^s = \underline{i}^{rT} \frac{d\underline{L}_{sr}^T}{d\theta} \underline{i}^s = \left(\underline{i}^{sT} \frac{d\underline{L}_{sr}}{d\theta} \underline{i}^r \right)^T$, the electromagnetic torque becomes:

$$T_e = P \underline{i}^{sT} \frac{d\underline{L}_{sr}}{d\theta} \underline{i}^r \quad (3.9c)$$

Substitution of currents from (3.3)-(3.4) and (3.7) into (3.9c) yields the torque equation in developed form:

$$T_e = -PM \left\{ \begin{aligned} & (i_{1s}i_{1r} + i_{2s}i_{2r} + i_{3s}i_{3r} + \dots + i_{ns}i_{nr}) \sin \theta + (i_{ns}i_{1r} + i_{1s}i_{2r} + i_{2s}i_{3r} + i_{3s}i_{4r} + \dots + i_{(n-1)s}i_{nr}) \sin(\theta + \alpha) + \\ & (i_{(n-1)s}i_{1r} + i_{ns}i_{2r} + i_{1s}i_{3r} + i_{2s}i_{4r} + \dots + i_{(n-2)s}i_{nr}) \sin(\theta + 2\alpha) + \\ & (i_{(n-2)s}i_{1r} + i_{(n-1)s}i_{2r} + i_{ns}i_{3r} + i_{1s}i_{4r} + \dots + i_{(n-3)s}i_{nr}) \sin(\theta + 3\alpha) + \\ & \dots + \\ & (i_{2s}i_{1r} + i_{3s}i_{2r} + i_{4s}i_{3r} + i_{5s}i_{4r} + \dots + i_{1s}i_{nr}) \sin(\theta + (n-1)\alpha) \end{aligned} \right\} \quad (3.10)$$

The equation of rotor motion is:

$$\frac{J}{P} \frac{d\omega}{dt} = T_e - T_L \quad (3.11)$$

where J and P are the inertia and number of pole pairs, respectively, ω is the electrical speed of rotation and T_L is the load torque. Mechanical loss torque is neglected.

The equations describing an n -phase machine are highly coupled and contain time varying coefficients. In order to simplify the mathematical model of an n -phase machine a decoupling transformation is applied and the machine is transformed to an equivalent two-phase machine. This transformation is demonstrated in the following sub-section.

3.3 Decoupling transformation

Let the correlation between any set of variables $[x]$ (voltages, currents, and flux linkages) in original old (phase) domain and new (transformed) domain be given with:

$$\begin{aligned} \underline{x}_{new} &= \underline{C} \underline{x}_{old} \\ \underline{x}_{old} &= \underline{C}^{-1} \underline{x}_{new} \end{aligned} \quad (3.12)$$

where a power invariant transformation matrix is selected so that $\underline{C}^{-1} = \underline{C}^T$. The decoupling transformation matrix is then given for an odd number of phases with [White and Woodson (1959)]:

$$\underline{C} = \sqrt{\frac{2}{n}} \begin{bmatrix} 1 & \cos \alpha & \cos 2\alpha & \cos 3\alpha & \dots & \cos 3\alpha & \cos 2\alpha & \cos \alpha \\ 0 & \sin \alpha & \sin 2\alpha & \sin 3\alpha & \dots & -\sin 3\alpha & -\sin 2\alpha & -\sin \alpha \\ 1 & \cos 2\alpha & \cos 4\alpha & \cos 6\alpha & \dots & \cos 6\alpha & \cos 4\alpha & \cos 2\alpha \\ 0 & \sin 2\alpha & \sin 4\alpha & \sin 6\alpha & \dots & -\sin 6\alpha & -\sin 4\alpha & -\sin 2\alpha \\ 1 & \cos 3\alpha & \cos 6\alpha & \cos 9\alpha & \dots & \cos 9\alpha & \cos 6\alpha & \cos 3\alpha \\ 0 & \sin 3\alpha & \sin 6\alpha & \sin 9\alpha & \dots & -\sin 9\alpha & -\sin 6\alpha & -\sin 3\alpha \\ 1 & \cos 4\alpha & \cos 8\alpha & \cos 12\alpha & \dots & \cos 12\alpha & \cos 8\alpha & \cos 4\alpha \\ 0 & \sin 4\alpha & \sin 8\alpha & \sin 12\alpha & \dots & -\sin 12\alpha & -\sin 8\alpha & -\sin 4\alpha \\ \dots & \dots \\ 1 & \cos \left(\frac{n-1}{2} \alpha \right) & \cos 2 \left(\frac{n-1}{2} \alpha \right) & \cos 3 \left(\frac{n-1}{2} \alpha \right) & \dots & \cos 3 \left(\frac{n-1}{2} \alpha \right) & \cos 2 \left(\frac{n-1}{2} \alpha \right) & \cos \left(\frac{n-1}{2} \alpha \right) \\ 0 & \sin \left(\frac{n-1}{2} \alpha \right) & \sin 2 \left(\frac{n-1}{2} \alpha \right) & \sin 3 \left(\frac{n-1}{2} \alpha \right) & \dots & -\sin 3 \left(\frac{n-1}{2} \alpha \right) & -\sin 2 \left(\frac{n-1}{2} \alpha \right) & -\sin \left(\frac{n-1}{2} \alpha \right) \\ \frac{1}{\sqrt{2}} & \frac{1}{\sqrt{2}} & \frac{1}{\sqrt{2}} & \frac{1}{\sqrt{2}} & \dots & \frac{1}{\sqrt{2}} & \frac{1}{\sqrt{2}} & \frac{1}{\sqrt{2}} \end{bmatrix} \quad (3.13a)$$

Here the first two rows define α - β components, the last row defines standard zero sequence component, while the remaining $(n-3)$ rows define $[(n-1)/2 - 1]$ pairs of x-y

components. Transformation matrix for an even number of phases is given with [White and Woodson (1959)]:

$$\underline{C} = \sqrt{\frac{2}{n}} \begin{bmatrix} 1 & \cos \alpha & \cos 2\alpha & \cos 3\alpha & \dots & \cos 3\alpha & \cos 2\alpha & \cos \alpha \\ 0 & \sin \alpha & \sin 2\alpha & \sin 3\alpha & \dots & -\sin 3\alpha & -\sin 2\alpha & -\sin \alpha \\ 1 & \cos 2\alpha & \cos 4\alpha & \cos 6\alpha & \dots & \cos 6\alpha & \cos 4\alpha & \cos 2\alpha \\ 0 & \sin 2\alpha & \sin 4\alpha & \sin 6\alpha & \dots & -\sin 6\alpha & -\sin 4\alpha & -\sin 2\alpha \\ 1 & \cos 3\alpha & \cos 6\alpha & \cos 9\alpha & \dots & \cos 9\alpha & \cos 6\alpha & \cos 3\alpha \\ 0 & \sin 3\alpha & \sin 6\alpha & \sin 9\alpha & \dots & -\sin 9\alpha & -\sin 6\alpha & -\sin 3\alpha \\ \dots & \dots \\ 1 & \cos \left\{ \frac{n-2}{2} \alpha \right\} & \cos 2 \left\{ \frac{n-2}{2} \alpha \right\} & \cos 3 \left\{ \frac{n-2}{2} \alpha \right\} & \dots & \cos 3 \left\{ \frac{n-2}{2} \alpha \right\} & \cos 2 \left\{ \frac{n-2}{2} \alpha \right\} & \cos \left\{ \frac{n-2}{2} \alpha \right\} \\ 0 & \sin \left\{ \frac{n-2}{2} \alpha \right\} & \sin 2 \left\{ \frac{n-2}{2} \alpha \right\} & \sin 3 \left\{ \frac{n-2}{2} \alpha \right\} & \dots & -\sin 3 \left\{ \frac{n-2}{2} \alpha \right\} & -\sin 2 \left\{ \frac{n-2}{2} \alpha \right\} & -\sin \left\{ \frac{n-2}{2} \alpha \right\} \\ \frac{1}{\sqrt{2}} & \frac{1}{\sqrt{2}} & \frac{1}{\sqrt{2}} & \frac{1}{\sqrt{2}} & \dots & \frac{1}{\sqrt{2}} & \frac{1}{\sqrt{2}} & \frac{1}{\sqrt{2}} \\ \frac{1}{\sqrt{2}} & -\frac{1}{\sqrt{2}} & \frac{1}{\sqrt{2}} & -\frac{1}{\sqrt{2}} & \dots & -\frac{1}{\sqrt{2}} & \frac{1}{\sqrt{2}} & -\frac{1}{\sqrt{2}} \end{bmatrix} \quad (3.13b)$$

Here the first two rows define α - β components, the last two rows define zero sequence components, while the remaining $(n-4)$ rows define $[(n-2)/2 - 1]$ pairs of x-y components. The inverse transformation for odd number of phases is:

$$\underline{C}^{-1} = \sqrt{\frac{2}{n}} \begin{bmatrix} 1 & 0 & 1 & 0 & 1 & 0 & \dots & 1 & 0 & \frac{1}{\sqrt{2}} \\ \cos \alpha & \sin \alpha & \cos 2\alpha & \sin 2\alpha & \cos 3\alpha & \sin 3\alpha & \dots & \cos \left\{ \frac{n-1}{2} \alpha \right\} & \sin \left\{ \frac{n-1}{2} \alpha \right\} & \frac{1}{\sqrt{2}} \\ \cos 2\alpha & \sin 2\alpha & \cos 4\alpha & \sin 4\alpha & \cos 6\alpha & \sin 6\alpha & \dots & \cos 2 \left\{ \frac{n-1}{2} \alpha \right\} & \sin 2 \left\{ \frac{n-1}{2} \alpha \right\} & \frac{1}{\sqrt{2}} \\ \cos 3\alpha & \sin 3\alpha & \cos 6\alpha & \sin 6\alpha & \cos 9\alpha & \sin 9\alpha & \dots & \cos 3 \left\{ \frac{n-1}{2} \alpha \right\} & \sin 3 \left\{ \frac{n-1}{2} \alpha \right\} & \frac{1}{\sqrt{2}} \\ \dots & \dots \\ \cos 3\alpha & -\sin 3\alpha & \cos 6\alpha & -\sin 6\alpha & \cos 9\alpha & -\sin 9\alpha & \dots & \cos 3 \left\{ \frac{n-1}{2} \alpha \right\} & -\sin 3 \left\{ \frac{n-1}{2} \alpha \right\} & \frac{1}{\sqrt{2}} \\ \cos 2\alpha & -\sin 2\alpha & \cos 4\alpha & -\sin 4\alpha & \cos 6\alpha & -\sin 6\alpha & \dots & \cos 2 \left\{ \frac{n-1}{2} \alpha \right\} & -\sin 2 \left\{ \frac{n-1}{2} \alpha \right\} & \frac{1}{\sqrt{2}} \\ \cos \alpha & -\sin \alpha & \cos 2\alpha & -\sin 2\alpha & \cos 3\alpha & -\sin 3\alpha & \dots & \cos \left\{ \frac{n-1}{2} \alpha \right\} & -\sin \left\{ \frac{n-1}{2} \alpha \right\} & \frac{1}{\sqrt{2}} \end{bmatrix} \quad (3.14a)$$

and for an even number of phases is:

$$\underline{C}^{-1} = \sqrt{\frac{2}{n}} \begin{bmatrix} 1 & 0 & 1 & 0 & 1 & 0 & \dots & 1 & 0 & \frac{1}{\sqrt{2}} & \frac{1}{\sqrt{2}} \\ \cos \alpha & \sin \alpha & \cos 2\alpha & \sin 2\alpha & \cos 3\alpha & \sin 3\alpha & \dots & \cos \left\{ \frac{n-2}{2} \alpha \right\} & \sin \left\{ \frac{n-2}{2} \alpha \right\} & \frac{1}{\sqrt{2}} & -\frac{1}{\sqrt{2}} \\ \cos 2\alpha & \sin 2\alpha & \cos 4\alpha & \sin 4\alpha & \cos 6\alpha & \sin 6\alpha & \dots & \cos 2 \left\{ \frac{n-2}{2} \alpha \right\} & \sin 2 \left\{ \frac{n-2}{2} \alpha \right\} & \frac{1}{\sqrt{2}} & \frac{1}{\sqrt{2}} \\ \cos 3\alpha & \sin 3\alpha & \cos 6\alpha & \sin 6\alpha & \cos 9\alpha & \sin 9\alpha & \dots & \cos 3 \left\{ \frac{n-2}{2} \alpha \right\} & \sin 3 \left\{ \frac{n-2}{2} \alpha \right\} & \frac{1}{\sqrt{2}} & -\frac{1}{\sqrt{2}} \\ \dots & \dots \\ \cos 3\alpha & -\sin 3\alpha & \cos 6\alpha & -\sin 6\alpha & \cos 9\alpha & -\sin 9\alpha & \dots & \cos 3 \left\{ \frac{n-2}{2} \alpha \right\} & -\sin 3 \left\{ \frac{n-2}{2} \alpha \right\} & \frac{1}{\sqrt{2}} & -\frac{1}{\sqrt{2}} \\ \cos 2\alpha & -\sin 2\alpha & \cos 4\alpha & -\sin 4\alpha & \cos 6\alpha & -\sin 6\alpha & \dots & \cos 2 \left\{ \frac{n-2}{2} \alpha \right\} & -\sin 2 \left\{ \frac{n-2}{2} \alpha \right\} & \frac{1}{\sqrt{2}} & \frac{1}{\sqrt{2}} \\ \cos \alpha & -\sin \alpha & \cos 2\alpha & -\sin 2\alpha & \cos 3\alpha & -\sin 3\alpha & \dots & \cos \left\{ \frac{n-2}{2} \alpha \right\} & -\sin \left\{ \frac{n-2}{2} \alpha \right\} & \frac{1}{\sqrt{2}} & -\frac{1}{\sqrt{2}} \end{bmatrix} \quad (3.14b)$$

3.4 Application of the decoupling transformation onto the phase domain model

Let the transformation according to (3.12), be defined with the following correlations:

$$\begin{aligned} \underline{v}_{\alpha\beta}^s &= \underline{C} \underline{v}^s & \underline{i}_{\alpha\beta}^s &= \underline{C} \underline{i}^s & \underline{\psi}_{\alpha\beta}^s &= \underline{C} \underline{\psi}^s \\ \underline{v}_{\alpha\beta}^r &= \underline{C} \underline{v}^r & \underline{i}_{\alpha\beta}^r &= \underline{C} \underline{i}^r & \underline{\psi}_{\alpha\beta}^r &= \underline{C} \underline{\psi}^r \end{aligned} \quad (3.15)$$

where new stator and rotor windings retain the speed of rotation of original windings. Substitution of (3.13a) or (3.13b), in conjunction with (3.15), into voltage equations of (3.1)-(3.2) leads to transformed form of the voltage equations:

$$\begin{bmatrix} \underline{v}_{\alpha\beta}^s \\ \underline{v}_{\alpha\beta}^r \end{bmatrix} = \begin{bmatrix} \underline{R}_s & 0 \\ 0 & \underline{R}_r \end{bmatrix} \begin{bmatrix} \underline{i}_{\alpha\beta}^s \\ \underline{i}_{\alpha\beta}^r \end{bmatrix} + \frac{d}{dt} \begin{bmatrix} \underline{\psi}_{\alpha\beta}^s \\ \underline{\psi}_{\alpha\beta}^r \end{bmatrix} \quad (3.16)$$

which remain to be of the same form as in original phase domain. Transformation of flux linkage equations results in:

$$\begin{bmatrix} \underline{\psi}_{\alpha\beta}^s \\ \underline{\psi}_{\alpha\beta}^r \end{bmatrix} = \begin{bmatrix} \underline{C} & 0 \\ 0 & \underline{C} \end{bmatrix} \begin{bmatrix} \underline{L}_s & \underline{L}_{sr} \\ \underline{L}_{rs} & \underline{L}_r \end{bmatrix} \begin{bmatrix} \underline{C}^{-1} & 0 \\ 0 & \underline{C}^{-1} \end{bmatrix} \begin{bmatrix} \underline{i}_{\alpha\beta}^s \\ \underline{i}_{\alpha\beta}^r \end{bmatrix} = \begin{bmatrix} \underline{L}_{\alpha\beta}^s & \underline{L}_{\alpha\beta}^{sr} \\ \underline{L}_{\alpha\beta}^{rs} & \underline{L}_{\alpha\beta}^r \end{bmatrix} \begin{bmatrix} \underline{i}_{\alpha\beta}^s \\ \underline{i}_{\alpha\beta}^r \end{bmatrix} \quad (3.17)$$

where

$$\underline{L}_{\alpha\beta} = \begin{bmatrix} \underline{L}_{\alpha\beta}^s & \underline{L}_{\alpha\beta}^{sr} \\ \underline{L}_{\alpha\beta}^{rs} & \underline{L}_{\alpha\beta}^r \end{bmatrix} = \begin{bmatrix} \underline{C} \underline{L}_s \underline{C}^{-1} & \underline{C} \underline{L}_{sr} \underline{C}^{-1} \\ \underline{C} \underline{L}_{rs} \underline{C}^{-1} & \underline{C} \underline{L}_r \underline{C}^{-1} \end{bmatrix} \quad (3.18)$$

Individual submatrices of (3.18) are further equal to:

$$\underline{L}_{\alpha\beta}^s = \begin{bmatrix} L_{ls} + (n/2)M & & & & & \\ & L_{ls} + (n/2)M & & & & \\ & & L_{ls} & & & \\ & & & L_{ls} & & \\ & & & & \dots & \\ & & & & & L_{ls} \end{bmatrix} \quad (3.19)$$

$$\underline{L}_{\alpha\beta}^r = \begin{bmatrix} L_{lr} + (n/2)M & & & & & \\ & L_{lr} + (n/2)M & & & & \\ & & L_{lr} & & & \\ & & & L_{lr} & & \\ & & & & \dots & \\ & & & & & L_{lr} \end{bmatrix} \quad (3.20)$$

Further

$$\underline{L}_{\alpha\beta}^{rs} = \frac{n}{2} M \begin{bmatrix} \cos(\theta) & \sin(\theta) & 0 & \dots & 0 \\ -\sin(\theta) & \cos(\theta) & 0 & \dots & 0 \\ 0 & 0 & 0 & \dots & 0 \\ \dots & \dots & \dots & \dots & \dots \\ 0 & 0 & 0 & \dots & 0 \end{bmatrix} = \frac{n}{2} M \begin{bmatrix} \cos \theta & \sin \theta & [0]^{2 \times (n-2)} \\ -\sin \theta & \cos \theta & [0]^{(n-2) \times (n-2)} \\ [0]^{(n-2) \times 2} & [0]^{(n-2) \times (n-2)} & \end{bmatrix} \quad (3.21)$$

and

$$\underline{L}_{\alpha\beta}^{sr} = \frac{n}{2} M \begin{bmatrix} \cos(\theta) & -\sin(\theta) & 0 & \dots & 0 \\ \sin(\theta) & \cos(\theta) & 0 & \dots & 0 \\ 0 & 0 & 0 & \dots & 0 \\ \dots & \dots & \dots & \dots & \dots \\ 0 & 0 & 0 & \dots & 0 \end{bmatrix} = \frac{n}{2} M \begin{bmatrix} \cos \theta & -\sin \theta & [0]^{2 \times (n-2)} \\ \sin \theta & \cos \theta & [0]^{(n-2) \times (n-2)} \\ [0]^{(n-2) \times 2} & [0]^{(n-2) \times (n-2)} & \end{bmatrix} \quad (3.22)$$

where θ denotes instantaneous rotor position. Hence x-y components of stator and rotor are not coupled. Of course, there is not any mutual coupling between the x-components and y-components of stator (rotor) either, since the windings are orthogonal. The torque developed by the machine is given by:

$$T_e = \frac{P}{2} \begin{bmatrix} i_{\alpha\beta}^{sT} & i_{\alpha\beta}^{rT} \end{bmatrix} \cdot \underline{\underline{\begin{bmatrix} \underline{C} & 0 \\ 0 & \underline{C} \end{bmatrix} \frac{d}{d\theta} \begin{bmatrix} 0 & \underline{L}_{sr} \\ \underline{L}_{rs} & 0 \end{bmatrix} \underline{C}^{-1} \begin{bmatrix} 0 & 0 \\ 0 & \underline{C}^{-1} \end{bmatrix} \begin{bmatrix} i_{\alpha\beta}^s \\ i_{\alpha\beta}^r \end{bmatrix}}}} \quad (3.23)$$

The product of the underlined matrices is further equal to $\begin{bmatrix} 0 & \underline{C} \frac{d}{d\theta} (\underline{L}_{sr}) \underline{C}^{-1} \\ \underline{C} \frac{d}{d\theta} (\underline{L}_{rs}) \underline{C}^{-1} & 0 \end{bmatrix}$.

The two sub-matrices are evaluated as follows:

$$\underline{C} \frac{d}{d\theta} \underline{L}_{sr} \underline{C}^{-1} = -\frac{n}{2} M \begin{bmatrix} \sin(\theta) & \cos(\theta) & 0 & \dots & 0 \\ -\cos(\theta) & \sin(\theta) & 0 & \dots & 0 \\ 0 & 0 & 0 & \dots & 0 \\ \dots & \dots & \dots & \dots & \dots \\ 0 & 0 & 0 & \dots & 0 \end{bmatrix} \quad (3.24)$$

and

$$\underline{C} \frac{d}{d\theta} \underline{L}_{rs} \underline{C}^{-1} = -\frac{n}{2} M \begin{bmatrix} \sin(\theta) & -\cos(\theta) & 0 & \dots & 0 \\ \cos(\theta) & \sin(\theta) & 0 & \dots & 0 \\ 0 & 0 & 0 & \dots & 0 \\ \dots & \dots & \dots & \dots & \dots \\ 0 & 0 & 0 & \dots & 0 \end{bmatrix} \quad (3.25)$$

so that the final form of the torque equation is:

$$T_e = PL_m \{ \cos \theta (i_{\alpha r} i_{\beta s} - i_{\beta r} i_{\alpha s}) - \sin \theta (i_{\alpha r} i_{\alpha s} + i_{\beta r} i_{\beta s}) \} \quad (3.26)$$

Here $L_m = (n/2)M$.

By substituting (3.19)-(3.22) into (3.17) and then into (3.16) and taking into account that the rotor winding is short-circuited, the voltage equilibrium equations can be written as:

$$\begin{aligned}
 v_{\alpha s} &= R_s i_{\alpha s} + \frac{d\psi_{\alpha s}}{dt} = R_s i_{\alpha s} + (L_{ls} + L_m) \frac{di_{\alpha s}}{dt} + L_m \frac{d}{dt} (i_{\alpha s} \cos \theta - i_{\beta r} \sin \theta) \\
 v_{\beta s} &= R_s i_{\beta s} + \frac{d\psi_{\beta s}}{dt} = R_s i_{\beta s} + (L_{ls} + L_m) \frac{di_{\beta s}}{dt} + L_m \frac{d}{dt} (i_{\alpha r} \sin \theta + i_{\beta r} \cos \theta) \\
 v_{x1s} &= R_s i_{x1s} + \frac{d\psi_{x1s}}{dt} = R_s i_{x1s} + L_{ls} \frac{di_{x1s}}{dt} \\
 v_{y1s} &= R_s i_{y1s} + \frac{d\psi_{y1s}}{dt} = R_s i_{y1s} + L_{ls} \frac{di_{y1s}}{dt} \\
 v_{x2s} &= R_s i_{x2s} + \frac{d\psi_{x2s}}{dt} = R_s i_{x2s} + L_{ls} \frac{di_{x2s}}{dt} \\
 v_{y2s} &= R_s i_{y2s} + \frac{d\psi_{y2s}}{dt} = R_s i_{y2s} + L_{ls} \frac{di_{y2s}}{dt} \\
 &\dots\dots\dots \\
 v_{0s} &= R_s i_{0s} + \frac{d\psi_{0s}}{dt} = R_s i_{0s} + L_{ls} \frac{di_{0s}}{dt}
 \end{aligned} \tag{3.27}$$

$$\begin{aligned}
 v_{\alpha r} = 0 &= R_r i_{\alpha r} + \frac{d\psi_{\alpha r}}{dt} = R_r i_{\alpha r} + (L_{lr} + L_m) \frac{di_{\alpha r}}{dt} + L_m \frac{d}{dt} (i_{\alpha s} \cos \theta + i_{\beta s} \sin \theta) \\
 v_{\beta r} = 0 &= R_r i_{\beta r} + \frac{d\psi_{\beta r}}{dt} = R_r i_{\beta r} + (L_{lr} + L_m) \frac{di_{\beta r}}{dt} + L_m \frac{d}{dt} (-i_{\alpha s} \sin \theta + i_{\beta s} \cos \theta) \\
 v_{x1r} = 0 &= R_r i_{x1r} + \frac{d\psi_{x1r}}{dt} = R_r i_{x1r} + L_{lr} \frac{di_{x1r}}{dt} \\
 v_{y1r} = 0 &= R_r i_{y1r} + \frac{d\psi_{y1r}}{dt} = R_r i_{y1r} + L_{lr} \frac{di_{y1r}}{dt} \\
 v_{x2r} = 0 &= R_r i_{x2r} + \frac{d\psi_{x2r}}{dt} = R_r i_{x2r} + L_{lr} \frac{di_{x2r}}{dt} \\
 v_{y2r} = 0 &= R_r i_{y2r} + \frac{d\psi_{y2r}}{dt} = R_r i_{y2r} + L_{lr} \frac{di_{y2r}}{dt} \\
 &\dots\dots\dots \\
 v_{0r} = 0 &= R_r i_{0r} + \frac{d\psi_{0r}}{dt} = R_r i_{0r} + L_{lr} \frac{di_{0r}}{dt}
 \end{aligned} \tag{3.28}$$

In the case of an even number of phases the last two equations are for zero sequence components so that the total number of pairs of x-y components is $[(n - 2)/2 - 1]$. For an odd number of phases the last equation only is the zero sequence component so that there are $[(n - 1)/2 - 1]$ pairs of x-y components.

One can see that the torque equation (3.26) has been reduced to a much simpler form than that of equation (3.10). The torque equation (3.26) shows that the machine's

torque is entirely developed due to the interaction of the stator and rotor α - β current components, regardless of the number of phases. Hence for any n -phase machine independent flux and torque control require only two current components. It can be seen from the rotor equation (3.28) that since the rotor is short-circuited and stator x-y components are decoupled from rotor x-y components, all rotor x-y components and zero sequence components are identically equal to zero. The same applies to the stator zero sequence components for odd phase numbers and one of the two zero sequence components for even phase numbers, since star connection is assumed.

3.5 Application of the rotational transformation

Since all the x-y components and zero sequence components of stator and rotor are decoupled, rotational transformation needs to be applied to α - β components only. The form of the transformation matrices for stator and rotor are [White and Woodson (1959)]:

$$\underline{D}_s = \begin{bmatrix} \cos \theta_s & \sin \theta_s & & & \\ -\sin \theta_s & \cos \theta_s & & & \\ & & 1 & & \\ & & & \dots & \\ & & & & 1 \end{bmatrix} \quad \underline{D}_s^{-1} = \begin{bmatrix} \cos \theta_s & -\sin \theta_s & & & \\ \sin \theta_s & \cos \theta_s & & & \\ & & 1 & & \\ & & & \dots & \\ & & & & 1 \end{bmatrix} \quad (3.29)$$

$$\underline{D}_r = \begin{bmatrix} \cos \beta & \sin \beta & & & \\ -\sin \beta & \cos \beta & & & \\ & & 1 & & \\ & & & \dots & \\ & & & & 1 \end{bmatrix} \quad \underline{D}_r^{-1} = \begin{bmatrix} \cos \beta & -\sin \beta & & & \\ \sin \beta & \cos \beta & & & \\ & & 1 & & \\ & & & \dots & \\ & & & & 1 \end{bmatrix}$$

Transformation of the stator and rotor variables is performed using the same transformation expressions, except that θ_s is replaced with β , where $\beta = \theta_s - \theta$. Here θ_s is the instantaneous angular position of the d-axis of the common reference frame with respect to the phase "a" magnetic axis of the stator, $\theta_s = \int \omega_a dt$, where ω_a is the arbitrary rotational speed of the d-axis of the common reference frame while β is the instantaneous angular position of the d-axis of the common reference frame and the phase "a" magnetic axis of the rotor. Setting $\omega_a = 0$ yields model in the stationary common reference frame.

Upon application of (3.29) in conjunction with the model (3.26)-(3.28), voltage and flux linkage equations for an odd phase number take the form:

$$\begin{aligned}
 v_{ds} &= R_s i_{ds} - \omega_a \psi_{qs} + p \psi_{ds} & v_{dr} &= 0 = R_r i_{dr} - (\omega_a - \omega) \psi_{qr} + p \psi_{dr} \\
 v_{qs} &= R_s i_{qs} + \omega_a \psi_{ds} + p \psi_{qs} & v_{qr} &= 0 = R_r i_{qr} + (\omega_a - \omega) \psi_{dr} + p \psi_{qr} \\
 v_{x1s} &= R_s i_{x1s} + p \psi_{x1s} & v_{x1r} &= 0 = R_r i_{x1r} + p \psi_{x1r} \\
 v_{y1s} &= R_s i_{y1s} + p \psi_{y1s} & v_{y1r} &= 0 = R_r i_{y1r} + p \psi_{y1r} \\
 v_{x2s} &= R_s i_{x2s} + p \psi_{x2s} & v_{x2r} &= 0 = R_r i_{x2r} + p \psi_{x2r} \\
 v_{y2s} &= R_s i_{y2s} + p \psi_{y2s} & v_{y2r} &= 0 = R_r i_{y2r} + p \psi_{y2r} \\
 \dots\dots\dots & & & \\
 v_{0s} &= R_s i_{0s} + p \psi_{0s} & v_{0r} &= R_r i_{0r} + p \psi_{0r}
 \end{aligned} \tag{3.30a}$$

In the case of an even phase number:

$$\begin{aligned}
 v_{ds} &= R_s i_{ds} - \omega_a \psi_{qs} + p \psi_{ds} & v_{dr} &= 0 = R_r i_{dr} - (\omega_a - \omega) \psi_{qr} + p \psi_{dr} \\
 v_{qs} &= R_s i_{qs} + \omega_a \psi_{ds} + p \psi_{qs} & v_{qr} &= 0 = R_r i_{qr} + (\omega_a - \omega) \psi_{dr} + p \psi_{qr} \\
 v_{x1s} &= R_s i_{x1s} + p \psi_{x1s} & v_{x1r} &= 0 = R_r i_{x1r} + p \psi_{x1r} \\
 v_{y1s} &= R_s i_{y1s} + p \psi_{y1s} & v_{y1r} &= 0 = R_r i_{y1r} + p \psi_{y1r} \\
 v_{x2s} &= R_s i_{x2s} + p \psi_{x2s} & v_{x2r} &= 0 = R_r i_{x2r} + p \psi_{x2r} \\
 v_{y2s} &= R_s i_{y2s} + p \psi_{y2s} & v_{y2r} &= 0 = R_r i_{y2r} + p \psi_{y2r} \\
 \dots\dots\dots & & & \\
 v_{o+s} &= R_s i_{o+s} + p \psi_{o+s} & v_{o+r} &= R_r i_{o+r} + p \psi_{o+r} \\
 v_{o-s} &= R_s i_{o-s} + p \psi_{o-s} & v_{o-r} &= R_r i_{o-r} + p \psi_{o-r}
 \end{aligned} \tag{3.30b}$$

where $p = d/dt$.

The flux linkage equations become (odd phase number):

$$\begin{aligned}
 \psi_{ds} &= (L_{ls} + L_m) i_{ds} + L_m i_{dr} & \psi_{dr} &= (L_{lr} + L_m) i_{dr} + L_m i_{ds} \\
 \psi_{qs} &= (L_{ls} + L_m) i_{qs} + L_m i_{qr} & \psi_{qr} &= (L_{lr} + L_m) i_{qr} + L_m i_{qs} \\
 \psi_{x1s} &= L_{ls} i_{x1s} & \psi_{x1r} &= L_{lr} i_{x1r} \\
 \psi_{y1s} &= L_{ls} i_{y1s} & \psi_{y1r} &= L_{lr} i_{y1r} \\
 \psi_{x2s} &= L_{ls} i_{x2s} & \psi_{x2r} &= L_{lr} i_{x2r} \\
 \psi_{y2s} &= L_{ls} i_{y2s} & \psi_{y2r} &= L_{lr} i_{y2r} \\
 \dots\dots\dots & & & \\
 \psi_{0s} &= L_{ls} i_{0s} & \psi_{0r} &= L_{lr} i_{0r}
 \end{aligned} \tag{3.31a}$$

Even phase number:

$$\begin{aligned}
 \psi_{ds} &= (L_{ls} + L_m) i_{ds} + L_m i_{dr} & \psi_{dr} &= (L_{lr} + L_m) i_{dr} + L_m i_{ds} \\
 \psi_{qs} &= (L_{ls} + L_m) i_{qs} + L_m i_{qr} & \psi_{qr} &= (L_{lr} + L_m) i_{qr} + L_m i_{qs} \\
 \psi_{x1s} &= L_{ls} i_{x1s} & \psi_{x1r} &= L_{lr} i_{x1r} \\
 \psi_{y1s} &= L_{ls} i_{y1s} & \psi_{y1r} &= L_{lr} i_{y1r} \\
 \psi_{x2s} &= L_{ls} i_{x2s} & \psi_{x2r} &= L_{lr} i_{x2r} \\
 \psi_{y2s} &= L_{ls} i_{y2s} & \psi_{y2r} &= L_{lr} i_{y2r} \\
 \dots\dots\dots & & & \\
 \psi_{o+s} &= L_{ls} i_{o+s} & \psi_{o+r} &= L_{lr} i_{o+r} \\
 \psi_{o-s} &= L_{ls} i_{o-s} & \psi_{o-r} &= L_{lr} i_{o-r}
 \end{aligned} \tag{3.31b}$$

Here once more $L_m = (n/2)M$. Torque equation is:

$$T_e = \frac{nP}{2} M [i_{dr} i_{qs} - i_{ds} i_{qr}] \quad (3.32)$$

$$T_e = PL_m [i_{dr} i_{qs} - i_{ds} i_{qr}]$$

The machine model described with (3.30)-(3.32) is identical to that describing a three-phase machine in the arbitrary reference frame, except for the presence of x-y components. As rotor flux and torque are independent of x-y components, vector control scheme for an n -phase induction machine will be the same as for a three-phase machine, except that coordinate transformation involves creation of n individual phase currents (rather than three) from the d-q axis stator current references.

3.6 Rotor flux oriented control of an n -phase current-fed induction machine

Rotor flux oriented control is achieved when the speed of the reference frame is selected as equal to the speed of rotation of the rotor flux space vector at all times. The real axis of the reference frame, d-axis, is at all times aligned with the rotor flux space vector, while the q-axis is perpendicular to it. Thus the reference frame is fixed to the rotor flux space vector via the d-axis and therefore [Krishnan (2001)]:

$$\begin{aligned} \theta_s &= \phi_r & \theta_r &= \phi_r - \theta \\ \omega_a &= \omega_r & \omega_r &= \frac{d\phi_r}{dt} \end{aligned} \quad (3.33)$$

where angle ϕ_r denotes instantaneous rotor flux space vector position. Rotor flux space vector becomes a pure real variable in this special frame of reference,

$$\underline{\psi}_r = \psi_{dr} + j\psi_{qr} = \psi_r \quad (3.34)$$

i.e., it follows that:

$$\psi_{dr} = \psi_r \quad \psi_{qr} = 0 \quad \frac{d\psi_{qr}}{dt} = 0 \quad (3.35)$$

It is assumed that the machine is supplied by a current controlled VSI with current control in the stationary reference frame. Taking the current control loops as ideal, the stator voltage equations can be omitted [Krishnan (2001)]. Thus by considering the

rotor flux linkage equation (3.34) and taking into account equation (3.35) the rotor current space vector can be written as:

$$\underline{i}_r = \frac{\psi_r - L_m \underline{i}_s}{L_r} \quad (3.36)$$

Substitution of (3.36) into the rotor voltage equation (3.30), taking into account (3.33), results in:

$$0 = \frac{R_r}{L_r} (\psi_r - L_m \underline{i}_s) + \frac{d\psi_r}{dt} + j(\omega_r - \omega)\psi_r \quad (3.37)$$

Defining rotor time constant as $T_r = L_r/R_r$ and separating equation (3.37) into real and imaginary parts results in:

$$\psi_r + T_r \frac{d\psi_r}{dt} = L_m i_{ds} \quad (3.38)$$

$$(\omega_r - \omega)\psi_r T_r = L_m i_{qs} \quad (3.39)$$

$$\omega_{sl} = \frac{L_m i_{qs}}{T_r \psi_r}$$

Here ω_{sl} is the electrical slip angular frequency. Taking into account equation (3.35) the torque developed by the machine can be written as:

$$T_e = P \frac{L_m}{L_r} \psi_r i_{qs} \quad (3.40)$$

The torque equation (3.40) is now of the same form as the torque equation of a DC machine or a three-phase induction machine. One can see that if the magnitude of the rotor flux is held constant the torque developed by the machine can be controlled via the q-axis current component. The machine will have instantaneous torque response similar to a DC machine provided that the rotor flux is not affected by changes in the stator q-axis current component. Equation (3.38) shows that the magnitude of the rotor flux is proportional to the d-axis current and so rotor flux can be held constant by controlling the d-axis current component. If the magnitude of the rotor flux is held constant then it follows from equation (3.39) that the slip frequency and hence the instantaneous torque can be controlled via the q-axis current component. It can be seen that there is no pull-out torque and theoretically any value of torque can be achieved by applying the appropriate stator q-axis current under constant rotor flux operation of the machine. Since there is no excitation for rotor x-y components and rotor zero sequence

components, only the first two (d-q) equations in the second column of (3.30) and (3.31) are required. Equations describing a rotor flux oriented n -phase induction machine (3.38)-(3.40) are the same as those for a three-phase induction machine. Since flux and torque producing currents in any n -phase AC machine are only the d-q components, it follows that the indirect rotor flux oriented control scheme for any induction machine, regardless of the number of phases, is similar to that of a traditional three-phase induction machine, the only difference being the coordinate transformation calculation. Consider an indirect vector control scheme for a three-phase machine [Krishnan (2001)], aimed at operation in the constant flux region only (i.e. base speed region). The corresponding configuration of the indirect vector controller for operation in the base speed region is illustrated in Fig. 3.1 for an n -phase induction machine.

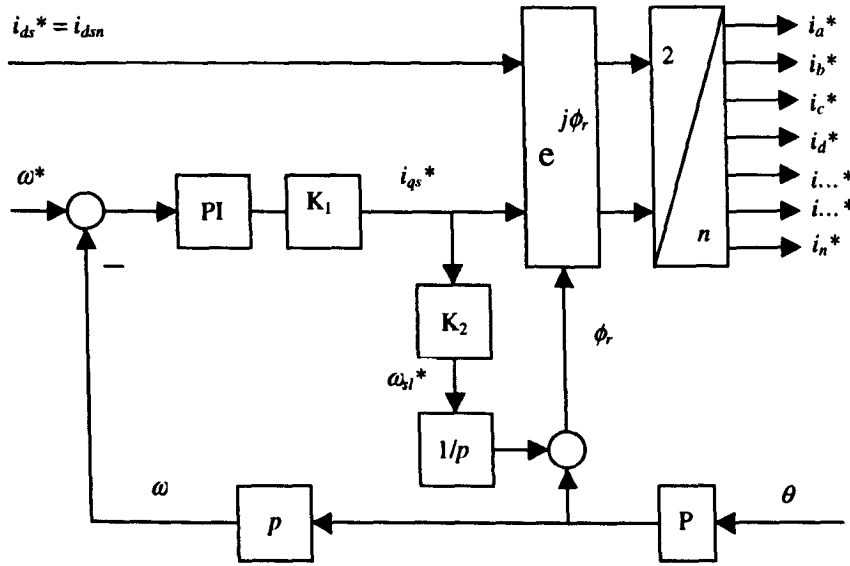


Fig. 3.1: Indirect vector controller for an n -phase induction machine.

The constant terms K_1 and K_2 are determined, on the basis of (3.39)-(3.40), with:

$$\begin{aligned} i_{qs}^* = K_1 T_e^* &\Rightarrow K_1 = i_{qs}^* / T_e^* = \frac{1}{P} \frac{L_r}{L_m} \frac{1}{\psi_r^*} = \frac{1}{P} \frac{L_r}{L_m^2} \frac{1}{i_{ds}^*} \\ \omega_{sl}^* = K_2 i_{qs}^* &\Rightarrow K_2 = \omega_{sl}^* / i_{qs}^* = \frac{L_m}{T_r \psi_r^*} = \frac{1}{T_r i_{ds}^*} \end{aligned} \quad (3.41)$$

3.7 Summary

This chapter has presented principles of mathematical modelling of an n -phase induction machine. It has been shown that application of decoupling and rotational transformations results in a greatly simplified mathematical model of an n -phase

machine. The transformation results in two current components (d-q) for stator and rotor which contribute to the torque developed by the machine (stator/rotor coupling) and $[(n-3)/2]$ pairs (odd phase number machine) or $[(n-4)/2]$ pairs (even phase number machine) of x-y components which do not. Since only one pair of stator d-q current components is needed for the flux and torque control in one machine, there is a possibility of using the existing degrees of freedom (i.e. $[(n - 3)/2]$ x-y pairs of stator current components in the odd phase number case) for control of other machines that would be connected in series with the first machine. However, if the control of the machines with series connected stator windings is to be decoupled one from the other, it is necessary that the flux/torque producing currents of one machine do not produce flux and torque in all the other machines in the group. Hence, if stator windings of $m = (n-1)/2$ (odd phase number case) or $m = (n-2)/2$ (even phase number case) multi-phase machines can be connected in such a way that what one machine sees as the d-q axis stator current components the other machines see as x-y current components, and vice versa, it would then be possible to completely independently control these machines while supplying them from a single current-controlled voltage source inverter. This explanation constitutes the basis of the multi-motor multi-phase drive system that is to be developed further on. In the general case a set of n -phase stator windings is to be supplied from a single n -phase current-controlled voltage source by connecting the stator windings in series and using the phase transposition, as illustrated in Fig. 1.2. As already noted phase transposition means shift in connection of the phases 1,2, ... n of one machine to the phases 1,2, ... n of the second machine, etc., where 1,2,3... n is the flux/torque producing phase sequence of the given machine according to the spatial distribution of the phases within the stator winding. The issue of required phase transposition is discussed in detail in the next chapter.

CHAPTER 4

SERIES CONNECTIONS OF n -PHASE MACHINES

4.1 Introduction

This chapter considers the machine-to-machine connection for all the possible odd and even phase number cases. In order to achieve fully decoupled control of each machine in the multi-phase multi-machine drive it is necessary to perform a phase transposition in series connection of machines. The chapter shows how to perform the required phase transposition and how to construct a connection table termed the connectivity matrix, which leads to the connection diagram. All phase numbers (both odd and even) are considered ignoring the physical limitations of constructing large phase number machines. The maximum number of connectable machines differs depending upon the properties of the phase number. The chapter analyses all the possible situations that can occur and summarises the results for the odd and even phase number case in table 4.15 and 4.16, respectively. It is shown that the maximum number of connectable machines for the odd phase number case $[(n-1)/2]$ is obtained when n is a prime number or a power of a prime number. For the even phase number case the maximum number of connectable machines $[(n-2)/2]$ is obtained when n is such that $n/2$ is a prime number or n is a power of 2. These situations provide the greatest advantage because the saving in the number of inverter legs is the greatest. Considerations of this chapter, related to even phase numbers, are detailed in Levi et al (2003a), while odd phase numbers are covered in Levi et al (2004a) and Levi et al (2004c).

4.2 Machine connectivity for a general n -phase case

If a set of n -phase machines is to be connected in series and the machines are to be controlled independently, it is necessary to make flux/torque producing currents of one machine non flux/torque producing currents in all the other machines. In other words d - q currents of one machine must appear as one of the x - y pairs of currents for all the

other machines. Simple series connection of stator windings will of course not yield the desired result. However, if a phase transposition is introduced between phases in series connection, the desired effect will automatically result. An answer to the question how the phase transposition needs to be done lies in the decoupling transformation matrix (3.13a/b) repeated here for convenience.

$$\underline{C} = \sqrt{\frac{2}{n}} \begin{bmatrix} 1 & \cos \alpha & \cos 2\alpha & \cos 3\alpha & \dots & \cos(n-1)\alpha \\ 0 & \sin \alpha & \sin 2\alpha & \sin 3\alpha & \dots & \sin(n-1)\alpha \\ 1 & \cos 2\alpha & \cos 4\alpha & \cos 6\alpha & \dots & \cos 2(n-1)\alpha \\ 0 & \sin 2\alpha & \sin 4\alpha & \sin 6\alpha & \dots & \sin 2(n-1)\alpha \\ 1 & \cos 3\alpha & \cos 6\alpha & \cos 9\alpha & \dots & \cos 3(n-1)\alpha \\ 0 & \sin 3\alpha & \sin 6\alpha & \sin 9\alpha & \dots & \sin 3(n-1)\alpha \\ 1 & \cos 4\alpha & \cos 8\alpha & \cos 12\alpha & \dots & \cos 4(n-1)\alpha \\ 0 & \sin 4\alpha & \sin 8\alpha & \sin 12\alpha & \dots & \sin 4(n-1)\alpha \\ \dots & \dots & \dots & \dots & \dots & \dots \\ 1 & \cos\left(\frac{n-1}{2}\alpha\right) & \cos 2\left(\frac{n-1}{2}\alpha\right) & \cos 3\left(\frac{n-1}{2}\alpha\right) & \dots & \cos(n-1)\left(\frac{n-1}{2}\alpha\right) \\ 0 & \sin\left(\frac{n-1}{2}\alpha\right) & \sin 2\left(\frac{n-1}{2}\alpha\right) & \sin 3\left(\frac{n-1}{2}\alpha\right) & \dots & \sin(n-1)\left(\frac{n-1}{2}\alpha\right) \\ 1/\sqrt{2} & 1/\sqrt{2} & 1/\sqrt{2} & 1/\sqrt{2} & \dots & 1/\sqrt{2} \end{bmatrix} \quad (3.13a)$$

$$\underline{C} = \sqrt{\frac{2}{n}} \begin{bmatrix} 1 & \cos \alpha & \cos 2\alpha & \cos 3\alpha & \dots & \cos(n-1)\alpha \\ 0 & \sin \alpha & \sin 2\alpha & \sin 3\alpha & \dots & \sin(n-1)\alpha \\ 1 & \cos 2\alpha & \cos 4\alpha & \cos 6\alpha & \dots & \cos 2(n-1)\alpha \\ 0 & \sin 2\alpha & \sin 4\alpha & \sin 6\alpha & \dots & \sin 2(n-1)\alpha \\ 1 & \cos 3\alpha & \cos 6\alpha & \cos 9\alpha & \dots & \cos 3(n-1)\alpha \\ 0 & \sin 3\alpha & \sin 6\alpha & \sin 9\alpha & \dots & \sin 3(n-1)\alpha \\ \dots & \dots & \dots & \dots & \dots & \dots \\ 1 & \cos\left(\frac{n-2}{2}\alpha\right) & \cos 2\left(\frac{n-2}{2}\alpha\right) & \cos 3\left(\frac{n-2}{2}\alpha\right) & \dots & \cos(n-1)\left(\frac{n-2}{2}\alpha\right) \\ 0 & \sin\left(\frac{n-2}{2}\alpha\right) & \sin 2\left(\frac{n-2}{2}\alpha\right) & \sin 3\left(\frac{n-2}{2}\alpha\right) & \dots & \sin(n-1)\left(\frac{n-2}{2}\alpha\right) \\ 1/\sqrt{2} & 1/\sqrt{2} & 1/\sqrt{2} & 1/\sqrt{2} & \dots & 1/\sqrt{2} \\ 1/\sqrt{2} & -1/\sqrt{2} & 1/\sqrt{2} & -1/\sqrt{2} & \dots & -1/\sqrt{2} \end{bmatrix} \quad (3.13b)$$

According to the transformation matrix (3.13), phase '1' of all the machines will be connected directly in series (the first column in (3.13)). The phase transposition for phase '1' is therefore 0 degrees and the phase step is zero. However, phase '2' of the first machine will be connected to phase '3' of the second machine, which will be further connected to phase '4' of the third machine and so on. The phase transposition moving from one machine to the other is the spatial angle α and the phase step is 1. This follows from the second column of the transformation matrix that contains cosine and sine terms with spatial displacements equal to $\alpha, 2\alpha, 3\alpha, 4\alpha, 5\alpha, \dots [(n-1)/2]\alpha$ for the odd phase number case and $[(n-2)/2]\alpha$ for the even phase number case. In a similar

manner phase '3' of the first machine (the third element in the first row of (3.13) with spatial displacement of 2α) is connected to phase '5' of the second machine, which further gets connected to phase '7' and so on. The phase transposition is 2α , and the phase step is 2. This follows from the third column of the transformation matrix, where spatial displacement equals $2\alpha, 4\alpha, 6\alpha, \dots, 2[(n-1)/2]\alpha$ (odd phase number) or $2[(n-2)/2]\alpha$ (even phase number). Further, phase '4' of the first machine needs to be connected to phase '7' of the second machine which gets connected to phase '10' of the third machine and so on. Here the phase step is equal to 3 and the phases are transposed by 3α . This corresponds to the fourth column in the transformation matrix, where terms with $3\alpha, 6\alpha, 9\alpha, 12\alpha, \dots, 3[(n-1)/2]\alpha$ (odd phase number) or $3[(n-2)/2]\alpha$ (even phase number) appear. For phase '5' of the first machine the phase transposition will equal 4α and phase step will be 4, for phase '6' the phase step will be 5 and phase transposition will equal 5α , and so on.

The above given explanation enables construction of a connection table, which is called further on connectivity matrix. In general, an n -phase system results in a connectivity matrix of the form given in Table 4.1 [Levi et al (2004a)]. Flux/torque producing phase sequence for any particular machine is denoted in Table 4.1 with symbols a,b,c,d,... rather than with numbers 1,2,3,... (both notations are used further on, depending on which one is more convenient for the given purpose). Double-line in Table 4.1 encircles the seven-phase case, while the bold box applies to the five-phase case. Dashed line encircles eleven-phase case, while solid line is the box for the thirteen-phase case. If a number in the table, obtained by substituting $a=1, b=2, c=3, d=4, \dots$, is greater than the number of phases n , resetting is performed by deducting $j \times n$ ($j = 1, 2, 3, \dots$) from the number so that the resulting number belongs to the set $[1, n]$. Source phases are in Table 4.1 identified with capital letters while the first column lists the motors.

Table 4.1: Connectivity matrix for the general n -phase case.

	A	B	C	D	E	F	G	H	I	J	K	L	M	N	O
M1	a	b	c	d	e	f	g	h	i	j	k	l	m	n	...
M2	a	b+1	c+2	d+3	e+4	f+5	g+6	h+7	i+8	j+9	k+10	l+11	m+12	n+13	...
M3	a	b+2	c+4	d+6	e+8	f+10	g+12	h+14	i+16	j+18	k+20	l+22	m+24	n+26	...
M4	a	b+3	c+6	d+9	e+12	f+15	g+18	h+21	i+24	j+27	k+30	l+33	m+36	n+39	...
M5	a	b+4	c+8	d+12	e+16	f+20	g+24	h+28	i+32	j+36	k+40	l+44	m+48	n+52	...
M6	a	b+5	c+10	d+15	e+20	f+25	g+30	h+35	i+40	j+45	k+50	l+55	m+60	n+65	...
M7	a	b+6	c+12	d+18	e+24	f+30	g+36	h+42	i+48	j+54	k+60	l+66	m+72	n+78	...
....

Connection rules, described here and summarized in Table 4.1, can be expressed in a form of symbolic equations. Let the machines be denoted as M_1, M_2, \dots, M_k , where k stands for the maximum number of connectable machines. Similarly, let the machine phase be denoted for each machine, according to the sequence of spatial ordering, with indices $1, 2, 3, \dots, n$ and let the source phases be $SP_1, SP_2, SP_3, \dots, SP_n$ (instead of A, B, C, D...). The connection of the appropriate machine phases to individual source phases then proceeds in accordance with the following symbolic equations [Levi et al (2004c)]:

$$\begin{aligned}
 SP_1 &= M_{1_1} \rightarrow M_{2_1} \rightarrow M_{3_1} \rightarrow M_{4_1} \rightarrow K \rightarrow M_{k_1} \\
 SP_2 &= M_{1_2} \rightarrow M_{2_{2+1}} \rightarrow M_{3_{2+2}} \rightarrow M_{4_{2+3}} \rightarrow K \rightarrow M_{k_{2+(k-1)}} \\
 SP_3 &= M_{1_3} \rightarrow M_{2_{3+2}} \rightarrow M_{3_{3+4}} \rightarrow M_{4_{3+6}} \rightarrow K \rightarrow M_{k_{3+2(k-1)}} \\
 SP_4 &= M_{1_4} \rightarrow M_{2_{4+3}} \rightarrow M_{3_{4+6}} \rightarrow M_{4_{4+9}} \rightarrow K \rightarrow M_{k_{4+3(k-1)}} \\
 &----- \\
 SP_n &= M_{1_n} \rightarrow M_{2_{n+(n-1)}} \rightarrow M_{3_{n+2(n-1)}} \rightarrow M_{4_{n+3(n-1)}} \rightarrow K \rightarrow M_{k_{n+(n-1)(k-1)}}
 \end{aligned} \tag{4.1}$$

Note that the meaning of the equality sign in (4.1) is “source phase consists of,” while the meaning of the symbol \rightarrow is “connect to.” On the basis of (4.1) it is possible to write a symbolic equation for the connection rule for any of the source phases $j = 1, 2, 3, \dots, n$ in the following form:

$$SP_j = M_{1_j} \rightarrow M_{2_{j+(j-1)}} \rightarrow M_{3_{j+2(j-1)}} \rightarrow M_{4_{j+3(j-1)}} \rightarrow K \rightarrow M_{k_{j+(j-1)(k-1)}} \tag{4.2}$$

Symbolic equation (4.2) can be finally given in a compact form:

$$SP_j = \sum_{i=1}^k M_{i_{j+(i-1)(j-1)}} \quad j = 1, 2, 3, \dots, n \tag{4.3}$$

where Σ has again only symbolic meaning.

4.3 Connectivity matrices and connection diagrams for machines with an odd number of phases

Connectivity matrix and the corresponding connection diagram are given in this sub-section for certain selected specific phase numbers. Selection is done in such a way as to aid the discussion of the classification of all the possible situations in section 4.5. Consider at first the five-phase case. Table 4.2 and Fig. 4.1 give the connectivity matrix and the connection diagram for the two five-phase machines, which are obtained from the general case shown in Table 4.1.

Table 4.2: Connectivity matrix for the five-phase case.

	A	B	C	D	E
M1	1	2	3	4	5
M2	1	3	5	2	4

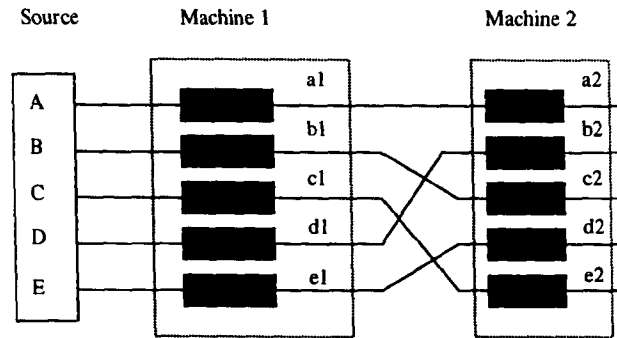


Fig. 4.1: Connection diagram for the five-phase case.

Situation that arises in the seven-phase case is shown in Table 4.3 and Fig. 4.2, where it can be seen that three seven-phase machines can now be connected in series, as follows from the discussion in sub-section 4.1. The two phase numbers considered so far are both prime numbers and the situation is simple. However, when the number of phases is not a prime number the situation becomes more involved.

Table 4.3: Connectivity matrix for the seven-phase case.

	A	B	C	D	E	F	G
M1	1	2	3	4	5	6	7
M2	1	3	5	7	2	4	6
M3	1	4	7	3	6	2	5

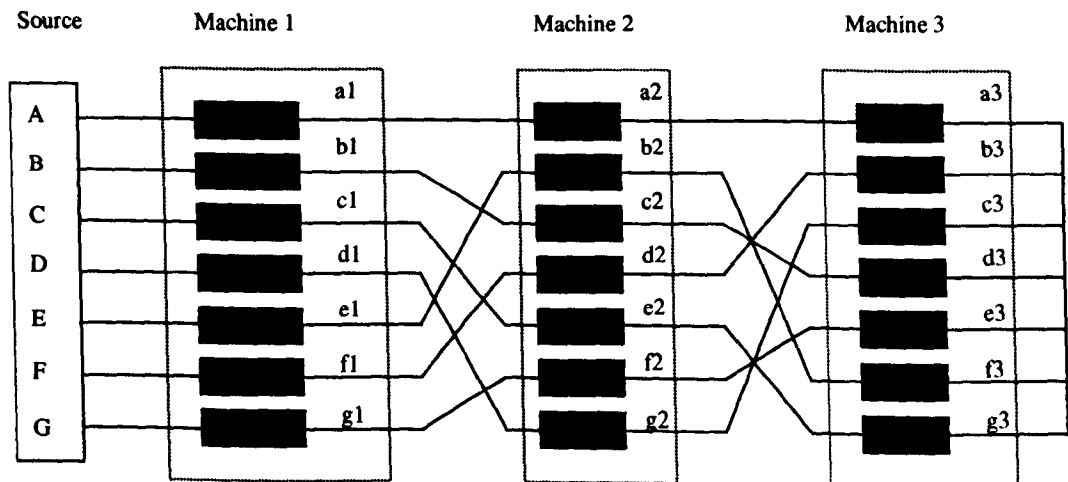


Fig. 4.2: Connection diagram for three seven-phase machines.

Consider the nine-phase case. Connectivity matrix, obtained from Table 4.1, is shown in Table 4.4. As can be seen in Table 4.4, only phases 1,4 and 7 of machine M3 (encircled with a dotted box) are utilized in the series connection. Since the spatial displacement between these phases is 120 degrees, this means that machine M3 is actually a three-phase rather than a nine-phase machine. Connection diagram is shown in Fig. 4.3. It has to be noted that a re-ordering of the machines has to be done if series connection comprises machines of different phase numbers, as shown in Fig. 4.3. All the machines with the highest phase number have to be connected at first in series to the source, respecting the required phase transposition. Next come all the machines with the second highest phase number, and so on. The sequence finishes with the smallest phase number. This is so since, taking the nine-phase case as the example, the three flux/torque producing currents of a nine-phase machine which enter any given phase of the three-phase machine sum to zero in any instant in time. This simultaneously means that the three-phase machine in Fig. 4.3 will not suffer any adverse effects due to the series connection with three nine-phase machines.

Table 4.4: Connectivity matrix for the nine-phase case.

	A	B	C	D	E	F	G	H	I
M1	1	2	3	4	5	6	7	8	9
M2	1	3	5	7	9	2	4	6	8
M3	1	4	7	1	4	7	1	4	7
M4	1	5	9	4	8	3	7	2	6

The connectivity matrix for the eleven-phase and thirteen-phase case is given in Tables 4.5 and 4.6, respectively. In these cases all the machines in the system are of equal phase number (the eleven-phase case utilises five eleven-phase machines and the thirteen-phase system utilises six thirteen-phase machines).

An especially interesting phase number is fifteen. The procedure described in section 4.2 results in the fifteen-phase connectivity matrix (Table 4.7) containing two five-phase machines M3 and M6 (identified with dotted line in the table) and a three-phase machine (identified with double solid line in the table). As five is not exactly divisible by three, it is not possible to connect these machines in series. An attempt to connect a five-phase machine M6 with a three-phase machine M5 leads to a complete short-circuiting of all terminals of the two machines since all five phases have to be connected to all three phases. The connectivity matrix given in table 4.7 can be re-ordered so that connection of a five-phase machine to a three-phase machine does not

appear in the sequence (Table 4.8). The machines in the group now have the following sequential phase numbers: 15,15,5,15,5,15,3. Thus machines M3 and M5 are five-phase, while machine M7 is 3-phase.

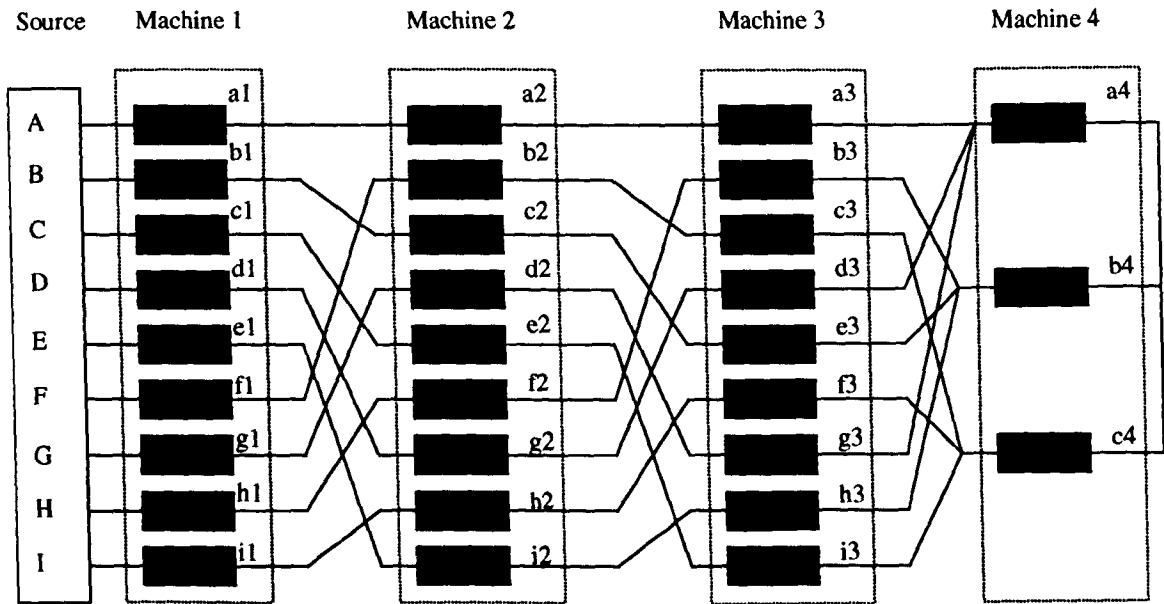


Fig. 4.3: Connection diagram for the nine-phase case: three nine-phase machines and one three-phase machine are connected in series.

Table 4.5: Connectivity matrix for the eleven-phase case.

	A	B	C	D	E	F	G	H	I	J	K
M1	1	2	3	4	5	6	7	8	9	10	11
M2	1	3	5	7	9	11	2	4	6	8	10
M3	1	4	7	10	2	5	8	11	3	6	9
M4	1	5	9	2	6	10	3	7	11	4	8
M5	1	6	11	5	10	4	9	3	8	2	7

Table 4.6: Connectivity matrix for the thirteen-phase case.

	A	B	C	D	E	F	G	H	I	J	K	L	M
M1	1	2	3	4	5	6	7	8	9	10	11	12	13
M2	1	3	5	7	9	11	13	2	4	6	8	10	12
M3	1	4	7	10	13	3	6	9	12	2	5	8	11
M4	1	5	9	13	4	8	12	3	7	11	2	6	10
M5	1	6	11	3	8	13	5	10	2	7	12	4	9
M6	1	7	13	6	12	5	11	4	10	3	9	2	8

Table 4.7: Connectivity matrix for the fifteen-phase case

	A	B	C	D	E	F	G	H	I	J	K	L	M	N	O
M1	1	2	3	4	5	6	7	8	9	10	11	12	13	14	15
M2	1	3	5	7	9	11	13	15	2	4	6	8	10	12	14
M3	1	4	7	10	13	1	4	7	10	13	1	4	7	10	13
M4	1	5	9	13	2	6	10	14	3	7	11	15	4	8	12
M5	1	6	11	1	6	11	1	6	11	1	6	11	1	6	11
M6	1	7	13	4	10	1	7	13	4	10	1	7	13	4	10
M7	1	8	15	7	14	6	13	5	12	4	11	3	10	2	9

Table 4.8: Connectivity matrix for the fifteen-phase case (re-ordered)

	A	B	C	D	E	F	G	H	I	J	K	L	M	N	O
M1	1	2	3	4	5	6	7	8	9	10	11	12	13	14	15
M2	1	3	5	7	9	11	13	15	2	4	6	8	10	12	14
M3	1	4	7	10	13	1	4	7	10	13	1	4	7	10	13
M4	1	5	9	13	2	6	10	14	3	7	11	15	4	8	12
M5	1	7	13	4	10	1	7	13	4	10	1	7	13	4	10
M6	1	8	15	7	14	6	13	5	12	4	11	3	10	2	9
M7	1	6	11	1	6	11	1	6	11	1	6	11	1	6	11

However it is not possible to connect in series a machine with a smaller number of phases before a machine with a larger number of phases. This can be shown if one considers the individual phase currents of all the seven machines and the source currents in the following way (source phases are identified with capital A, B, C... letters; machine phases are identified with lower case a, b, c, \dots letters; machines are identified with indices 1, 2, 3, ...; machines 1, 2, 4 and 6 are 15-phase; machines 3 and 5 are five-phase; machine 7 is three-phase; reference currents equal actual currents due to assumed ideal current feeding):

$$\begin{aligned}
i_A &= i_{a1}^* + i_{a2}^* + (1/3)i_{a3}^* + i_{a4}^* + (1/3)i_{a5}^* + i_{a6}^* + (1/5)i_{a7}^* \\
i_B &= i_{b1}^* + i_{c2}^* + (1/3)i_{b3}^* + i_{e4}^* + (1/3)i_{c5}^* + i_{h6}^* + (1/5)i_{b7}^* \\
i_C &= i_{c1}^* + i_{e2}^* + (1/3)i_{c3}^* + i_{i4}^* + (1/3)i_{e5}^* + i_{o6}^* + (1/5)i_{c7}^* \\
i_D &= i_{d1}^* + i_{g2}^* + (1/3)i_{d3}^* + i_{m4}^* + (1/3)i_{b5}^* + i_{g6}^* + (1/5)i_{d7}^* \\
i_E &= i_{e1}^* + i_{i2}^* + (1/3)i_{e3}^* + i_{b4}^* + (1/3)i_{d5}^* + i_{n6}^* + (1/5)i_{e7}^* \\
i_F &= i_{f1}^* + i_{k2}^* + (1/3)i_{a3}^* + i_{f4}^* + (1/3)i_{d5}^* + i_{f6}^* + (1/5)i_{c7}^* \\
i_G &= i_{g1}^* + i_{m2}^* + (1/3)i_{b3}^* + i_{j4}^* + (1/3)i_{c5}^* + i_{m6}^* + (1/5)i_{a7}^* \\
i_H &= i_{h1}^* + i_{o2}^* + (1/3)i_{c3}^* + i_{n4}^* + (1/3)i_{e5}^* + i_{e6}^* + (1/5)i_{b7}^* \\
i_I &= i_{i1}^* + i_{b2}^* + (1/3)i_{d3}^* + i_{c4}^* + (1/3)i_{b5}^* + i_{i6}^* + (1/5)i_{c7}^* \\
i_J &= i_{j1}^* + i_{d2}^* + (1/3)i_{e3}^* + i_{g4}^* + (1/3)i_{d5}^* + i_{d6}^* + (1/5)i_{a7}^* \\
i_K &= i_{k1}^* + i_{f2}^* + (1/3)i_{a3}^* + i_{k4}^* + (1/3)i_{a5}^* + i_{k6}^* + (1/5)i_{b7}^* \\
i_L &= i_{l1}^* + i_{h2}^* + (1/3)i_{b3}^* + i_{o4}^* + (1/3)i_{c5}^* + i_{c6}^* + (1/5)i_{c7}^* \\
i_M &= i_{m1}^* + i_{j2}^* + (1/3)i_{c3}^* + i_{d4}^* + (1/3)i_{e5}^* + i_{j6}^* + (1/5)i_{a7}^* \\
i_N &= i_{n1}^* + i_{i2}^* + (1/3)i_{d3}^* + i_{h4}^* + (1/3)i_{b5}^* + i_{b6}^* + (1/5)i_{b7}^* \\
i_O &= i_{o1}^* + i_{n2}^* + (1/3)i_{e3}^* + i_{i4}^* + (1/3)i_{d5}^* + i_{i6}^* + (1/5)i_{c7}^*
\end{aligned} \tag{4.4}$$

Individual phase currents for the seven machines are then as follows:

Machine 1 (15-phase):

$$\begin{aligned}
i_{a1} &= i_A; & i_{b1} &= i_B; & i_{c1} &= i_C; & i_{d1} &= i_D; & i_{e1} &= i_E; \\
i_{f1} &= i_F; & i_{g1} &= i_G; & i_{h1} &= i_H; & i_{i1} &= i_I; & i_{e1} &= i_J; \\
i_{k1} &= i_K; & i_{l1} &= i_L; & i_{m1} &= i_M; & i_{n1} &= i_N; & i_{o1} &= i_O;
\end{aligned} \tag{4.5}$$

Machine 2 (15-phase):

$$\begin{aligned}
 i_{a2} &= i_A; & i_{b2} &= i_I; & i_{c2} &= i_B; & i_{d2} &= i_J; & i_{e2} &= i_C; \\
 i_{f2} &= i_K; & i_{g2} &= i_D; & i_{h2} &= i_L; & i_{i2} &= i_E; & i_{j2} &= i_M; \\
 i_{k2} &= i_F; & i_{l2} &= i_N; & i_{m2} &= i_G; & i_{n2} &= i_O; & i_{o2} &= i_H;
 \end{aligned} \tag{4.6}$$

Machine 3 (5-phase):

$$\begin{aligned}
 i_{a3} &= i_A + i_F + i_K = i_{a3}^* + i_{a5}^* \\
 i_{b3} &= i_B + i_G + i_L = i_{b3}^* + i_{c5}^* \\
 i_{c3} &= i_C + i_H + i_M = i_{c3}^* + i_{e5}^* \\
 i_{d3} &= i_D + i_I + i_N = i_{d3}^* + i_{b5}^* \\
 i_{e3} &= i_E + i_J + i_O = i_{e3}^* + i_{d5}^*
 \end{aligned} \tag{4.7}$$

Machine 4 (15-phase):

$$\begin{aligned}
 i_{a4} &= i_{f4} = i_{k4} = (1/3)(i_A + i_F + i_K) \\
 i_{e4} &= i_{j4} = i_{o4} = (1/3)(i_B + i_G + i_L) \\
 i_{d4} &= i_{i4} = i_{n4} = (1/3)(i_C + i_H + i_M) \\
 i_{c4} &= i_{h4} = i_{m4} = (1/3)(i_D + i_I + i_N) \\
 i_{b4} &= i_{g4} = i_{l4} = (1/3)(i_E + i_J + i_O)
 \end{aligned} \tag{4.8}$$

Machine 5 (5-phase):

$$\begin{aligned}
 i_{a5} &= i_{a4} + i_{f4} + i_{k4} = i_A + i_F + i_K = i_{a3}^* + i_{a5}^* \\
 i_{b5} &= i_{m4} + i_{c4} + i_{h4} = i_D + i_I + i_N = i_{d3}^* + i_{b5}^* \\
 i_{c5} &= i_{e4} + i_{j4} + i_{o4} = i_B + i_G + i_L = i_{b3}^* + i_{c5}^* \\
 i_{d5} &= i_{b4} + i_{g4} + i_{l4} = i_E + i_J + i_O = i_{e3}^* + i_{d5}^* \\
 i_{e5} &= i_{i4} + i_{n4} + i_{d4} = i_C + i_H + i_M = i_{c3}^* + i_{e5}^*
 \end{aligned} \tag{4.9}$$

Machine 6 (15-phase):

$$\begin{aligned}
 i_{a6} &= i_{f6} = i_{k6} = (1/3)(i_A + i_F + i_K) \\
 i_{e6} &= i_{j6} = i_{o6} = (1/3)(i_C + i_H + i_M) \\
 i_{d6} &= i_{i6} = i_{n6} = (1/3)(i_E + i_J + i_O) \\
 i_{c6} &= i_{h6} = i_{m6} = (1/3)(i_B + i_G + i_L) \\
 i_{b6} &= i_{g6} = i_{l6} = (1/3)(i_D + i_I + i_N)
 \end{aligned} \tag{4.10}$$

Machine 7 (3-phase):

$$\begin{aligned}
 i_{a7} &= i_{a6} + i_{g6} + i_{m6} + i_{d6} + i_{j6} = (1/3)(i_A + i_B + i_C + i_D + i_E + i_F + i_G + i_H + i_I + i_J + i_K + i_L + i_M + i_N + i_O) \\
 i_{b7} &= i_{h6} + i_{n6} + i_{e6} + i_{k6} + i_{b6} = (1/3)(i_A + i_B + i_C + i_D + i_E + i_F + i_G + i_H + i_I + i_J + i_K + i_L + i_M + i_N + i_O) \\
 i_{c7} &= i_{o6} + i_{f6} + i_{l6} + i_{c6} + i_{i6} = (1/3)(i_A + i_B + i_C + i_D + i_E + i_F + i_G + i_H + i_I + i_J + i_K + i_L + i_M + i_N + i_O)
 \end{aligned} \tag{4.11}$$

Information about currents for the machine M4, as well as the information about currents for the remaining fifteen-phase machine M6 are completely lost in the transition from M3 to M4 because certain currents cancel out in machine three leaving only those currents shown in equation (4.7). The currents shown in (4.11) obviously sum to zero, confirming that it is not possible to connect both five-phase and three-phase machines in the same multi-motor system. It is therefore not possible to go from the lower number of phases towards higher number of phases in the connection diagram, looking from the source side. The only way that one can connect this multi-motor system is to order at first all four fifteen-phase machines, followed by the two five-phase machines. However, since $5/3$ is not an integer, the three-phase machine cannot be connected at the end of the group (short circuited terminals). Thus, instead of being able to connect seven machines in series, in the fifteen-phase case one can connect at most six machines in series (four fifteen-phase plus two five-phase). Alternatively, one can connect four fifteen-phase machines in series with one three-phase machine and this gives total number of connectable machines as five, instead of seven. With only five machines and 15 inverter legs any potential advantage (smaller number of inverter legs) is lost over the equivalent drive with five three-phase machines supplied from five three-legged inverters.

On the basis of these considerations it follows that: i) all machines with a higher number of phases have to precede all the machines with a smaller number of phases; and, ii) it is not possible to connect in series with phase transposition machines whose phase numbers equal two different prime numbers.

4.4 Connectivity matrices and connection diagrams for machines with an even number of phases

The minimum even number of phases that will enable series connection is $n = 6$. The corresponding connectivity matrix, obtained on the basis of the given procedure, is given in Table 4.9. It can be seen from the last row of this matrix that only phases 1,3 and 5 of the second machine are utilised. As spatial displacement between these phases is 120° , it follows that the second machine is a three-phase machine rather than a six-phase machine. The corresponding connection diagram is given in Fig. 4.4. Note that the flux/torque producing currents of the six-phase machine mutually cancel at the

connection points with the three-phase machine. This means that the three-phase machine will not suffer from any adverse effects due to the series connection with the six-phase machine. This of course does not hold true for the six-phase machine.

In the case of an eight-phase system it is possible to connect three machines in series. The connectivity matrix is the one given in Table 4.10. The first and the third machine are eight-phase, however the second machine is four-phase since only phases 1,3,5,7 are utilised (and spatial displacement is therefore 90 degrees). It is important to note that like in the odd phase number case, when connecting the machines in series to the source, all the machines with the highest phase number must come first. This means that the actual sequence of connection of the three machines to the source has to be M1, M3, M2, as shown in the connection diagram in Fig. 4.5. This is so since flux/torque producing currents of the machine with a higher phase number cancel when entering the machine with the lower phase number (for example, in the six-phase case of Fig. 4.4. phase currents *a*1 and *d*1 of the six-phase machine are in phase opposition, so that their sum at the point of entry into the phase *a*2 of the second machine is zero).

Ten-phase case is illustrated in Table 4.11 and Fig. 4.6. It is now possible to connect four machines in series. Two of them are ten-phase (M1 and M3), while the remaining two (M2 and M4) are five-phase. Such a situation will always exist when the even phase number *n* is such that *n*/2 is a prime number, as discussed in the next section. Once more, the two machines with the higher phase number have to be connected at first in series with the source. Five-phase machines are then added at the end of the chain, as shown in Fig. 4.6.

Table 4.9: Connectivity matrix for the six-phase drive system.

	A	B	C	D	E	F
M1	1	2	3	4	5	6
M2	1	3	5	1	3	5

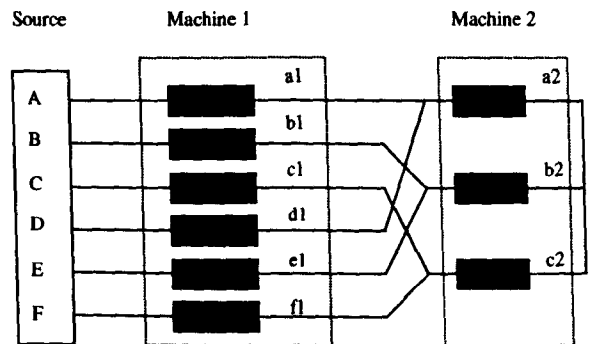


Fig. 4.4. Connection diagram for the six-phase two-motor system

Table 4.10: Connectivity matrix for the eight-phase drive system.

	A	B	C	D	E	F	G	H
M1	1	2	3	4	5	6	7	8
M2	1	3	5	7	1	3	5	7
M3	1	4	7	2	5	8	3	6

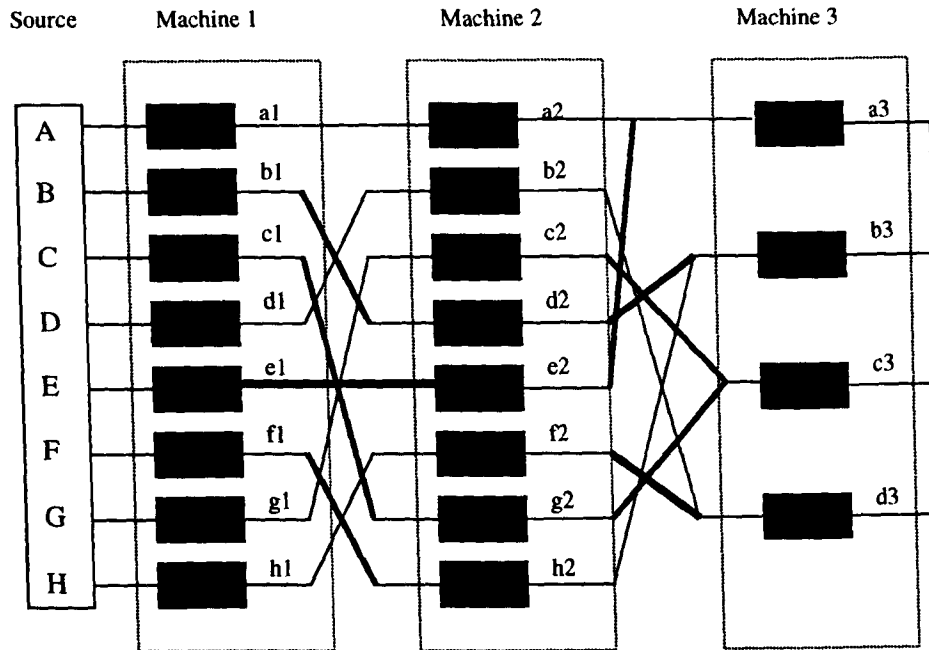


Fig. 4.5. Connection diagram for the eight-phase drive system.

Table 4.11: Connectivity matrix for the ten-phase drive system.

	A	B	C	D	E	F	G	H	I	J
M1	1	2	3	4	5	6	7	8	9	10
M2	1	3	5	7	9	1	3	5	7	9
M3	1	4	7	10	3	6	9	2	5	8
M4	1	5	9	3	7	1	5	9	3	7

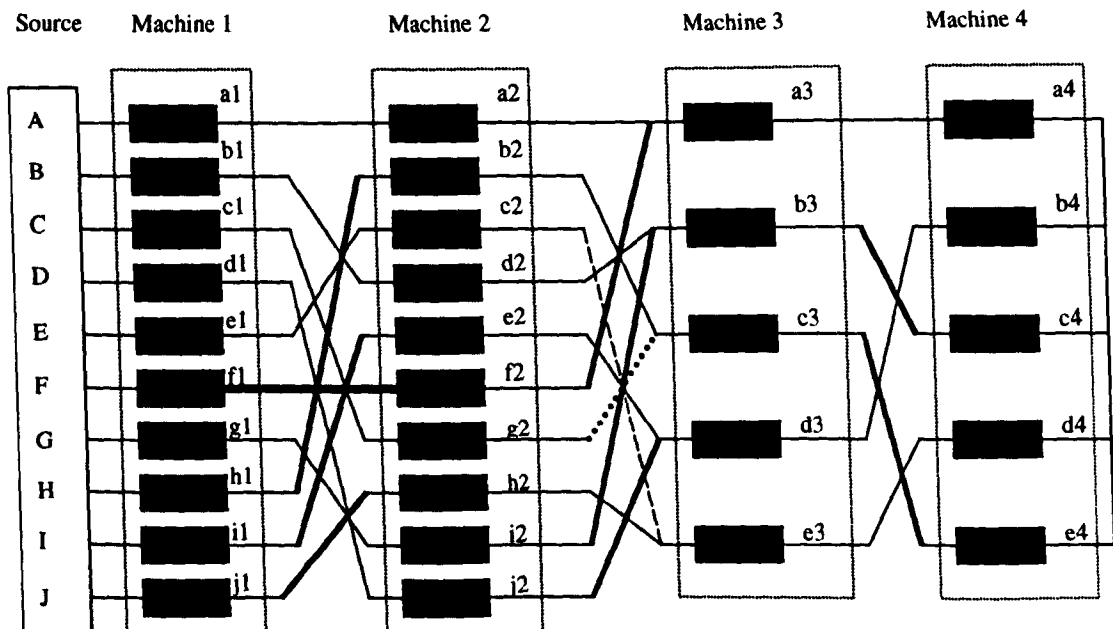


Fig. 4.6. Series connection of two ten-phase and two five-phase machines to the ten-phase source.

In the three cases illustrated so far it was possible to connect the maximum possible number $k = (n-2)/2$ of machines. Indeed, for any even phase number one

expects, on the basis of the considerations given so far, that the number of connectable machines will be $k = (n-2)/2$. This is however not always the case. Consider for example a twelve-phase system. Connectivity matrix is shown in Table 4.12. Machines M1 and M5 are twelve-phase, machine M2 is six-phase, machine M3 is four-phase, and machine M4 is three-phase. Hence, it is not possible to connect all five machines in series since the ratio $4/3$ is not an integer (an attempt to connect a four-phase machine to a three-phase machine leads to short-circuiting of all the terminals). At most four machines can be connected in series, two twelve-phase, followed by the six-phase and three-phase. The ordering is M1,M5,M2,M4.

Table 4.13 summarises the situation, which arises for all the even phase numbers up to eighteen [Levi et al (2003a)]. Bold boxes apply to the phase numbers such that $n/2$ is a prime number. As can be seen from the table, only $k/2$ machines are n -phase, while the remaining $k/2$ machines are $n/2$ -phase. In the eighteen-phase case the number of connectable machines is smaller than eight (at most seven), since the ratio $9/6$ is not an integer. Similar situation arises in the twenty-phase case (Table 4.14), where both four-phase and five-phase machines appear. There are four twenty-phase machines (M1,M3,M7,M9), two ten-phase machines (M2,M6), two five-phase machines (M4,M8) and one four-phase machine (M5). At most eight machines can be connected using the sequence M1,M3,M7,M9,M2,M6,M4,M8 (four twenty-phase, two ten-phase, and two five-phase). But, eight machines can be connected in series with the odd number of phases $n = 17$, which requires three inverter legs less.

Table 4.12: Connectivity matrix for the twelve-phase system.

	A	B	C	D	E	F	G	H	I	J	K	L
M1	1	2	3	4	5	6	7	8	9	10	11	12
M2	1	3	5	7	9	11	1	3	5	7	9	11
M3	<i>1</i>	<i>4</i>	<i>7</i>	<i>10</i>	<i>1</i>	<i>4</i>	<i>7</i>	<i>10</i>	<i>1</i>	<i>4</i>	<i>7</i>	<i>10</i>
M4	<u>1</u>	<u>5</u>	<u>9</u>	<u>1</u>	<u>5</u>	<u>9</u>	<u>1</u>	<u>5</u>	<u>9</u>	<u>1</u>	<u>5</u>	<u>9</u>
M5	1	6	11	4	9	2	7	12	5	10	3	8

Table 4.13: Phase numbers of individual machines for the even supply phase numbers up to eighteen.

Number of the supply phases	6	8	10	12	14	16	18
Number of phases and ordering of connectable machines (before re-ordering)	6 3	8 4 8	10 5 10 5	12 6 4 3 12	14 7 14 7 14	16 8 16 4 16 8 16	18 9 6 9 18 3 18 9

Table 4.14: Connectivity matrix for the twenty-phase drive system.

	A	B	C	D	E	F	G	H	I	J	K	L	M	N	O	P	Q	R	S	T
M1	1	2	3	4	5	6	7	8	9	10	11	12	13	14	15	16	17	18	19	20
M2	1	3	5	7	9	11	13	15	17	19	1	3	5	7	9	11	13	15	17	19
M3	1	4	7	10	13	16	19	2	5	8	11	14	17	20	3	6	9	12	15	18
M4	1	5	9	13	17	1	5	9	13	17	1	5	9	13	17	1	5	9	13	17
M5	1	6	11	16	1	6	11	16	1	6	11	16	1	6	11	16	1	6	11	16
M6	1	7	13	19	5	11	17	3	9	15	1	7	13	19	5	11	17	3	9	15
M7	1	8	15	2	9	16	3	10	17	4	11	18	5	12	19	6	13	20	7	14
M8	1	9	17	5	13	1	9	17	5	13	1	9	17	5	13	1	9	17	5	13
M9	1	10	19	8	17	6	15	4	13	2	11	20	9	18	7	16	5	14	3	12

4.5 Machine connectivity related general considerations

4.5.1 Odd number of phases

A set of multi-phase machines, connected to a supply with an odd number of phases, equal to n , is under consideration. Depending on the properties of the phase number n , three different situations may arise with respect to the number of connectable machines and the individual phase numbers of connectable machines.

a) Let the number of phases n be a prime number. The number of machines that can be connected in series with phase transposition then equals:

$$k = \frac{n-1}{2} \quad (4.12)$$

since there are $(n-1)/2$ pairs of current components that can be used for independent flux and torque control in this multi-phase machine set (the remaining component, zero sequence component, will not exist since the connection of the multi-phase multi-drive system is in star). All the machines are in this case of the same number of phases equal to n . The phase numbers belonging to this category are:

$$n = 3, 5, 7, 11, 13, 17, 19, 23, 29, 31, 37, 41, 43, 47, \dots \quad (4.13)$$

and section 4.3 has elaborated four such phase numbers: five, seven, eleven and thirteen.

b) Consider next the number of phases n that is not a prime number, but it satisfies the condition

$$n = 3^m, \quad m = 2, 3, 4, \dots \quad (4.14)$$

The number of machines that can be connected remains to be given with (4.12), i.e. $k = (n-1)/2$. However, not all k machines are in this case of the phase number equal to

n . As shown in section 4.3 using the nine-phase case as the example ($n = 9, m = 2$), the number of machines that can be connected is equal, according to (4.12) to $k = 4$. However, only $k - 1$ machines have nine phases, while the last machine is three-phase. In the case of $n = 27$ coefficient m equals $m = 3$, meaning that although a total of $k = 13$ machines can be connected in series, only certain number of these will be with twenty-seven phases while there will be machines with nine phases and with three phases as well. Actually, there will be one three-phase machine, three nine-phase machines and nine twenty-seven-phase machines. Hence for the general case of $m > 1$ the phase numbers of the machines that can be connected in series will be:

$$n, \frac{n}{3}, \frac{n}{3^2}, \dots, \frac{n}{3^{m-1}} \quad (4.15)$$

This case can be generalised for the total number of phases n equal to:

$$n = l^m, \quad m = 2, 3, 4, \dots \quad (4.16)$$

where l is a prime number. For example, for $n = 25, l = 5$ and $m = 2$. Hence 12 machines can be connected in series. Ten of these will be with 25 phases while two will be five-phase. Hence the number of phases of connectable machines will be:

$$n, \frac{n}{l}, \frac{n}{l^2}, \dots, \frac{n}{l^{m-1}} \quad (4.17)$$

The phase numbers encompassed by this category are:

$$n = 9, 25, 27, 49, 81, 121, 125, 169, 243, \dots \quad (4.18)$$

It should be noted that the number of machines with smaller number of phases than n , which can be used within any multi-drive system, is limited. For example, for $n = 9, 27, 81 \dots$ there can be no more than one three-phase machine; and no more than three nine-phase machines, etc. Similarly for $n = 25, 125 \dots$ there can be no more than two five-phase machines. For $n = 49$ there can be no more than three seven-phase machines, for $n = 121$ there can be no more than five eleven-phase machines, etc.

e) The third possible case arises when n is not a prime number and is not divisible by l^m . However, n is divisible by two or more prime numbers (for example, for $n = 15$ the two prime numbers are 3 and 5). Let these prime numbers be denoted as n_1, n_2, n_3, \dots . The number of machines that can be connected is now:

$$k < \frac{n-1}{2} \quad (4.19)$$

Ordering of machines in series connection has to follow the following rule: all the n -phase machines are at first connected in series to the source, with phase transposition. Next follow the machines with the largest prime number value out of n_1, n_2, n_3, \dots (say, n_1). This should be followed by connection of all the machines with the second largest prime number, say n_2 , etc. This rule has to be observed, since its violation makes operation of a higher phase number machine, connected after a lower phase number machine, impossible. For example, in fifteen-phase case, considered previously in section 4.3, an attempt to connect at first a five-phase machine and then a fifteen-phase machine means that the information regarding currents required for the operation of the 15-phase machine will be lost through current cancellation in the five-phase machine. One thus ultimately reaches the stage where one n_1 phase machine is to be connected to a machine with n_2 phases. This is not possible since the ratio n_1/n_2 is not an integer. This is so since an attempt to connect machines of phase numbers equal to different prime numbers leads to the short-circuiting of terminals.

Again, as already discussed, among these k machines only a certain number will be with n phases. The other machines that should be connectable in the multi-drive system will have phase numbers equal to n_1, n_2, n_3, \dots . However, in general, the group will be composed of machines with the phase numbers equal to n and one of the prime numbers n_1, n_2, n_3, \dots :

$$n, n_1 \quad \text{or} \quad n, n_2 \quad \text{or} \quad n, n_3 \dots \dots \quad \text{or} \quad n, n_j \quad (4.20)$$

where:

$$n = n_1 \cdot n_2 \cdot n_3 \cdot \dots \cdot n_j \quad (4.21)$$

Note that this category encompasses the situation where some of the numbers $n_1, n_2, n_3, \dots, n_j$ may be the same prime number, but there is at least one other prime number in this sequence. In other words, situation where $n = n_1 \cdot n_2 \cdot \dots \cdot n_j \cdot l^m$, $m = 2, 3, 4, \dots$ is included. The phase numbers belonging to this category are:

$$n = 15, 21, 33, 35, 39, 45, 51, 55, 57, 63, 65, 69, 75, 77, \dots \quad (4.22)$$

It is to be noted that categories b) and c) can be regarded as sub-categories of a more general case for which n is not a prime number. They have in common that two or more

phase numbers appear in the series connection with phase transposition of the multi-phase machines. However, the total number of connectable machines is not the same (it is given with (4.12) and (4.19), respectively). A summary of all possible situations that can arise with $n = \text{odd number}$ is given in Table 4.15.

Table 4.15: Possible situations with phase number $n = \text{an odd number}$.

$n = \text{an odd number, } \geq 5$			
		Number of connectable machines	Number of phases of machines in the multi-drive system
$n = \text{a prime number}$		$k = \frac{n-1}{2}$	n
$n \neq \text{a prime number}$	$n = l^m, \quad m = 2,3,4,\dots$	$k = \frac{n-1}{2}$	$n, \frac{n}{l}, \frac{n}{l^2}, \dots, \frac{n}{l^{m-1}}$
	$n = n_1 \cdot n_2 \cdot n_3 \cdot \dots \cdot n_j$	$k < \frac{n-1}{2}$	$n, n_1 \text{ or } n, n_2 \text{ or } n, n_3 \dots$ or n, n_j
	$n = n_1 \cdot n_2 \cdot \dots \cdot n_j \cdot l^m, \quad m = 2,3,4,\dots$	$k < \frac{n-1}{2}$	$n, n_1 \text{ or } n, n_2 \dots \text{ or } n, n_j$ or $\frac{n}{l}, \frac{n}{l^2} \dots \frac{n}{l^{m-1}}$

4.5.2 Even number of phases

Consider a set of multi-phase machines that are supplied from a source with an even number of phases, equal to n . There are three different situations that may arise, depending on the properties of the phase number n .

a) Let the number $n/2$ be a prime number. The maximum number of machines that can be connected in series with phase transposition equals:

$$k = \frac{n-2}{2} \tag{4.23}$$

since there are $(n - 2)/2$ pairs of current/voltage/flux components that can be used for independent flux and torque control in this multi-phase machine set. In general the remaining two components, zero sequence components, cannot be used for control purposes. The number of phases of individual k machines will be as follows: $k/2$ machines will be n -phase and $k/2$ machines will be $n/2$ -phase. The ordering of machines has to follow the rule that higher number of phases comes first. Hence the first $k/2$ machines are n -phase, while the subsequent $k/2$ machines are $n/2$ -phase. Note that this means that one half of the machines are with an even number of phases, while

the rest are with an odd number of phases. The phase numbers belonging to this category are:

$$n = 6, 10, 14, 22, 26, 34, 38, 46, 58, 62, 74, \dots \quad (4.24)$$

b) Consider next the number of phases n such that $n/2$ is not a prime number, but it satisfies the condition that:

$$n = 2^m, \quad m = 3, 4, 5, \dots \quad (4.25)$$

Note that minimum value of m that will enable machine interconnectivity is $m = 3$. The number of machines that can be connected remains to be given with (4.23):

$$k = \frac{n-2}{2} \quad (4.26)$$

However, again not all k machines are of the phase number equal to n . Consider for example the situation which arises when $n = 8$. In this case $m = 3$ and the number of machines that can be connected is equal, according to (4.23) to $k = 3$. However, only two machines are eight-phase, while the third one is four-phase. Hence for the general case of $m \geq 3$ the phase numbers of the machines that can be connected in series will be:

$$n, \frac{n}{2}, \frac{n}{2^2}, \dots, \frac{n}{2^{m-2}} \quad (4.27)$$

This case arises when the phase number of the multi-drive system takes values of:

$$n = 8, 16, 32, 64, \dots \quad (4.28)$$

c) The third possible case arises for all the other n that are even numbers. The number of machines that can be connected is now:

$$k < \frac{n-2}{2} \quad (4.29)$$

The same situation arises as in case c) of the odd number of phases. An attempt to connect machines of different phase numbers that are not exactly divisible (i.e. the result of division is not an integer) is not possible, since it leads to the short-circuiting of terminals. For example, $n = 12$ leads to theoretical interconnection of five machines; two of these are twelve-phase, one is six-phase, one is four-phase and one is three-phase; however, four-phase and three-phase machines can not be connected in series,

since all terminals of the four-phase machine would need to be connected to all terminals of the three-phase machine, leading to a complete short-circuit after the point of this connection. It is therefore not possible to connect five machines in series. However, ordering the machines as twelve-phase, twelve-phase, six-phase and three-phase enables interconnection of four machines. This however has no advantage whatsoever, since four machines can be connected with a nine-phase system. Similarly, for $n = 20$ one ends up with the need to interconnect a four-phase and a five-phase machine, which cannot be done, so that the resulting number of machines is smaller than $(n-2)/2$. For $n = 18$ there are three eighteen-phase, three nine-phase, one six-phase and one three-phase machine, giving theoretical number of inter-connectable machines as eight. But, a nine-phase machine cannot be connected to a six-phase machine, so that maximum number of machines in the group is seven (18, 18, 18, 9, 9, 9, 3-phase). So, 18 legs would be required for seven machines, while with 17 legs ($n = 17$) one can connect eight machines (similarly, fifteen-phase case in section 4.5.1 yields maximum number of connectable machines as six, rather than seven).

Again, among these k machines only a certain number will be with n phases. The other machines that should be connectable in the multi-drive system will have phase numbers equal to $n/2, n/3, n/4, \dots$ as appropriate. There will be at least three different phase numbers among the multi-machine set. Phase numbers that belong to this group are:

$$n = 12, 18, 20, 24, 28, 30, 36, 40, \dots$$

Cases b) and c) can be regarded as sub-cases of a general case for which $n/2$ is not a prime number. They have in common that two or more phase numbers appear in the series connection with phase transposition of multi-phase machines. The total number of connectable machines is however not the same, as given with (4.26) and (4.29), respectively.

With reference to Table 4.13, columns for $n = 6, 10$ and 14 correspond to case a) when $n/2$ is a prime number, while columns for $n = 8$ and 16 correspond to case b) where $n = 2^m$, $m = 3, 4, 5, \dots$. Finally, the cases of $n = 12$ and 18 are from the sub-group c). A summary of all possible situations that can arise with $n =$ an even phase number is given in Table 4.16.

Table 4.16: Possible situation that can arise with $n =$ even number.

$n =$ an even number, ≥ 6			
		Number of connectable machines	Number of phases of machines in the multi-drive system
$n/2 =$ a prime number		$k = \frac{n-2}{2}$	$k/2$ are n -phase and $k/2$ are $n/2$ - phase
$n/2 \neq$ a prime number	$n = 2^m, m = 3, 4, 5, \dots$	$k = \frac{n-2}{2}$	$n, \frac{n}{2}, \frac{n}{2^2}, \dots, \frac{n}{2^{m-2}}$
	All other even numbers	$k < \frac{n-2}{2}$	$n, n/2, n/3, n/4, \dots$ as appropriate

4.6 Summary

In order to connect a set of n -phase machines in series and control them independently, it is necessary to perform a phase transposition in the machine-to-machine connection. This chapter demonstrated how to perform the phase transposition for both the odd and even phase numbers using the decoupling transformation matrix. This allows the construction of a connection table termed the connectivity matrix. Connectivity matrices were developed for a general n -phase case and selected set of phase numbers. It was shown that the number of connectable machines and the phase number of each machine in the system are dependent on the properties of the supply phase number. For systems containing machines with different phase numbers it is important that the machines are ordered beginning with the machines having the highest number of phases and to continue in descending order. Detailed analysis of all the odd and even phase numbers has shown that the number of connectable machines equals the maximum expected number $[(n-1)/2$ for odd numbers and $(n-2)/2$ for even numbers] only for certain supply phase numbers. From the practical point of view only supply phase numbers that allow series connection of the maximum number of connectable machines are of potential importance. This is so since such a situation enables saving of the maximum number of inverter legs, when compared with an equivalent three-phase system. As far as saving in inverter legs is concerned, the viable multi-phase drive systems are therefore those for which the number of supply phases is either a prime number or a power of the prime number (for the odd phase number case) or n is such that $n/2$ is a prime number or is a power of two (for the even phase number case).

CHAPTER 5

SIMULATION STUDIES FOR ODD PHASE NUMBERS

5.1 Introduction

The concept of a multi-phase multi-machine drive with decoupled dynamic control is verified in this chapter for five, nine and fifteen-phase cases by computer simulation. Considerations of this chapter can be found in Levi et al (2003b), Levi et al (2004b), Levi et al (2004c) and Jones et al (2003a). Considerations related to the seven-phase three-motor drive can be found in Jones et al (2003b).

Initially the phase-domain model of a five-phase induction machine is derived and simulated. The phase-domain model is next used in the simulation of a current-fed induction machine under indirect rotor flux oriented vector control. As a further step, d-q model of the machine is applied in simulations thus allowing the results to be compared. Simulation of two five-phase machines connected in series using both modelling methods is carried out in order to verify the concept. This allows vector control of a five-phase two-motor drive to be considered. Simulations are performed for both torque mode and speed mode of operation in order to validate the concept which is further extended to the nine-phase and fifteen-phase cases. Once again, each configuration is tested via simulation. Both the nine-phase and the fifteen-phase cases are of particular interest because of the arrangement of the machines within the multi-machine groups.

5.2 The five-phase single motor drive

5.2.1 Phase-domain model of a five-phase induction machine

A five-phase induction machine is constructed using ten phase belts, each of 36 degrees, along the circumference of the stator. The spatial displacement between phase mmfs is therefore 72 degrees. The rotor winding is treated as an equivalent five-phase winding, of the same properties as the stator winding. Once more it is assumed that the

rotor winding has already been referred to stator winding, using winding transformation ratio, so that the maximum value of the mutual stator to rotor inductance terms equals in value mutual inductance within the five-phase stator winding and mutual inductance within the five-phase rotor winding (M). Let a five-phase induction machine be fed from an ideal current source, with a system of five-phase sinusoidal currents:

$$\begin{aligned} i_a &= \sqrt{2}I \sin(\omega_s t) \\ i_b &= \sqrt{2}I \sin(\omega_s t - \alpha) \\ i_c &= \sqrt{2}I \sin(\omega_s t - 2\alpha) \\ i_d &= \sqrt{2}I \sin(\omega_s t + 2\alpha) \\ i_e &= \sqrt{2}I \sin(\omega_s t + \alpha) \end{aligned} \quad (5.1)$$

Since stator currents are known, their derivatives are known as well:

$$\begin{aligned} di_a / dt &= \sqrt{2}I \omega_s \cos(\omega_s t) \\ di_b / dt &= \sqrt{2}I \omega_s \cos(\omega_s t - \alpha) \\ di_c / dt &= \sqrt{2}I \omega_s \cos(\omega_s t - 2\alpha) \\ di_d / dt &= \sqrt{2}I \omega_s \cos(\omega_s t + 2\alpha) \\ di_e / dt &= \sqrt{2}I \omega_s \cos(\omega_s t + \alpha) \end{aligned} \quad (5.2)$$

Under the assumption of ideal current feeding stator voltage equations can be omitted from further consideration of the model of the machine. Rotor voltage equation in matrix form is from (3.2):

$$\underline{v}_{abcde}^r = \underline{R}_r \underline{i}_{abcde}^r + p \underline{\Psi}_{abcde}^r \quad (5.3)$$

Expanding the flux linkage term using (3.2) results in:

$$\underline{v}_{abcde}^r = \underline{R}_r \underline{i}_{abcde}^r + p (\underline{L}_r \underline{i}_{abcde}^r + \underline{L}_{rs} \underline{i}_{abcde}^s) \quad (5.4)$$

Performing the differentiation gives:

$$\underline{v}_{abcde}^r = \underline{R}_r \underline{i}_{abcde}^r + \underline{L}_r p(\underline{i}_{abcde}^r) + [p(\underline{L}_{rs})] \underline{i}_{abcde}^s + \underline{L}_{rs} p(\underline{i}_{abcde}^s) \quad (5.5)$$

Equation (5.5) needs to be solved in order to determine the rotor currents. Taking into account that the rotor is short circuited, one has from (5.5):

$$p(\underline{i}_{abcde}^r) = -\underline{L}_r^{-1} (\underline{R}_r \underline{i}_{abcde}^r + [p(\underline{L}_{rs})] \underline{i}_{abcde}^s + \underline{L}_{rs} p(\underline{i}_{abcde}^s)) \quad (5.6)$$

Performing the differentiation as indicated above and expanding the sub matrices using (3.6)-(3.7) enables formulation of the equations in state-space form as follows:

$$\begin{bmatrix} pi_{ar} \\ pi_{br} \\ pi_{cr} \\ pi_{dr} \\ pi_{er} \end{bmatrix} = - \begin{bmatrix} L_{lr} + M & M \cos \alpha & M \cos 2\alpha & M \cos 2\alpha & M \cos \alpha \\ M \cos \alpha & L_{lr} + M & M \cos \alpha & M \cos 2\alpha & M \cos 2\alpha \\ M \cos 2\alpha & M \cos \alpha & L_{lr} + M & M \cos \alpha & M \cos 2\alpha \\ M \cos 2\alpha & M \cos 2\alpha & M \cos \alpha & L_{lr} + M & M \cos \alpha \\ M \cos \alpha & M \cos 2\alpha & M \cos 2\alpha & M \cos \alpha & L_{lr} + M \end{bmatrix}^{-1} \times$$

$$\left[\begin{array}{l} -\omega M \begin{bmatrix} \sin(\theta) & \sin(\theta - \alpha) & \sin(\theta - 2\alpha) & \sin(\theta + 2\alpha) & \sin(\theta + \alpha) \\ \sin(\theta + \alpha) & \sin(\theta) & \sin(\theta - \alpha) & \sin(\theta - 2\alpha) & \sin(\theta + 2\alpha) \\ \sin(\theta + 2\alpha) & \sin(\theta + \alpha) & \sin(\theta) & \sin(\theta - \alpha) & \sin(\theta - 2\alpha) \\ \sin(\theta - 2\alpha) & \sin(\theta + 2\alpha) & \sin(\theta + \alpha) & \sin(\theta) & \sin(\theta - \alpha) \\ \sin(\theta - \alpha) & \sin(\theta - 2\alpha) & \sin(\theta + 2\alpha) & \sin(\theta + \alpha) & \sin(\theta) \end{bmatrix} \begin{bmatrix} i_{as} \\ i_{bs} \\ i_{cs} \\ i_{ds} \\ i_{es} \end{bmatrix} \\ + M \begin{bmatrix} \cos(\theta) & \cos(\theta - \alpha) & \cos(\theta - 2\alpha) & \cos(\theta + 2\alpha) & \cos(\theta + \alpha) \\ \cos(\theta + \alpha) & \cos(\theta) & \cos(\theta - \alpha) & \cos(\theta - 2\alpha) & \cos(\theta + 2\alpha) \\ \cos(\theta + 2\alpha) & \cos(\theta + \alpha) & \cos(\theta) & \cos(\theta - \alpha) & \cos(\theta - 2\alpha) \\ \cos(\theta - 2\alpha) & \cos(\theta + 2\alpha) & \cos(\theta + \alpha) & \cos(\theta) & \cos(\theta - \alpha) \\ \cos(\theta - \alpha) & \cos(\theta - 2\alpha) & \cos(\theta + 2\alpha) & \cos(\theta + \alpha) & \cos(\theta) \end{bmatrix} \begin{bmatrix} pi_{as} \\ pi_{bs} \\ pi_{cs} \\ pi_{ds} \\ pi_{es} \end{bmatrix} \\ + \begin{bmatrix} R_r & 0 & 0 & 0 & 0 \\ 0 & R_r & 0 & 0 & 0 \\ 0 & 0 & R_r & 0 & 0 \\ 0 & 0 & 0 & R_r & 0 \\ 0 & 0 & 0 & 0 & R_r \end{bmatrix} \begin{bmatrix} i_{ar} \\ i_{br} \\ i_{cr} \\ i_{dr} \\ i_{er} \end{bmatrix} \end{array} \right] \quad (5.7)$$

Stator voltages are in the case of current feeding output variables and are calculated according to:

$$\underline{v}_{abcde}^s = \underline{R}_s \underline{i}_{abcde}^s + \underline{L}_s p(\underline{i}_{abcde}^s) + [p(\underline{L}_{sr})] \underline{i}_{abcde}^r + \underline{L}_{sr} p(\underline{i}_{abcde}^r) \quad (5.8)$$

Expanding (5.8) by means of (3.5)-(3.7) gives expressions for stator phase voltages:

$$\begin{bmatrix} v_{as} \\ v_{bs} \\ v_{cs} \\ v_{ds} \\ v_{es} \end{bmatrix} = \begin{bmatrix} R_s & & & & \\ & R_s & & & \\ & & R_s & & \\ & & & R_s & \\ & & & & R_s \end{bmatrix} \begin{bmatrix} i_{as} \\ i_{bs} \\ i_{cs} \\ i_{ds} \\ i_{es} \end{bmatrix} + \begin{bmatrix} L_{ls} + M & M \cos \alpha & M \cos 2\alpha & M \cos 2\alpha & M \cos \alpha \\ M \cos \alpha & L_{ls} + M & M \cos \alpha & M \cos 2\alpha & M \cos 2\alpha \\ M \cos 2\alpha & M \cos \alpha & L_{ls} + M & M \cos \alpha & M \cos 2\alpha \\ M \cos 2\alpha & M \cos 2\alpha & M \cos \alpha & L_{ls} + M & M \cos \alpha \\ M \cos \alpha & M \cos 2\alpha & M \cos 2\alpha & M \cos \alpha & L_{ls} + M \end{bmatrix} \begin{bmatrix} pi_{as} \\ pi_{bs} \\ pi_{cs} \\ pi_{ds} \\ pi_{es} \end{bmatrix} -$$

$$-\omega M \begin{bmatrix} \sin(\theta) & \sin(\theta + \alpha) & \sin(\theta + 2\alpha) & \sin(\theta - 2\alpha) & \sin(\theta - \alpha) \\ \sin(\theta - \alpha) & \sin(\theta) & \sin(\theta + \alpha) & \sin(\theta + 2\alpha) & \sin(\theta - 2\alpha) \\ \sin(\theta - 2\alpha) & \sin(\theta - \alpha) & \sin(\theta) & \sin(\theta + \alpha) & \sin(\theta + 2\alpha) \\ \sin(\theta + 2\alpha) & \sin(\theta - 2\alpha) & \sin(\theta - \alpha) & \sin(\theta) & \sin(\theta + \alpha) \\ \sin(\theta + \alpha) & \sin(\theta + 2\alpha) & \sin(\theta - 2\alpha) & \sin(\theta - \alpha) & \sin(\theta) \end{bmatrix} \begin{bmatrix} i_{ar} \\ i_{br} \\ i_{cr} \\ i_{dr} \\ i_{er} \end{bmatrix} +$$

$$+ M \begin{bmatrix} \cos(\theta) & \cos(\theta + \alpha) & \cos(\theta + 2\alpha) & \cos(\theta - 2\alpha) & \cos(\theta - \alpha) \\ \cos(\theta - \alpha) & \cos(\theta) & \cos(\theta + \alpha) & \cos(\theta + 2\alpha) & \cos(\theta - 2\alpha) \\ \cos(\theta - 2\alpha) & \cos(\theta - \alpha) & \cos(\theta) & \cos(\theta + \alpha) & \cos(\theta + 2\alpha) \\ \cos(\theta + 2\alpha) & \cos(\theta - 2\alpha) & \cos(\theta - \alpha) & \cos(\theta) & \cos(\theta + \alpha) \\ \cos(\theta + \alpha) & \cos(\theta + 2\alpha) & \cos(\theta - 2\alpha) & \cos(\theta - \alpha) & \cos(\theta) \end{bmatrix} \begin{bmatrix} pi_{ar} \\ pi_{br} \\ pi_{cr} \\ pi_{dr} \\ pi_{er} \end{bmatrix} \quad (5.9)$$

The electromagnetic torque developed by the machine can be calculated, using stator and rotor phase currents and (3.10), as:

$$T_e = -PM \left\{ \begin{aligned} & (i_{as}i_{ar} + i_{bs}i_{br} + i_{cs}i_{cr} + i_{ds}i_{dr} + i_{es}i_{er}) \sin \theta + (i_{es}i_{ar} + i_{as}i_{br} + i_{bs}i_{cr} + i_{cs}i_{dr} + i_{ds}i_{er}) \sin(\theta + \alpha) + \\ & (i_{ds}i_{ar} + i_{es}i_{br} + i_{as}i_{cr} + i_{bs}i_{dr} + i_{cs}i_{er}) \sin(\theta + 2\alpha) + (i_{cs}i_{ar} + i_{ds}i_{br} + i_{es}i_{cr} + i_{as}i_{dr} + i_{bs}i_{er}) \\ & \sin(\theta - 2\alpha) + (i_{bs}i_{ar} + i_{cs}i_{br} + i_{ds}i_{cr} + i_{es}i_{dr} + i_{as}i_{er}) \sin(\theta - \alpha) \end{aligned} \right\} \quad (5.10)$$

The mechanical equation of motion depends on the characteristics of the load, which may differ widely from one application to another. It is assumed, for simplicity, that the load torque consists only of an inertial torque and a constant load torque. The electrical speed of the machine and the rotor position can therefore be expressed from (3.11) as:

$$\begin{aligned} \frac{d\omega}{dt} &= \frac{P}{J} (T_e - T_L) \\ \frac{d\theta}{dt} &= \omega \end{aligned} \quad (5.11)$$

In order to determine the equivalent circuit parameters of an induction machine it is necessary to perform some tests. These tests produce parameter values suitable for steady-state phasor and d-q models. However, in order to model the machine in the phase-domain it is necessary to convert the equivalent circuit parameters to their phase-domain equivalent. The relationship between these parameters can be seen in the derivation of the d-q model of the machine (chapter 3), where only the mutual inductance value differs from that in the phase variable form. In this study, per-phase phasor equivalent circuit parameters (Fig. 5.1) of an existing three-phase induction machine are taken as the starting point (Table 5.1). Regardless of the number of phases of the induction machine under consideration, per-phase phasor equivalent circuit parameters are assumed to be always the same. Such an approach is adopted since it enables simple verification of the correctness of the simulation programs and subsequent simulation results. Per-phase phasor equivalent circuit parameters of Table 5.1 apply to a three-phase four-pole 50Hz machine with rated rms phase voltage of 220V, rated rms current of 2.1A and rated torque of 5Nm (1.67Nm per phase). Relevant data for vector control of a corresponding n -phase multi-phase drive system are given in Appendix C. The mutual inductance value of the equivalent circuit is divided by 2.5 for the five-phase case to yield the value for M in phase variable model.

The parameters of the five-phase induction machine are given in Table 5.1 in the right-hand column for the phase-domain model.

Table 5.1: Five-phase machine parameters.

Equivalent circuit parameters	Phase-domain model
$L_{lr} = 0.04 \text{ H}$	$L_{lr} = 0.04 \text{ H}$
$L_{ls} = 0.04 \text{ H}$	$L_{ls} = 0.04 \text{ H}$
$L_m = 0.42 \text{ H}$	$M = L_m/2.5 = 0.168 \text{ H}$
$R_r = 6.3 \Omega$	$R_r = 6.3 \Omega$
$R_s = 10 \Omega$	$R_s = 10 \Omega$

The inertia of all machines simulated further on is equal to $J = 0.03 \text{ kgm}^2$. All the machines are four-pole.

5.2.2 Simulation of a single five-phase induction machine (phase-domain model)

The equations (5.7)-(5.11) allow a simulation program for a five-phase induction machine to be written using MATLAB/SIMULINK software. The machine is modelled as current-fed to allow the simplest realisation of an indirect rotor flux oriented induction motor drive (to be described later). The source currents were assumed to be ideal balanced sinusoidal currents, of 2.1A rms and frequency 50Hz (Fig. 5.2). The simulation was run for an imaginary scenario of direct on-line starting under no-load conditions. A load torque of 4 Nm was applied in a stepwise manner at $t = 6\text{s}$. The torque and speed behaviour of the machine (Fig. 5.2b) show that the machine takes 3.8s to reach synchronous speed. Synchronous speed is attained because the effects of friction have been neglected in the mathematical model. The acceleration of the machine is very slow and this is because the torque developed by the machine takes a long time to reach its maximum value. The long acceleration time is a result of the limitation of the source current to rated value. This can be explained by considering the rotor flux magnitude (Fig. 5.2c), which indicates that the rotor flux is very small near standstill and slowly increases to above rated value (rated = $\sqrt{5} \times 0.5683$). The reason for this becomes clear if one considers the steady-state equivalent circuit of an induction machine, illustrated in Fig. 5.1. At standstill the slip is unity and the majority of the current flows into the rotor branch so that magnetising flux is small. During acceleration of the motor the slip value decreases, thus allowing the development of

greater flux and torque.

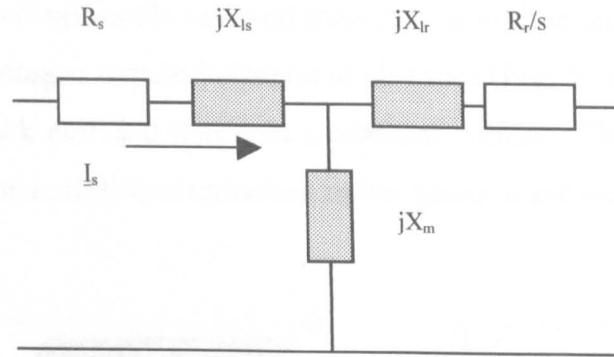
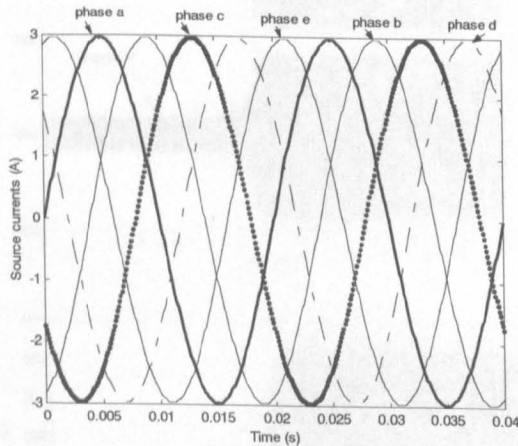
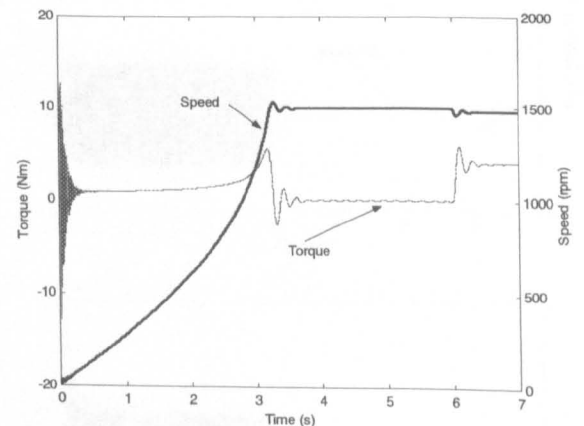


Fig. 5.1: Per-phase phasor equivalent circuit of a current-fed induction machine.

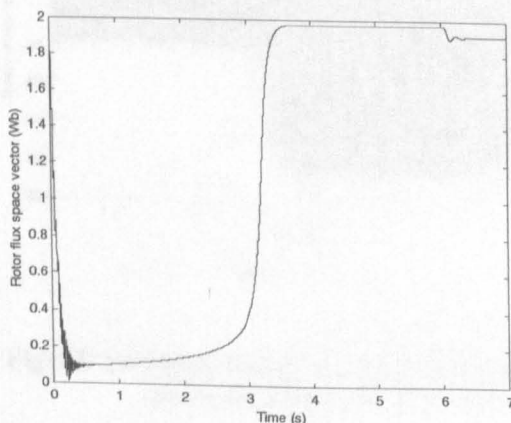
The current supplied to the machine is held constant and rated. When the machine reaches synchronous speed the current completely flows through the magnetizing branch. Therefore rotor flux reaches a value greater than rated. It can be seen from the no-load acceleration graphs that the initial torque transient is rather large (Fig. 5.2b). This is due to the fact that the simulation is applying a step stator current to the machine (Fig 5.2a), while the current in a real machine cannot be stepped due to the inductive nature of the windings.



(a)



(b)



(c)

Fig 5.2: Simulation of a five-phase current-fed induction machine direct on-line starting using phase-domain model: stator input currents (a), rotor speed and torque response (b), and rotor flux space vector amplitude (c).

This stepped stator current produces an instantaneous rotor flux of 1.97 Wb (Fig. 5.2c) at time equal to zero (impossible in a real machine, as at time equal to zero rotor flux is zero). The stator voltages remain balanced at all times (Fig. 5.3a) and increase in order to counteract the back emf and maintain a constant current. The application of a load torque to the machine results in a reduction in the speed of the machine, since there is

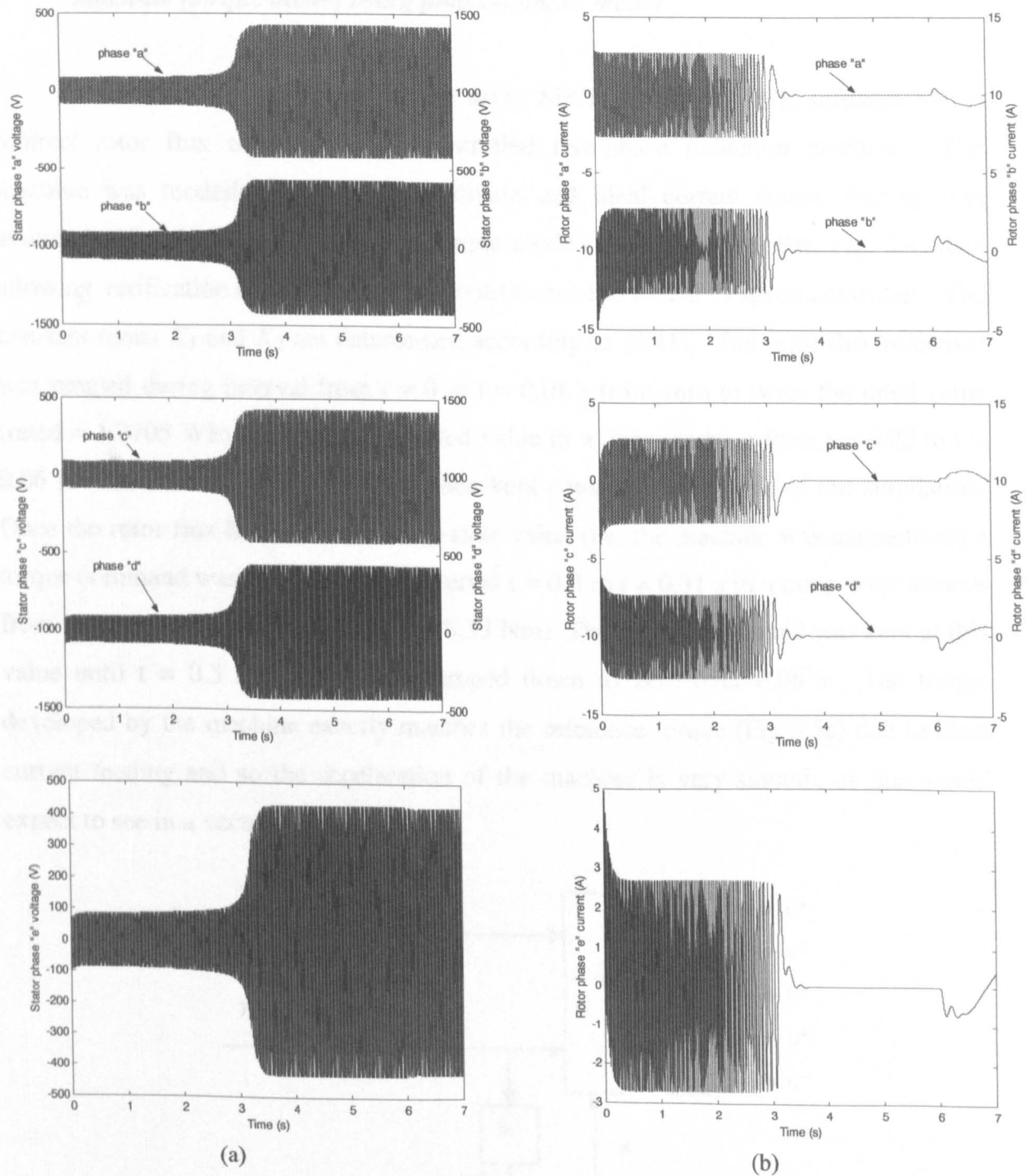


Fig 5.3: Simulation results of a five-phase current-fed induction machine direct on-line starting using phase-domain model: stator phase voltages (a) and rotor phase currents (b).

voltages experience a small decrease with the application of the load, this is due to the increase in slip resulting in a reduction in back emf and an increase in rotor current (Fig. 5.3b).

5.2.3 Simulation of indirect vector control of a current-fed five-phase induction machine (torque mode) using phase-domain model

A simulation program was written using MATLAB/SIMULINK software for an indirect rotor flux oriented vector controlled five-phase induction machine. The machine was modelled in the phase-domain and ideal current source feeding was assumed. The drive was operated in torque mode (no speed controller, Fig. 5.4) thus allowing verification of the concept without the need to tune a PI speed controller. The constant terms K_1 and K_2 are determined according to (3.41). The rotor flux reference was ramped during interval from $t = 0$ to $t = 0.01$ s from zero to twice the rated value (rated = 1.2705 Wb) and reduced to rated value in a linear fashion from $t = 0.05$ to $t = 0.06$ s. The rotor flux reference was then kept constant for the rest of the simulation. Once the rotor flux had reached steady-state value (i.e. the machine was magnetised) a torque command was applied during interval $t = 0.3$ to $t = 0.31$ s in a ramp wise manner from zero to twice rated value (rated = 8.33 Nm). The torque command was kept at this value until $t = 0.5$ s, when it was ramped down to zero over 0.06 s. The torque developed by the machine exactly matches the reference torque (Fig 5.5a) due to ideal current feeding and so the acceleration of the machine is very smooth, as one would expect to see in a vector-controlled drive.

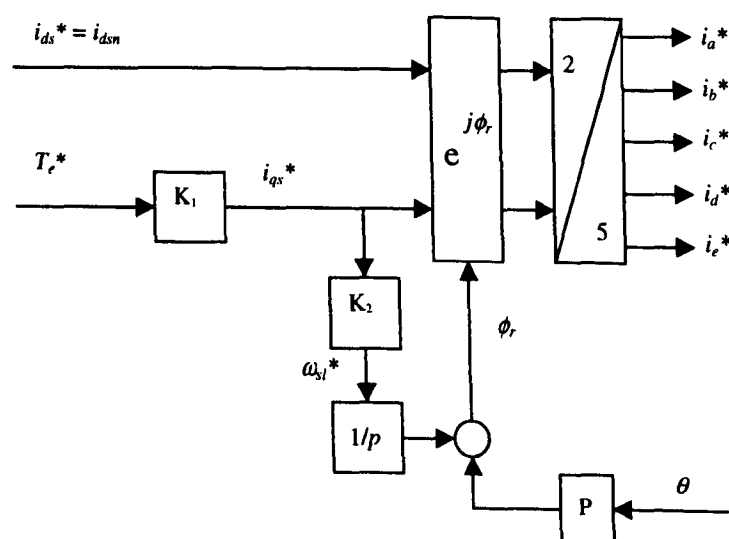


Fig 5.4: Indirect vector controller (torque mode).

The torque does not affect the rotor flux and vice versa (Figs. 5.5a-b) thus proving that decoupled flux and torque control has been achieved and that the rotor flux position has been correctly calculated. Fig. 5.6 shows that the rotor currents, after initial excitation, remain at zero until the torque command is applied. Stator currents and voltages are shown in Figs. 5.5c and d respectively.

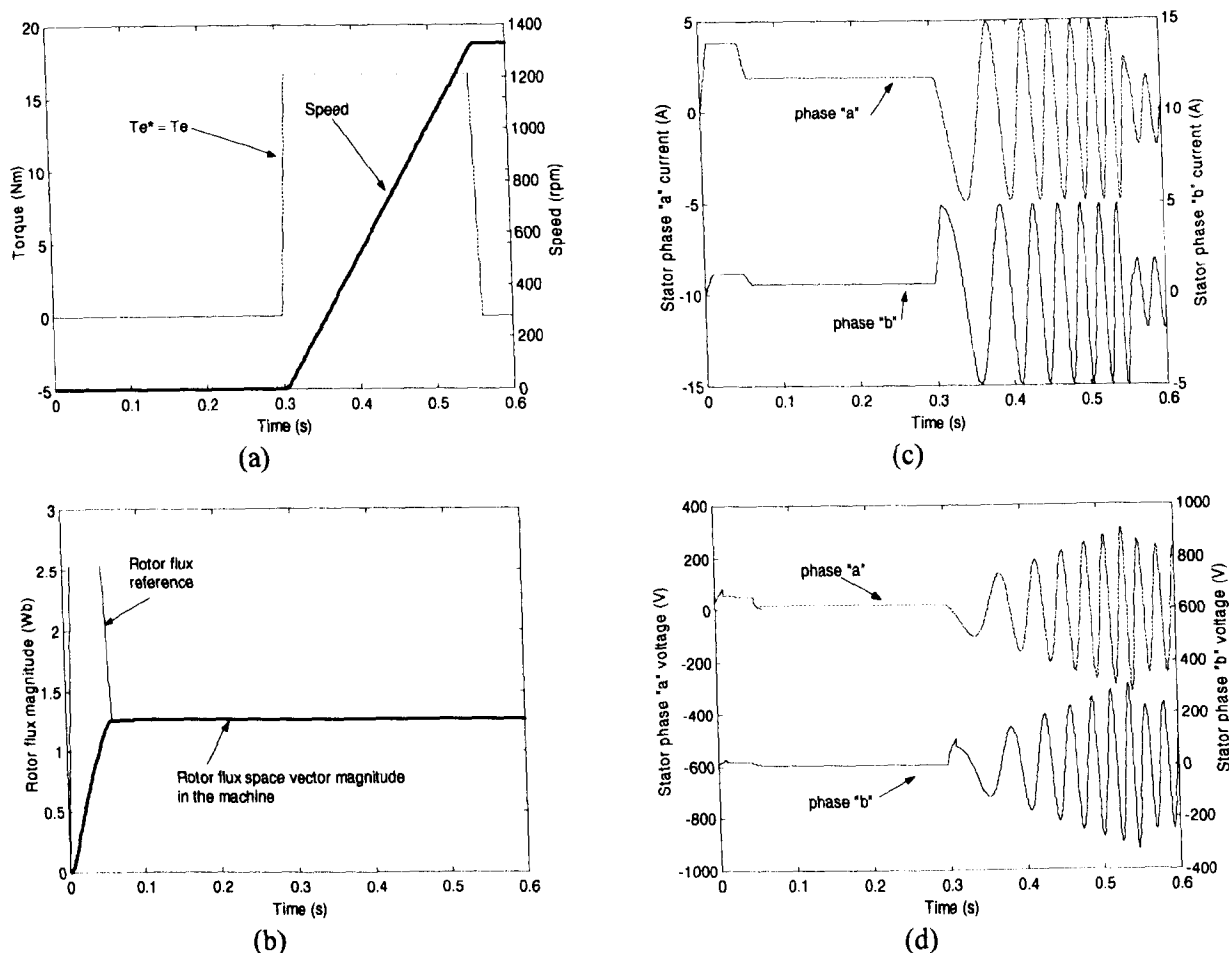


Fig. 5.5: Rotor flux oriented control of a single five-phase induction machine (torque mode) using phase-domain model: torque and speed response (a), rotor flux reference and magnitude in the machine (b), stator phase “a” and phase “b” currents (c), stator phase “a” and phase “b” voltages (d).

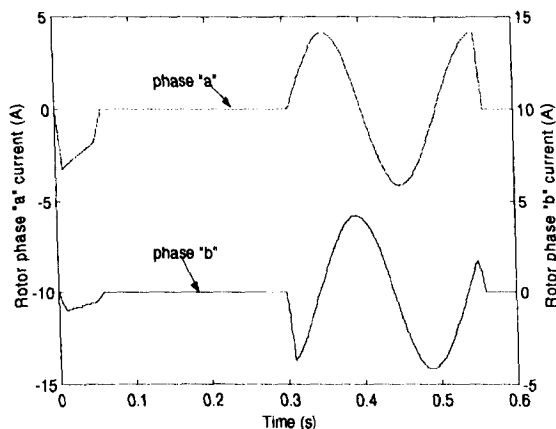


Fig. 5.6: Rotor flux oriented control of a single five-phase induction machine (torque mode) using phase-domain model: rotor phase “a” and phase “b” currents.

5.2.4 Simulation of indirect vector control of a current-fed five-phase induction machine (torque mode) using stationary reference frame model

The stationary reference frame model of a five-phase induction machine (as described in section 3.5) is used here in the simulation. Identical conditions to those in section 5.2.3 were used in order to compare like for like results and hence verify the modelling approach. By comparing the results for the stationary reference frame model (Fig. 5.7) with those obtained using the phase-domain model (Fig. 5.5-5.6) it is clear that the both methods produces identical results. This has been confirmed for all phases whilst the figures given represent the first two phases. whilst the figures given represent the first two phases.

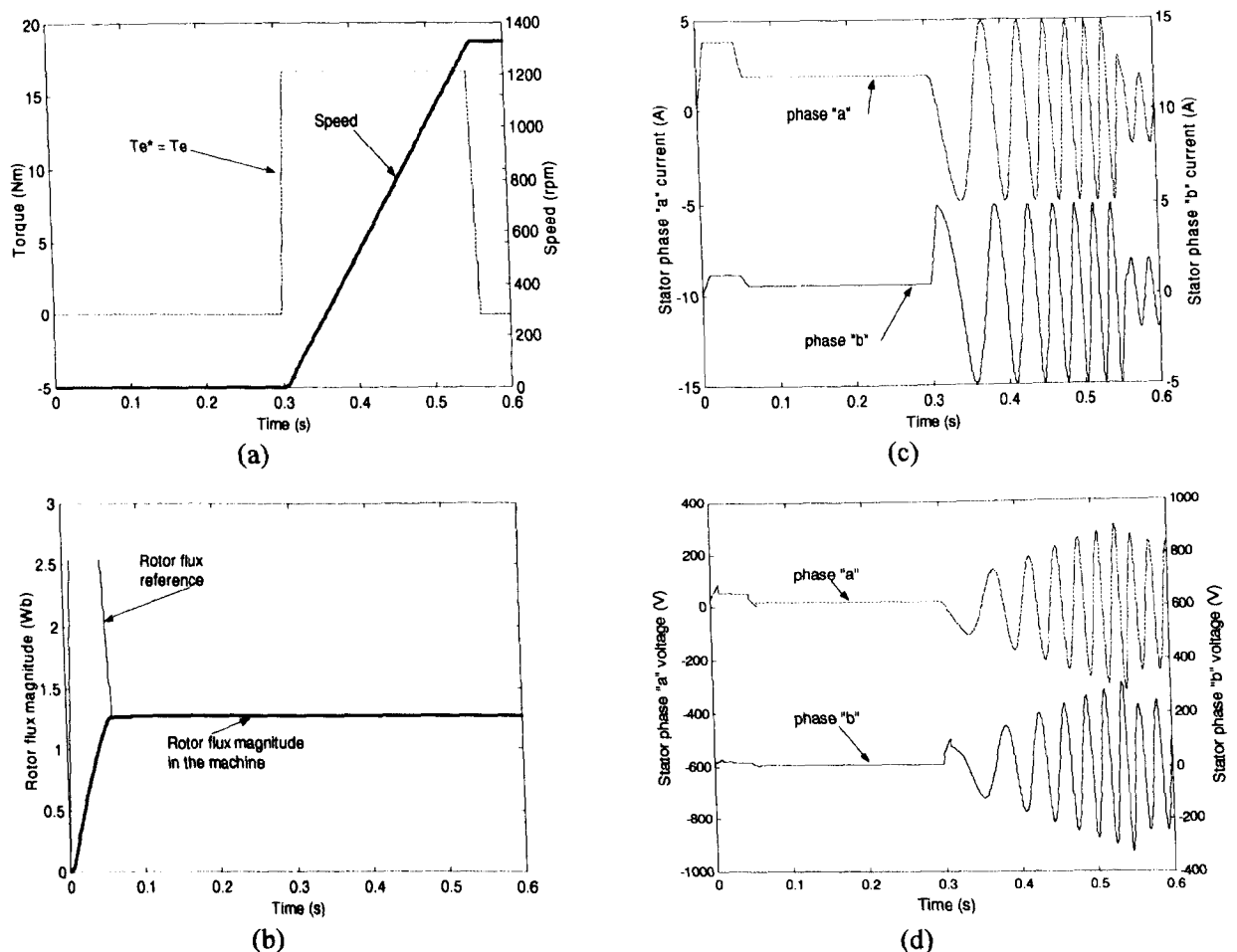


Fig. 5.7: Rotor flux oriented control of a single five-phase induction machine using stationary reference frame model. Torque and speed response (a), rotor flux reference and magnitude in the machine (b), stator phase "a" and phase "b" currents (c) and stator phase "a" and phase "b" voltages (d).

5.3 The five-phase two-motor drive

In order to verify that it is possible to connect two five-phase induction machines in series and feed them via a single five-phase inverter whilst independently controlling

the speed of each machine it is necessary to at first consider steady-state operation with ideal sinusoidal current. The connection diagram for assumed ideal current source supply without vector controllers is illustrated in Fig. 5.8.

Let the phase sequence of the source be A,B,C,D,E and let the flux-torque producing phase sequence for both machines be a,b,c,d,e. Assume that machine 1 is supplied for purposes of torque and flux production with ideal sinusoidal currents of rms value and frequency equal to I_1, ω_1 respectively. Similarly, machine 2 is supplied with a flux and torque producing set of currents of rms value and frequency I_2, ω_2 . According to Fig. 5.8, source phase currents are simultaneously corresponding phase currents for machine 1:

$$\begin{aligned}
 i_A = i_{a1} &= \sqrt{2}I_1 \sin(\omega_1 t) + \underline{\underline{\sqrt{2}I_2 \sin(\omega_2 t)}} \\
 i_B = i_{b1} &= \sqrt{2}I_1 \sin(\omega_1 t - \alpha) + \underline{\underline{\sqrt{2}I_2 \sin(\omega_2 t - 2\alpha)}} \\
 i_C = i_{c1} &= \sqrt{2}I_1 \sin(\omega_1 t - 2\alpha) + \underline{\underline{\sqrt{2}I_2 \sin(\omega_2 t + \alpha)}} \\
 i_D = i_{d1} &= \sqrt{2}I_1 \sin(\omega_1 t + 2\alpha) + \underline{\underline{\sqrt{2}I_2 \sin(\omega_2 t - \alpha)}} \\
 i_E = i_{e1} &= \sqrt{2}I_1 \sin(\omega_1 t + \alpha) + \underline{\underline{\sqrt{2}I_2 \sin(\omega_2 t + 2\alpha)}}
 \end{aligned} \tag{5.12}$$

However, machine 2 is connected to the source via a "phase transposition" operation, so that the machine is supplied with the following currents:

$$\begin{aligned}
 i_{a2} = i_A &= \underline{\underline{\sqrt{2}I_1 \sin(\omega_1 t)}} + \sqrt{2}I_2 \sin(\omega_2 t) \\
 i_{b2} = i_D &= \underline{\underline{\sqrt{2}I_1 \sin(\omega_1 t + 2\alpha)}} + \sqrt{2}I_2 \sin(\omega_2 t - \alpha) \\
 i_{c2} = i_B &= \underline{\underline{\sqrt{2}I_1 \sin(\omega_1 t - \alpha)}} + \sqrt{2}I_2 \sin(\omega_2 t - 2\alpha) \\
 i_{d2} = i_E &= \underline{\underline{\sqrt{2}I_1 \sin(\omega_1 t + \alpha)}} + \sqrt{2}I_2 \sin(\omega_2 t + 2\alpha) \\
 i_{e2} = i_C &= \underline{\underline{\sqrt{2}I_1 \sin(\omega_1 t - 2\alpha)}} + \sqrt{2}I_2 \sin(\omega_2 t + \alpha)
 \end{aligned} \tag{5.13}$$

Supplying the machines with the above currents makes it possible to independently control the speed of each machine by controlling frequencies f_1 and f_2 respectively, together with current magnitudes. This can be explained by considering the underlined terms in equations (5.12) and (5.13). The spatial mmf distribution in a five-phase AC machine is given by:

$$\begin{aligned}
 F_a &= Ni_a \cos(\epsilon) \\
 F_b &= Ni_b \cos(\epsilon - \alpha) \\
 F_c &= Ni_c \cos(\epsilon - 2\alpha) \\
 F_d &= Ni_d \cos(\epsilon + 2\alpha) \\
 F_e &= Ni_e \cos(\epsilon + \alpha)
 \end{aligned} \tag{5.14}$$

The origin of ε is chosen to be the magnetic axis of phase “a”. The resultant mmf at point ε is:

$$F(\varepsilon) = F_a(\varepsilon) + F_b(\varepsilon) + F_c(\varepsilon) + F_d(\varepsilon) + F_e(\varepsilon) \quad (5.15)$$

Therefore the total mmf produced in machine 2 by the underlined terms in (5.13) is given with:

$$\begin{aligned} & \sqrt{2}NI_1 \left[\sin(\omega_1 t) \cos(\varepsilon) + \sin(\omega_1 t + 2\alpha) \cos(\varepsilon - \alpha) + \sin(\omega_1 t - \alpha) \cos(\varepsilon - 2\alpha) + \right. \\ & \left. + \sin(\omega_1 t + \alpha) \cos(\varepsilon + 2\alpha) + \sin(\omega_1 t - 2\alpha) \cos(\varepsilon + \alpha) \right] = \\ & = \sqrt{2}NI_1 \frac{1}{4j} \left[\left(e^{j\omega_1 t} - e^{-j\omega_1 t} \right) \left(e^{j\varepsilon} + e^{-j\varepsilon} \right) + \left(e^{j(\omega_1 t + 2\alpha)} - e^{-j(\omega_1 t + 2\alpha)} \right) \left(e^{j(\varepsilon - \alpha)} + e^{-j(\varepsilon - \alpha)} \right) + \right. \\ & \left. + \left(e^{j(\omega_1 t - \alpha)} - e^{-j(\omega_1 t - \alpha)} \right) \left(e^{j(\varepsilon - 2\alpha)} + e^{-j(\varepsilon - 2\alpha)} \right) + \left(e^{j(\omega_1 t + \alpha)} - e^{-j(\omega_1 t + \alpha)} \right) \left(e^{j(\varepsilon + 2\alpha)} + e^{-j(\varepsilon + 2\alpha)} \right) \right. \\ & \left. + \left(e^{j(\omega_1 t - 2\alpha)} - e^{-j(\omega_1 t - 2\alpha)} \right) \left(e^{j(\varepsilon + \alpha)} + e^{-j(\varepsilon + \alpha)} \right) \right] = \\ & = \sqrt{2}NI_1 \frac{1}{4j} \left[e^{j\omega_1 t} e^{j\varepsilon} \left(1 + e^{j\alpha} + e^{-j3\alpha} + e^{j3\alpha} + e^{-j\alpha} \right) - e^{-j\omega_1 t} e^{-j\varepsilon} \left(1 + e^{-j\alpha} + e^{j3\alpha} + e^{-j3\alpha} + e^{j\alpha} \right) + \right. \\ & \left. e^{j\omega_1 t} e^{-j\varepsilon} \left(1 + e^{j3\alpha} + e^{j\alpha} + e^{-j\alpha} + e^{-j3\alpha} \right) - e^{-j\omega_1 t} e^{j\varepsilon} \left(1 + e^{-j3\alpha} + e^{-j\alpha} + e^{j\alpha} + e^{j3\alpha} \right) \right] = 0 \end{aligned} \quad (5.16)$$

Thus the currents that produce a rotating field in machine 1 do not produce a rotating field in machine 2 and vice versa. Application of the transformation matrix (3.13a) on stator currents of the two machines given with (5.12)-(5.13) produces the results summarised in Table 5.2 [Levi et al (2003b)]. Table 5.2 shows that, due to the phase transposition in the series connection of the two machines, torque/flux producing currents of machine 1 produce α - β components in machine 1 and x-y components in machine 2, and vice versa. It is this fact which makes it possible to independently control each motor in the multi-motor drive.

Table 5.2: Stator current components in series-connected motors in steady-state

Current components	M1	M2
α	$\sqrt{5}I_1 \sin \omega_1 t$	$\sqrt{5}I_2 \sin \omega_2 t$
β	$-\sqrt{5}I_1 \cos \omega_1 t$	$-\sqrt{5}I_2 \cos \omega_2 t$
x1	$\sqrt{5}I_2 \sin \omega_2 t$	$\sqrt{5}I_1 \sin \omega_1 t$
y1	$-\sqrt{5}I_2 \cos \omega_2 t$	$\sqrt{5}I_1 \cos \omega_1 t$
0	0	0

The source phase voltages are calculated using the voltages of the two machines, according to:

$$\begin{aligned}
 v_A &= v_{as1} + v_{as2} \\
 v_B &= v_{bs1} + v_{bs2} \\
 v_C &= v_{cs1} + v_{cs2} \\
 v_D &= v_{ds1} + v_{ds2} \\
 v_E &= v_{es1} + v_{es2}
 \end{aligned}
 \tag{5.17}$$

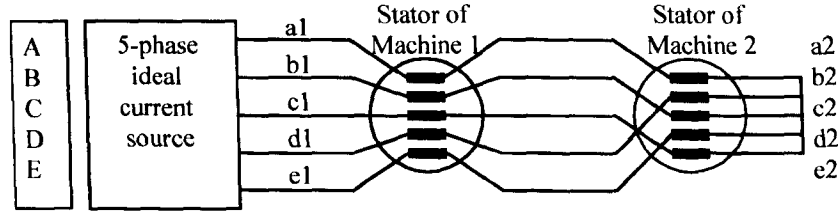


Fig. 5.8: Series connection of two five-phase machines without controllers and with ideal current source feeding.

5.3.1 Simulation of series connection of two five-phase machines with phase transposition (phase-domain model)

A program was written using MATLAB/SIMULINK software in order to verify the concept developed in section 5.3. The program simulates two identical induction machines, the first of which (IM1) is supplied with rated current 2.1A at 50Hz and is loaded at $t = 6$ s in a stepped manner. The second machine (IM2) is supplied with rated current 2.1A at 25Hz and is loaded at $t = 2$ s in a stepped manner. Both machines are modelled in the phase-domain as described in section 5.2.1. The input stator currents of the two machines are shown in Fig. 5.9 and are obtained according to (5.12) and (5.13).

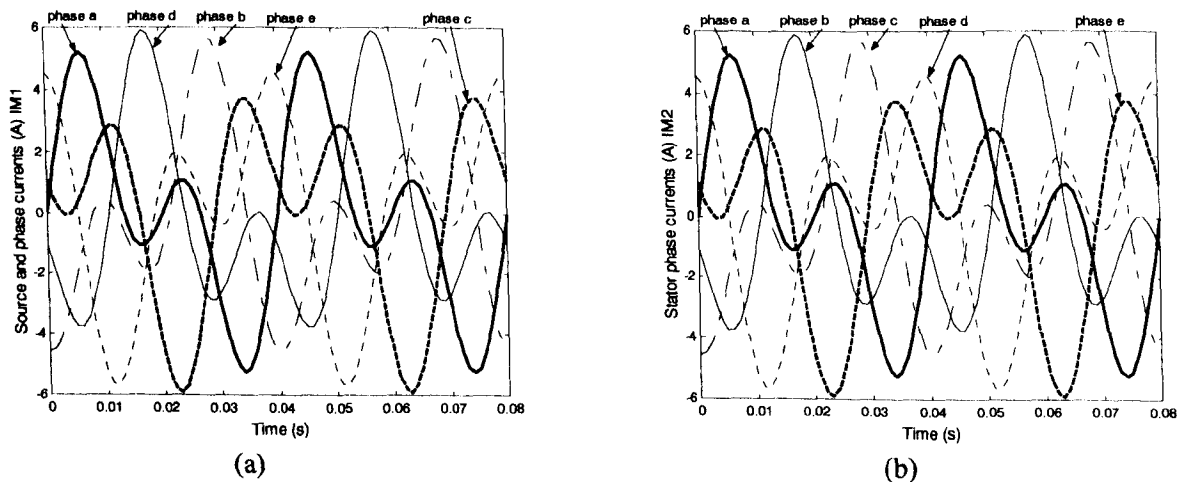


Fig. 5.9: Simulation results for the two five-phase induction machines connected in series, during direct on-line starting (phase-domain model): stator phase currents of machine 1 (a) and machine 2 (b).

Torque and speed responses of the two machines are illustrated in Fig. 5.10. Other simulation results are shown in Figs. 5.11 and 5.12. Fig. 5.10 shows that the

torque and therefore the speed response of IM1 is identical to that obtained with a single five-phase machine (Fig 5.2), while IM2 is operating at half the speed of IM1 as one would expect. Therefore the two machines are operating independently of each other. In other words, operating state of IM2 does not affect in any way rotor flux and torque in IM1, and vice versa.

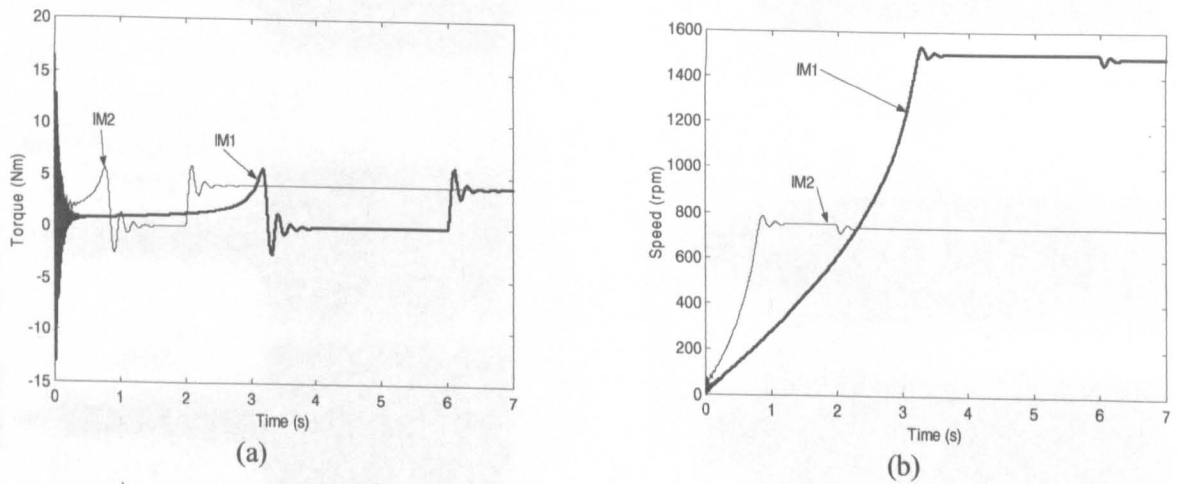


Fig. 5.10: Torque (a) and speed (b) response of the two series-connected five-phase machines during direct on-line starting (phase-domain model).

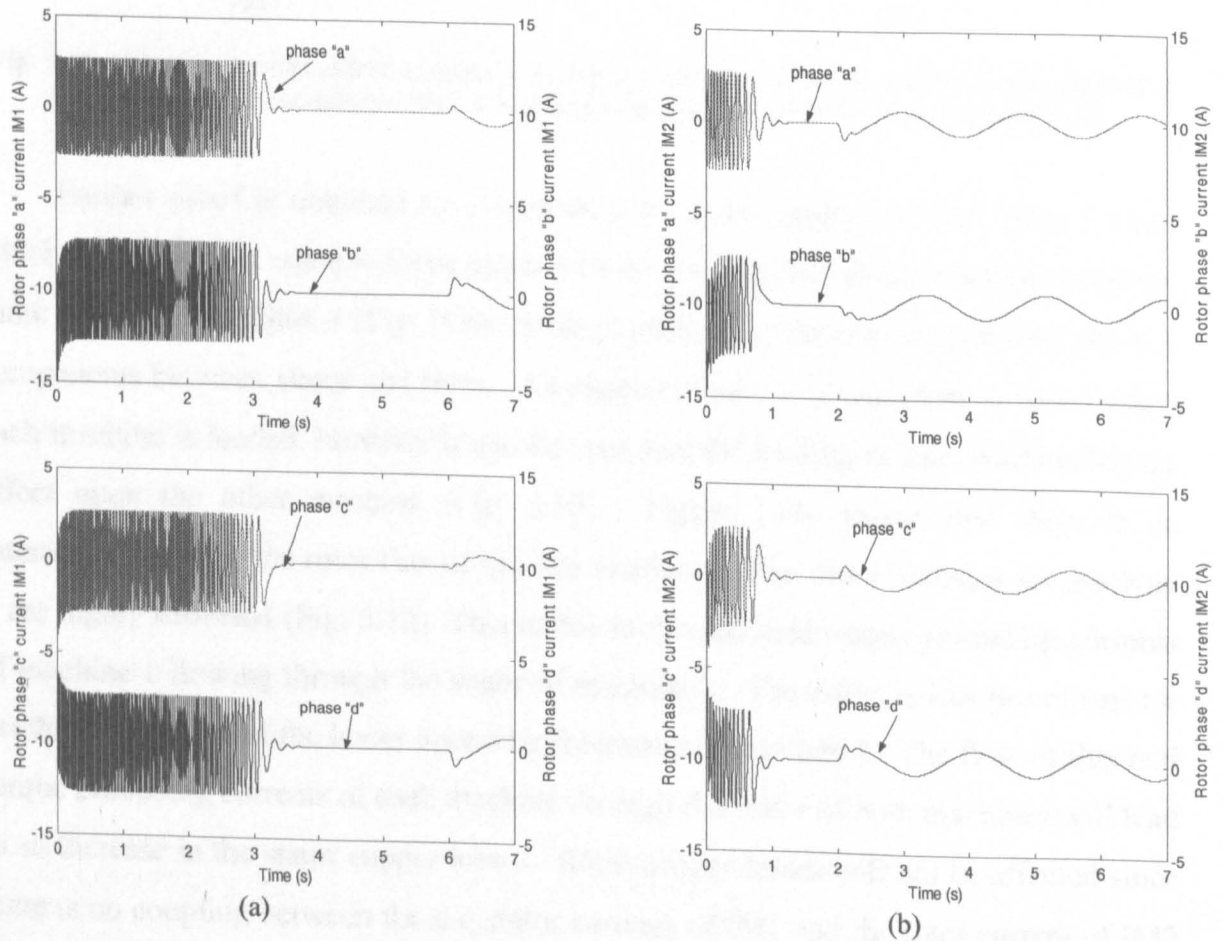


Fig. 5.11: Simulation results of two five-phase induction machines connected in series during direct on-line starting (phase-domain model): rotor currents in IM1 (a) and IM2 (b).

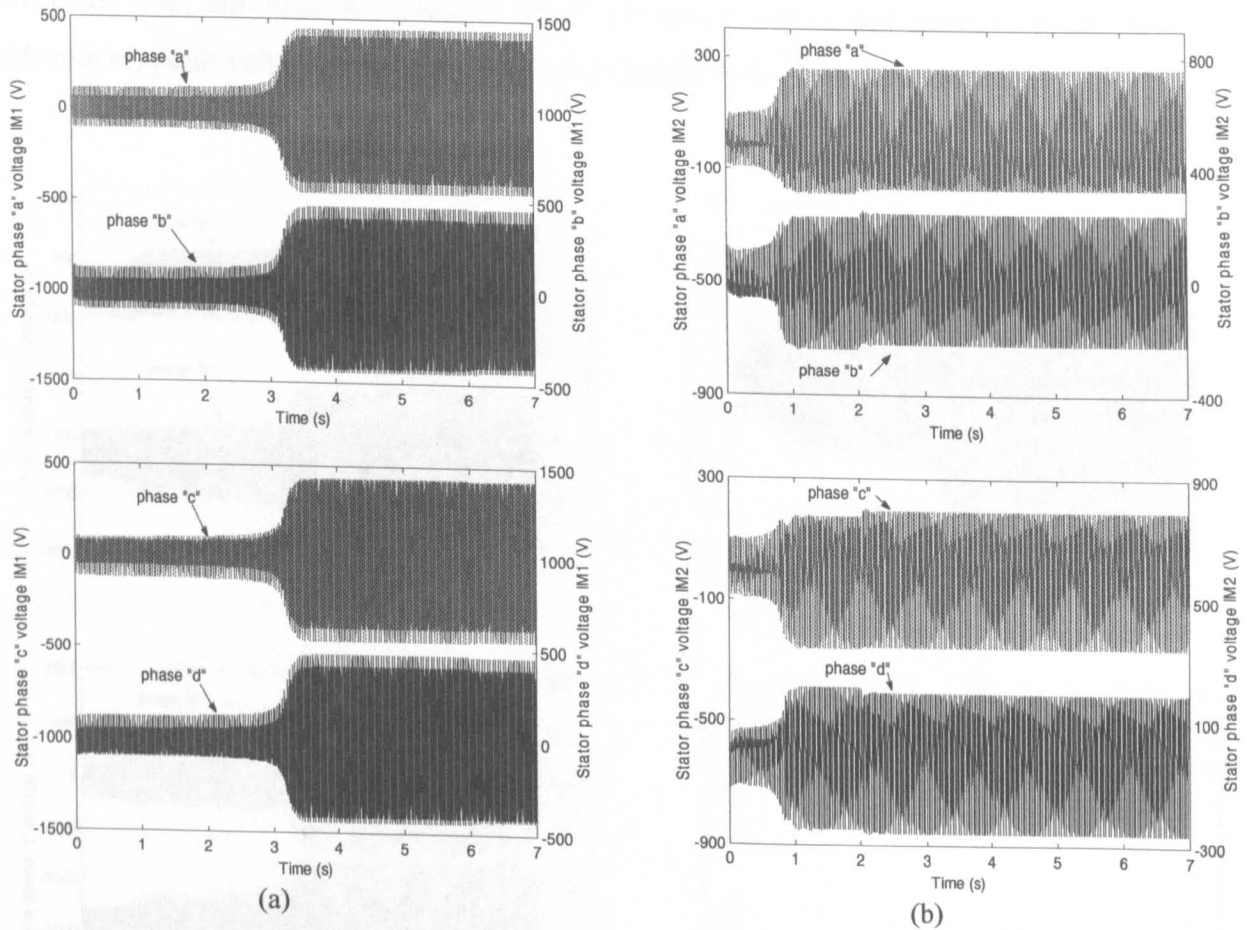


Fig. 5.12: Simulation results of two five-phase induction machines connected in series during direct on-line starting (phase-domain model): stator phase voltages of machine 1 (a) and machine 2 (b).

Further proof is obtained by considering the rotor currents of IM1 (Fig. 5.11a), which are identically equal to those obtained with a single five-phase machine under the same operating conditions (Fig. 5.3b) demonstrating that there is no coupling for x - y components between stator and rotor. As expected there is a reduction in speed when each machine is loaded, however it can be seen that the loading of one machine has no effect upon the other machine (Fig. 5.10). Figure 5.13c shows that there is no interaction between the rotor flux of the two machines. The stator voltages for machine 2 are highly distorted (Fig. 5.12). This is due to the flux and torque producing currents of machine 1 flowing through the stator of machine 2. The effect is less prominent for machine 1 because of the lower operating frequency of machine 2. The flow of flux and torque producing currents of each machine through the stator of both machines will lead to an increase in the stator copper losses. Rotor copper losses will not be affected since there is no coupling between the d - q stator currents of IM1 and the rotor current of IM2 and the d - q stator currents of IM2 and the rotor currents of IM1. Finally, source voltages obtained using (5.17) are displayed in Fig. 5.13a and b. They are highly

distorted and, although AC, clearly have different negative and positive peak values. Moreover, peak values of individual phase voltages may differ substantially.

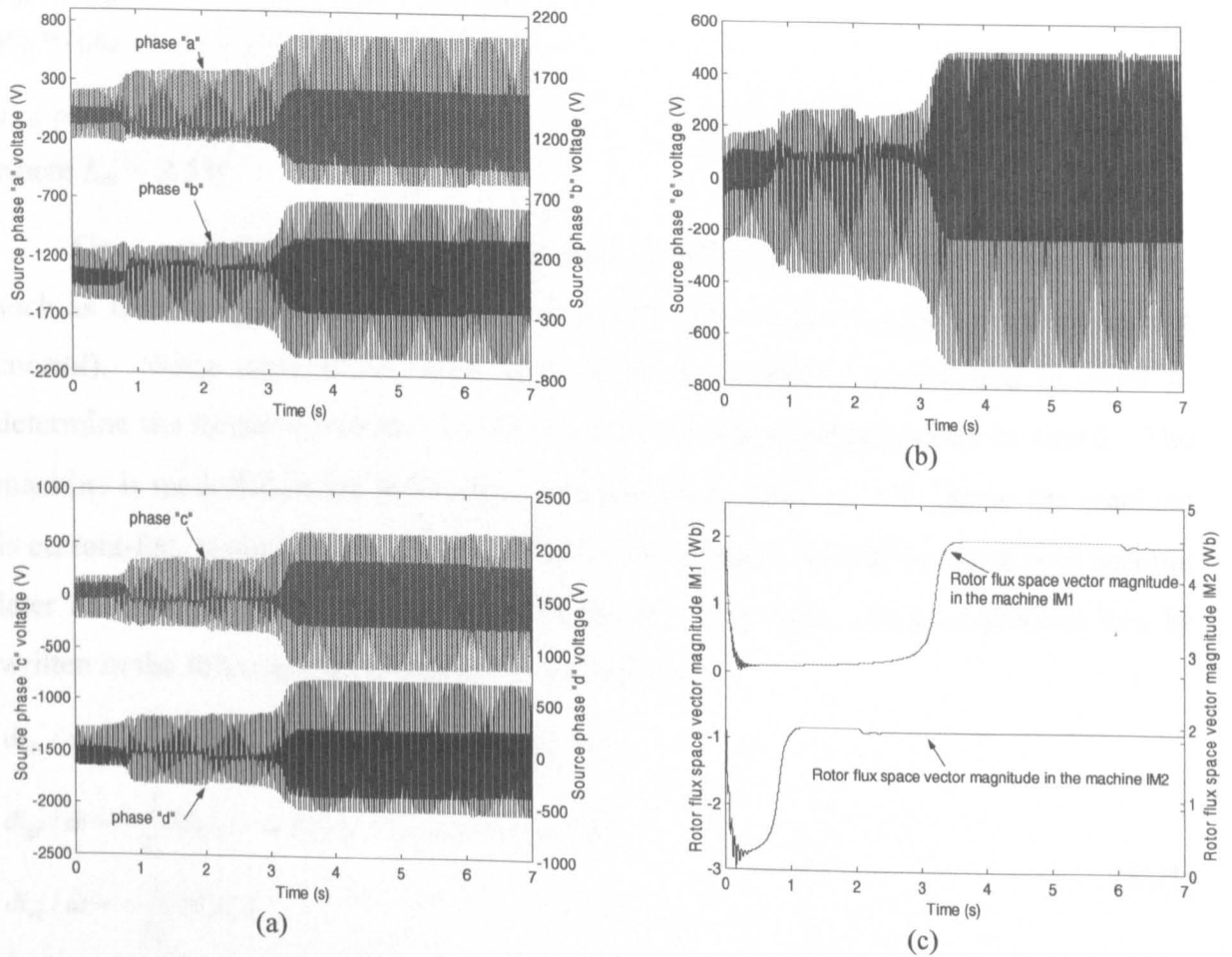


Fig. 5.13: Simulation results of two five-phase induction machines connected in series during direct on-line starting (phase-domain model): source phase “a-d” voltages (a), source phase “e” voltage (b) and rotor flux magnitude in each machine (c).

5.3.2 Series connection of two five-phase machines using stationary reference frame model

From the common reference frame model (rotating at arbitrary speed) of an n -phase induction machine given with (3.30)-(3.32), one has for the five-phase machine the following:

$$\begin{aligned}
 v_{ds} &= R_s i_{ds} - \omega_a \psi_{qs} + p \psi_{ds} & v_{dr} &= R_r i_{dr} - (\omega_a - \omega) \psi_{qr} + p \psi_{dr} \\
 v_{qs} &= R_s i_{qs} + \omega_a \psi_{ds} + p \psi_{qs} & v_{qr} &= R_r i_{qr} + (\omega_a - \omega) \psi_{dr} + p \psi_{qr} \\
 v_{xs} &= R_s i_{xs} + p \psi_{xs} & v_{xr} &= R_r i_{xr} + p \psi_{xr} \\
 v_{ys} &= R_s i_{ys} + p \psi_{ys} & v_{yr} &= R_r i_{yr} + p \psi_{yr} \\
 v_{os} &= R_s i_{os} + p \psi_{os} & v_{or} &= R_r i_{or} + p \psi_{or}
 \end{aligned} \tag{5.18}$$

$$\begin{aligned}
 \psi_{ds} &= (L_{ls} + L_m)i_{ds} + L_m i_{dr} & \psi_{dr} &= (L_{lr} + L_m)i_{dr} + L_m i_{ds} \\
 \psi_{qs} &= (L_{ls} + L_m)i_{qs} + L_m i_{qr} & \psi_{qr} &= (L_{lr} + L_m)i_{qr} + L_m i_{qs} \\
 \psi_{xs} &= L_{ls} i_{xs} & \psi_{xr} &= L_{lr} i_{xr} \\
 \psi_{ys} &= L_{ls} i_{ys} & \psi_{yr} &= L_{lr} i_{yr} \\
 \psi_{os} &= L_{ls} i_{os} & \psi_{or} &= L_{lr} i_{or}
 \end{aligned} \tag{5.19}$$

$$T_e = PL_m [i_{dr} i_{qs} - i_{ds} i_{qr}] \tag{5.20}$$

where $L_m = 2.5M$

Once again the machine is considered as being fed by an ideal current source, such as for example a current controlled voltage source inverter (with perfect current control). Stator currents and their derivatives are therefore known and in order to determine the torque developed by the machine the rotor currents must be found. The machine is modelled in the stationary reference frame; thus $\omega_d = 0$. Since the machine is current-fed, stator voltage equations are omitted again and will be taken into account later on in calculation of stator phase voltages. The rotor voltage equations can be written in the following form suitable for simulation:

$$\begin{aligned}
 di_{dr} / dt &= -\frac{1}{L_r} (R_r i_{dr} + \omega (L_r i_{qr} + L_m i_{\beta s}) + L_m di_{\alpha s} / dt) \\
 di_{qr} / dt &= -\frac{1}{L_r} (R_r i_{qr} - \omega (L_r i_{dr} + L_m i_{\alpha s}) + L_m di_{\beta s} / dt) \\
 di_{xr} / dt &= -\frac{1}{L_{lr}} (R_r i_{xr}) \\
 di_{yr} / dt &= -\frac{1}{L_{lr}} (R_r i_{yr})
 \end{aligned} \tag{5.21}$$

The equation for zero sequence components is omitted since there is no possibility of having such a component in the short-circuited rotor. Furthermore x-y components of rotor current will be identically equal to zero since there is no excitation in this part of the electric circuit. This is so since x-y components of the rotor are not coupled with x-y components of the stator (and are not coupled with α - β components either), so that there are no induced voltages in x-y circuits of rotor that could give rise to x-y rotor current components. This means that the second pair of equations in (5.21) can be omitted from further consideration. The stator voltages are reconstructed by finding at first the stator voltage α - β and x-y components according to:

$$\begin{aligned}
 v_{\alpha s} &= R_s i_{\alpha s} + L_s p i_{\alpha s} + L_m p i_{dr} \\
 v_{\beta s} &= R_s i_{\beta s} + L_s p i_{\beta s} + L_m p i_{qr} \\
 v_{xs} &= R_s i_{xs} + L_{ls} p i_{xs} \\
 v_{ys} &= R_s i_{ys} + L_{ls} p i_{ys} \\
 v_{0s} &= R_s i_{0s} + L_{ls} p i_{0s}
 \end{aligned} \tag{5.22}$$

Zero sequence components, although included in (5.22), will not exist due to star connection of the winding. Equation (5.22) is further used to calculate the phase voltages of the machine. Correlation between known stator phase currents and stator current components required in (5.21), as well as the correlation between calculated stator voltage components of (5.22) and actual stator phase voltages are governed with the decoupling transformation matrix \underline{C} and its inverse, obtained from (3.13)-(3.14) by setting $n = 5$:

$$\underline{C} = \sqrt{\frac{2}{5}} \begin{bmatrix} 1 & \cos \alpha & \cos 2\alpha & \cos 2\alpha & \cos \alpha \\ 0 & \sin \alpha & \sin 2\alpha & -\sin 2\alpha & -\sin \alpha \\ 1 & \cos 2\alpha & \cos 4\alpha & \cos 4\alpha & \cos 2\alpha \\ 0 & \sin 2\alpha & \sin 4\alpha & -\sin 4\alpha & -\sin 2\alpha \\ \frac{1}{\sqrt{2}} & \frac{1}{\sqrt{2}} & \frac{1}{\sqrt{2}} & \frac{1}{\sqrt{2}} & \frac{1}{\sqrt{2}} \end{bmatrix} \quad \underline{C}^{-1} = \sqrt{\frac{2}{5}} \begin{bmatrix} 1 & 0 & 1 & 0 & \frac{1}{\sqrt{2}} \\ \cos \alpha & \sin \alpha & \cos 2\alpha & \sin 2\alpha & \frac{1}{\sqrt{2}} \\ \cos 2\alpha & \sin 2\alpha & \cos 4\alpha & \sin 4\alpha & \frac{1}{\sqrt{2}} \\ \cos 2\alpha & -\sin 2\alpha & \cos 4\alpha & -\sin 4\alpha & \frac{1}{\sqrt{2}} \\ \cos \alpha & -\sin \alpha & \cos 2\alpha & -\sin 2\alpha & \frac{1}{\sqrt{2}} \end{bmatrix} \quad (5.23a)$$

so that:

$$\underline{i}_{\alpha\beta}^s = \underline{C} \underline{i}_{abcde}^s \quad \underline{v}_{abcde}^s = \underline{C}^{-1} \underline{v}_{\alpha\beta}^s \quad (5.23b)$$

The rotor currents are reconstructed into phase-variable form by applying the inverse transformation to the d-q rotor currents taking into account the rotational transformation. In other words calculation of actual rotor currents requires application of the complete transformation matrix (i.e. both decoupling and rotational transformation matrices):

$$\begin{aligned} i_{ar} &= \sqrt{\frac{2}{5}} (i_{\alpha r} \cos \beta - i_{\beta r} \sin \beta) \\ i_{br} &= \sqrt{\frac{2}{5}} (i_{\alpha r} \cos(\beta - \alpha) - i_{\beta r} \sin(\beta - \alpha)) \\ i_{cr} &= \sqrt{\frac{2}{5}} (i_{\alpha r} \cos(\beta - 2\alpha) - i_{\beta r} \sin(\beta - 2\alpha)) \\ i_{dr} &= \sqrt{\frac{2}{5}} (i_{\alpha r} \cos(\beta + 2\alpha) - i_{\beta r} \sin(\beta + 2\alpha)) \\ i_{er} &= \sqrt{\frac{2}{5}} (i_{\alpha r} \cos(\beta + \alpha) - i_{\beta r} \sin(\beta + \alpha)) \end{aligned} \quad (5.24)$$

where $\beta = -\theta$, $\theta = \int \omega dt$. The zero sequence components and the x-y components of rotor currents are all zero and are therefore omitted from (5.24). The rotor flux

$$\begin{aligned}\psi_{dr} &= L_r i_{dr} + L_m i_{\alpha s} \\ \psi_{qr} &= L_r i_{qr} + L_m i_{\beta s} \\ \psi_r &= \sqrt{(\psi_{dr})^2 + (\psi_{qr})^2}\end{aligned}\tag{5.25}$$

The electrical speed of the machine and the electromagnetic torque are given by:

$$\omega = \frac{P}{J} \int (T_e - T_l) dt\tag{5.26a}$$

$$T_e = PL_m (i_{dr} i_{\beta s} - i_{\alpha s} i_{qr})\tag{5.26b}$$

The two machines are connected in the same manner as in the phase-domain case (Fig. 5.8). The input stator currents for the first and the second machine are transformed separately using the transformation matrix \underline{C} . The model of the machine is then solved independently for the two machines and stator voltage components are calculated. Stator phase voltages for the two machines are then found using the inverse transformation matrix \underline{C}^{-1} . Finally, source phase voltages are calculated by means of (5.17).

5.3.3 Simulation of two five-phase induction machines using model in the stationary reference frame

In order to investigate the correctness of the machine model of section 5.3.2 a program is created using MATLAB/SIMULINK software. A simulation is run with each machine operating under identical conditions as those used for the phase-domain model in section 5.3.1. Therefore the stator phase currents of each machine remain as shown in Fig. 5.9. The torque and speed response of each machine are illustrated in Fig. 5.14a, where it can be seen that the response is identical to that shown in Fig. 5.10, where the phase-domain machine models were used. Figures 5.14b, 5.14c and 5.14d show the rotor currents, source voltages and machine voltages for the first two phases (phase “a” and “b”), respectively, and are identical to those shown in Figs. 5.11–5.13. Figure 5.14b also shows the rotor flux response of each machine, which is again identical to that shown in Fig. 5.13c. Thus it is proven that the modelling the two machines in the stationary reference frame provides the same results as those obtained using the phase-domain models, however the stationary reference frame model is much simpler and requires less processing time.

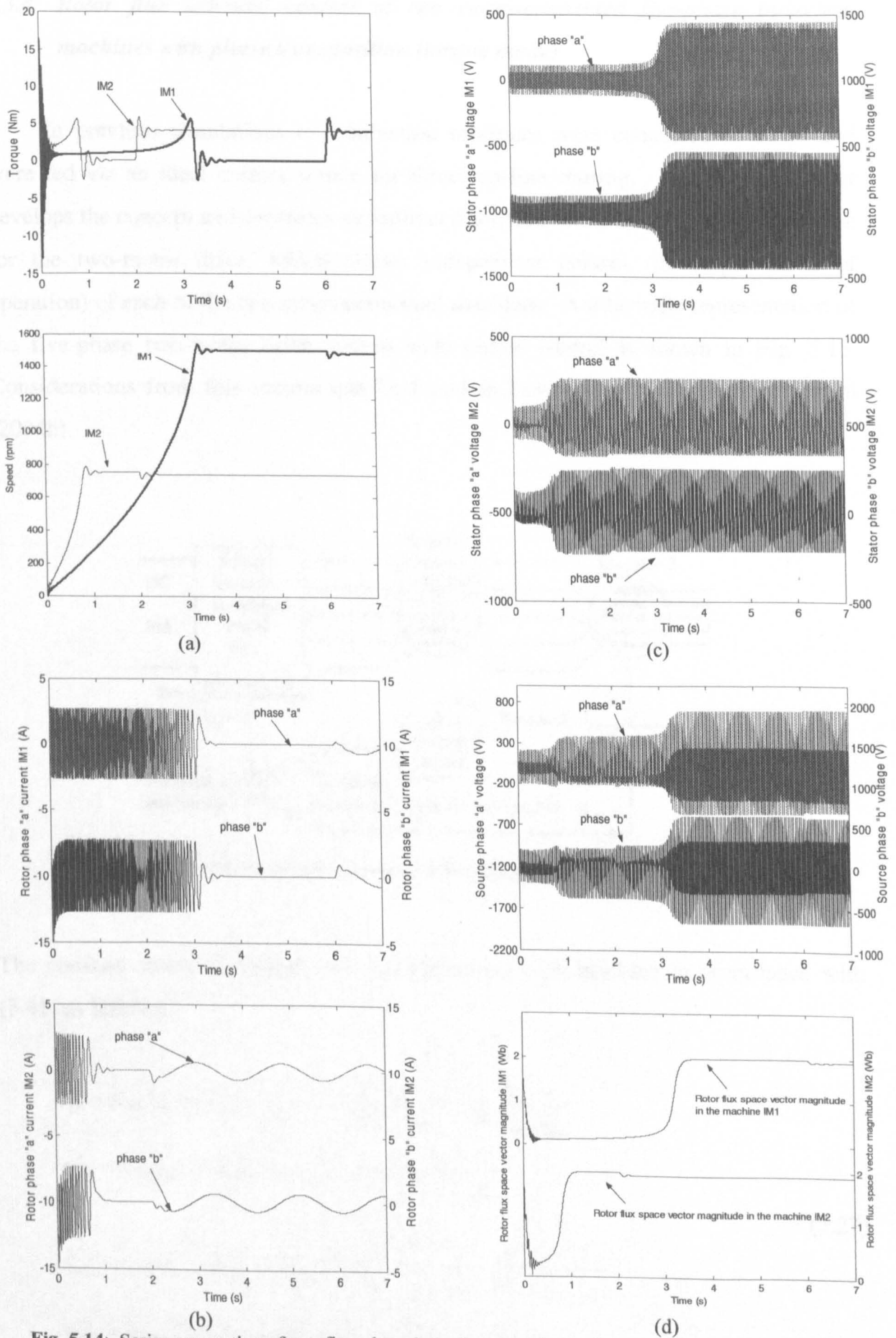


Fig. 5.14: Series connection of two five-phase induction machines using stationary reference frame model: Speed and torque response, IM1, IM2 (a), phase "a-b" rotor currents IM1, IM2 (b), phase "a-b" stator voltage, IM1, IM2 (c), source phase "a-b" voltages and rotor flux magnitude in each machine (d).

5.3.4 Rotor flux oriented control of two series-connected five-phase induction machines with phase transposition (torque mode)

In previous simulations two induction machines were connected in series and were fed via an ideal current source for direct on-line starting. This section further develops the concept and considers an indirect rotor flux oriented vector control scheme for the two-motor drive, which allows independent control (in torque mode of operation) of each of the two series-connected machines. A schematic representation of the five-phase two-motor drive system with vector control is shown in Fig. 5.15. Considerations from this section can be found in Levi et al (2003b) and Levi et al (2004b).

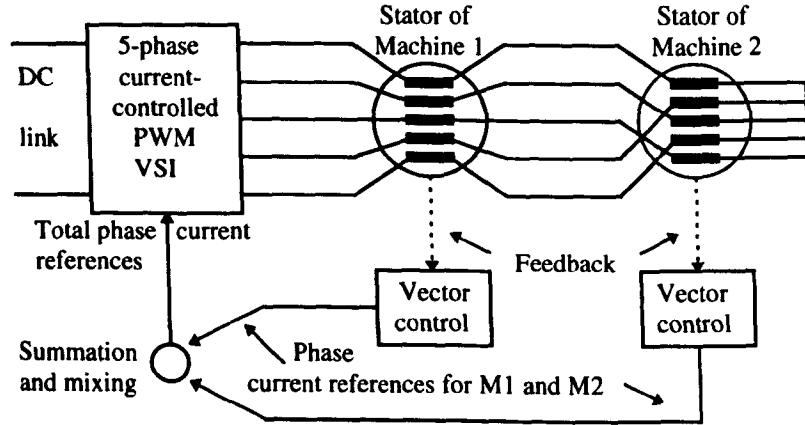


Fig.5.15: Vector control scheme for a five-phase two-motor drive system.

The constant terms K_1 and K_2 are determined for each machine in accordance with (3.41) as follows:

$$\begin{aligned}
 i_{qs1}^* &= K_{1(1)} T_{e1}^* \Rightarrow K_{1(1)} = i_{qs1}^* / T_{e1}^* = \frac{1}{P_1} \frac{L_{r1}}{L_{m1}} \frac{1}{\psi_{r1}^*} = \frac{1}{P_1} \frac{L_{r1}}{L_{m1}^2} \frac{1}{i_{ds1}^*} \\
 \omega_{sl1}^* &= K_{2(1)} i_{qs1}^* \Rightarrow K_{2(1)} = \omega_{sl1}^* / i_{qs1}^* = \frac{L_{m1}}{T_{r1} \psi_{r1}^*} = \frac{1}{T_{r1} i_{ds1}^*} \\
 i_{qs2}^* &= K_{1(2)} T_{e2}^* \Rightarrow K_{1(2)} = i_{qs2}^* / T_{e2}^* = \frac{1}{P_2} \frac{L_{r2}}{L_{m2}} \frac{1}{\psi_{r2}^*} = \frac{1}{P_2} \frac{L_{r2}}{L_{m2}^2} \frac{1}{i_{ds2}^*} \\
 \omega_{sl2}^* &= K_{2(2)} i_{qs2}^* \Rightarrow K_{2(2)} = \omega_{sl2}^* / i_{qs2}^* = \frac{L_{m2}}{T_{r2} \psi_{r2}^*} = \frac{1}{T_{r2} i_{ds2}^*}
 \end{aligned}
 \tag{5.27}$$

Phase current references are further formed separately for the two machines, as follows:

$$\begin{aligned}
 i_{a1}^* &= \sqrt{\frac{2}{5}}(i_{ds1}^* \cos \phi_{r1} - i_{qs1}^* \sin \phi_{r1}) \\
 i_{b1}^* &= \sqrt{\frac{2}{5}}(i_{ds1}^* \cos(\phi_{r1} - \alpha) - i_{qs1}^* \sin(\phi_{r1} - \alpha)) \\
 i_{c1}^* &= \sqrt{\frac{2}{5}}(i_{ds1}^* \cos(\phi_{r1} - 2\alpha) - i_{qs1}^* \sin(\phi_{r1} - 2\alpha)) \\
 i_{d1}^* &= \sqrt{\frac{2}{5}}(i_{ds1}^* \cos(\phi_{r1} + 2\alpha) - i_{qs1}^* \sin(\phi_{r1} + 2\alpha)) \\
 i_{e1}^* &= \sqrt{\frac{2}{5}}(i_{ds1}^* \cos(\phi_{r1} + \alpha) - i_{qs1}^* \sin(\phi_{r1} + \alpha)) \\
 \\
 i_{a2}^* &= \sqrt{\frac{2}{5}}(i_{ds2}^* \cos \phi_{r2} - i_{qs2}^* \sin \phi_{r2}) \\
 i_{b2}^* &= \sqrt{\frac{2}{5}}(i_{ds2}^* \cos(\phi_{r2} - \alpha) - i_{qs2}^* \sin(\phi_{r2} - \alpha)) \\
 i_{c2}^* &= \sqrt{\frac{2}{5}}(i_{ds2}^* \cos(\phi_{r2} - 2\alpha) - i_{qs2}^* \sin(\phi_{r2} - 2\alpha)) \\
 i_{d2}^* &= \sqrt{\frac{2}{5}}(i_{ds2}^* \cos(\phi_{r2} + 2\alpha) - i_{qs2}^* \sin(\phi_{r2} + 2\alpha)) \\
 i_{e2}^* &= \sqrt{\frac{2}{5}}(i_{ds2}^* \cos(\phi_{r2} + \alpha) - i_{qs2}^* \sin(\phi_{r2} + \alpha))
 \end{aligned} \tag{5.28}$$

Resultant inverter current references are given with:

$$\begin{aligned}
 i_A^* &= i_{a1}^* + i_{a2}^* \equiv i_A \\
 i_B^* &= i_{b1}^* + i_{c2}^* \equiv i_B \\
 i_C^* &= i_{c1}^* + i_{e2}^* \equiv i_C \\
 i_D^* &= i_{d1}^* + i_{b2}^* \equiv i_D \\
 i_E^* &= i_{e1}^* + i_{d2}^* \equiv i_E
 \end{aligned} \tag{5.29}$$

Due to assumed ideal current feeding these are identically equal to the actual inverter output currents, as indicated in (5.29). Currents of (5.29) are therefore simultaneously the input currents of machine 1. Due to phase transposition, the input phase currents of machine 2 are:

$$\begin{aligned}
 i_{a2} &= i_A = i_A^* \\
 i_{b2} &= i_D = i_D^* \\
 i_{c2} &= i_B = i_B^* \\
 i_{d2} &= i_E = i_E^* \\
 i_{e2} &= i_C = i_C^*
 \end{aligned} \tag{5.30}$$

Source phase voltages are determined using equation (5.17).

5.3.5 Simulation of series connection of two five-phase machines (torque mode) using phase-domain model

The system was initially investigated using the phase-domain machine model and later investigated using the d-q machine model in the stationary reference frame. Rotor flux reference (stator d-axis current reference) is applied at first to excite the machines. Different profiles of rotor flux reference are applied to each machine (Fig. 5.16c). Once the rated rotor flux in both machines has been established, torque command is first applied to machine one (IM1) at $t = 0.3$ s and removed at $t = 0.55$ s in a ramp wise manner. Torque reference is applied at $t = 0.35$ s and removed at $t = 0.5$ s for the second machine (IM2) in a ramp wise manner. Torque reference for the first machine equals twice the rated torque (16.67 Nm), while torque reference for the second machine is the rated value (8.33 Nm). It is assumed that the inverter is ideal and so inverter current references match actual inverter currents.

As can be seen from Fig. 5.16a torque references and actual torques developed by the machines are mutually indistinguishable. Application of the torque command to one of the machines has no effect upon the torque developed by the other machine. Speed response of each machine is smooth, with maximum allowed rate of change, Fig. 5.16b. Stator phase “a” current references for the two machines are shown in Fig. 5.16d and are similar to those seen in a standard vector controlled three-phase machine. Rotor flux remains undisturbed in both machines during torque transients indicating that decoupled control has been achieved. High level of distortion is evident in both source currents and source voltages (Figs. 5.17a and 5.17b, respectively). The same applies to individual machine phase voltages illustrated in Fig. 5.18b for phase “a”. Rotor currents remain identical to the situation when only one machine is present (Fig. 5.18a) showing that x-y currents don’t flow in the rotors of the machines.

As already noted, the flow of torque and flux producing currents of each machine through the stator of both machines is the main drawback of this system. The flow of non torque/flux producing currents through the stator of each machine will lead to an increase in the stator copper losses and reduce the efficiency of the system. Another drawback, caused by this current flow is the voltage drop produced by the x-y stator current components in both machines. This will impact on the voltage rating of the inverter semiconductors.

5.3.6. Simulation of series connection of two five-phase machines (torque mode) using stationary reference frame machine model

Once again a program was written using the stationary reference frame machine model for the identical situation to the one previously presented. Once more, the same results were obtained as with the phase variable model. These figures are therefore not shown. Fig. 5.19 shows the stator α - β and x-y current components in the stationary reference frame, respectively, as seen by machine 1. One can see that the α - β components correspond to the stator phase current references of machine 1, while x-y components correspond to stator phase current references of machine 2. In particular, α -axis current equals phase "a" current reference of machine 1 in Fig. 5.16d, while x-axis current equals phase "a" current reference of machine 2 in Fig. 5.16d, except for the scaling factor in the transformation.

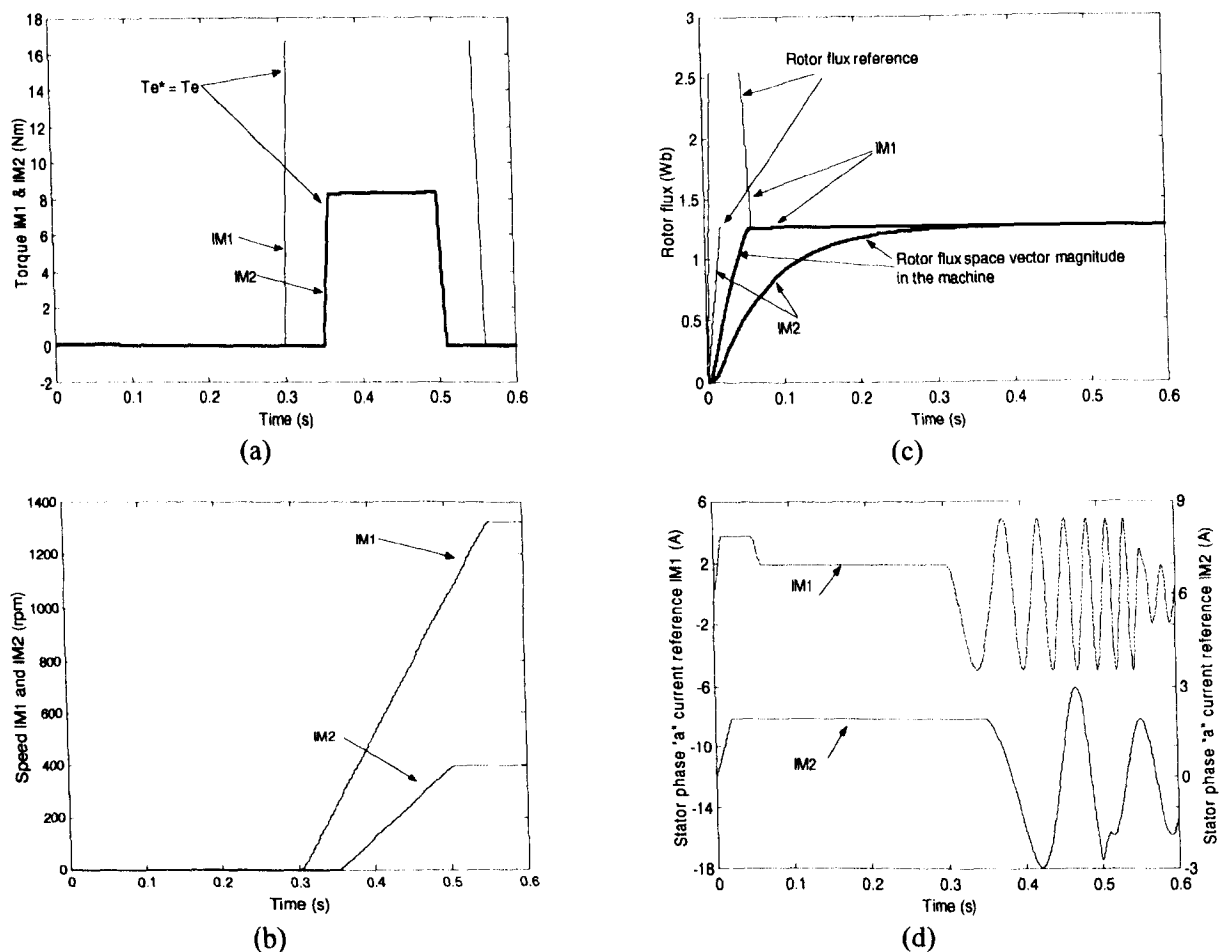


Fig. 5.16: Indirect vector control of two series-connected five-phase induction machines using phase variable machine model. Torque response (a), speed responses (b), rotor flux reference and rotor flux magnitude in the machines (c) and stator phase "a" current reference (d).

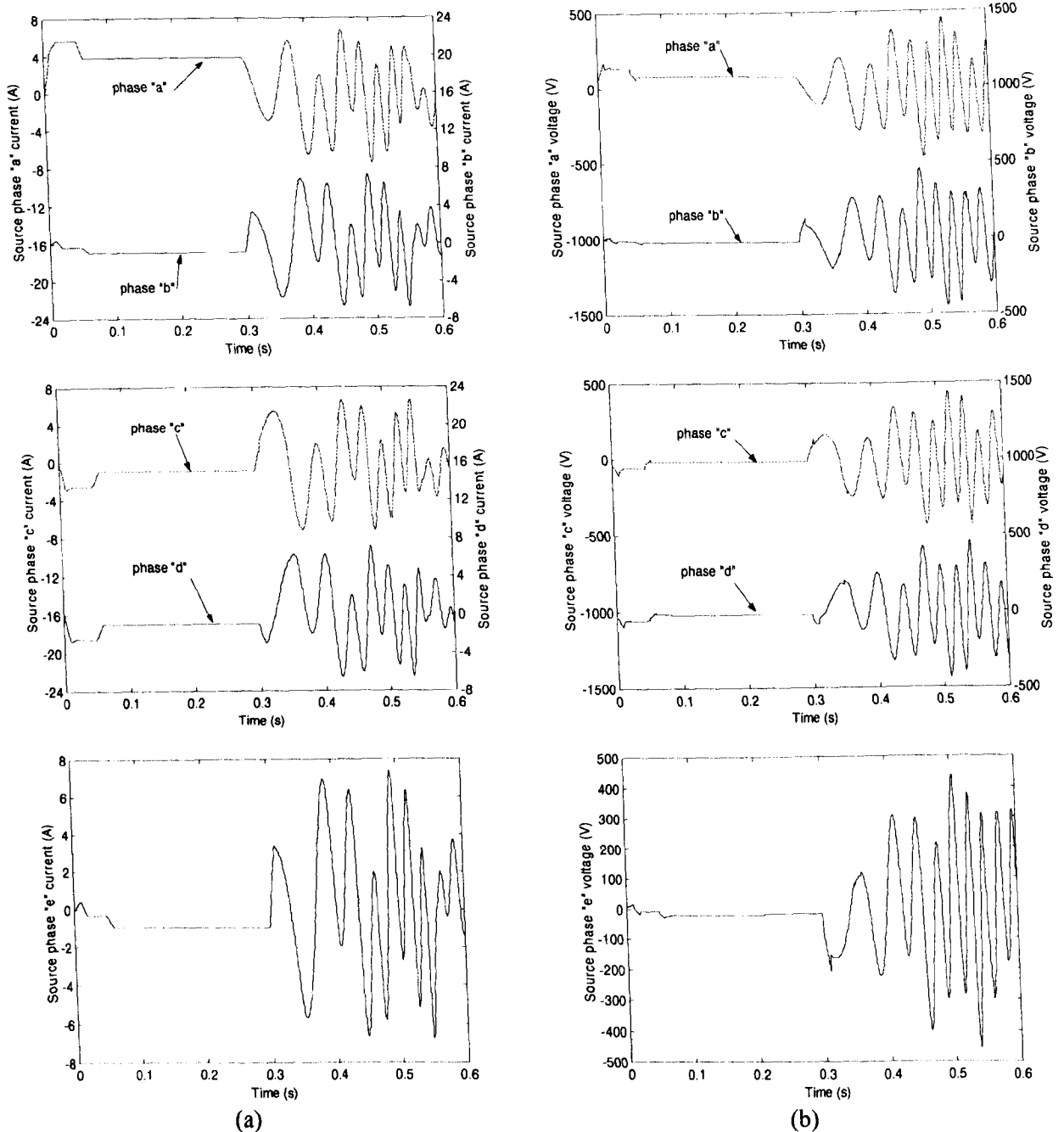


Fig. 5.17: Indirect vector control of two series-connected five-phase induction machines using phase variable machine model. Source currents (a) and source voltages (b).

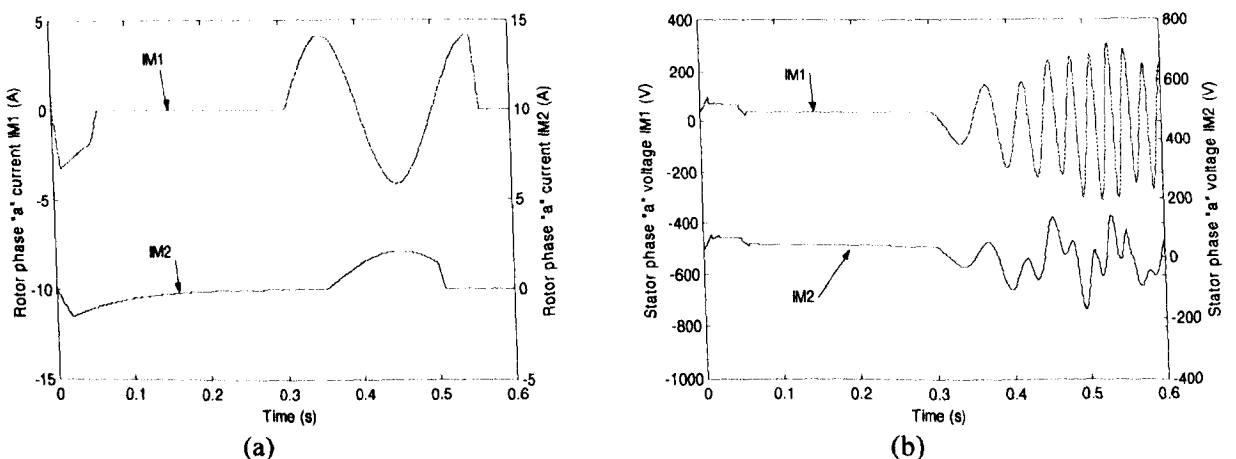


Fig. 5.18: Indirect vector control of two series-connected five-phase induction machines using phase variable machine model. Rotor phase "a" currents (a) and stator phase "a" voltages (b) for the two machines.

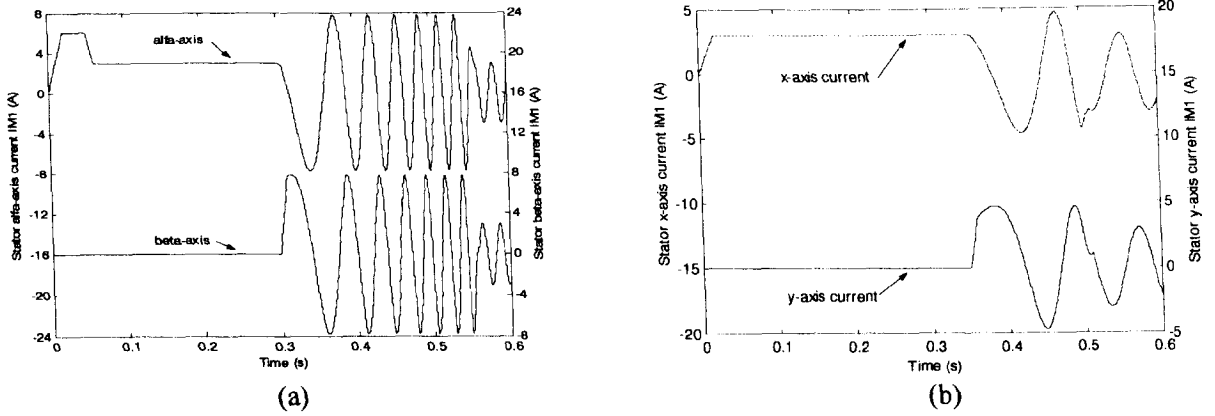


Fig. 5.19: Indirect vector control of two series-connected five-phase induction machines using stationary reference frame machine model. Stator current α - β components (a) and x-y components (b) in machine 1.

5.3.7 Rotor flux oriented control of two series-connected five-phase induction machines (speed mode)

Many applications require precise control of motor speed and so operation of the multi-phase multi-machine drive using closed loop speed control (i.e., including a speed controller (PI) as in Figure 3.1) is examined next. Figure 5.20 shows the structure of the speed control loop. The inverter is assumed as ideal and so delays associated with the inverter are ignored along with any signal processing delays.

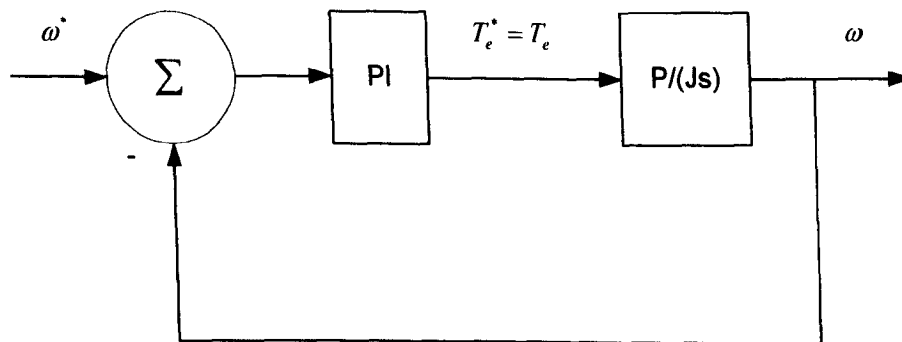


Fig. 5.20: Structure of the speed control loop

The transfer function for the PI controller is:

$$G_{PI}(s) = K_p + K_i \frac{1}{s} = K_p \left(1 + \frac{1}{T_i s} \right) \quad (5.31)$$

The characteristic equation of the above speed control loop is solved for $1 + G_{PI}(s)H(s) = 0$, where according to Fig. 5.20 $H(s) = 1/(Js/P)$. Hence the characteristic equation is:

$$s^2 + 66.67K_p s + \omega_0^2 = 0 \quad (5.32)$$

The coefficients of (5.32) are equated with those in (5.33), which defines the desired closed loop dynamic response in terms of damping ratio ξ and natural frequency ω_0 :

$$s^2 + 2\xi\omega_0 s + \omega_0^2 = 0 \quad (5.33)$$

Damping ratio is selected as 0.707. The natural frequency for the speed control loop is dependent on the bandwidth of the inner current loop. For the purpose of the speed controller design, current loop bandwidth is taken as 100 Hz [Iqbal (2003)]. Taking the speed control bandwidth as one tenth of this value (10 Hz) and approximating the natural frequency with the bandwidth, one has $\omega_0 = 62.8318$ rad/s. Substitution of the damping ratio and natural frequency values into (5.33) and comparison with (5.32) yield the following values for the speed controller parameters; $K_p = 1.332$, $K_i = 59.214$ and $T_i = 0.0225$ s. These values were fine-tuned and PI controller gains used further on in all simulations (regardless of the number of phases of the system and the number of motors in the group) are $K_p = 1.5$, $K_i = 75$ ($T_i = 0.02$ s). In order to avoid problems with integral wind-up during operation in the torque limit, an anti wind-up PI controller is used.

5.3.8 Simulation of series connection of two five-phase machines (speed mode)

The two machines are represented using the phase-domain model and are excited using the same rotor flux reference profile as illustrated in Fig. 5.21c. It is assumed that the inverter is ideal and so inverter phase currents exactly match inverter phase current references. A speed command is applied to each machine at different times once the rotor flux has reached rated value. A speed command of rated value (299 rad/s) is applied to machine 1 in a ramp wise manner (rise time $t = 0.3 - 0.31$ s), while a speed command of one half rated (149 rad/s) is applied to machine 2 in a ramp wise manner (rise time $t = 0.4 - 0.41$ s). The torque limit of both machines is set to twice the rated value (16.67 Nm). A load torque of 4 Nm was applied to machine 2 at $t = 0.65$ s in a stepwise manner.

The torque almost instantly steps to the maximum allowed value upon application

of the speed command and stays there until the desired speed has been reached (Fig 5.21a). Once again one can see from the resulting graphs that decoupled flux and torque control has been achieved for both machines and each machine is controlled independently. Application of a load to machine 2 results in a very small deviation in the speed of the machine from the commanded value, which is very quickly corrected. The application of a load to machine 2 in no way affects the speed or torque developed by machine 1 (Fig. 5.21a-b).

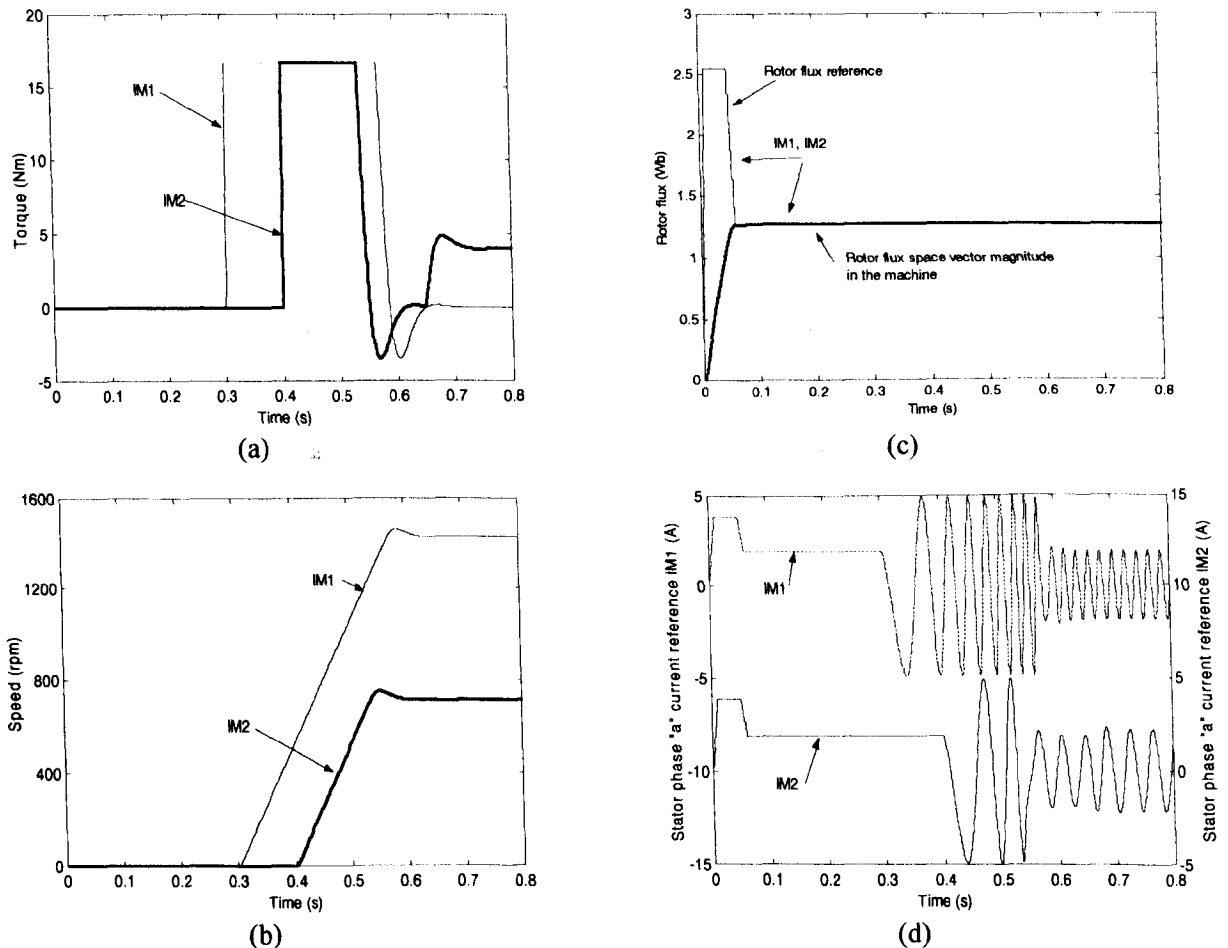


Fig. 5.21: Rotor flux oriented control of two series-connected five-phase induction motors in the speed mode using phase variable model. Torque response (a), speed response (b), rotor flux reference and rotor flux response (c) and stator phase “a” current references for the two machines (d).

Stator phase current references for the two machines are shown for phase “a” in Fig. 5.21d. Source currents and source voltages are illustrated in Fig. 5.22. The same considerations as those given in conjunction with Figs. 5.16-5.19 for torque are also valid here.

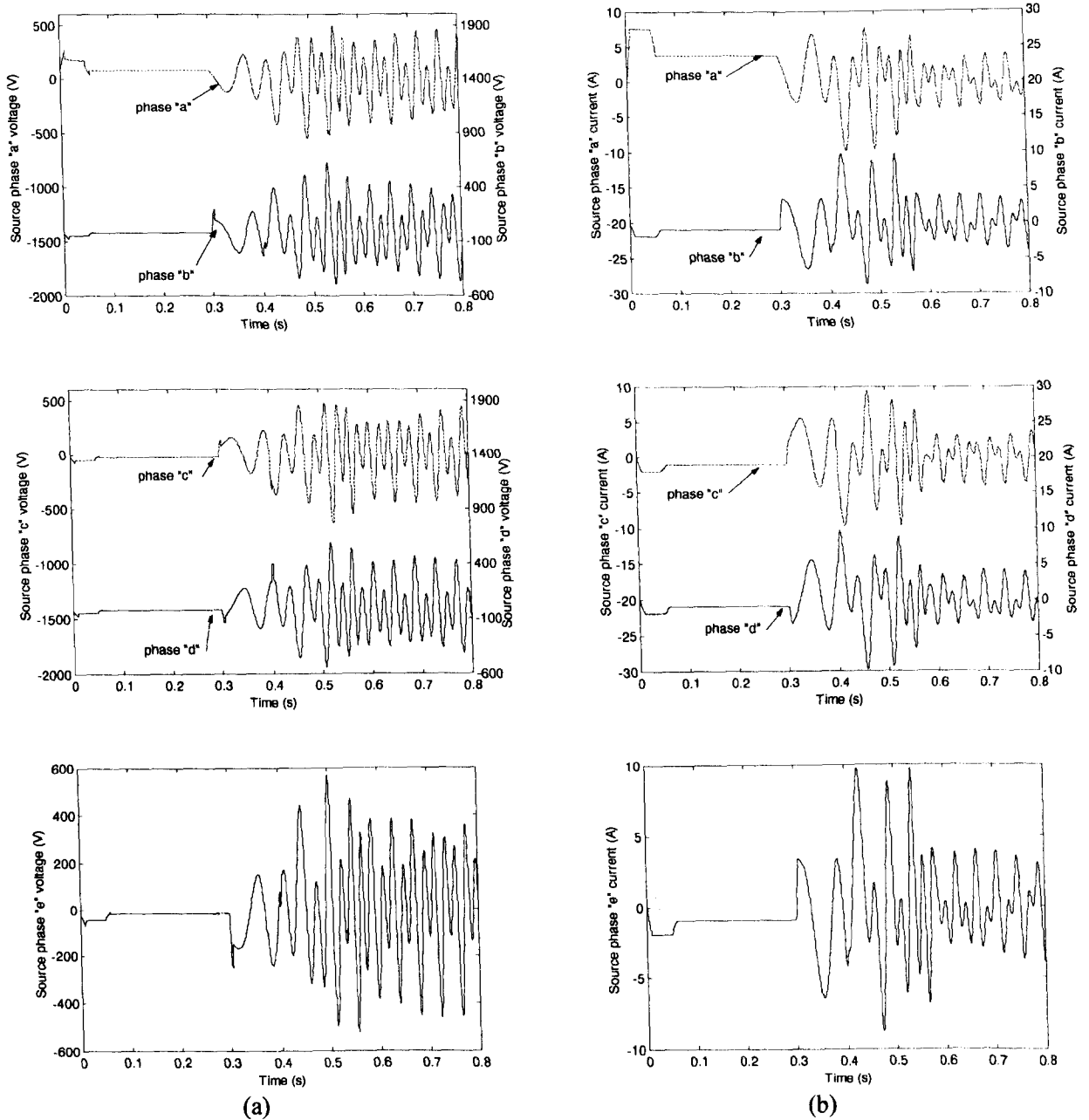


Fig. 5.22: Rotor flux oriented control of two series-connected five-phase induction motors in the speed mode using phase variable model. Source voltages (a) and source currents (b).

5.4 The nine-phase four-motor drive

This section examines the nine-phase four-motor drive and includes results published in Jones et al (2003a). The nine-phase case is of particular interest because it falls under category b in section 4.5.1, where it is shown that the number of connectable machines remains to be given with $(n-1)/2$. However, the number of phases is not a prime number and satisfies the condition $n = 3^m$. Thus only three of the machines will be nine-phase. The remaining machine will have three-phases as shown in the

connectivity matrix given in Table 4.4. The connection diagram given in Fig. 4.3 is repeated for convenience in Fig. 5.23. As discussed in section 4.3 the position of the three-phase machine is of critical importance and it must be connected last (with respect to the nine-phase source) in the multi-phase multi-motor drive.

The connection diagram shown in Fig 5.23 governs inverter phase voltages. They are determined with an appropriate summation of stator phase voltages of individual machines respecting the phase transposition.

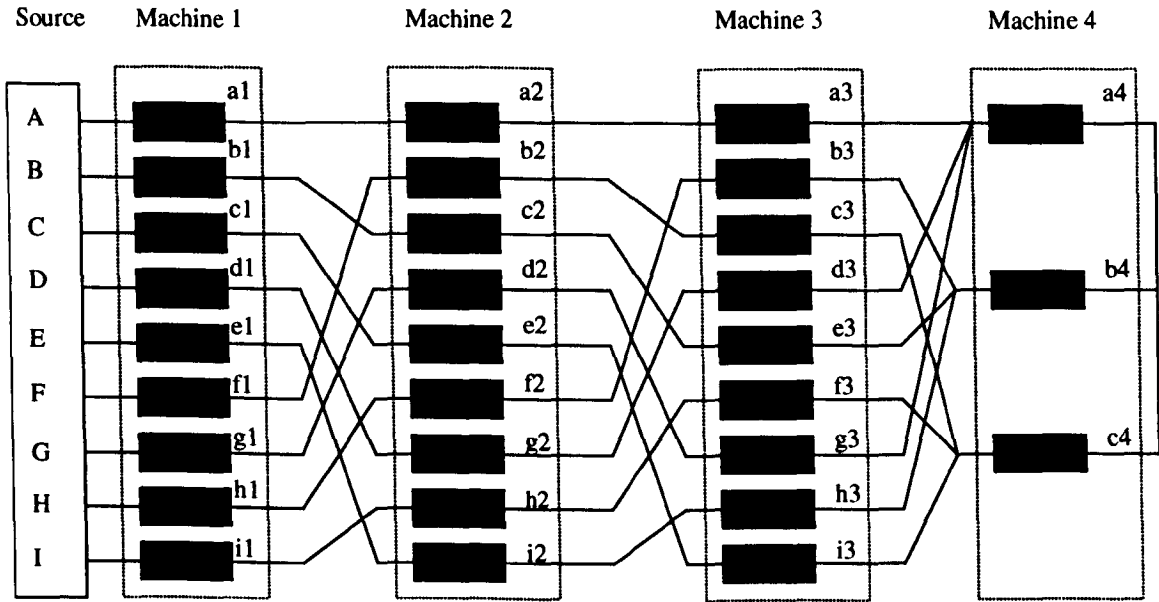


Fig. 5.23: Connection diagram for the nine-phase case: three nine-phase machines and one three-phase machine are connected in series.

$$\begin{aligned}
 v_A &= v_{as1} + v_{as2} + v_{as3} + v_{as4} \\
 v_B &= v_{bs1} + v_{cs2} + v_{es3} + v_{bs4} \\
 v_C &= v_{cs1} + v_{es2} + v_{is3} + v_{cs4} \\
 v_D &= v_{ds1} + v_{gs2} + v_{ds3} + v_{as4} \\
 v_E &= v_{es1} + v_{is2} + v_{hs3} + v_{bs4} \\
 v_F &= v_{fs1} + v_{bs2} + v_{cs3} + v_{cs4} \\
 v_G &= v_{gs1} + v_{ds2} + v_{gs3} + v_{as4} \\
 v_H &= v_{hs1} + v_{fs2} + v_{bs3} + v_{bs4} \\
 v_I &= v_{is1} + v_{hs2} + v_{fs3} + v_{cs4}
 \end{aligned} \tag{5.34}$$

The individual machine phase current references generated by the controllers are summed according to the phase transposition in Fig. 5.23. Thus the inverter current references are given as [Jones et al (2003a)]:

$$\begin{aligned}
 i_A^* &= i_{a1}^* + i_{a2}^* + i_{a3}^* + (1/3)_{a4}^* \\
 i_B^* &= i_{b1}^* + i_{c2}^* + i_{e3}^* + (1/3)_{b4}^* \\
 i_C^* &= i_{c1}^* + i_{e2}^* + i_{i3}^* + (1/3)_{c4}^* \\
 i_D^* &= i_{d1}^* + i_{g2}^* + i_{d3}^* + (1/3)_{a4}^* \\
 i_E^* &= i_{e1}^* + i_{i2}^* + i_{h3}^* + (1/3)_{b4}^* \\
 i_F^* &= i_{f1}^* + i_{b2}^* + i_{c3}^* + (1/3)_{c4}^* \\
 i_G^* &= i_{g1}^* + i_{d2}^* + i_{g3}^* + (1/3)_{a4}^* \\
 i_H^* &= i_{h1}^* + i_{f2}^* + i_{b3}^* + (1/3)_{b4}^* \\
 i_i^* &= i_{i1}^* + i_{h2}^* + i_{f3}^* + (1/3)_{c4}^*
 \end{aligned} \tag{5.35}$$

5.4.1 Simulation of rotor flux oriented control of three nine-phase and one three-phase induction machines connected in series (torque mode)

The system was verified by simulating the acceleration transient during torque mode of operation. The machines were modelled in the stationary reference frame as described in chapter 3. Initially the machines are magnetised using the same procedure as described in section 5.3.8 (respecting the different rotor flux ratings). Torque references are applied and removed using ramps of 0.01s duration as shown in Table 5.3. Each machine accelerates smoothly (Fig. 5.24a) and no variation in rotor flux can be seen for any of the machines (Fig. 5.24b) during the acceleration transient, meaning that completely decoupled flux and torque control has been achieved not only in one machine but between the machines as well. The torque response of each machine follows the reference torque without any deviation (Fig 5.24c) and so the speed response of each machine is the fastest possible. The stator phase “a” current reference is shown in Fig 5.25a for each of the four machines. The inverter currents for the first four phases are given in Fig 5.25b. The current references are essentially sinusoidal in final steady-state. Inverter currents are a summation of the current references taking into account the phase transposition and are therefore highly distorted. The same applies to the stator phase voltages of the nine-phase machines, which are shown in Fig. 5.26 together with the overall inverter output phase voltages for the first four phases.

Due to series connection of the stator windings, x-y voltage components exist in all the nine-phase machines, leading to distorted stator voltage waveforms. The worst level of distortion can be clearly seen in machine three. This is because this machine has the lowest speed of rotation of all the nine-phase machines. It can be seen that the

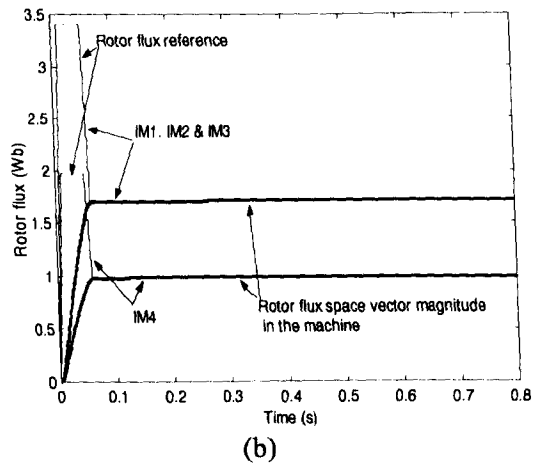
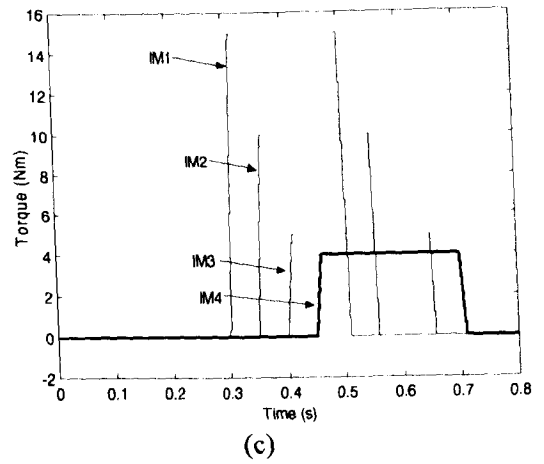
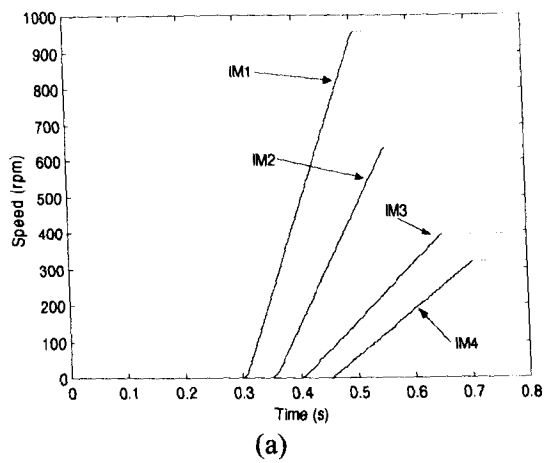


Fig. 5.24: Vector control of the four-motor nine-phase drive: Speed response (a) rotor flux reference and responses (b) and torque responses (c).

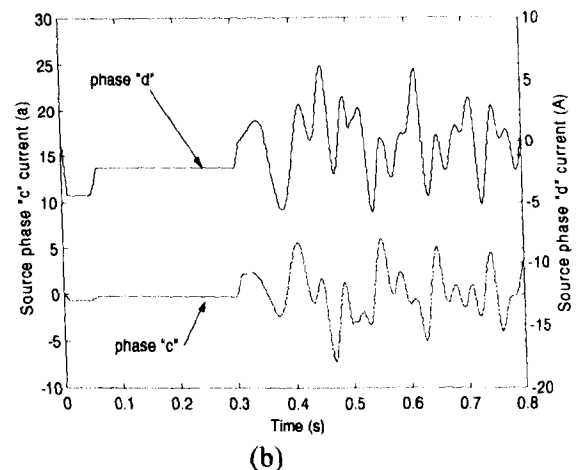
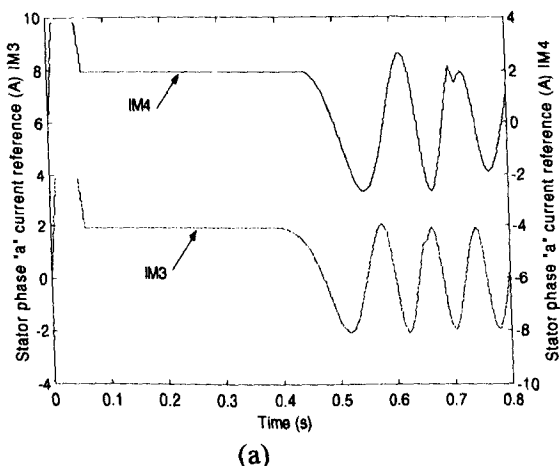
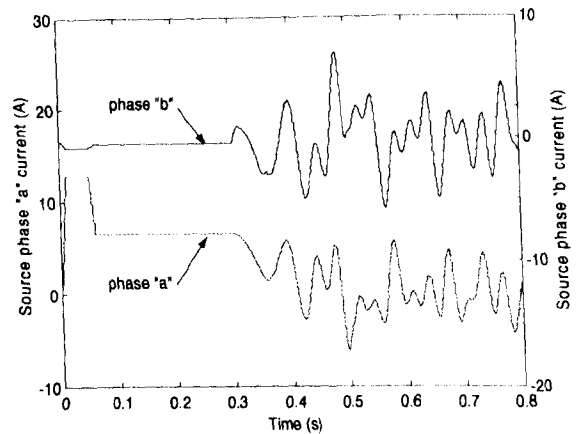
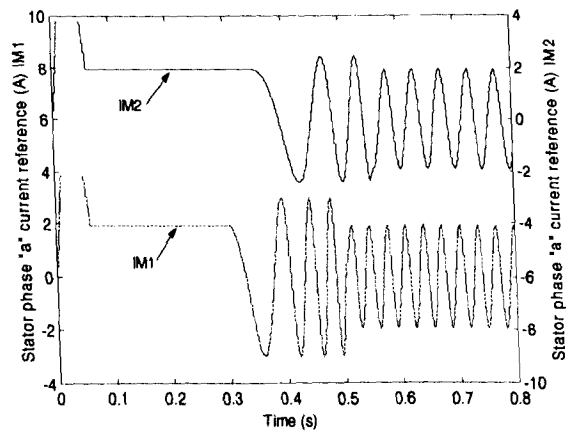


Fig. 5.25: Vector control of the four-motor nine-phase drive: Stator phase "a" current references (a) and source currents for the first four phases (b).

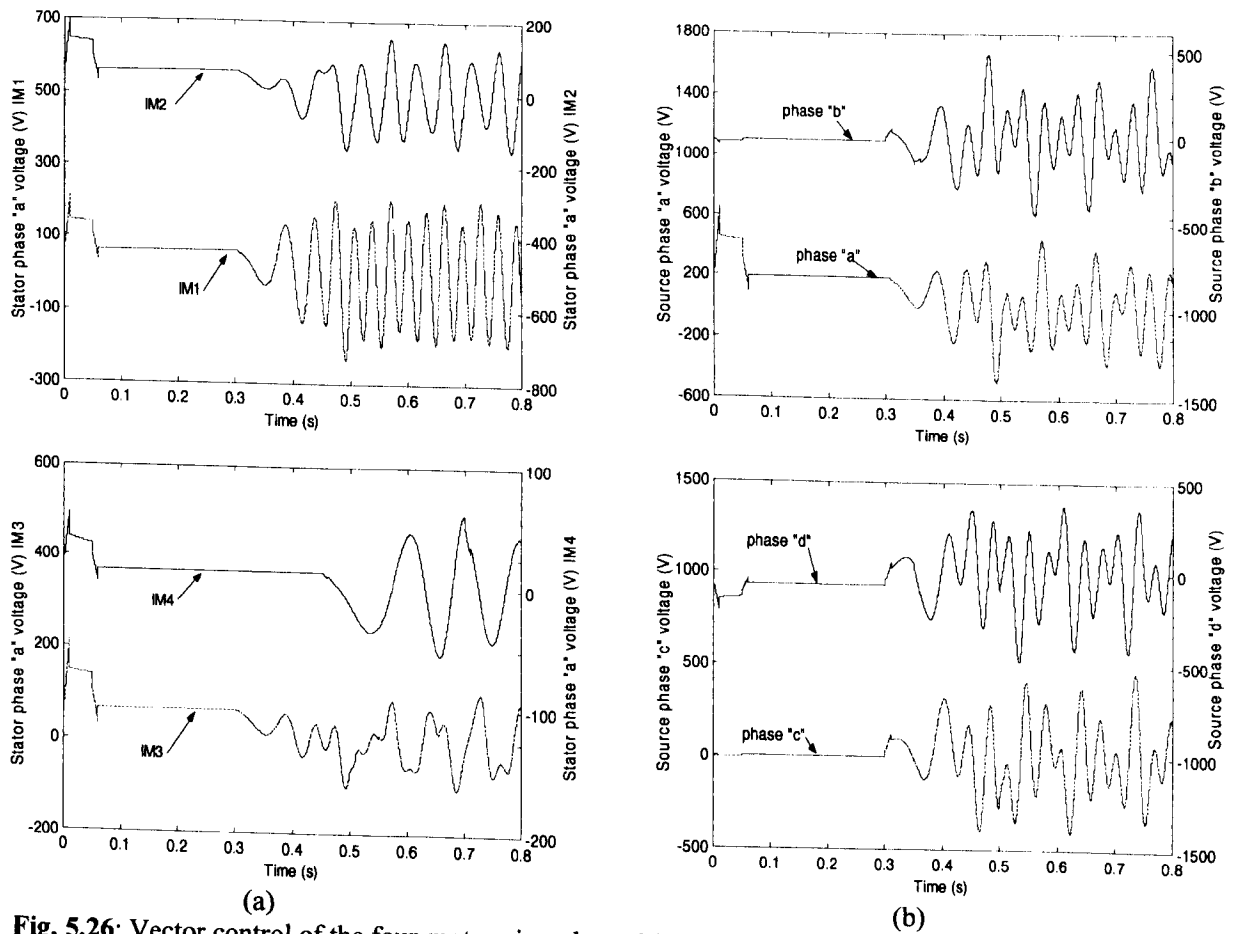


Fig. 5.26: Vector control of the four-motor nine-phase drive. Stator phase “a” voltage (a) and source voltages for the first four phases (b).

three-phase machine is not affected in any adverse manner by the series connection to the other three machines. This is because the torque and flux producing currents of the other machines mutually cancel at the point of connection with the three-phase machine. Hence no x-y currents flow in the three-phase machine.

Table 5.3: Torque command application and removal for each machine.

Machine	T_e^*	Applied at	Removed at
IM1 (9-phase)	T_{en}	$t = 0.3 \text{ s}$	$t = 0.5 \text{ s}$
IM2 (9-phase)	$(2/3)T_{en}$	$t = 0.35 \text{ s}$	$t = 0.55 \text{ s}$
IM3 (9-phase)	$(1/3)T_{en}$	$t = 0.4 \text{ s}$	$t = 0.65 \text{ s}$
IM4 (3-phase)	$0.8T_{en}$	$t = 0.45 \text{ s}$	$t = 0.7 \text{ s}$

5.5 The fifteen-phase six-motor drive

As shown in chapter 4, the fifteen-phase transformation matrix results in a connectivity table which can not be realised in practise. The number of machines that can be connected in series for the fifteen-phase case is at most six. The reasons behind

this conclusion are elaborated in section 4.3 and will not be repeated here. The six machines which can be connected in series consist of four fifteen-phase and two five-phase machines as shown in Table 5.4, obtained on the basis of Table 4.7.

Table 5.4: Realisable connectivity matrix for the fifteen-phase case

	A	B	C	D	E	F	G	H	I	J	K	L	M	N	O
IM1	1	2	3	4	5	6	7	8	9	10	11	12	13	14	15
IM2	1	3	5	7	9	11	13	15	2	4	6	8	10	12	14
IM3	1	5	9	13	2	6	10	14	3	7	11	15	4	8	12
IM4	1	8	15	7	14	6	13	5	12	4	11	3	10	2	9
IM5	1	4	7	10	13	1	4	7	10	13	1	4	7	10	13
IM6	1	7	13	4	10	1	7	13	4	10	1	7	13	4	10

5.5.1 Simulation of rotor flux oriented control of four fifteen-phase and two five-phase induction machines connected in series (torque mode)

In order to prove the validity of the connections given in Table 5.4, a simulation program was written utilising a rotor flux oriented control scheme for operation in torque mode as previously described. Magnetising of the machines took place in the same fashion as described in section 5.3.8. The torque commands were applied in a ramp wise manner after the machines had been magnetised (Table 5.5). Fig. 5.27 shows that decoupled torque and flux control has been achieved and that the speed response is the fastest and smoothest possible. The same conclusions as those previously mentioned can be drawn from the remaining plots of currents and voltages and these are therefore omitted from this section.

5.6 Current cancellation

Independent control of each machine in the multi-phase multi-machine drive is made possible by the phase transposition introduced between the stator phase connections of the machines. Regardless of the number of phases the inverter has, summing the individual machine current references according to the phase transposition forms inverter phase current references. As a result of the summation it is possible that a steady-state may result in which individual machine phase current references cancel

each other and so the resulting inverter phase current reference becomes zero[⊗]. Note that due to the phase transposition this may happen with only one inverter current reference. This section considers the possibility of such an occurrence in the case of the five-phase two-motor drive presented in section 5.3.

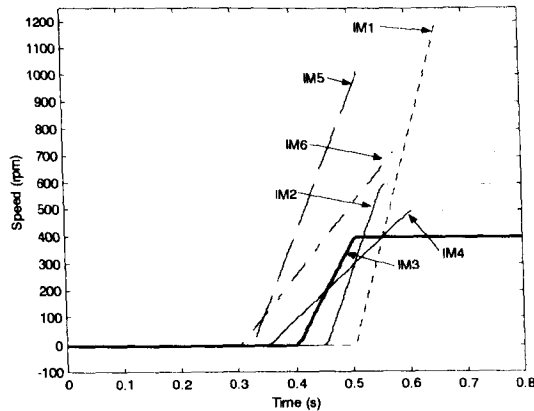


Fig. 5.27(a): Six-motor fifteen-phase case: Speed responses.

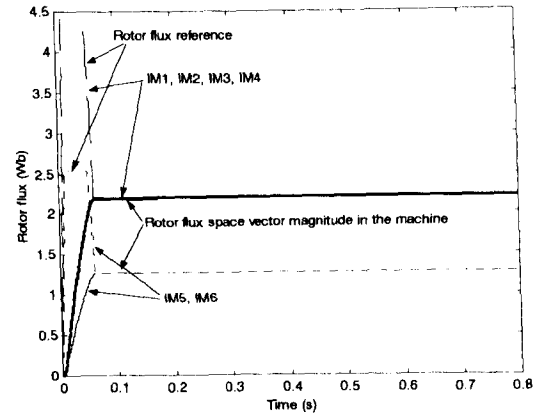


Fig. 5.27(c): Six-motor fifteen-phase case: Rotor flux reference and responses.

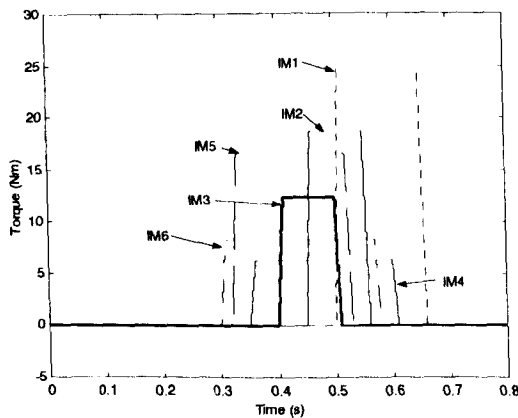


Fig. 5.27(b): Six-motor fifteen-phase case: Torque responses.

Table. 5.5 Torque command application and removal for each machine.

Machine	T_e^*	Applied at	Removed at
IM1 (15-phase)	T_{en}	$t = 0.5$	$t = 0.65$
IM2 (15-phase)	$(3/4)T_{en}$	$t = 0.45$	$t = 0.55$
IM3 (15-phase)	$(1/2)T_{en}$	$t = 0.4$	$t = 0.5$
IM4 (15-phase)	$(1/4)T_{en}$	$t = 0.35$	$t = 0.6$
IM5 (5-phase)	T_{en}	$t = 0.32$	$t = 0.52$
IM6 (5-phase)	$(1/2)T_{en}$	$t = 0.3$	$t = 0.57$

In the example examined here both five-phase machines are identical and operate under identical conditions ($I_1 = I_2 = I$, $\omega_1 = \omega_2 = \omega_s$). It is assumed that a speed command of 1500 rpm (50 Hz) is applied to machine 2 following an identical speed command given to machine 1 10ms earlier. This results in a 180° phase shift of the IM2 phase “a” flux/torque producing current with respect to phase “a” flux/torque producing current of IM1. Once both machines have accelerated to the required speed the steady-state inverter phase current reference will be [Levi et al (2004b)]:

[⊗] This issue was raised by Professor R.D. Lorenz during the discussion of the paper Levi et al (2003b).

$$\begin{aligned}
 i_A^* &= \sqrt{2}I_1 \sin(\omega_1 t) + \sqrt{2}I_2 \sin(\omega_2 t - \pi) = 0 \\
 i_B^* &= \sqrt{2}I_1 \sin(\omega_1 t - \alpha) + \sqrt{2}I_2 \sin(\omega_2 t - 2\alpha - \pi) = 2I \sqrt{1 + \cos(3\alpha/2)} \sin(\alpha t - \alpha/4) \\
 i_C^* &= \sqrt{2}I_1 \sin(\omega_1 t - 2\alpha) + \sqrt{2}I_2 \sin(\omega_2 t - 4\alpha - \pi) = 2I \sqrt{1 + \cos(\alpha/2)} \sin(\alpha t - 7\alpha/4) \\
 i_D^* &= \sqrt{2}I_1 \sin(\omega_1 t - 3\alpha) + \sqrt{2}I_2 \sin(\omega_2 t - \alpha - \pi) = 2I \sqrt{1 + \cos(\alpha/2)} \sin(\alpha t - 13\alpha/4) \\
 i_E^* &= \sqrt{2}I_1 \sin(\omega_1 t - 4\alpha) + \sqrt{2}I_2 \sin(\omega_2 t - 3\alpha - \pi) = 2I \sqrt{1 + \cos(3\alpha/2)} \sin(\alpha t - 19\alpha/4)
 \end{aligned} \tag{5.36}$$

This can be written as:

$$\begin{aligned}
 i_A^* &= 0 \\
 i_B^* &= \underline{\sqrt{2}I \sin(\alpha t - \alpha)} - \underline{\sqrt{2}I \sin(\alpha t - 2\alpha)} \\
 i_C^* &= \underline{\sqrt{2}I \sin(\alpha t - 2\alpha)} - \underline{\sqrt{2}I \sin(\alpha t - 4\alpha)} \\
 i_D^* &= \underline{\sqrt{2}I \sin(\alpha t - 3\alpha)} - \underline{\sqrt{2}I \sin(\alpha t - \alpha)} \\
 i_E^* &= \underline{\sqrt{2}I \sin(\alpha t - 4\alpha)} - \underline{\sqrt{2}I \sin(\alpha t - 3\alpha)}
 \end{aligned} \tag{5.37}$$

The spatial mmf distribution in the first five-phase machine is given by:

$$\begin{aligned}
 F_a &= Ni_A \cos(\varepsilon) \\
 F_b &= Ni_B \cos(\varepsilon - \alpha) \\
 F_c &= Ni_C \cos(\varepsilon - 2\alpha) \\
 F_d &= Ni_D \cos(\varepsilon + 2\alpha) \\
 F_e &= Ni_E \cos(\varepsilon + \alpha)
 \end{aligned} \tag{5.38}$$

The current references created by the vector controller of machine 1 (single-underlined terms in 5.37) create the following mmf in machine one:

$$\begin{aligned}
 F_b &= 0.5\sqrt{2}NI(\sin(\alpha t + \varepsilon - 2\alpha) + \sin(\alpha t - \varepsilon)) \\
 F_c &= 0.5\sqrt{2}NI(\sin(\alpha t + \varepsilon - 4\alpha) + \sin(\alpha t - \varepsilon)) \\
 F_d &= 0.5\sqrt{2}NI(\sin(\alpha t + \varepsilon + 4\alpha) + \sin(\alpha t - \varepsilon)) \\
 F_e &= 0.5\sqrt{2}NI(\sin(\alpha t + \varepsilon + 2\alpha) + \sin(\alpha t - \varepsilon))
 \end{aligned} \tag{5.39}$$

Therefore the total mmf produced in machine 1 by the current components belonging to machine 1 is:

$$-0.5\sqrt{2}NI \sin(\alpha t + \varepsilon) + 2\sqrt{2}NI \sin(\alpha t - \varepsilon) \tag{5.40}$$

Consider next current references generated by the vector controller of machine 2 (double underlined terms in (5.37)) flowing in the stator of machine 1 (5.38) one has:

$$\begin{aligned}
 F_b &= -0.5\sqrt{2}NI(\sin(\alpha t + \varepsilon - 3\alpha) + \sin(\alpha t - \varepsilon + \alpha)) \\
 F_c &= -0.5\sqrt{2}NI(\sin(\alpha t + \varepsilon - \alpha) + \sin(\alpha t - \varepsilon + 3\alpha)) \\
 F_d &= -0.5\sqrt{2}NI(\sin(\alpha t + \varepsilon + \alpha) + \sin(\alpha t - \varepsilon - 3\alpha)) \\
 F_e &= -0.5\sqrt{2}NI(\sin(\alpha t + \varepsilon + 3\alpha) + \sin(\alpha t - \varepsilon + \alpha))
 \end{aligned} \tag{5.41}$$

Therefore the total mmf produced in machine 1 by the current components belonging to machine 2 is:

$$0.5\sqrt{2}NI \sin(\alpha + \varepsilon) + 0.5\sqrt{2}NI \sin(\alpha - \varepsilon) \quad (5.42)$$

Taking into account that both machines are identical and operating under identical conditions phase current references of two machines have the same frequency and magnitude. Therefore summation of (5.40) and (5.42) gives the resultant mmf wave in the air gap of the five-phase machine (machine 1) as:

$$2.5\sqrt{2}NI \sin(\alpha - \varepsilon) \quad (5.43)$$

Obviously, the same result also follows for machine 2. The resultant mmf shows that there is no loss in mmf and that the current components of each machine re-enforce each other. Thus the drive should operate as normal without any loss in performance or control decoupling. This is so since in the proposed five-phase two-motor drive system only four degrees of freedom are utilised. The fifth is redundant, meaning that there is one degree of redundancy that remains for utilisation in safety critical applications, in the case of failure of one inverter leg. Further proof of completely decoupled control of both machines under the described conditions can be obtained if one applies the decoupling transformation (3.13a) to stator currents of machine 1 (5.36) and the stator currents of machine 2, resulting in Table 5.6. Comparison of Table 5.6 with equivalent results under normal operating conditions (Table 5.2) shows that only the phases of the current components change but not the magnitudes and so both machines will operate as normal.

Table 5.6: Stator current components in five-phase series-connected motors with phase “a” current cancellation (steady-state).

Current components	M1	M2
α	$\sqrt{5}I \sin \alpha$	$-\sqrt{5}I \sin \alpha$
β	$-\sqrt{5}I \cos \alpha$	$\sqrt{5}I \cos \alpha$
$x1$	$-\sqrt{5}I \sin \alpha$	$\sqrt{5}I \sin \alpha$
$y1$	$\sqrt{5}I \cos \alpha$	$\sqrt{5}I \cos \alpha$
0	0	0

5.6.1 Simulation verification (five-phase case)

Verification that the five-phase series-connected two-motor drive will operate as predicted in section 5.6 is provided by simulation, for the case when inverter phase “a” current reference becomes zero. As previously mentioned both machines are assumed to be identical and operating under identical conditions. Once rated rotor flux is established in both five-phase machines a speed command (314 rad/s) is applied to machine 1 at $t = 0.3\text{s}$. At $t = 0.35\text{s}$ an identical speed command is applied to machine 2. As can be seen in Fig. 5.28 both machines accelerate to the required speed as before. Once both machines reach the required speed, the individual machine phase current references are of the same magnitude and frequency as shown in Fig. 5.28. However phase “a” machine current references are in phase opposition and so they cancel each other when they are summed according to the phase transposition (5.29). Thus the inverter phase “a” current reference becomes zero, as shown in Fig. 5.28. Torque and rotor flux response of each machine are presented in Fig. 5.28, where it can be seen that the cancellation of the inverter phase “a” current reference has no effect upon the performance of the drive. Each machine is loaded in the same manner at $t = 0.9\text{s}$ with a load of 5 Nm. The torque responses of two machines are illustrated in Fig 5.28a where it can be seen that the torque developed by the machines rapidly responds to the applied load. Rotor flux is in no way affected by the application of the load, thus proving that decoupled control has been maintained. A small dip in speed can be seen in Fig 5.28a when the load is applied, however this is quickly corrected by the control system. Inverter phase “a” current reference shown in Fig. 5.28b remains at zero when the load torque is applied because the load torque is applied to both machines in an identical manner. Thus individual machine phase “a” current references remain of the same magnitude and frequency but in phase opposition during the application of the load to both machines. Stator phase “a” voltage of each machine can be seen in Fig. 5.28b. The voltage does not become zero once the machines have reached the required speed; this voltage is due to the flow of currents in the other phases which link with phase “a” through the mutual inductances. The example considered here demonstrates that the five-phase series-connected two-motor drive will operate when phase “a” of the inverter current reference becomes zero, however the same conclusion may be drawn for any of the inverter phase references. In the five-phase case it is not possible for more than one inverter phase current reference to cancel, because of the phase transposition.

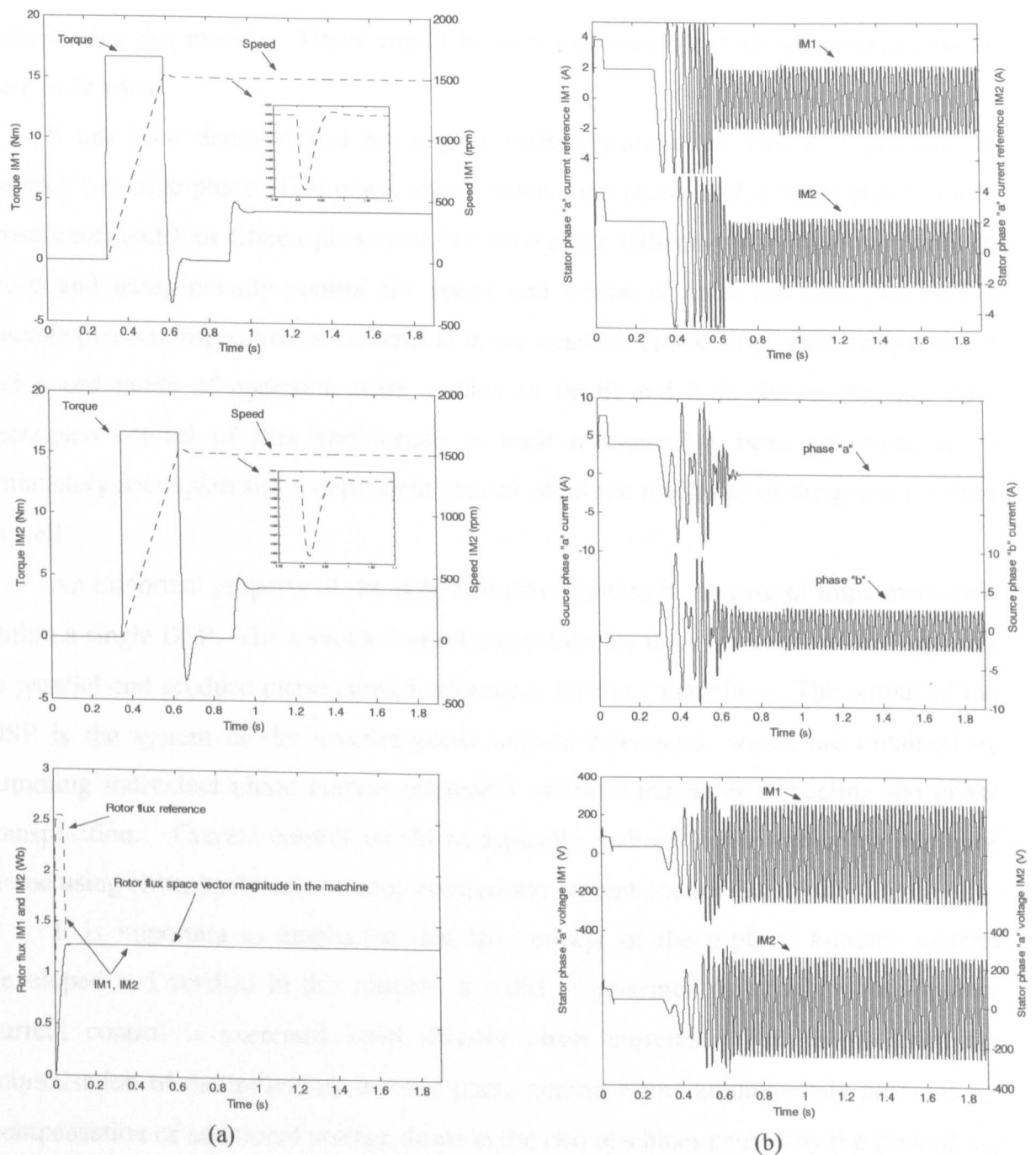


Fig. 5.28: Vector control of series-connected five-phase two-motor drive with inverter phase “a” current cancellation: Torque, speed and rotor flux response (a), Stator phase “a” current, inverter phase “a-b” currents and stator phase “a-b” voltage (b).

5.7 Summary

Both phase-domain and stationary reference frame modelling of five phase induction machines have been considered and it has been demonstrated by a number of simulations that both models return identical results. This is, although expected, important because it allows the further development of simulation programs for

phases using d-q models. These would be very cumbersome if phase-domain models were to be used.

It has been demonstrated by way of various simulations that it is possible to connect two five-phase (five-phase case), three nine-phase and a three-phase (nine-phase case) and four fifteen-phase and two five-phase (fifteen-phase case) machines in series and independently control the speed and torque of each machine, provided a suitable phase transposition is introduced in the machine connection. Both torque mode and speed mode of operation were studied in detail and it is shown that not only decoupled control of flux and torque in each machine has been achieved, but a completely decoupled and independent control of all the machines of the group resulted as well.

An important property of the proposed drive system is the ease of implementation within a single DSP. The k vector control algorithms for the k machines need to operate in parallel and produce phase current references for the k machines. The output of the DSP is the system of the inverter phase current references, which are obtained by summing individual phase current references of the k machines respecting the phase transposition. Current control would be typically realised in the stationary reference frame using either hysteresis or ramp comparison current control.

It is important to emphasise that the concept of the n -phase k -motor system, developed and verified in this chapter, is valid in presented form only when inverter current control is exercised upon inverter phase currents. This is so since the minimisation of the individual inverter phase current errors automatically provides for compensation of additional voltage drops in the two machines caused by the flow of x-y stator current components. Modifications of the concept, required if current control is to be performed in the rotating reference frame, will be discussed at a later stage.

The flow of torque/flux producing currents of all machines in the system through the stators of all machines presents a significant disadvantage of this system, since the efficiency of the overall system is reduced. Clearly, such a situation will lead to an increased amount of stator copper losses in the machines (rotor copper losses will not be affected).

Determination of the additional amount of the stator winding losses depends on the machine ratings and operating conditions. Consider the two-motor five-phase case. For simplicity, it is assumed that the two machines are identical and operate with the same load (i.e. current) and at the same speed (i.e. frequency). In other words the

situation described with (5.12) and (5.37) is considered. Using either (5.12) or (5.37), it can be easily shown that the amount of stator winding loss will double in each machine in this series connection, compared to the case when a single five-phase machine operates under the same conditions. It should be noted however, that distribution of the additional winding loss is uneven among the phases (for example if (5.12) applies then phase “a” losses of both machines will quadruple, while if (5.37) applies there will be no losses at all in phase “a” of both machines). The second shortcoming is the voltage drop produced by x-y stator current components in both machines, which will impact on the voltage rating of the inverter semiconductors. This means that the voltage rating will have to be higher (but only slightly, since these voltage drops appear across stator leakage impedance and are therefore rather small) than twice the rating of a single five-phase motor drive. Current rating of the inverter will have to correspond to the sum of current ratings of the two machines.

Simulations of the nine-phase four-machine drive demonstrated that the three-phase machine connected at the end of the system (from the point of view of the inverter) did not suffer any adverse effects due to series connection with the nine-phase machines. This is so because the flux/torque producing currents of the other machines cancel out at the point of connection to the three-phase machine and hence the efficiency of the three-phase machine remains unaffected.

Due to the nature of the multi-phase series-connected multi-motor drive it is possible that stator current references may cancel when forming the inverter current references. This situation is examined for the five-phase case and it is shown that the drive performance is not affected.

CHAPTER 6

SIMULATION STUDIES FOR EVEN PHASE NUMBERS

6.1 Introduction

This chapter considers the situation when the inverter number of phases is an even number. Simulations are performed for the six-phase and ten-phase drives. For even phase numbers, any saving in the number of inverter legs comes into existence only when the number of phases is equal to or greater than eight. As discussed in chapter 4, the even phase case results in series connection of at most $(n-2)/2$ machines. However, not all of the machines in the system are of the same phase number and so the case studies in this chapter fall under categories a) and b) of section 4.5.2.

The even phase numbers are inferior to odd phase numbers from the point of view of the saving in the number of inverter legs, since more legs can be saved with an odd phase number than the subsequent even phase number. Nevertheless, the fact that the connectable machines are always of different phase numbers appears to offer an advantage over the odd phase numbers in certain situations. Consider for example the six-phase case and suppose that a six-phase motor drive is selected for a certain application for the reasons of high power. If the application requires one more controllable drive for certain auxiliary function, of low voltage and low power rating, then this drive can be selected as a three-phase drive and connected in series with the six-phase motor. This means that control of the second (three-phase) drive can be achieved at no extra cost. Hence, although there is no saving in the number of inverter legs, there is an actual benefit since a separate three-phase inverter is not required. The three-phase machine is not adversely affected by series connection to the six-phase machine and the three-phase machine (of low power) will have negligible impact on efficiency of the six-phase machine (high power). The drive system appears to be a very viable solution for the described type of application.

The main research results of this chapter have been published in Jones et al (2004a) and Levi et al (2003a).

6.2. The six-phase two-motor drive

Application of the transformation matrix (3.13b) allows the construction of a connectivity matrix as discussed in section 4.2. The connectivity matrix for the six-phase case and corresponding connection diagram, already given in section 4.4, are repeated for convenience in Table 6.1 and Fig 6.1, respectively. In order to simplify the initial analysis the controller and inverter are omitted and the supply is assumed to be an ideal sinusoidal current source.

Let the phase sequence of the source be A,B,C,D,E,F and let the flux-torque producing phase sequence for the two machines be a,b,c,d,e,f and a,b,c. Assume that machine 1 (six-phase) is supplied for purposes of torque and flux production with ideal sinusoidal currents of rms value and frequency equal to I_1, ω_1 . Similarly, machine 2 (three-phase) is supplied with a flux and torque producing set of currents of rms value and frequency I_2, ω_2 . According to the connection diagram (Fig. 6.1), source phase currents are simultaneously corresponding phase currents for machine 1:

Table 6.1: Connectivity matrix for the six-phase drive system.

	A	B	C	D	E	F
M1	1	2	3	4	5	6
M2	1	3	5	1	3	5

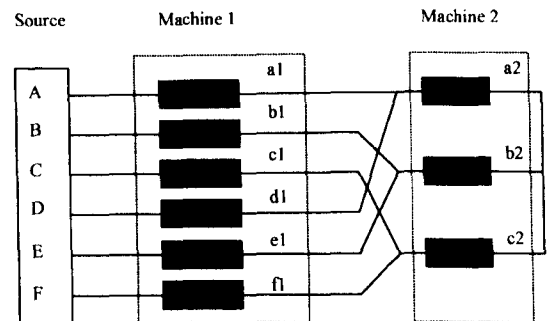


Fig. 6.1: Connection diagram for the six-phase two-motor system

$$\begin{aligned}
 i_A = i_{a1} &= \sqrt{2}I_1 \sin(\omega_1 t) + \underline{\underline{0.5 \cdot \sqrt{2}I_2 \sin(\omega_2 t)}} \\
 i_B = i_{b1} &= \sqrt{2}I_1 \sin(\omega_1 t - \alpha) + \underline{\underline{0.5 \cdot \sqrt{2}I_2 \sin(\omega_2 t - 2\alpha)}} \\
 i_C = i_{c1} &= \sqrt{2}I_1 \sin(\omega_1 t - 2\alpha) + \underline{\underline{0.5 \cdot \sqrt{2}I_2 \sin(\omega_2 t - 4\alpha)}} \\
 i_D = i_{d1} &= \sqrt{2}I_1 \sin(\omega_1 t - 3\alpha) + \underline{\underline{0.5 \cdot \sqrt{2}I_2 \sin(\omega_2 t)}} \\
 i_E = i_{e1} &= \sqrt{2}I_1 \sin(\omega_1 t - 4\alpha) + \underline{\underline{0.5 \cdot \sqrt{2}I_2 \sin(\omega_2 t - 2\alpha)}} \\
 i_F = i_{f1} &= \sqrt{2}I_1 \sin(\omega_1 t - 5\alpha) + \underline{\underline{0.5 \cdot \sqrt{2}I_2 \sin(\omega_2 t - 4\alpha)}}
 \end{aligned} \tag{6.1}$$

Machine 1 (six-phase) and machine 2 (three-phase) are connected via a phase transposition which results in machine 2 being supplied with the following currents:

$$\begin{aligned}
 i_{a2} = i_A + i_D &= \sqrt{2}I_1 \sin(\omega_1 t) + \sqrt{2}I_1 \sin(\omega_1 t - 3\alpha) + \sqrt{2}I_2 \sin(\omega_2 t) \\
 i_{b2} = i_B + i_E &= \sqrt{2}I_1 \sin(\omega_1 t - \alpha) + \sqrt{2}I_1 \sin(\omega_1 t - 4\alpha) + \sqrt{2}I_2 \sin(\omega_2 t - 2\alpha) \\
 i_{c2} = i_C + i_F &= \sqrt{2}I_1 \sin(\omega_1 t - 2\alpha) + \sqrt{2}I_1 \sin(\omega_1 t - 5\alpha) + \sqrt{2}I_2 \sin(\omega_2 t - 4\alpha)
 \end{aligned} \tag{6.2}$$

By supplying the machines with the currents given in (6.1)-(6.2) it is possible to independently control the speed of each machine by controlling frequencies f_1 and f_2 together with current magnitudes I_1 and I_2 , respectively, provided that the currents that produce a rotating field in machine 1 do not produce a rotating field in machine 2 and vice versa. This is achieved through the phase transposition operation. Application of the decoupling transformation matrix on the stator currents of the two machines given with (6.1)-(6.2) produces the results shown in Table 6.2 [Jones et al (2004a)] and can be explained by considering the underlined terms in equations (6.1) and (6.2), respectively. It is obvious that in any of the phase currents of machine 2 in (6.2) the two underlined terms cancel each other since they are in phase opposition. Similarly, mmfs produced in machine 1 in (6.1) due to the flow of machine 2 related currents (underlined terms) cancel each other since the currents in any two phases displaced by 180 degrees are the same (so that mmfs are of the same value but of the opposite signs).

Table 6.2: Stator current components in series-connected motors in steady-state (six-phase case).

Current components	M1	M2
α	$\sqrt{6}I_1 \sin \omega_1 t$	$\sqrt{3}I_2 \sin \omega_2 t$
β	$-\sqrt{6}I_1 \cos \omega_1 t$	$-\sqrt{3}I_2 \cos \omega_2 t$
$x1$	$\sqrt{6} \frac{I_2}{2} \sin \omega_2 t$	—
$y1$	$-\sqrt{6} \frac{I_2}{2} \cos \omega_2 t$	
$0+$	0	0
$0-$	0	0

6.2.1 Rotor flux oriented control of a six-phase and a three-phase induction machine connected in series with phase transposition

A standard method of indirect rotor flux oriented control is again considered here. Current control is once more performed in the stationary reference frame, using inverter phase currents. It is important to notice that the so far presented form of the vector-

controlled multi-phase multi-motor drive system is valid when the current control is exercised in the stationary reference frame, as already noted in chapter 5. This is so since minimisation of the inverter phase current errors through inverter switching automatically generates appropriate voltages required for compensation of the additional voltage drops in the machines, caused by the flow of x-y current components. Either ramp-comparison or hysteresis current control can be used. Generation of individual machine phase current references is determined with (superscript j stands for the machine under consideration, 1 or 2; $\alpha = 2\pi/n = 60^\circ$ for machine 1 and $\alpha = 2\pi/n = 120^\circ$ for machine 2; $n = 6$ for M1 and $n = 3$ for M2):

$$\begin{aligned}
 i_1^{*(j)} &= \sqrt{\frac{2}{n}} [i_{ds}^{*(j)} \cos \phi_r^{(j)} - i_{qs}^{*(j)} \sin \phi_r^{(j)}] \\
 i_2^{*(j)} &= \sqrt{\frac{2}{n}} [i_{ds}^{*(Mj)} \cos(\phi_r^{(Mj)} - \alpha) - i_{qs}^{*(Mj)} \sin(\phi_r^{(j)} - \alpha)] \\
 \dots\dots\dots \\
 i_n^{*(j)} &= \sqrt{\frac{2}{n}} [i_{ds}^{*(j)} \cos(\phi_r^{(j)} - (n-1)\alpha) - i_{qs}^{*(j)} \sin(\phi_r^{(j)} - (n-1)\alpha)]
 \end{aligned} \tag{6.3}$$

Inverter reference currents are further built, according to the connection diagram (Fig 6.1). Inverter reference current creation has to take into account the existence of machines with different phase numbers within the group. Thus for the six-phase inverter with a six-phase and a three-phase machine, illustrated in Fig. 6.1 and Table 6.1, the inverter current references are determined with:

$$\begin{aligned}
 i_A^* &= i_{a1}^* + 0.5i_{a2}^* & i_B^* &= i_{b1}^* + 0.5i_{b2}^* \\
 i_C^* &= i_{c1}^* + 0.5i_{c2}^* & i_D^* &= i_{d1}^* + 0.5i_{d2}^* \\
 i_E^* &= i_{e1}^* + 0.5i_{e2}^* & i_F^* &= i_{f1}^* + 0.5i_{f2}^*
 \end{aligned} \tag{6.4}$$

The inverter output phase voltages follow directly from Fig. 6.1:

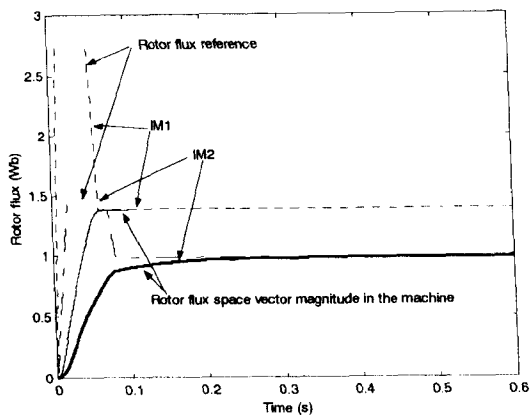
$$\begin{aligned}
 v_A &= v_{a1} + v_{a2} & v_B &= v_{b1} + v_{b2} & v_C &= v_{c1} + v_{c2} \\
 v_D &= v_{d1} + v_{d2} & v_E &= v_{e1} + v_{e2} & v_F &= v_{f1} + v_{f2}
 \end{aligned} \tag{6.5}$$

6.2.2 Simulation of rotor flux oriented control of a six-phase and a three-phase induction machine with phase transposition (torque mode)

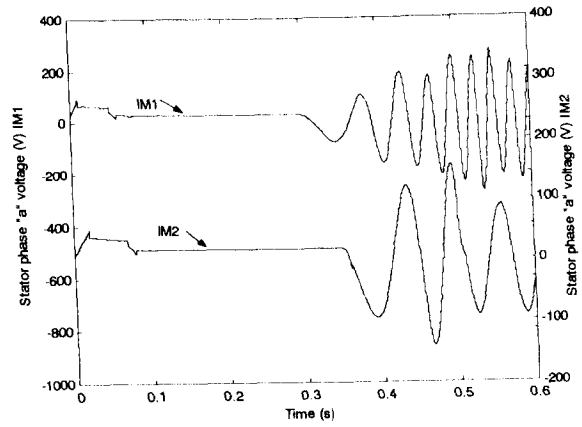
Both induction machines under consideration were modelled in the stationary reference frame as described in chapter 3 respecting the number of phases and the

spacial displacement between windings. Both machines are assumed to have the same per-phase equivalent circuit parameters and ratings. Once again, it is assumed that the inverter generates ideal currents as requested by the control system. A different d-axis current reference (rotor flux reference) was applied to each machine. The d-axis current reference of machine 1 was initially ramped to twice its rated value between $t = 0$ and $t = 0.01$ s. It was later reduced in a ramp wise manner back to the rated value from $t = 0.05$ s to $t = 0.06$ s. For machine 2 the stator d-axis current reference was ramped to 1.5 times the rated value from 0 to 0.02s and kept at 1.5 times the rated value until 0.07s when it was ramped downwards to rated value between 0.07s to 0.08s. The torque reference for machine 1 was ramped at $t = 0.3$ from zero to 1.5 times rated (15Nm) and maintained at this value until $t = 0.55$ s when it was ramped down to zero. The torque reference for machine 2 was applied from $t = 0.35$ to 0.5s in a ramp wise manner from zero to twice rated (10Nm) and then back to zero. Duration of all ramps for torque reference application was 0.01 second.

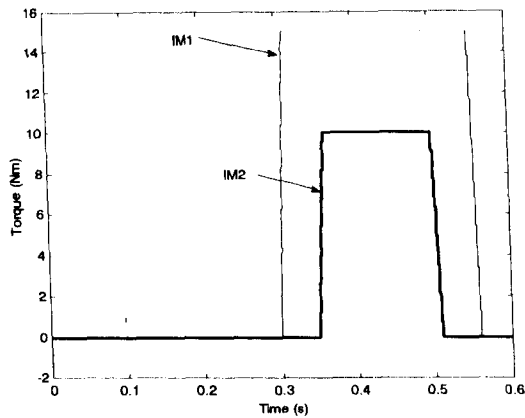
The rotor flux reference and the corresponding response of the two machines can be seen in Fig 6.2a. The magnetising of each machine is in no way disturbed by the other machine and rotor flux attains the reference value and remains at that value for the remainder of the simulation, confirming the absence of any x-y rotor currents. Torque references and torque responses (which are mutually indistinguishable because of assumed ideal current feeding) are shown in Fig. 6.2b. It can be seen that the torque response of each machine is in no way affected by the torque response of the other machine in the system and the torque and flux response of each machine are completely decoupled. This means that independent torque and flux control has been achieved for both machines. The speed response of each machine is smooth (Fig. 6.2c) due to the complete decoupling of the torque control of both machines. Once again, the stator current references for each machine (Fig 6.2d) are sinusoidal in steady-state. However, the inverter phase currents (Fig 6.2g) are highly distorted due to the summation given by (6.4). Stator phase “a” voltages of the two machines are shown in Fig 6.2e where it can be seen that the stator voltage of machine 2 (three-phase machine) is not affected by the torque command to machine 1 ($t = 0.3$ s). This is because the torque and flux producing currents of machine 1 do not flow through the stator of machine 2 and so machine 2 is not adversely affected by machine 1. However the flux and torque producing currents of machine 2 flows through the stator of machine 1 and cause voltage distortion, as can be seen in Fig. 6.2e. The flow of x-y currents through the



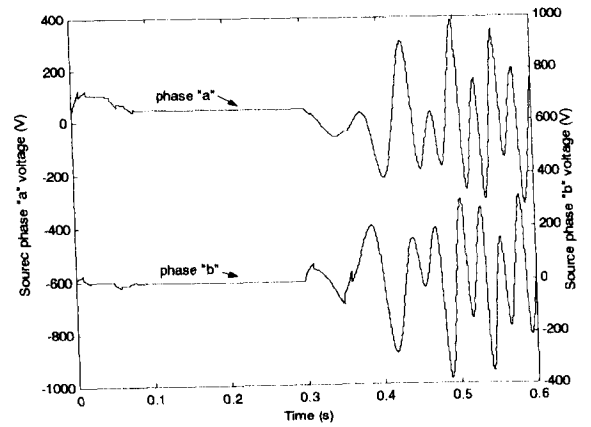
(a)



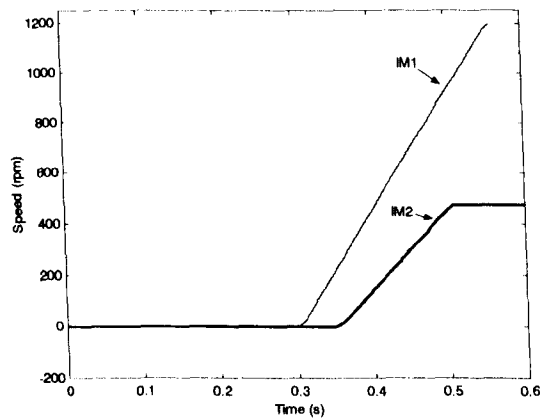
(e)



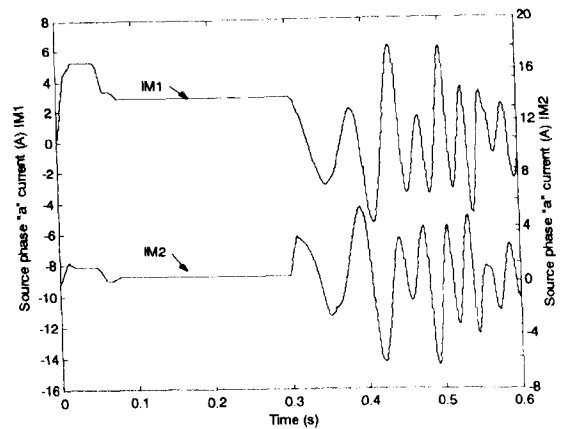
(b)



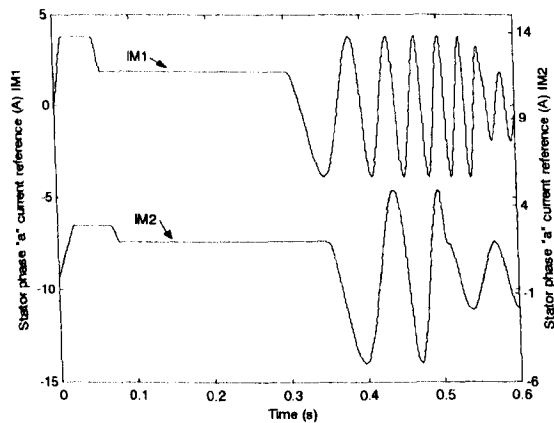
(f)



(c)



(g)



(d)

Fig. 6.2: Six-phase two-motor drive: Rotor flux and rotor flux reference (a), torque responses (b), speed responses (c). Stator phase "a" current reference (d) and voltage for each machine (e). Phase "a" and "b" source voltages (f) and currents (g).

stator of machine 1 increases winding losses of the machine. Stator iron losses will very slightly increase as well, due to the increased phase voltage of the six-phase machine caused by the flow of x-y current components. This will in general reduce the efficiency of the six-phase machine and will therefore reduce the total efficiency of the six-phase two-motor drive in comparison to the equivalent three-phase two-motor drive. However, as discussed in section 6.1, reduction in the efficiency of the six-phase machine will be negligibly small if the six-phase machine is of high power and the three-phase machine is of low power.

As illustrated in Fig. 6.2f, the source voltages required from the inverter are highly distorted. However, this does not present a problem provided that fast inverter current control with a high switching frequency is used.

6.3 The ten-phase four-motor drive

Application of the transformation matrix (3.13b), as described in chapter 4, results in the connectivity matrix and connection diagram given in Table 4.11 and Fig. 4.6, respectively. The windings of the second and fourth machines are 72 degrees apart and therefore represent the windings of two five-phase machines. The system therefore contains two ten-phase machines and two five-phase machines and results in a saving of two inverter legs when compared to the equivalent three-phase four-motor drive. The inverter current references are generated according to the phase transposition given in Fig. 4.6 as:

$$\begin{aligned}
 i_A^* &= i_{a1}^* + i_{a2}^* + 0.5i_{a3}^* + 0.5i_{a4}^* & i_F^* &= i_{f1}^* + i_{f2}^* + 0.5i_{a3}^* + 0.5i_{a4}^* \\
 i_B^* &= i_{b1}^* + i_{d2}^* + 0.5i_{b3}^* + 0.5i_{c4}^* & i_G^* &= i_{g1}^* + i_{i2}^* + 0.5i_{b3}^* + 0.5i_{c4}^* \\
 i_C^* &= i_{c1}^* + i_{g2}^* + 0.5i_{c3}^* + 0.5i_{e4}^* & i_H^* &= i_{h1}^* + i_{b2}^* + 0.5i_{c3}^* + 0.5i_{e4}^* \\
 i_D^* &= i_{d1}^* + i_{j2}^* + 0.5i_{d3}^* + 0.5i_{b4}^* & i_J^* &= i_{j1}^* + i_{e2}^* + 0.5i_{d3}^* + 0.5i_{b4}^* \\
 i_E^* &= i_{e1}^* + i_{c2}^* + 0.5i_{e3}^* + 0.5i_{d4}^* & i_K^* &= i_{k1}^* + i_{h2}^* + 0.5i_{e3}^* + 0.5i_{d4}^*
 \end{aligned} \tag{6.6}$$

The inverter output voltages are calculated using the same connection diagram:

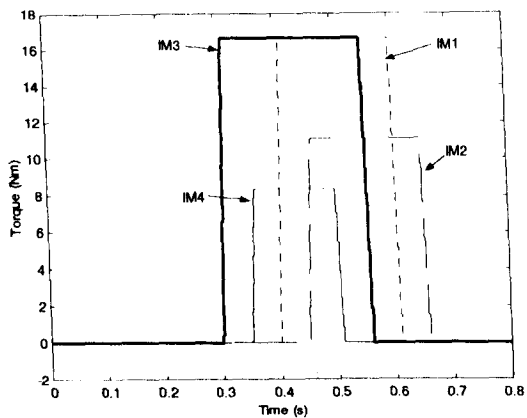
$$\begin{aligned}
 v_A &= v_{a1} + v_{a2} + v_{a3} + v_{a4} & v_F &= v_{f1} + v_{f2} + v_{a3} + v_{a4} \\
 v_B &= v_{b1} + v_{d2} + v_{b3} + v_{c4} & v_G &= v_{g1} + v_{i2} + v_{b3} + v_{c4} \\
 v_C &= v_{c1} + v_{g2} + v_{c3} + v_{e4} & v_H &= v_{h1} + v_{b2} + v_{c3} + v_{e4} \\
 v_D &= v_{d1} + v_{j2} + v_{d3} + v_{b4} & v_I &= v_{i1} + v_{e2} + v_{d3} + v_{b4} \\
 v_E &= v_{e1} + v_{c2} + v_{e3} + v_{d4} & v_J &= v_{j1} + v_{h2} + v_{e3} + v_{d4}
 \end{aligned} \tag{6.7}$$

6.3.1 Simulation of rotor flux oriented control of two ten-phase and two five-phase induction machines connected in series with phase transposition (torque mode)

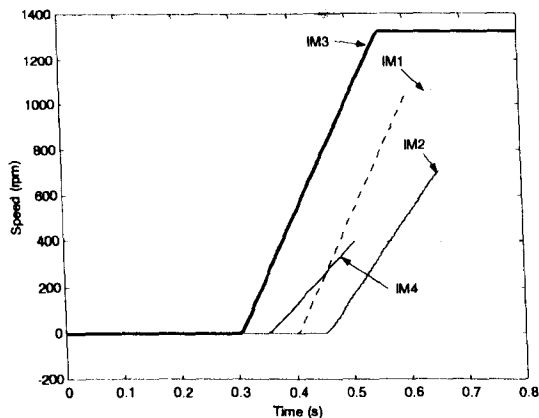
Independent rotor flux oriented control of each machine in the system is achieved in an identical manner to that previously described. Each machine is modelled in the stationary reference frame, as explained in Chapter 3 and Levi et al (2003a). Each machine is assumed to have the same per-phase equivalent circuit parameters and ratings. All the machines are initially pre-magnetised in the manner described in section 5.3.8, as illustrated in Figs. 6.3c and 6.3d. Once the rotor flux has reached steady-state, a torque command was applied and later removed using ramps of 0.01 seconds duration as per the schedule given in Table 6.3. Simulation results are given in Figs. 6.3 and 6.4. Once again the torque response of each machine is the fastest possible and the machines accelerate smoothly from zero and in the shortest possible time. The control of rotor flux and torque of each machine is decoupled and also independent of the control of other machines in the system (Fig. 6.3a and b respectively). The stator phase “a” current references shown in Fig. 6.3d are again similar to those seen in three-phase rotor flux oriented drives, however the source currents are the result of the summation given by (6.6) and are highly distorted. The application of the torque command to each of the two five-phase machines (IM3 and IM4 at $t = 0.3$ and $t = 0.35$ seconds respectively) clearly affects the stator voltages of the ten-phase machines (Fig. 6.3e). The five-phase machines are given the torque commands identical to those in section 5.3.6, where only two five-phase machines were connected in series. The stator voltages of each five-phase machine (Fig. 6.3e) are identical (except for time scaling) to those of Fig. 5.18b (five-phase two-motor case). This confirms that the five-phase machines only affect each other and are not adversely affected by the ten-phase machines in the group. One can conclude that the torque/flux producing currents of the ten-phase machines do not flow through the stators of the five-phase machines, while every machine in the group affects the ten-phase machines. The efficiency of the multi-machine system for the ten-phase configuration is therefore expected to be better when compared to the equivalent four-machine system with an odd phase number (nine-phase case), elaborated in section 5.4.

Table: 6.3: Torque command application and removal for each machine

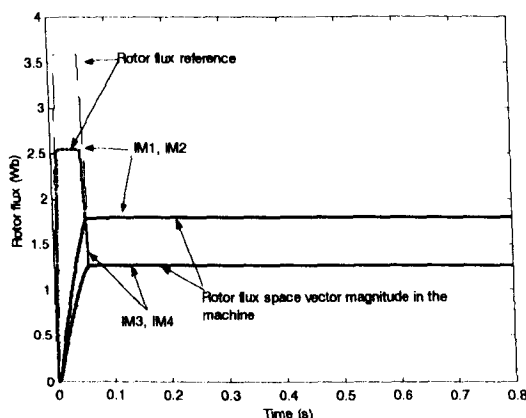
Machine	T_e^*	Applied at	Removed at
IM1 (10-phase)	T_{en}	$t = 0.4$ s	$t = 0.6$ s
IM2 (10-phase)	$2/3 T_{en}$	$t = 0.45$ s	$t = 0.65$ s
IM3 (5-phase)	$2T_{en}$	$t = 0.3$ s	$t = 0.55$ s
IM4 (5-phase)	T_{en}	$t = 0.35$ s	$t = 0.5$ s



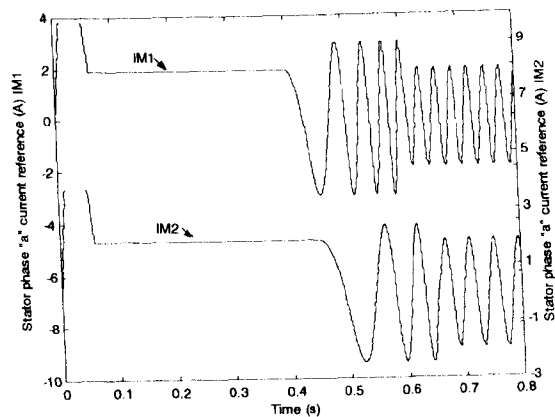
(a)



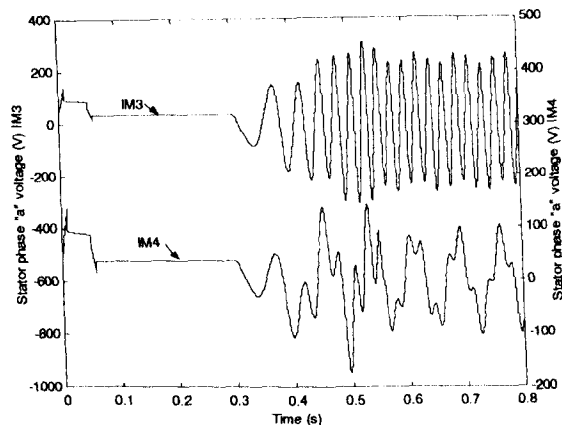
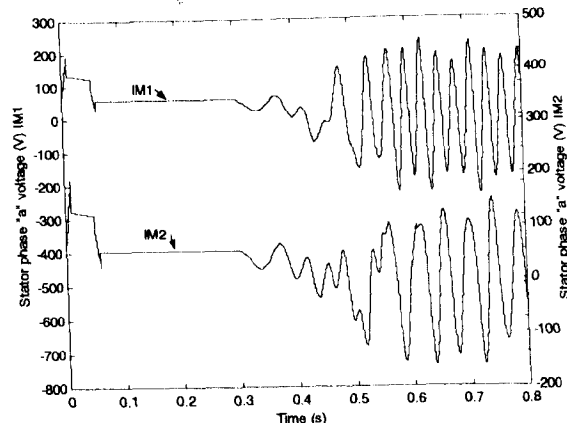
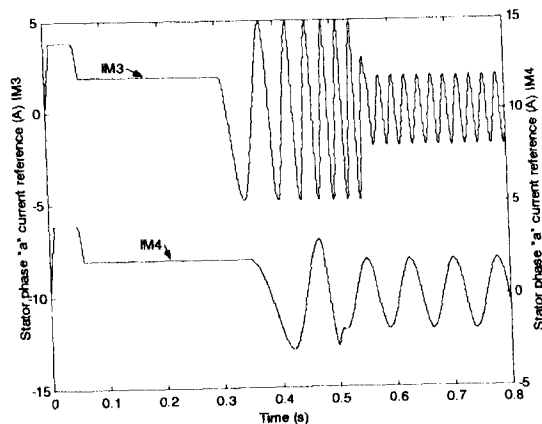
(b)



(c)



(d)



(e)

Fig. 6.3: Ten-phase four-motor drive system: Torque (a), speed responses (b), rotor flux and rotor flux reference (c), stator phase "a" current reference (d) and Stator phase "a" voltage (e).

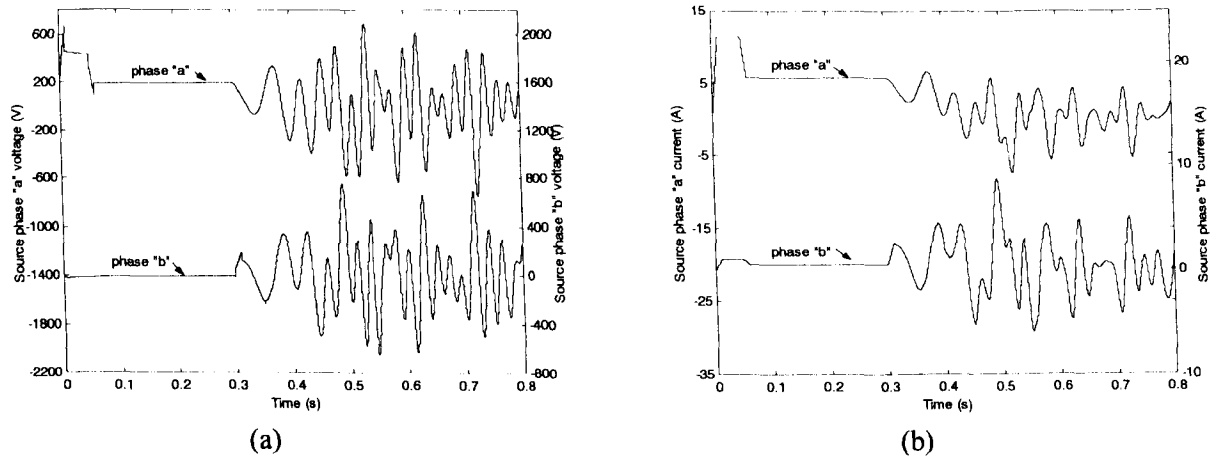


Fig. 6.4: Ten-phase four-motor drive system: Source voltages for the first two phases (a) and currents for the first two phases (b)

6.4 Current cancellation

It is explained in section 5.6 that the generation of the inverter phase current references according to the phase transposition may cause one phase of the inverter current reference to become zero. This phenomenon is examined in this section for the six-phase two-motor drive. The example examined here considers the case when phase “a” inverter current reference becomes zero. For this situation to occur it is necessary for stator current references of the three-phase machine to have twice the magnitude and the same frequency as the six-phase machine ($I_2 = 2I_1$; $I_1 = 0.5I_2 = I$, $\omega_1 = \omega_2 = \omega_s$). If both machines are given a speed command of 314 rad/s 10ms apart from one another, once both machines have reached the required speed (supply frequency of each machine is 50Hz) the steady-state inverter phase current references will be:

$$\begin{aligned}
 i_A^* &= \sqrt{2}I_1 \sin(\omega_1 t) + 1/2 \sqrt{2}I_2 \sin(\omega_2 t - \pi) \\
 i_B^* &= \sqrt{2}I_1 \sin(\omega_1 t - \alpha) + 1/2 \sqrt{2}I_2 \sin(\omega_2 t - 2\alpha - \pi) \\
 i_C^* &= \sqrt{2}I_1 \sin(\omega_1 t - 2\alpha) + 1/2 \sqrt{2}I_2 \sin(\omega_2 t - 4\alpha - \pi) \\
 i_D^* &= \sqrt{2}I_1 \sin(\omega_1 t - 3\alpha) + 1/2 \sqrt{2}I_2 \sin(\omega_2 t - \pi) \\
 i_E^* &= \sqrt{2}I_1 \sin(\omega_1 t - 4\alpha) + 1/2 \sqrt{2}I_2 \sin(\omega_2 t - 2\alpha - \pi) \\
 i_F^* &= \sqrt{2}I_1 \sin(\omega_1 t - 5\alpha) + 1/2 \sqrt{2}I_2 \sin(\omega_2 t - 4\alpha - \pi)
 \end{aligned} \tag{6.8}$$

This can be written as:

$$\begin{aligned}
 i_A^* &= 0 \\
 i_B^* &= \sqrt{2}I \sin(\omega_s t - \alpha) - \underline{\underline{\sqrt{2}I \sin(\omega_s t - 2\alpha)}} \\
 i_C^* &= \sqrt{2}I \sin(\omega_s t - 2\alpha) - \underline{\underline{\sqrt{2}I \sin(\omega_s t - 4\alpha)}} \\
 i_D^* &= \sqrt{2}I \sin(\omega_s t - 3\alpha) - \underline{\underline{\sqrt{2}I \sin(\omega_s t)}} \\
 i_E^* &= \sqrt{2}I \sin(\omega_s t - 4\alpha) - \underline{\underline{\sqrt{2}I \sin(\omega_s t - 2\alpha)}} \\
 i_F^* &= \sqrt{2}I \sin(\omega_s t - 5\alpha) - \underline{\underline{\sqrt{2}I \sin(\omega_s t - 4\alpha)}}
 \end{aligned} \tag{6.9}$$

The spatial mmf distribution in a symmetrical six-phase machine is given by:

$$\begin{aligned}
 F_a &= NI_A \cos(\varepsilon) \\
 F_b &= NI_B \cos(\varepsilon - \alpha) \\
 F_c &= NI_C \cos(\varepsilon - 2\alpha) \\
 F_d &= NI_D \cos(\varepsilon - 3\alpha) \\
 F_e &= NI_E \cos(\varepsilon - 4\alpha) \\
 F_f &= NI_F \cos(\varepsilon - 5\alpha)
 \end{aligned} \tag{6.10}$$

The current references created by the vector controller of the six-phase machine (single-underlined terms in (6.9)) create the following mmf in the six-phase machine:

$$\begin{aligned}
 F_b &= 0.5\sqrt{2}NI(\sin(\omega_s t + \varepsilon - 2\alpha) + \sin(\omega_s t - \varepsilon)) \\
 F_c &= 0.5\sqrt{2}NI(\sin(\omega_s t + \varepsilon - 4\alpha) + \sin(\omega_s t - \varepsilon)) \\
 F_d &= 0.5\sqrt{2}NI(\sin(\omega_s t + \varepsilon) + \sin(\omega_s t - \varepsilon)) \\
 F_e &= 0.5\sqrt{2}NI(\sin(\omega_s t + \varepsilon - 2\alpha) + \sin(\omega_s t - \varepsilon)) \\
 F_f &= 0.5\sqrt{2}NI(\sin(\omega_s t + \varepsilon + 2\alpha) + \sin(\omega_s t - \varepsilon))
 \end{aligned} \tag{6.11}$$

The total mmf produced in machine 1 by current components belonging to machine 1 is:

$$-0.5\sqrt{2}I \sin(\omega_s t + \varepsilon) + 2.5\sqrt{2}I \sin(\omega_s t - \varepsilon) \tag{6.12}$$

Consider the current references of machine 2 (double-underlined terms of (6.9)) flowing in the stator of machine 1:

$$\begin{aligned}
 F_b &= -0.5\sqrt{2}I(\sin(\omega_s t + \varepsilon - 3\alpha) + \sin(\omega_s t - \varepsilon - \alpha)) \\
 F_c &= -0.5\sqrt{2}I(\sin(\omega_s t + \varepsilon) + \sin(\omega_s t - \varepsilon - 2\alpha)) \\
 F_d &= -0.5\sqrt{2}I(\sin(\omega_s t + \varepsilon - 3\alpha) + \sin(\omega_s t - \varepsilon + 3\alpha)) \\
 F_e &= -0.5\sqrt{2}I(\sin(\omega_s t + \varepsilon) + \sin(\omega_s t - \varepsilon - 2\alpha)) \\
 F_f &= -0.5\sqrt{2}I(\sin(\omega_s t + \varepsilon + 3\alpha) + \sin(\omega_s t - \varepsilon + \alpha))
 \end{aligned} \tag{6.13}$$

Summation of (6.13) gives the following result:

$$0.5\sqrt{2}I \sin(\omega_s t + \varepsilon) + 0.5\sqrt{2}I \sin(\omega_s t - \varepsilon) \tag{6.14}$$

Summation of (6.12) and (6.14) gives the resultant mmf wave in the air gap of the six-phase machine (machine 1) as:

$$3\sqrt{2}I \sin(\omega_s t - \varepsilon) \quad (6.15)$$

Consider the currents supplied to machine 2:

$$\begin{aligned} i_{a2} &= i_A + i_D = \sqrt{2}I \sin(\omega_s t - 3\alpha) + \sqrt{2}I \sin(\omega_s t - \pi) = 2\sqrt{2}I \sin(\omega_s t - \pi) \\ i_{b2} &= i_B + i_E = \underline{\sqrt{2}I \sin(\omega_s t - \alpha)} + \underline{\sqrt{2}I \sin(\omega_s t - 4\alpha)} + 2\sqrt{2}I \sin(\omega_s t - 2\alpha - \pi) \\ i_{c2} &= i_C + i_F = \underline{\sqrt{2}I \sin(\omega_s t - 2\alpha)} + \underline{\sqrt{2}I \sin(\omega_s t - 5\alpha)} + 2\sqrt{2}I \sin(\omega_s t - 4\alpha - \pi) \end{aligned} \quad (6.16)$$

It can be seen that the underlined terms cancel while the phase “a” current sums to the required amplitude and phase. This demonstrates that both machines will operate without any loss in developed torque or performance. Further proof is obtained by application of the decoupling transformation (3.14b) to the inverter current references (6.8) and the stator currents of machine 2. The results can be seen in Table 6.4.

Table 6.4: Stator current components in six-phase case with phase “a” current cancellation (steady-state).

Current components	M1	M2
α	$\sqrt{6}I_1 \sin \omega_1 t$	$-\sqrt{12}I_2 \sin \omega_2 t$
β	$-\sqrt{6}I_1 \cos \omega_1 t$	$\sqrt{12}I_2 \cos \omega_2 t$
$x1$	$-\sqrt{6}I_2 \sin \omega_2 t$	—
$y1$	$\sqrt{6}I_2 \cos \omega_2 t$	
$0+$	0	0
$0-$	0	0

6.4.1 Simulation verification (six-phase case)

The performance of the six-phase two-motor drive under the conditions laid out in the previous section is verified here by simulation. It is assumed that the inverter is ideal and that the six-phase machine and the three-phase machine are equivalent in terms of the maximum torque they can develop. The torque limit of both machines is therefore 10Nm. A speed command of 314rad/s is applied to the six-phase machine and the three-phase machine in an identical manner at $t = 0.3s$ and $t = 0.301s$, respectively. Inverter phase “a” current cancellation can be seen in Fig. 6.5b when both machines

have reached the commanded speed. The torque, speed and rotor flux developed by each machine can be seen in Fig. 6.5a where it is obvious that neither of the machines is negatively affected due to cancellation of the inverter phase “a” current. Stator phase “a” current reference of the three-phase machine is twice that of the six-phase machine (Fig. 6.5c), thus resulting in cancellation of the inverter phase “a” current when summed according to (6.4). Stator phase “a” voltages of each machine are presented in Fig. 6.5c.

6.5 Summary

The multi-phase multi-machine drive concept for an even supply phase number has been investigated in detail for the six-phase and the ten-phase case. This chapter has demonstrated that series connection of machines within a multi-machine drive system fed by a single even phase number inverter allows independent control of each machine provided a suitable phase transposition is introduced in the connection of the machines in the group. In the even phase case the minimum required number of inverter phases is six. However, saving in the number of inverter legs, compared to a traditional three-phase multi-machine system, is not achieved unless the number of phases is equal to or greater than eight. Simulations were performed for the six-phase and ten-phase case for torque mode of operation. It was shown that both systems allow independent control of all the machines within the group.

The major disadvantage of the even phase system in comparison to the odd phase number case is that the number of inverter legs saved is the same for an even number and the previous odd number. However, an even phase number always results in a multi-machine system having motors with at least two different phase numbers. It was shown that all the machines in the group with a smaller phase number are not affected by the series connection to the larger phase number machines. The increase in losses and therefore reduced efficiency of the multi-phase multi-machine system is expected to be less pronounced for the even phase number system than for the equivalent odd phase number system, allowing the connection of the same number of machines. One particularly attractive possibility is the use of the six-phase high power machine in series connection to a low-power three-phase machine. Although there is no saving in the number of inverter legs, the supply and control of the three-phase machine can be obtained at no extra cost.

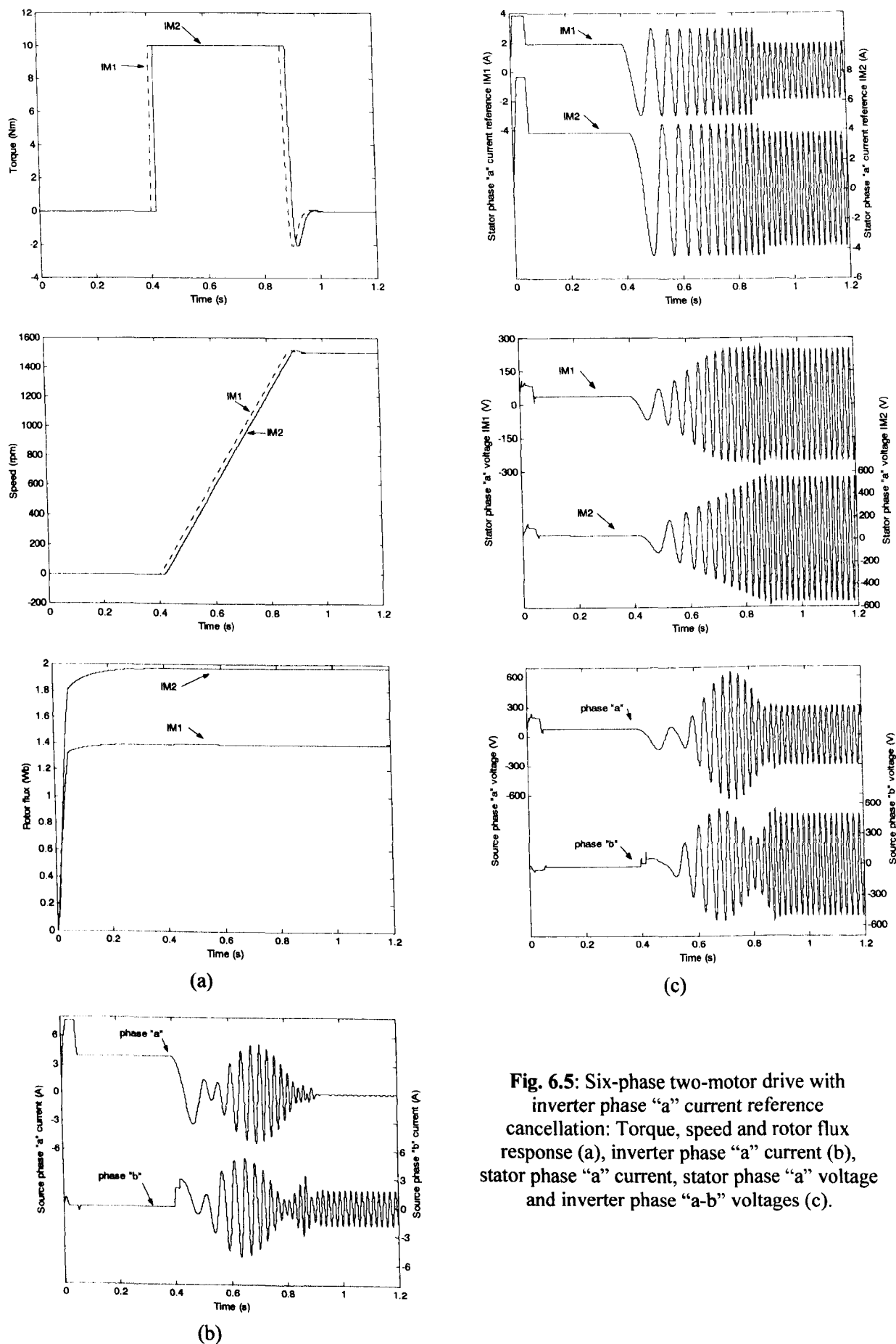


Fig. 6.5: Six-phase two-motor drive with inverter phase “a” current reference cancellation: Torque, speed and rotor flux response (a), inverter phase “a” current (b), stator phase “a” current, stator phase “a” voltage and inverter phase “a-b” voltages (c).

CHAPTER 7

CONNECTION OF DIFFERENT TYPES OF AC MACHINES

7.1 Introduction

There are many situations that require the use of different types of machines within a multi-motor drive. This chapter considers the connection of different types of multi-phase AC machines in the multi-machine drive. On the basis of the considerations of chapter 4 one can expect that the concept of multi-phase multi-motor drive systems, investigated in detail in chapters 5 and 6 using induction machines, is completely independent of the machine type and is equally applicable to all multi-phase machines with sinusoidal field distribution. The construction of the machines differs only in terms of the rotor and this fact allows the machines to be connected in series regardless of the type, provided a phase transposition is introduced in the same manner as explained in chapters 4 to 6. In order to prove such a situation, the connection of different machine types in the seven-phase drive system is considered in this chapter. It is shown in Jones et al (2003b) that this configuration allows series connection of three induction machines. However, the three machines under consideration in this chapter include: a surface mounted permanent magnet synchronous machine (PMSM), a synchronous reluctance machine (Syn-Rel) and an induction machine. Independent control of each machine within the seven-phase multi-motor drive is made possible by introducing a phase transposition between the stator windings of the machines as illustrated in Fig. 4.2. Considerations of this chapter can be found in Jones et al (2004). An explanation of how independent control of each machine is achieved becomes clear if one considers operation of the drive under steady state conditions.

Let us assume that machine 1 (IM1) is supplied with ideal sinusoidal currents of rms value and frequency equal to I_1 , ω_1 , machine 2 (IM2) is supplied with I_2 , ω_2 and machine 3 (IM3) is supplied with I_3 , ω_3 . Then the phase currents for machine 1 can be written as:

$$\begin{aligned}
 i_A = i_{a1} &= \sqrt{2}I_1 \sin(\omega_1 t) + \sqrt{2}I_2 \sin(\omega_2 t) + \sqrt{2}I_3 \sin(\omega_3 t) \\
 i_B = i_{b1} &= \sqrt{2}I_1 \sin(\omega_1 t - \alpha) + \sqrt{2}I_2 \sin(\omega_2 t - 2\alpha) + \sqrt{2}I_3 \sin(\omega_3 t - 3\alpha) \\
 i_C = i_{c1} &= \sqrt{2}I_1 \sin(\omega_1 t - 2\alpha) + \sqrt{2}I_2 \sin(\omega_2 t + 3\alpha) + \sqrt{2}I_3 \sin(\omega_3 t + \alpha) \\
 i_D = i_{d1} &= \sqrt{2}I_1 \sin(\omega_1 t - 3\alpha) + \sqrt{2}I_2 \sin(\omega_2 t + \alpha) + \sqrt{2}I_3 \sin(\omega_3 t - 2\alpha) \\
 i_E = i_{e1} &= \sqrt{2}I_1 \sin(\omega_1 t + 3\alpha) + \sqrt{2}I_2 \sin(\omega_2 t - \alpha) + \sqrt{2}I_3 \sin(\omega_3 t + 2\alpha) \\
 i_F = i_{f1} &= \sqrt{2}I_1 \sin(\omega_1 t + 2\alpha) + \sqrt{2}I_2 \sin(\omega_2 t - 3\alpha) + \sqrt{2}I_3 \sin(\omega_3 t - \alpha) \\
 i_G = i_{g1} &= \sqrt{2}I_1 \sin(\omega_1 t + \alpha) + \sqrt{2}I_2 \sin(\omega_2 t + 2\alpha) + \sqrt{2}I_3 \sin(\omega_3 t + 3\alpha)
 \end{aligned} \tag{7.1}$$

By examining Fig. 4.2 it can be seen that the currents given in equation (7.1) also represent the source currents. The spatial mmf distribution in a seven-phase AC machine is given by:

$$\begin{aligned}
 F_a &= NI_a \cos(\varepsilon) \\
 F_b &= NI_b \cos(\varepsilon - \alpha) \\
 F_c &= NI_c \cos(\varepsilon - 2\alpha) \\
 F_d &= NI_d \cos(\varepsilon - 3\alpha) \\
 F_e &= NI_e \cos(\varepsilon + 3\alpha) \\
 F_f &= NI_f \cos(\varepsilon + 2\alpha) \\
 F_g &= NI_g \cos(\varepsilon + \alpha)
 \end{aligned} \tag{7.2}$$

The total mmf produced in machine 1 by the second set of terms in equation (7.1) is given by:

$$\begin{aligned}
 &\sqrt{2}NI_2 \left[\begin{array}{l} \sin(\omega_2 t)\cos(\varepsilon) + \sin(\omega_2 t - 2\alpha)\cos(\varepsilon - \alpha) + \sin(\omega_2 t - 3\alpha)\cos(\varepsilon - 2\alpha) + \\ \sin(\omega_2 t + \alpha)\cos(\varepsilon - 3\alpha) + \sin(\omega_2 t - \alpha)\cos(\varepsilon + 3\alpha) + \sin(\omega_2 t - 3\alpha)\cos(\varepsilon + 2\alpha) + \\ \sin(\omega_2 t + 2\alpha)\cos(\varepsilon + \alpha) \end{array} \right] = \\
 &= \sqrt{2}NI_2 \frac{1}{4j} \left[\begin{array}{l} e^{j\omega_2 t} e^{j\varepsilon} (1 + e^{-j\alpha} + e^{j\alpha} + e^{-j2\alpha} + e^{j2\alpha} + e^{-j3\alpha} + e^{j3\alpha}) \\ -e^{-j\omega_2 t} e^{-j\varepsilon} (1 + e^{-j\alpha} + e^{j\alpha} + e^{-j2\alpha} + e^{j2\alpha} + e^{-j3\alpha} + e^{j3\alpha}) \\ e^{j\omega_2 t} e^{-j\varepsilon} (1 + e^{-j\alpha} + e^{j\alpha} + e^{-j4\alpha} + e^{j4\alpha} + e^{-j5\alpha} + e^{j5\alpha}) \\ -e^{-j\omega_2 t} e^{j\varepsilon} (1 + e^{-j\alpha} + e^{j\alpha} + e^{-j4\alpha} + e^{j4\alpha} + e^{-j5\alpha} + e^{j5\alpha}) \end{array} \right] = 0
 \end{aligned} \tag{7.3}$$

The total mmf produced in machine 1 by the third set of terms in equation (7.1) is given by:

$$\begin{aligned}
 &\sqrt{2}NI_3 \left[\begin{array}{l} \sin(\omega_3 t)\cos(\varepsilon) + \sin(\omega_3 t - 3\alpha)\cos(\varepsilon - \alpha) + \sin(\omega_3 t + \alpha)\cos(\varepsilon - 2\alpha) + \\ \sin(\omega_3 t - 2\alpha)\cos(\varepsilon - 3\alpha) + \sin(\omega_3 t + 2\alpha)\cos(\varepsilon + 3\alpha) + \sin(\omega_3 t - \alpha)\cos(\varepsilon + 2\alpha) + \\ \sin(\omega_3 t + 3\alpha)\cos(\varepsilon + \alpha) \end{array} \right] = \\
 &= \sqrt{2}NI_3 \frac{1}{4j} \left[\begin{array}{l} e^{j\omega_3 t} e^{j\varepsilon} (1 + e^{-j\alpha} + e^{j\alpha} + e^{-j4\alpha} + e^{j4\alpha} + e^{-j5\alpha} + e^{j5\alpha}) \\ -e^{-j\omega_3 t} e^{-j\varepsilon} (1 + e^{-j\alpha} + e^{j\alpha} + e^{-j4\alpha} + e^{j4\alpha} + e^{-j5\alpha} + e^{j5\alpha}) \\ e^{j\omega_3 t} e^{-j\varepsilon} (1 + e^{-j\alpha} + e^{j\alpha} + e^{-j2\alpha} + e^{j2\alpha} + e^{-j3\alpha} + e^{j3\alpha}) \\ -e^{-j\omega_3 t} e^{j\varepsilon} (1 + e^{-j\alpha} + e^{j\alpha} + e^{-j2\alpha} + e^{j2\alpha} + e^{-j3\alpha} + e^{j3\alpha}) \end{array} \right] = 0
 \end{aligned} \tag{7.4}$$

Thus it can be seen that currents, which produce a rotating field in machines 2 and 3, do not produce a rotating field in machine 1. Likewise it can also be shown that the currents that produce a rotating field in machines 2 and 3 do not affect any of the other two machines in the system. Application of the decoupling transformation matrix (3.13a) on the inverter currents (7.1) gives the current components shown in Table 7.1. It can be seen that the torque/flux producing currents (α - β) of machine 1 produce x-y current components in the other machines in the group and vice versa.

Table 7.1: Stator current components in series-connected motors in steady state (seven-phase case)

Current components	M1	M2	M3
α	$\sqrt{7}I_1 \sin \omega_1 t$	$\sqrt{7}I_2 \sin \omega_2 t$	$\sqrt{7}I_3 \sin \omega_3 t$
β	$-\sqrt{7}I_1 \cos \omega_1 t$	$-\sqrt{7}I_2 \cos \omega_2 t$	$-\sqrt{7}I_3 \cos \omega_3 t$
x1	$\sqrt{7}I_2 \sin \omega_2 t$	$\sqrt{7}I_3 \sin \omega_3 t$	$\sqrt{7}I_1 \sin \omega_1 t$
y1	$-\sqrt{7}I_2 \cos \omega_2 t$	$\sqrt{7}I_3 \cos \omega_3 t$	$\sqrt{7}I_1 \cos \omega_1 t$
x2	$\sqrt{7}I_3 \sin \omega_3 t$	$\sqrt{7}I_1 \sin \omega_1 t$	$\sqrt{7}I_2 \sin \omega_2 t$
y2	$-\sqrt{7}I_3 \cos \omega_3 t$	$\sqrt{7}I_1 \cos \omega_1 t$	$-\sqrt{7}I_2 \cos \omega_2 t$
0	0	0	0

7.2 Modelling of permanent magnet and synchronous reluctance machines

The permanent magnet synchronous machines and synchronous reluctance machines under consideration here have seven-phase stator windings, which are sinusoidally distributed around the circumference and therefore generate a sinusoidal field. Both the PMSM machine and the Syn-Rel machine do not have any windings on rotor. The PMSM is of so-called surface mounted structure and, like the name suggests, the permanent magnets are mounted on the surface of the rotor. The difference between the quadrature and direct axis inductances in this machine is small and the machine can be usually considered as having a uniform air-gap (i.e. $L_d = L_q = L_s$). In such a PMSM torque is produced solely due to the existence of flux developed by the permanent

magnets attached to the rotor while in a Syn-Rel the rotor is of a salient construction and torque (reluctance torque) exists solely due to the uneven air-gap. Therefore inductances along d and q-axis are substantially different in a Syn-Rel machine.

Modelling of multi-phase synchronous machines in d-q domain can be performed by analogy with corresponding three-phase synchronous machine modelling and multi-phase induction machine modelling. One important observation is that all synchronous machines, regardless of the type and the number of phases, have to be modelled in the rotating frame firmly fixed to the rotor. This is so since, in general, d-q axis inductances of synchronous machines are mutually different. In such a case only selection of the rotating frame fixed to the rotor (i.e. synchronous rotating frame) leads to elimination of the phase domain inductance dependence on the rotor angular position.

In general, one defines the following d-q axis inductances for a synchronous machine without rotor windings [Krishnan (2001)]:

$$\begin{aligned} L_d &= L_{ls} + L_{md} \\ L_q &= L_{ls} + L_{mq} \end{aligned} \quad (7.5)$$

Transformation of the phase variable model of an n -phase synchronous machine to the d-q reference frame is achieved using the decoupling transformation matrices (3.13a)-(3.14a) and the rotational transformation matrices (3.29). Due to (7.5) the common reference frame is fixed to the rotor. The rotational transformation applies to d-q axis components only and the transformation for x-y components is therefore the decoupling transformation only.

The voltage equilibrium equations upon application of (3.13a) and (3.29) and taking into account that:

$$\underline{v}_{dq}^s = \underline{D}_s \underline{C} \underline{v}_{abcde}^s \quad \underline{i}_{dq}^s = \underline{D}_s \underline{C} \underline{i}_{abcde}^s \quad \underline{\psi}_{dq}^s = \underline{D}_s \underline{C} \underline{\psi}_{abcde}^s \quad (7.6)$$

are for both PMSM and a Syn-Rel with a seven-phase winding given with:

$$\begin{aligned} v_{ds} &= R_s i_{ds} - \omega \psi_{qs} + p \psi_{ds} \\ v_{qs} &= R_s i_{qs} + \omega \psi_{ds} + p \psi_{qs} \\ v_{xs} &= R_s i_{x1s} + p \psi_{x1s} \\ v_{ys} &= R_s i_{y1s} + p \psi_{y1s} \\ v_{ys} &= R_s i_{x2s} + p \psi_{x2s} \\ v_{ys} &= R_s i_{y2s} + p \psi_{y2s} \\ v_{os} &= R_s i_{os} + p \psi_{os} \end{aligned} \quad (7.7)$$

Flux linkage equations of a PMSM take the following form:

$$\begin{aligned}
 \psi_{ds} &= (L_{ls} + L_{md})i_{ds} + \psi_m = L_s i_{ds} + \psi_m \\
 \psi_{qs} &= (L_{ls} + L_{mq})i_{qs} = L_s i_{qs} \\
 \psi_{x1s} &= L_{ls} i_{x1s} \\
 \psi_{y1s} &= L_{ls} i_{y1s} \\
 \psi_{x2s} &= L_{ls} i_{x2s} \\
 \psi_{y2s} &= L_{ls} i_{y2s} \\
 \psi_{os} &= L_{ls} i_{os}
 \end{aligned} \tag{7.8}$$

since $L_{md} = L_{mq} = L_m$, while for a Syn-Rel machine flux linkages are given with:

$$\begin{aligned}
 \psi_{ds} &= (L_{ls} + L_{md})i_{ds} = L_d i_{ds} \\
 \psi_{qs} &= (L_{ls} + L_{mq})i_{qs} = L_q i_{qs} \\
 \psi_{x1s} &= L_{ls} i_{x1s} \\
 \psi_{y1s} &= L_{ls} i_{y1s} \\
 \psi_{x2s} &= L_{ls} i_{x2s} \\
 \psi_{y2s} &= L_{ls} i_{y2s} \\
 \psi_{os} &= L_{ls} i_{os}
 \end{aligned} \tag{7.9}$$

Torque equation of a PMSM is:

$$\begin{aligned}
 T_e &= P(\psi_{ds} i_{qs} - \psi_{qs} i_{ds}) \\
 T_e &= P[\psi_m i_{qs} + (L_d - L_q) i_{ds} i_{qs}] = P \psi_m i_{qs}
 \end{aligned} \tag{7.10}$$

while for a Syn-Rel machine torque can be expressed as:

$$\begin{aligned}
 T_e &= P(\psi_{ds} i_{qs} - \psi_{qs} i_{ds}) \\
 T_e &= P(L_d - L_q) i_{ds} i_{qs}
 \end{aligned} \tag{7.11}$$

It should be noted that the two inductances L_{md}, L_{mq} are again related through the coefficient $n/2$ with the corresponding phase domain inductances. These two inductances can be given with:

$$\begin{aligned}
 L_{md} &= (n/2)(M + M_1) \\
 L_{mq} &= (n/2)(M - M_1)
 \end{aligned} \tag{7.12}$$

where M has the same meaning as for an induction motor while M_1 is the amplitude of the second harmonic of the mutual inductance terms in the stator winding, caused by the existence of the saliency (and is the reason why transformation into synchronous reference frame is the only one which eliminates angular dependency of the phase domain inductances).

7.2.1 PMSM parameters

The per-phase data required for the simulation of an n -phase PMSM are given in Table 7.2, and are based on a three-phase PMSM utilised in Ibrahim (1999). The given value of the permanent magnet flux is rms and needs to be multiplied with \sqrt{n} for use in n -phase machine d-q model.

Table 7.2: PMSM data on rms and per-phase basis

	PMSM1
Peak per-phase torque, $T_{e\max}$ (Nm)	6.9
Rated per-phase torque, T_{en} (Nm)	2.033
Rated per-phase current, I_n (A) (rms)	6.2
Peak per-phase current, I_{\max} (A) (rms)	21
Rated speed, ω_n (rad/s) n_n (rpm)	180 (1720 rpm)
Inertia J (kgm ²)	0.00176
Winding per-phase resistance, R_s (Ω)	1.4
Winding per-phase inductance, L_s (mH)	5.6
Stator leakage inductance L_{ls} (mH)	0.56
Magnet flux, Ψ_m (Vs/rad) (rms value)	0.1093
Rated frequency, f_n (Hz)	86
Pole pair number	3

Using the per-phase values given in Table 7.2, one has for a seven-phase PMSM: $T_{e\max} = 7 \cdot 6.9 = 48.3$ Nm, $T_{en} = 7 \cdot 2.033 = 14.231$ Nm, $|\underline{\psi}_m| = \sqrt{7} \cdot 0.1093 = 0.2891$ Wb. In order to slow down the acceleration of the machine an inertial load was assumed, increasing the total inertia to 0.0536 kgm².

7.2.2 Syn-Rel machine parameters

The per-phase data of a Syn-Rel machine are given in Table 7.3 and are taken from Jovanovic (1996), where a three-phase Syn-Rel machine was considered. According to Jovanovic (1996) saturation along the d-axis is significant and the work lists both saturated and unsaturated values of the inductances. The issue of saturation (which asks for significantly more elaborate machine models) is of no relevance here

and the synchronous inductance along the d-axis is therefore taken as the mean value of the unsaturated and the saturated value of the d-axis inductance.

Table 7.3: Per-phase data of a Syn-Rel.

	Syn-Rel data
Stator phase rated current (A) (rms)	14.3
Rated per-phase torque (Nm)	12.333 Nm
Number of pole pairs	2
Rated frequency (Hz)	50 Hz
Rated speed (rad/s and rpm)	157.08 (1500)
Motor inertia (kgm^2)	0.23
Maximum per-phase stator current (A) (rms)	20 A
Maximum per-phase torque (Nm)	19
Stator per-phase resistance (Ohms)	0.6
Synchronous d-axis inductance L_d (mH)	82.95
Synchronous q-axis inductance L_q (mH)	9.8
Stator leakage inductance L_{ls} (mH)	4.17

Calculation of rated no-load and rated torque components of rated per phase stator current closely follows the procedure for an induction machine and results in $I_{dsn} = 7.91$ A and $I_{qsn} = 11.91$ A (rms). Hence, for a seven-phase Syn-Rel one has, using data of Table 7.3, the following values:

$$T_{emax} = 7 \cdot 19 = 133 \text{ Nm}, T_{en} = 7 \cdot 12.33 = 86.31 \text{ Nm},$$

$$i_{dsn} = \sqrt{7} \cdot 7.91 = 20.92 \text{ A and } i_{qsn} = \sqrt{7} \cdot 11.91 = 31.51 \text{ A}$$

7.3 Vector control of a PMSM and a Syn-Rel machine

The equations given in section 7.2 are already in the rotor flux oriented reference frame for a PMSM, since d-axis coincides with the direction of the permanent magnet flux. Inductances along d-q axes are assumed to be equal, and base speed region is considered only. Assuming that current control is performed in the stationary reference frame, the vector controller takes the form given in Fig 7.1. The controller structure is the same for both PMSM and Syn-Rel machines. The stator d-axis (i_{ds}^*) current is held at zero for the PMSM as the machine will be limited to operation in the base speed region. For the Syn-Rel the simplest possible method of vector control, called constant d-axis current control, is used. Hence stator d-axis current command will be kept at the constant rated value throughout.

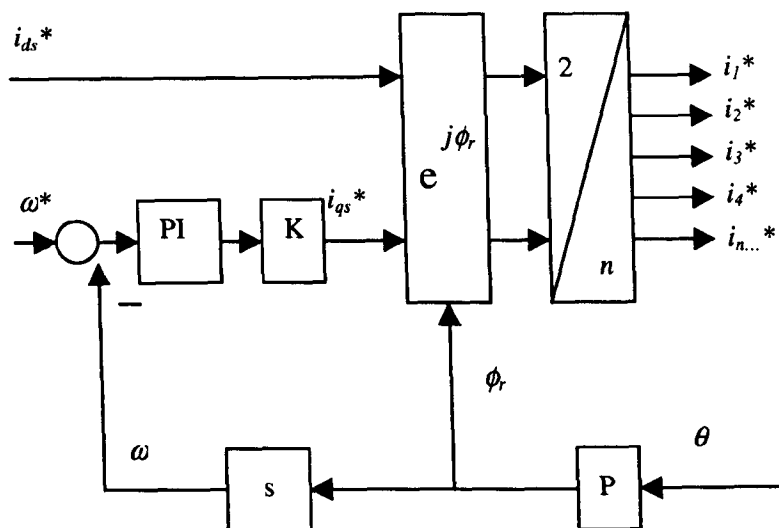


Fig. 7.1: Vector controller for an n -phase PMSM or Syn-Rel ($i_{ds}^* = 0$ for PMSM, $i_{ds}^* = i_{ds_n}$ for Syn-Rel).

Assuming that the output of the speed controller is the torque reference, constant k in Fig.7.1 equals for a PMSM $k = 1/(P\psi_m)$ while for the Syn-Rel: $k = 1/[P(L_d - L_q)I_{dsn}]$.

7.3.1 Simulation of the seven-phase drive comprising an induction machine, a PMSM and a Syn-Rel machine (torque mode)

The seven-phase case allows the possibility of connecting three seven-phase machines in series as demonstrated in Jones et al (2003b). These are taken as a seven-phase induction machine, a synchronous reluctance machine and a permanent magnet synchronous machine. A simulation program was developed using MATLAB/SIMULINK software considering the torque mode of operation under no-load conditions.

The induction machine was magnetised in the same way as described in previous chapters and a torque command was applied to each machine according to the schedule shown in Table 7.4. The torque response of each machine exactly matched the applied torque command and hence each machine accelerated smoothly and in the fastest possible time (Fig 7.2a-b). Despite the higher torque developed by the Syn-Rel the machine takes the longest time to accelerate to the rated speed, because of the relatively high inertia. The rotor flux of the induction machine remains unaffected by the application of the torque command to any of the machines in the group and remains at the commanded value at all times (Fig 7.2c), thus demonstrating that completely

decoupled flux and torque control has been achieved. The stator current reference for each machine becomes sinusoidal once the torque command is applied (Fig 7.2d). The stator current reference is at the maximum value during the acceleration of the machines, due to operation in the torque limit. The effect of the rotor flux command can be seen on the induction machine stator current reference. Likewise the stator current reference of the Syn-Rel machine shows an initial value of 11.18A due to the pre-excitation in simulation with $i_{dsn} = 20.92A$. The PMSM however requires no magnetising current and therefore the initial current reference is zero (Fig 7.2d). Once the PMSM has reached the required speed and the torque command is removed the stator current reference returns to zero. This is again due to the fact that there is no need for the magnetising current, since permanent magnets provide the required flux.

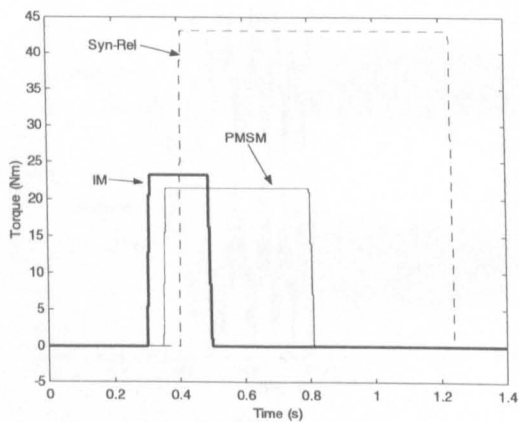
The source currents are highly distorted due to the summing of the machine current references respecting the phase transposition. The effect of the PMSM current reference upon the source currents can be seen (Fig 7.3a) between $t = 0.35$ and $t = 0.8s$ where the PMSM current references dominate because of their high value. Once the PMSM has reached the required speed the source currents no longer contain components of the PMSM stator currents and become less distorted. It can be seen that the source voltages are highly distorted (Fig 7.3b). The individual stator voltages of the machines can be seen in Fig 7.3c. The stator voltages of each machine are once more highly distorted due to the flow of torque/flux producing currents of other machines in the group through the stators of all machines. The PMSM only affects the other machine voltages when the PMSM is accelerating because no currents flow once the machine has reached the required speed. This of course holds true for no-load operation only, considered here. After 0.8s the stator voltages of the IM and Syn-Rel machine contain only two components, related to operating frequencies of these two machines. The PMSM voltage is affected by all the machines in the group. Under loaded conditions the PMSM would operate with non-zero current and the situation would be the same as in the case of three induction motors, considered in Jones (2003b).

Table 7.4: Application of torque command.

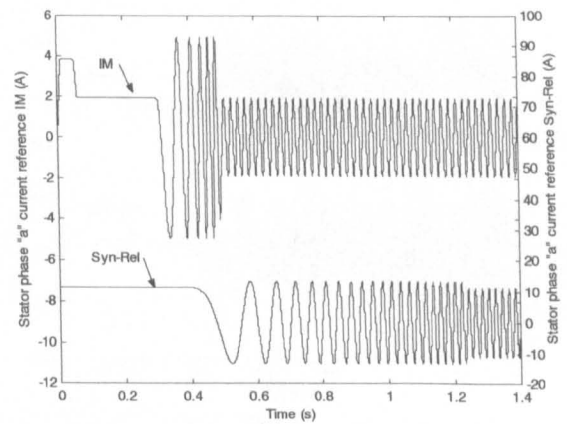
Machine	T_e^* (Nm)	Applied at (s)	Removed at (s)
IM	$2T_{en} = 23.34$	$t = 0.3$	$t = 0.49$
PMSM	$1.5T_{en} = 21.35$	$t = 0.35$	$t = 0.8$
Syn-Rel	$0.5T_{en} = 43.16$	$t = 0.4$	$t = 1.23$

7.4 Summary

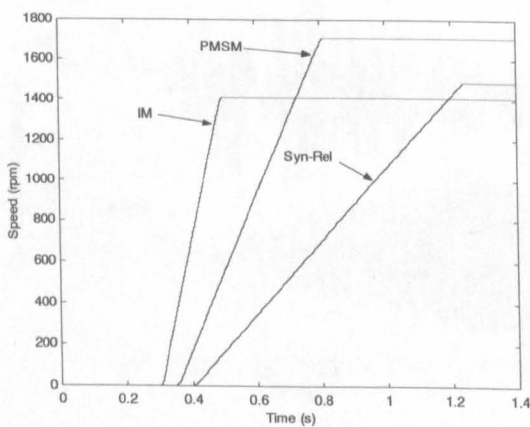
This chapter has verified the possibility of connecting the different types of multi-phase AC machines in series and independently controlling all the machines in the group. A seven-phase three-motor drive was considered in detail, consisting of an induction machine, a permanent magnet synchronous machine and a synchronous reluctance machine. Since the concept of the multi-phase multi-motor drive system



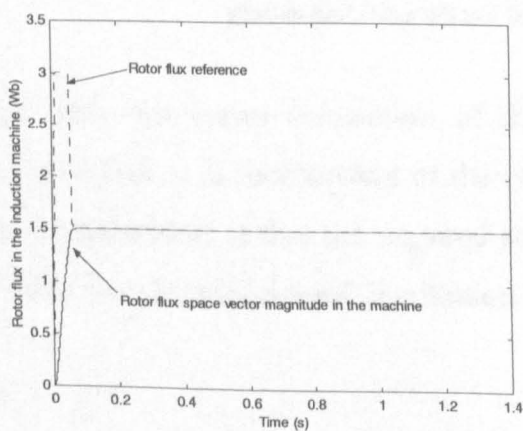
(a)



(d)



(b)



(c)

Fig.7.2: Seven-phase three-motor drive: Torque responses (a), speed response (b), rotor flux and rotor flux reference of induction machine (c) and stator phase "a" current reference (d).

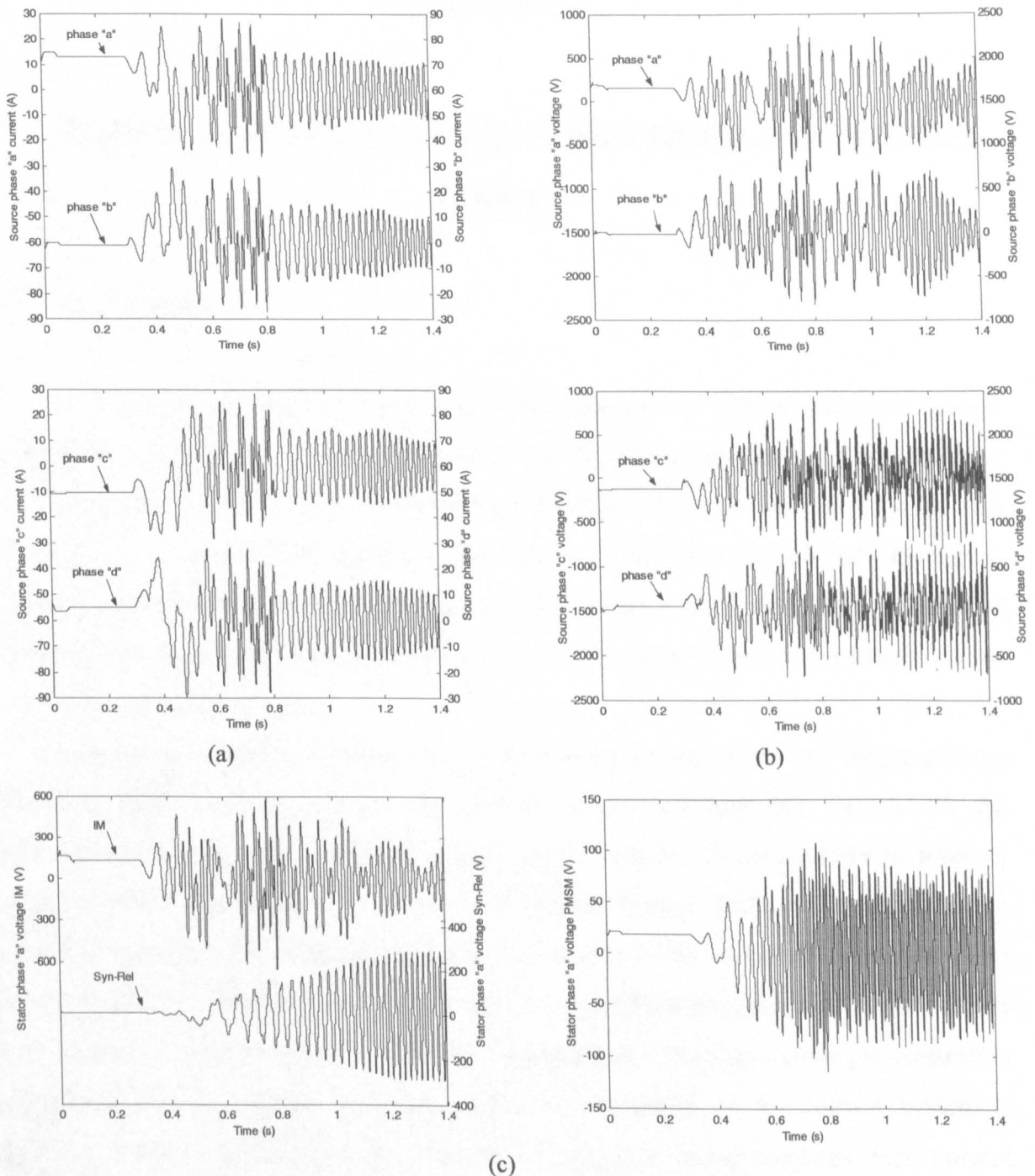


Fig. 7.3: Seven-phase three-motor drive source currents (a) and source voltages (b) for the first four phases and stator phase "a" voltage of the three machines (c).

asks only for series connection of the stator windings with an appropriate phase transposition, it is independent of the type of rotor (i.e. the type of AC machine). The only requirement is that the required stator currents of the AC machine are sinusoidal (that is that the spatial mmf distribution is sinusoidal).

CHAPTER 8

CURRENT CONTROL IN THE SYNCHRONOUS REFERENCE FRAME

8.1 Introduction

The majority of field oriented high performance AC drives utilise a current regulated pulse width modulated (PWM) VSI as the power converter. Field oriented controllers that provide voltage commands are feasible. However, if phase currents are selected as the controlled variables then stator dynamics (effects of resistance, inductance and induced emf) are eliminated. This allows a relatively simple method of achieving decoupled flux and torque control by instantaneous stator current space vector amplitude and position control.

All current control techniques essentially belong to one of the two major groups. The first group encompasses all the current control methods that operate in the stationary reference frame while the second group includes current control techniques with controllers operating in the rotational reference frame. In the work presented so far, only vector control schemes with current control in the stationary reference have been considered. However, current control in the stationary reference frame suffers from inherent problems and is usually built using combined digital-analogue realisation (current control is usually analogue, while the remainder of the control system is digital). Current control in the stationary reference frame requires that current controllers process alternating signals, which can be of a large frequency range. Furthermore, controller characteristics in steady-state depend on the operating frequency and machine impedance [Brod and Novotny (1985)]. These shortcomings can be partially but not completely eliminated by different modifications of the basic current control principles.

At low operating speeds the induced rotational electromotive force is small and current control enables very good tracking between reference and actual currents, with respect to both amplitude and phase. However at higher speeds, due to limited voltage capability of the inverter and finite switching frequency, tracking worsens and an error

is met in both amplitude and phase of actual currents compared to reference currents.

The inherent problems of regulating AC signals in the stationary reference frame were originally recognized by Schauder and Caddy (1982). They showed that the stationary reference frame ramp comparison controller is only one of an infinite number of possible controllers. In effect controllers implemented in other reference frames exhibit quite different characteristics. This stems from the fact that the frequency of the controlled currents is different in different reference frames and so the controllers' performance will be different in different reference frames. It therefore follows that a current controller operating in the synchronous reference frame will operate upon steady-state currents that are DC and a simple PI controller will result in zero steady-state error. The performance of the synchronous reference frame controller is therefore superior to the stationary reference frame controller in all aspects. It is, however, considerably more hardware-intensive, requiring an additional transformation between stationary and synchronous variables.

The work presented in this chapter will consider the five-phase and six-phase two-machine drive with current control performed in the synchronous reference frame, which, as well as offering the advantages previously mentioned also allows for complete digital realisation. When current control is performed in the synchronous reference frame the outputs of the control system become voltage references. The final goal (for rotor flux oriented control) remains orientation of stator current space vector along the rotor flux space vector, however the appropriate stator voltage space vector that enables achievement of this goal has to be determined. In other words, stator voltage space vector has to have such a magnitude and has to be put in such a position that resulting stator current space vector attains exactly the magnitude and position with respect to rotor flux space vector that are needed to realise decoupled flux and torque control; i.e., stator current space vector is controlled indirectly by direct control of stator voltage space vector. For this reason the machine can no longer be considered as current fed and so the modelling of the machine becomes more complex.

This chapter will therefore begin with the voltage fed model of the five-phase and six-phase series-connected drives. Next, simulation studies will be presented for a single five-phase machine and later the five-phase two-machine drive system. This will allow a comparison of the two cases and it will be shown that the series-connected multi-phase multi-machine drive suffers deterioration in dynamic performance due to the flow of x-y currents. In order to solve this problem two schemes are developed; one

using a feed-forward method and the other requiring a modification of the decoupling circuit. Both schemes are verified via simulation for the five-phase two-machine case and the six-phase two-machine case. Considerations of this chapter can be found in Jones et al (2004a), Jones et al (2004b), Jones et al (2004c) and Jones et al (2005).

8.2 Phase domain modelling of the voltage-fed series-connected five-phase two-motor drive

In order for current control to be implemented in the synchronous reference frame the machine has to be considered as voltage fed. This significantly complicates the modelling of the machine because stator dynamics now have to be taken into consideration. The phase variable model of the two-motor five-phase drive connected in series according to Fig. 4.1 is developed in state space form. Due to the series connection of two stator windings according to Fig. 4.1 the following holds true:

$$\begin{aligned}
 v_A &= v_{as1} + v_{as2} \\
 v_B &= v_{bs1} + v_{cs2} \\
 v_C &= v_{cs1} + v_{es2} \\
 v_D &= v_{ds1} + v_{bs2} \\
 v_E &= v_{es1} + v_{ds2}
 \end{aligned} \tag{8.1}$$

$$\begin{aligned}
 i_A &= i_{as1} = i_{as2} \\
 i_B &= i_{bs1} = i_{cs2} \\
 i_C &= i_{cs1} = i_{es2} \\
 i_D &= i_{ds1} = i_{bs2} \\
 i_E &= i_{es1} = i_{ds2}
 \end{aligned} \tag{8.2}$$

Capital letters stand for inverter phase-to-neutral voltages and inverter currents in equations (8.1)-(8.2).

In a general case the two machines, although both five-phase, may be different and therefore be with different parameters. Let the index '1' denote induction machine directly connected to the five-phase inverter and let the index '2' stand for the second induction machine, connected after the first machine through phase transposition.

Voltage equation for the complete system can be written in compact matrix form as:

$$\underline{v} = \underline{R}i + \frac{d(\underline{L}i)}{dt} \tag{8.3}$$

where the system is of the 15th order and

$$\underline{v} = \begin{bmatrix} \underline{v}^{INV} \\ \underline{0} \\ \underline{0} \end{bmatrix} \quad \underline{i} = \begin{bmatrix} \underline{i}^{INV} \\ \underline{i}_{r1} \\ \underline{i}_{r2} \end{bmatrix} \quad (8.4)$$

$$\begin{aligned} \underline{v}^{INV} &= [v_A \quad v_B \quad v_C \quad v_D \quad v_E]^T \\ \underline{i}^{INV} &= [i_A \quad i_B \quad i_C \quad i_D \quad i_E]^T \end{aligned} \quad (8.5)$$

$$\begin{aligned} \underline{i}_{r1} &= [i_{ar1} \quad i_{br1} \quad i_{cr1} \quad i_{dr1} \quad i_{er1}]^T \\ \underline{i}_{r2} &= [i_{ar2} \quad i_{br2} \quad i_{cr2} \quad i_{dr2} \quad i_{er2}]^T \end{aligned} \quad (8.6)$$

The resistance and inductance matrices of (3.2) can be written as:

$$\underline{R} = \begin{bmatrix} \underline{R}_{s1} + \underline{R}_{s2} & & & & \\ & & \underline{R}_{r1} & & \\ & & & & \\ & & & & \\ & & & & \underline{R}_{r2} \end{bmatrix} \quad (8.7)$$

$$\underline{L} = \begin{bmatrix} \underline{L}_{s1} + \underline{L}_{s2}' & \underline{L}_{sr1} & \underline{L}_{sr2}' \\ \underline{L}_{rs1} & \underline{L}_{r1} & \underline{0} \\ \underline{L}_{rs2}' & \underline{0} & \underline{L}_{r2} \end{bmatrix} \quad (8.8)$$

Superscript ' in (8.8) denotes sub-matrices of machine 2 that have been modified through the phase transposition operation, compared to their original form given in (3.5), (3.6). The sub-matrices of (8.7)-(8.8) are all five by five matrices and are given with the following expressions:

$$\begin{aligned} \underline{R}_{s1} &= \text{diag}(R_{s1} \quad R_{s1} \quad R_{s1} \quad R_{s1} \quad R_{s1}) \\ \underline{R}_{s2} &= \text{diag}(R_{s2} \quad R_{s2} \quad R_{s2} \quad R_{s2} \quad R_{s2}) \\ \underline{R}_{r1} &= \text{diag}(R_{r1} \quad R_{r1} \quad R_{r1} \quad R_{r1} \quad R_{r1}) \\ \underline{R}_{r2} &= \text{diag}(R_{r2} \quad R_{r2} \quad R_{r2} \quad R_{r2} \quad R_{r2}) \end{aligned} \quad (8.9)$$

$$\underline{L}_{s1} = \begin{bmatrix} L_{ls1} + M_1 & M_1 \cos \alpha & M_1 \cos 2\alpha & M_1 \cos 2\alpha & M_1 \cos \alpha \\ M_1 \cos \alpha & L_{ls1} + M_1 & M_1 \cos \alpha & M_1 \cos 2\alpha & M_1 \cos 2\alpha \\ M_1 \cos 2\alpha & M_1 \cos \alpha & L_{ls1} + M_1 & M_1 \cos \alpha & M_1 \cos 2\alpha \\ M_1 \cos 2\alpha & M_1 \cos 2\alpha & M_1 \cos \alpha & L_{ls1} + M_1 & M_1 \cos \alpha \\ M_1 \cos \alpha & M_1 \cos 2\alpha & M_1 \cos 2\alpha & M_1 \cos \alpha & L_{ls1} + M_1 \end{bmatrix} \quad (8.10)$$

$$\underline{L}_{s2}' = \begin{bmatrix} L_{ls2} + M_1 & M_2 \cos 2\alpha & M_2 \cos \alpha & M_2 \cos \alpha & M_2 \cos 2\alpha \\ M_2 \cos 2\alpha & L_{ls2} + M_2 & M_2 \cos 2\alpha & M_2 \cos \alpha & M_2 \cos \alpha \\ M_2 \cos \alpha & M_2 \cos 2\alpha & L_{ls2} + M_2 & M_2 \cos 2\alpha & M_2 \cos \alpha \\ M_2 \cos \alpha & M_2 \cos \alpha & M_2 \cos 2\alpha & L_{ls2} + M_2 & M_2 \cos 2\alpha \\ M_2 \cos 2\alpha & M_2 \cos \alpha & M_2 \cos \alpha & M_2 \cos 2\alpha & L_{ls2} + M_2 \end{bmatrix} \quad (8.11)$$

$$\underline{L}_{r1} = \begin{bmatrix} L_{lr1} + M_1 & M_1 \cos \alpha & M_1 \cos 2\alpha & M_1 \cos 2\alpha & M_1 \cos \alpha \\ M_1 \cos \alpha & L_{lr1} + M_1 & M_1 \cos \alpha & M_1 \cos 2\alpha & M_1 \cos 2\alpha \\ M_1 \cos 2\alpha & M_1 \cos \alpha & L_{lr1} + M_1 & M_1 \cos \alpha & M_1 \cos 2\alpha \\ M_1 \cos 2\alpha & M_1 \cos 2\alpha & M_1 \cos \alpha & L_{lr1} + M_1 & M_1 \cos \alpha \\ M_1 \cos \alpha & M_1 \cos 2\alpha & M_1 \cos 2\alpha & M_1 \cos \alpha & L_{lr1} + M_1 \end{bmatrix} \quad (8.12)$$

$$\underline{L}_{r2} = \begin{bmatrix} L_{lr2} + M_2 & M_2 \cos \alpha & M_2 \cos 2\alpha & M_2 \cos 2\alpha & M_2 \cos \alpha \\ M_2 \cos \alpha & L_{lr2} + M_2 & M_2 \cos \alpha & M_2 \cos 2\alpha & M_2 \cos 2\alpha \\ M_2 \cos 2\alpha & M_2 \cos \alpha & L_{lr2} + M_2 & M_2 \cos \alpha & M_2 \cos 2\alpha \\ M_2 \cos 2\alpha & M_2 \cos 2\alpha & M_2 \cos \alpha & L_{lr2} + M_2 & M_2 \cos \alpha \\ M_2 \cos \alpha & M_2 \cos 2\alpha & M_2 \cos 2\alpha & M_2 \cos \alpha & L_{lr2} + M_2 \end{bmatrix} \quad (8.13)$$

$$\underline{L}_{sr1} = M_1 \begin{bmatrix} \cos \theta_1 & \cos(\theta_1 + \alpha) & \cos(\theta_1 + 2\alpha) & \cos(\theta_1 - 2\alpha) & \cos(\theta_1 - \alpha) \\ \cos(\theta_1 - \alpha) & \cos \theta_1 & \cos(\theta_1 + \alpha) & \cos(\theta_1 + 2\alpha) & \cos(\theta_1 - 2\alpha) \\ \cos(\theta_1 - 2\alpha) & \cos(\theta_1 - \alpha) & \cos \theta_1 & \cos(\theta_1 + \alpha) & \cos(\theta_1 + 2\alpha) \\ \cos(\theta_1 + 2\alpha) & \cos(\theta_1 - 2\alpha) & \cos(\theta_1 - \alpha) & \cos \theta_1 & \cos(\theta_1 + \alpha) \\ \cos(\theta_1 + \alpha) & \cos(\theta_1 + 2\alpha) & \cos(\theta_1 - 2\alpha) & \cos(\theta_1 - \alpha) & \cos \theta_1 \end{bmatrix} \quad (8.14)$$

$$\underline{L}_{rs1} = \underline{L}_{sr1}^T$$

$$\underline{L}_{sr2}' = M_2 \begin{bmatrix} \cos \theta_2 & \cos(\theta_2 + \alpha) & \cos(\theta_2 + 2\alpha) & \cos(\theta_2 - 2\alpha) & \cos(\theta_2 - \alpha) \\ \cos(\theta_2 - 2\alpha) & \cos(\theta_2 - \alpha) & \cos \theta_2 & \cos(\theta_2 + \alpha) & \cos(\theta_2 + 2\alpha) \\ \cos(\theta_2 + \alpha) & \cos(\theta_2 + 2\alpha) & \cos(\theta_2 - 2\alpha) & \cos(\theta_2 - \alpha) & \cos \theta_2 \\ \cos(\theta_2 - \alpha) & \cos \theta_2 & \cos(\theta_2 + \alpha) & \cos(\theta_2 + 2\alpha) & \cos(\theta_2 - 2\alpha) \\ \cos(\theta_2 + 2\alpha) & \cos(\theta_2 - 2\alpha) & \cos(\theta_2 - \alpha) & \cos \theta_2 & \cos(\theta_2 + \alpha) \end{bmatrix} \quad (8.15)$$

$$\underline{L}_{rs2}' = \underline{L}_{sr2}'^T$$

Expansion of (8.3) yields:

$$\underline{v} = \begin{bmatrix} \underline{v}^{INV} \\ \underline{0} \\ \underline{0} \end{bmatrix} = \begin{bmatrix} \underline{R}_{s1} + \underline{R}_{s2} & & \\ & \underline{R}_{r1} & \\ & & \underline{R}_{r2} \end{bmatrix} \begin{bmatrix} \underline{i}^{INV} \\ \underline{i}_{r1} \\ \underline{i}_{r2} \end{bmatrix} + \begin{bmatrix} \underline{L}_{s1} + \underline{L}_{s2}' & \underline{L}_{sr1} & \underline{L}_{sr2}' \\ \underline{L}_{rs1} & \underline{L}_{r1} & \underline{0} \\ \underline{L}_{rs2}' & \underline{0} & \underline{L}_{r2} \end{bmatrix} \frac{d}{dt} \begin{bmatrix} \underline{i}^{INV} \\ \underline{i}_{r1} \\ \underline{i}_{r2} \end{bmatrix} + \begin{bmatrix} \underline{0} & \frac{d}{dt} \underline{L}_{sr1} & \frac{d}{dt} \underline{L}_{sr2}' \\ \frac{d}{dt} \underline{L}_{rs1} & \underline{0} & \underline{0} \\ \frac{d}{dt} \underline{L}_{rs2}' & \underline{0} & \underline{0} \end{bmatrix} \begin{bmatrix} \underline{i}^{INV} \\ \underline{i}_{r1} \\ \underline{i}_{r2} \end{bmatrix} \quad (8.16)$$

Torque equations of the two machines in terms of inverter currents and their respective rotor currents and rotor positions are obtained by using (3.10). Replacing motor stator

currents with corresponding inverter currents of (8.2):

$$T_{e1} = -P_1 M_1 \left\{ \begin{array}{l} (i_A i_{ar1} + i_B i_{br1} + i_C i_{cr1} + i_D i_{dr1} + i_E i_{er1}) \sin \theta_1 + \\ (i_E i_{ar1} + i_A i_{br1} + i_B i_{cr1} + i_C i_{dr1} + i_D i_{er1}) \sin(\theta_1 + \alpha) + \\ (i_D i_{ar1} + i_E i_{br1} + i_A i_{cr1} + i_B i_{dr1} + i_C i_{er1}) \sin(\theta_1 + 2\alpha) + \\ (i_C i_{ar1} + i_D i_{br1} + i_E i_{cr1} + i_A i_{dr1} + i_B i_{er1}) \sin(\theta_1 - 2\alpha) + \\ (i_B i_{ar1} + i_C i_{br1} + i_D i_{cr1} + i_E i_{dr1} + i_A i_{er1}) \sin(\theta_1 - \alpha) \end{array} \right\} \quad (8.17)$$

$$T_{e2} = -P_2 M_2 \left\{ \begin{array}{l} (i_A i_{ar2} + i_D i_{br2} + i_B i_{cr2} + i_E i_{dr2} + i_C i_{er2}) \sin \theta_2 + \\ (i_C i_{ar2} + i_A i_{br2} + i_D i_{cr2} + i_B i_{dr2} + i_E i_{er2}) \sin(\theta_2 + \alpha) + \\ (i_E i_{ar2} + i_C i_{br2} + i_A i_{cr2} + i_D i_{dr2} + i_B i_{er2}) \sin(\theta_2 + 2\alpha) + \\ (i_B i_{ar2} + i_E i_{br2} + i_C i_{cr2} + i_A i_{dr2} + i_D i_{er2}) \sin(\theta_2 - 2\alpha) + \\ (i_D i_{ar2} + i_B i_{br2} + i_E i_{cr2} + i_C i_{dr2} + i_A i_{er2}) \sin(\theta_2 - \alpha) \end{array} \right\} \quad (8.18)$$

8.2.1 Transformation of the two-motor five-phase series-connected model into the stationary reference frame

In order to simplify the phase-domain model of section 8.2, the decoupling transformation (3.13a) is applied to the phase-domain model (8.3). Rotational transformation (3.29) is next applied to the rotor equations of both machine 1 and 2 of the two-motor system model to obtain the model in the stationary reference frame (8.19) – (8.22). A thorough explanation and derivation of this procedure can be found in Iqbal (2003) and Levi et al (2003c). Inverter voltage equations are:

$$\begin{aligned} v_\alpha^{INV} &= R_{s1} i_\alpha^{INV} + (L_{ls1} + L_{m1}) \frac{di_\alpha^{INV}}{dt} + L_{m1} \frac{di_{dr1}}{dt} + R_{s2} i_\alpha^{INV} + L_{ls2} \frac{di_\alpha^{INV}}{dt} \\ v_\beta^{INV} &= R_{s1} i_\beta^{INV} + (L_{ls1} + L_{m1}) \frac{di_\beta^{INV}}{dt} + L_{m1} \frac{di_{qr1}}{dt} + R_{s2} i_\beta^{INV} + L_{ls2} \frac{di_\beta^{INV}}{dt} \\ v_x^{INV} &= R_{s1} i_x^{INV} + L_{ls1} \frac{di_x^{INV}}{dt} + R_{s2} i_x^{INV} + (L_{ls2} + L_{m2}) \frac{di_x^{INV}}{dt} + L_{m2} \frac{di_{dr2}}{dt} \\ v_y^{INV} &= R_{s1} i_y^{INV} + L_{ls1} \frac{di_y^{INV}}{dt} + R_{s2} i_y^{INV} + (L_{ls2} + L_{m2}) \frac{di_y^{INV}}{dt} + L_{m2} \frac{di_{qr2}}{dt} \end{aligned} \quad (8.19)$$

Rotor voltage equations of machine 1:

$$\begin{aligned} 0 &= R_{r1} i_{dr1} + L_{m1} \frac{di_\alpha^{INV}}{dt} + (L_{lr1} + L_{m1}) \frac{di_{dr1}}{dt} + \omega_{l1} (L_{m1} i_\beta^{INV} + (L_{lr1} + L_{m1}) i_{qr1}) \\ 0 &= R_{r1} i_{qr1} + L_{m1} \frac{di_\beta^{INV}}{dt} + (L_{lr1} + L_{m1}) \frac{di_{qr1}}{dt} - \omega_{l1} (L_{m1} i_\alpha^{INV} + (L_{lr1} + L_{m1}) i_{dr1}) \end{aligned} \quad (8.20)$$

Rotor voltage equations of machine 2:

$$\begin{aligned} 0 &= R_{r2}i_{dr2} + L_{m1} \frac{di_x^{INV}}{dt} + (L_{lr2} + L_{m2}) \frac{di_{dr1}}{dt} + \omega_{22} (L_{m2}i_y^{INV} + (L_{lr2} + L_{m2})i_{qr2}) \\ 0 &= R_{r2}i_{qr2} + L_{m2} \frac{di_y^{INV}}{dt} + (L_{lr2} + L_{m2}) \frac{di_{qr2}}{dt} - \omega_{22} (L_{m1}i_x^{INV} + (L_{lr2} + L_{m2})i_{dr2}) \end{aligned} \quad (8.21)$$

Torque equations:

$$\begin{aligned} T_{e1} &= PL_{m1} [i_{dr1}i_{\beta}^{INV} - i_{\alpha}^{INV}i_{qr1}] \\ T_{e2} &= PL_{m2} [i_{dr2}i_y^{INV} - i_x^{INV}i_{qr2}] \end{aligned} \quad (8.22)$$

In addition to these equations that describe the two machines in series with phase transposition, one needs correlation between inverter phase and α - β voltages and currents,

$$\begin{bmatrix} v_{\alpha}^{INV} \\ v_{\beta}^{INV} \\ v_x^{INV} \\ v_y^{INV} \\ v_0^{INV} \end{bmatrix} = \underline{C} \begin{bmatrix} v_A \\ v_B \\ v_C \\ v_D \\ v_E \end{bmatrix} \quad \begin{bmatrix} i_A^{INV} \\ i_B^{INV} \\ i_C^{INV} \\ i_D^{INV} \\ i_E^{INV} \end{bmatrix} = \underline{C}^T \begin{bmatrix} i_d^{INV} \\ i_q^{INV} \\ i_x^{INV} \\ i_y^{INV} \\ i_0^{INV} \end{bmatrix} \quad (8.23)$$

Correlation between inverter current components and stator current components of the two machines is, using (3.2) and the second of (8.23), given with:

$$\begin{aligned} i_{\alpha}^{INV} &= i_{\alpha s1} = i_{xs2} \\ i_{\beta}^{INV} &= i_{\beta s1} = -i_{ys2} \\ i_x^{INV} &= i_{xs1} = i_{\alpha s2} \\ i_y^{INV} &= i_{ys1} = i_{\beta s2} \\ i_0^{INV} &= i_{0s1} = i_{0s2} \end{aligned} \quad (8.24)$$

The equation (8.24) implies that the α -axis and β -axis inverter current components are equal to the α -axis and β -axis stator current components of machine 1 and simultaneously x-axis and y-axis (in reverse direction) current components of machine 2. Similarly, x-axis and y-axis inverter current components are equal to the x-axis and y-axis stator current components of machine 1 and to α -axis and β -axis current components of machine 2. Further, in order to calculate stator phase voltages for

individual machines, one observes from (8.23) and (8.1) that:

$$\begin{aligned}
 v_{\alpha}^{INV} &= v_{\alpha s1} + v_{xs2} \\
 v_{\beta}^{INV} &= v_{\beta s1} - v_{ys2} \\
 v_x^{INV} &= v_{xs1} + v_{\alpha s2} \\
 v_y^{INV} &= v_{ys1} + v_{\beta s2} \\
 v_0^{INV} &= v_{0s1} + v_{0s2}
 \end{aligned} \tag{8.25}$$

This implies that the d-axis and q-axis circuits of machine 1 are connected in series with x-axis and y-axis circuits of machine 2, respectively and vice versa. Hence:

$$\begin{aligned}
 v_{\alpha s1} &= R_{s1} i_{\alpha}^{INV} + (L_{ls1} + L_{m1}) \frac{di_{\alpha}^{INV}}{dt} + L_{m1} \frac{di_{dr1}}{dt} \\
 v_{\beta s1} &= R_{s1} i_{\beta}^{INV} + (L_{ls1} + L_{m1}) \frac{di_{\beta}^{INV}}{dt} + L_{m1} \frac{di_{qr1}}{dt} \\
 v_{xs1} &= R_{s1} i_x^{INV} + L_{ls1} \frac{di_x^{INV}}{dt} \\
 v_{ys1} &= R_{s1} i_y^{INV} + L_{ls1} \frac{di_y^{INV}}{dt} \\
 v_{\alpha s2} &= R_{s2} i_x^{INV} + (L_{ls2} + L_{m2}) \frac{di_x^{INV}}{dt} + L_{m2} \frac{di_{dr2}}{dt} \\
 v_{\beta s2} &= R_{s2} i_y^{INV} + (L_{ls2} + L_{m2}) \frac{di_y^{INV}}{dt} + L_{m2} \frac{di_{qr2}}{dt} \\
 v_{xs2} &= R_{s2} i_{\alpha}^{INV} + L_{ls2} \frac{di_{\alpha}^{INV}}{dt} \\
 -v_{ys2} &= R_{s2} i_{\beta}^{INV} + L_{ls2} \frac{di_{\beta}^{INV}}{dt}
 \end{aligned} \tag{8.26}$$

Individual machine phase voltages are then determined with:

$$\begin{bmatrix} v_{as1} \\ v_{bs1} \\ v_{cs1} \\ v_{ds1} \\ v_{es1} \end{bmatrix} = \underline{C}^T \begin{bmatrix} v_{\alpha s1} \\ v_{\beta s1} \\ v_{xs1} \\ v_{ys1} \\ v_{0s1} \end{bmatrix} \qquad \begin{bmatrix} v_{as2} \\ v_{bs2} \\ v_{cs2} \\ v_{ds2} \\ v_{es2} \end{bmatrix} = \underline{C}^T \begin{bmatrix} v_{\alpha s2} \\ v_{\beta s2} \\ v_{xs2} \\ v_{ys2} \\ v_{0s2} \end{bmatrix} \tag{8.27}$$

8.3 Phase domain modelling of the voltage-fed series-connected six-phase two-motor drive

In order to design an appropriate current control scheme in the synchronous reference frame the six-phase two-motor drive model is developed in state-space form.

Due to the series connection of two stator windings according to Fig. 6.1 the following holds true:

$$\begin{aligned} v_A &= v_{a1} + v_{a2} & v_B &= v_{b1} + v_{b2} & v_C &= v_{c1} + v_{c2} \\ v_D &= v_{d1} + v_{d2} & v_E &= v_{e1} + v_{e2} & v_F &= v_{f1} + v_{f2} \end{aligned} \quad (8.28)$$

$$\begin{aligned} i_A &= i_{a1} + 0.5i_{a2} & i_B &= i_{b1} + 0.5i_{b2} \\ i_C &= i_{c1} + 0.5i_{c2} & i_D &= i_{d1} + 0.5i_{d2} \\ i_E &= i_{e1} + 0.5i_{e2} & i_F &= i_{f1} + 0.5i_{f2} \end{aligned} \quad (8.29)$$

Voltage equations of the complete two-motor system are to be formulated in terms of inverter currents and voltages. The system is however of the 15th order, since a three-phase machine is connected in series to the six-phase machine. The complete set of voltage equations can be written as:

$$\begin{bmatrix} \underline{v}^{INV} \\ \underline{0} \\ \underline{0} \end{bmatrix} = \begin{bmatrix} \underline{R}_{s1} + \underline{R}_{s2}' & & \\ & \underline{R}_{r1} & \\ & & \underline{R}_{r2} \end{bmatrix} \begin{bmatrix} \underline{i}^{INV} \\ \underline{i}_{r1} \\ \underline{i}_{r2} \end{bmatrix} + \frac{d}{dt} \left\{ \begin{bmatrix} \underline{L}_{s1} + \underline{L}_{s2}' & \underline{L}_{sr1} & \underline{L}_{sr2}' \\ \underline{L}_{rs1} & \underline{L}_{r1} & \underline{0} \\ \underline{L}_{rs2}' & \underline{0} & \underline{L}_{r2} \end{bmatrix} \begin{bmatrix} \underline{i}^{INV} \\ \underline{i}_{r1} \\ \underline{i}_{r2} \end{bmatrix} \right\} \quad (8.30)$$

Let the index '1' denote induction machine directly connected to the six-phase inverter and let the index '2' stand for the second induction machine (three-phase), connected after the first machine through phase transposition. Inductance and resistance matrices remain as in (3.3)-(3.8). Primed sub-matrices are again those that have been modified, with respect to their original form, in the process of series connection of two machines through the phase transposition operation. These sub-matrices are now equal to:

$$\underline{R}_{s2}' = \begin{bmatrix} \underline{R}_{s2} & \underline{R}_{s2} \\ \underline{R}_{s2} & \underline{R}_{s2} \end{bmatrix} \quad (8.31)$$

$$\underline{L}_{s2}' = \begin{bmatrix} \underline{L}_{s2} & \underline{L}_{s2} \\ \underline{L}_{s2} & \underline{L}_{s2} \end{bmatrix} \quad (8.32)$$

$$\begin{aligned} \underline{L}_{sr2}' &= \begin{bmatrix} \underline{L}_{sr2} \\ \underline{L}_{sr2} \end{bmatrix} \\ \underline{L}_{rs2}' &= \begin{bmatrix} \underline{L}_{rs2} & \underline{L}_{rs2} \end{bmatrix} = \begin{bmatrix} \underline{L}_{sr2}^T & \underline{L}_{sr2}^T \end{bmatrix} \end{aligned} \quad (8.33)$$

where inductance and resistance matrices for each machine are given in equations (3.5) to (3.8). Inverter voltages are:

$$\underline{v}^{INV} = \begin{bmatrix} v_A \\ v_B \\ v_C \\ v_D \\ v_E \\ v_F \end{bmatrix} = \begin{bmatrix} v_{as1} + v_{as2} \\ v_{bs1} + v_{cs2} \\ v_{cs1} + v_{es2} \\ v_{ds1} + v_{as2} \\ v_{es1} + v_{cs2} \\ v_{fs1} + v_{es2} \end{bmatrix} \quad (8.34)$$

Correlation between machine currents and inverter currents is still:

$$\underline{i}_{s1} = \begin{bmatrix} i_{as1} \\ i_{bs1} \\ i_{cs1} \\ i_{ds1} \\ i_{es1} \\ i_{fs1} \end{bmatrix} = \begin{bmatrix} i_A \\ i_B \\ i_C \\ i_D \\ i_E \\ i_F \end{bmatrix} = \underline{i}^{INV} \quad \underline{i}_{s2} = \begin{bmatrix} i_{as2} \\ i_{bs2} \\ i_{cs2} \\ i_{ds2} \\ i_{es2} \\ i_{fs2} \end{bmatrix} = \begin{bmatrix} i_A + i_D \\ 0 \\ i_B + i_E \\ 0 \\ i_C + i_F \\ 0 \end{bmatrix} \quad (8.35)$$

Torque equations of the two machines in terms of inverter currents and their respective rotor currents and rotor positions are obtained by using (3.10) and replacing motor stator currents with corresponding inverter currents of (8.35):

$$T_{e1} = -P_1 M_1 \left\{ \begin{aligned} & (i_A i_{ar1} + i_B i_{br1} + i_C i_{cr1} + i_D i_{dr1} + i_E i_{er1} + i_F i_{fr1}) \sin \theta_1 + \\ & (i_F i_{ar1} + i_A i_{br1} + i_B i_{cr1} + i_C i_{dr1} + i_D i_{er1} + i_E i_{fr1}) \sin(\theta_1 - 5\alpha) + \\ & (i_E i_{ar1} + i_F i_{br1} + i_A i_{cr1} + i_B i_{dr1} + i_C i_{er1} + i_D i_{fr1}) \sin(\theta_1 - 4\alpha) + \\ & (i_D i_{ar1} + i_E i_{br1} + i_F i_{cr1} + i_A i_{dr1} + i_B i_{er1} + i_C i_{fr1}) \sin(\theta_1 - 3\alpha) + \\ & (i_C i_{ar1} + i_D i_{br1} + i_E i_{cr1} + i_F i_{dr1} + i_A i_{er1} + i_B i_{fr1}) \sin(\theta_1 - 2\alpha) + \\ & (i_B i_{ar1} + i_C i_{br1} + i_D i_{cr1} + i_E i_{dr1} + i_F i_{er1} + i_A i_{fr1}) \sin(\theta_1 - \alpha) \end{aligned} \right\} \quad (8.36)$$

$$T_{e2} = -P_2 M_2 \left\{ \begin{aligned} & ((i_A + i_D) i_{ar2} + (i_B + i_E) i_{cr2} + (i_C + i_F) i_{er2}) \sin \theta_2 + \\ & ((i_C + i_F) i_{ar2} + (i_A + i_D) i_{cr2} + (i_B + i_E) i_{er2}) \sin(\theta_2 - 4\alpha) + \\ & ((i_B + i_E) i_{ar2} + (i_C + i_F) i_{cr2} + (i_A + i_D) i_{er2}) \sin(\theta_2 - 2\alpha) \end{aligned} \right\} \quad (8.37)$$

8.3.1 Transformation of the two-motor six-phase series-connected machine model into the stationary reference frame

Once again the phase domain state-space model of the six-phase two-motor drive

is considerably simplified with the application of the decoupling transformation (3.14b) and the rotational transformation (3.29) as shown in Jones et al (2004c). The inverter voltage equations in the stationary common reference frame are given in Iqbal and Levi (2004) as:

$$\begin{aligned}
 v_{\alpha}^{INV} &= R_{s1}i_{\alpha}^{INV} + (L_{ls1} + L_{m1})\frac{di_{\alpha}^{INV}}{dt} + L_{m1}\frac{di_{dr1}}{dt} \\
 v_{\beta}^{INV} &= R_{s1}i_{\beta}^{INV} + (L_{ls1} + L_{m1})\frac{di_{\beta}^{INV}}{dt} + L_{m1}\frac{di_{qr1}}{dt} \\
 v_x^{INV} &= R_{s1}i_x^{INV} + L_{ls1}\frac{di_x^{INV}}{dt} + \sqrt{2}\left\{R_{s2}\sqrt{2}i_x^{INV} + (L_{ls2} + L_{m2})\frac{d\sqrt{2}i_x^{INV}}{dt} + L_{m2}\frac{di_{dr2}}{dt}\right\} \\
 v_y^{INV} &= R_{s1}i_y^{INV} + L_{ls1}\frac{di_y^{INV}}{dt} + \sqrt{2}\left\{R_{s2}\sqrt{2}i_y^{INV} + (L_{ls2} + L_{m2})\frac{d\sqrt{2}i_y^{INV}}{dt} + L_{m2}\frac{di_{qr2}}{dt}\right\} \\
 v_{0+}^{INV} &= R_{s1}i_{0+}^{INV} + L_{ls1}\frac{di_{0+}^{INV}}{dt} + \sqrt{2}\left\{R_{s2}\sqrt{2}i_{0+}^{INV} + L_{ls2}\frac{d\sqrt{2}i_{0+}^{INV}}{dt}\right\} \\
 v_{0-}^{INV} &= R_{s1}i_{0-}^{INV} + L_{ls1}\frac{di_{0-}^{INV}}{dt}
 \end{aligned} \tag{8.38}$$

The rotor equations are:

$$\begin{aligned}
 0 &= R_{r1}i_{dr1} + L_{m1}\frac{di_{\alpha}^{INV}}{dt} + (L_{lr1} + L_{m1})\frac{di_{dr1}}{dt} + \omega_{r1}(L_{m1}i_{\beta}^{INV} + (L_{lr1} + L_{m1})i_{qr1}) \\
 0 &= R_{r1}i_{qr1} + L_{m1}\frac{di_{\beta}^{INV}}{dt} + (L_{lr1} + L_{m1})\frac{di_{qr1}}{dt} - \omega_{r1}(L_{m1}i_{\alpha}^{INV} + (L_{lr1} + L_{m1})i_{dr1})
 \end{aligned} \tag{8.39}$$

$$\begin{aligned}
 0 &= R_{r2}i_{dr2} + \sqrt{2}L_{m2}\frac{di_x^{INV}}{dt} + (L_{lr2} + L_{m2})\frac{di_{dr2}}{dt} + \omega_{r2}(L_{m2}\sqrt{2}i_y^{INV} + (L_{lr2} + L_{m2})i_{qr2}) \\
 0 &= R_{r2}i_{qr2} + \sqrt{2}L_{m2}\frac{di_y^{INV}}{dt} + (L_{lr2} + L_{m2})\frac{di_{qr2}}{dt} - \omega_{r2}(L_{m2}\sqrt{2}i_x^{INV} + (L_{lr2} + L_{m2})i_{dr2})
 \end{aligned} \tag{8.40}$$

Torque equations are:

$$\begin{aligned}
 T_{e1} &= PL_{m1}[i_{dr1}i_{\beta}^{INV} - i_{\alpha}^{INV}i_{qr1}] \\
 T_{e2} &= \sqrt{2}PL_{m2}[i_{dr2}i_y^{INV} - i_x^{INV}i_{qr2}]
 \end{aligned} \tag{8.41}$$

Inverter voltages can be represented as:

$$\begin{bmatrix} v_{\alpha}^{INV} \\ v_{\beta}^{INV} \\ v_x^{INV} \\ v_y^{INV} \\ v_{0+}^{INV} \\ v_{0-}^{INV} \end{bmatrix} = \underline{C} \begin{bmatrix} v_{a1} + v_{a2} \\ v_{b1} + v_{c2} \\ v_{c1} + v_{e2} \\ v_{d1} + v_{a2} \\ v_{e1} + v_{c2} \\ v_{f1} + v_{e2} \end{bmatrix} = \begin{bmatrix} v_{\alpha s1} \\ v_{\beta s1} \\ v_{xs1} + \sqrt{2}v_{\alpha s2} \\ v_{ys1} + \sqrt{2}v_{\beta s2} \\ v_{0+s1} + \sqrt{2}v_{0s2} \\ v_{0-s1} \end{bmatrix} \quad (8.42)$$

Hence in this case

$$\begin{aligned} v_{\alpha}^{INV} &= v_{\alpha s1} \\ v_{\beta}^{INV} &= v_{\beta s1} \\ v_x^{INV} &= v_{xs1} + \sqrt{2}v_{\alpha s2} \\ v_y^{INV} &= v_{ys1} + \sqrt{2}v_{\beta s2} \\ v_{0+}^{INV} &= v_{0+s1} + \sqrt{2}v_{0s2} \\ v_{0-}^{INV} &= v_{0-s1} \end{aligned} \quad (8.43)$$

On the other hand, correlation between inverter current axis components and axis current components of individual machines is, taking into account (8.29):

$$\begin{aligned} i_{\alpha}^{INV} &= i_{\alpha s1} \\ i_{\beta}^{INV} &= i_{\beta s1} \\ i_x^{INV} &= i_{xs1} = i_{\alpha s2} / \sqrt{2} \\ i_y^{INV} &= i_{ys1} = i_{\beta s2} / \sqrt{2} \\ i_{0+}^{INV} &= i_{0+s1} = i_{0s2} / \sqrt{2} \\ i_{0-}^{INV} &= i_{0-s1} \end{aligned} \quad (8.44)$$

Hence, in terms of inverter axis current components, one has the following machines' axis current components:

$$\begin{aligned} i_{\alpha s1} &= i_{\alpha}^{INV} \\ i_{\beta s1} &= i_{\beta}^{INV} \\ i_{xs1} &= i_x^{INV} \\ i_{ys1} &= i_y^{INV} \\ i_{0+s1} &= i_{0+}^{INV} \\ i_{0-s1} &= i_{0-}^{INV} \end{aligned} \quad (8.45)$$

$$\begin{aligned}
 i_{\alpha s2} &= \sqrt{2}i_x^{INV} \\
 i_{\beta s2} &= \sqrt{2}i_y^{INV} \\
 i_{0s2} &= \sqrt{2}i_{0+}^{INV}
 \end{aligned}
 \tag{8.46}$$

8.4 Vector control of a five-phase induction machine with current control in the synchronous reference frame

In order to investigate the possibility of current control in the synchronous reference frame for a multi-phase machine, a five-phase induction machine is initially considered. Indirect rotor flux oriented control in the constant flux region is assumed (Fig. 8.1a). Standard vector control scheme that enables creation of phase voltage references in the same manner as it is done for a three-phase machine is shown in Fig. 8.1b. In this scheme d-q axis voltage references are calculated by summing the outputs of the stator d-q axis current PI controllers with decoupling voltages. Decoupling circuits are introduced to decouple the d-axis and q-axis components of stator voltage and current [Novotny and Lipo (1997)]. Decoupling voltages are, for constant rotor flux operation, given with:

$$\begin{aligned}
 e_d &= -\omega_r \sigma L_s i_{qs}^* \\
 e_q &= \omega_r (L_s / L_m) \psi_r^* = \omega_r L_s i_{ds}^*
 \end{aligned}
 \tag{8.47a}$$

where the total leakage coefficient is given by:

$$\sigma = 1 - (L_m^2 / L_s L_r)
 \tag{8.47b}$$

It is assumed that reference rather than estimated stator current d-q axis components are utilized in (8.47). Stator d-q axis voltage references for the machine are obtained using:

$$v_{ds}^* = v_d' + e_d \quad v_{qs}^* = v_q' + e_q
 \tag{8.48}$$

where superscript ' in d-q axis voltage components denotes outputs of the synchronous current controllers. Machine phase voltage references are generated next as:

$$\begin{aligned}
 v_{as}^* &= \sqrt{\frac{2}{5}} [v_{ds}^* \cos \phi_{rj} - v_{qs}^* \sin \phi_{rj}] \\
 v_{bs}^* &= \sqrt{\frac{2}{5}} [v_{ds}^* \cos(\phi_{rj} - \alpha) - v_{qs}^* \sin(\phi_{rj} - \alpha)]
 \end{aligned} \tag{8.49}$$

$$v_{es}^* = \sqrt{\frac{2}{5}} [v_{ds}^* \cos(\phi_{rj} - 4\alpha) - v_{qs}^* \sin(\phi_{rj} - 4\alpha)]$$

where $\alpha = 2\pi/5$. The voltages are then impressed in reality using a method of PWM. Here however, inverter and the PWM method are not modelled. Instead, voltages of (8.49) will be directly impressed onto machine stator windings.

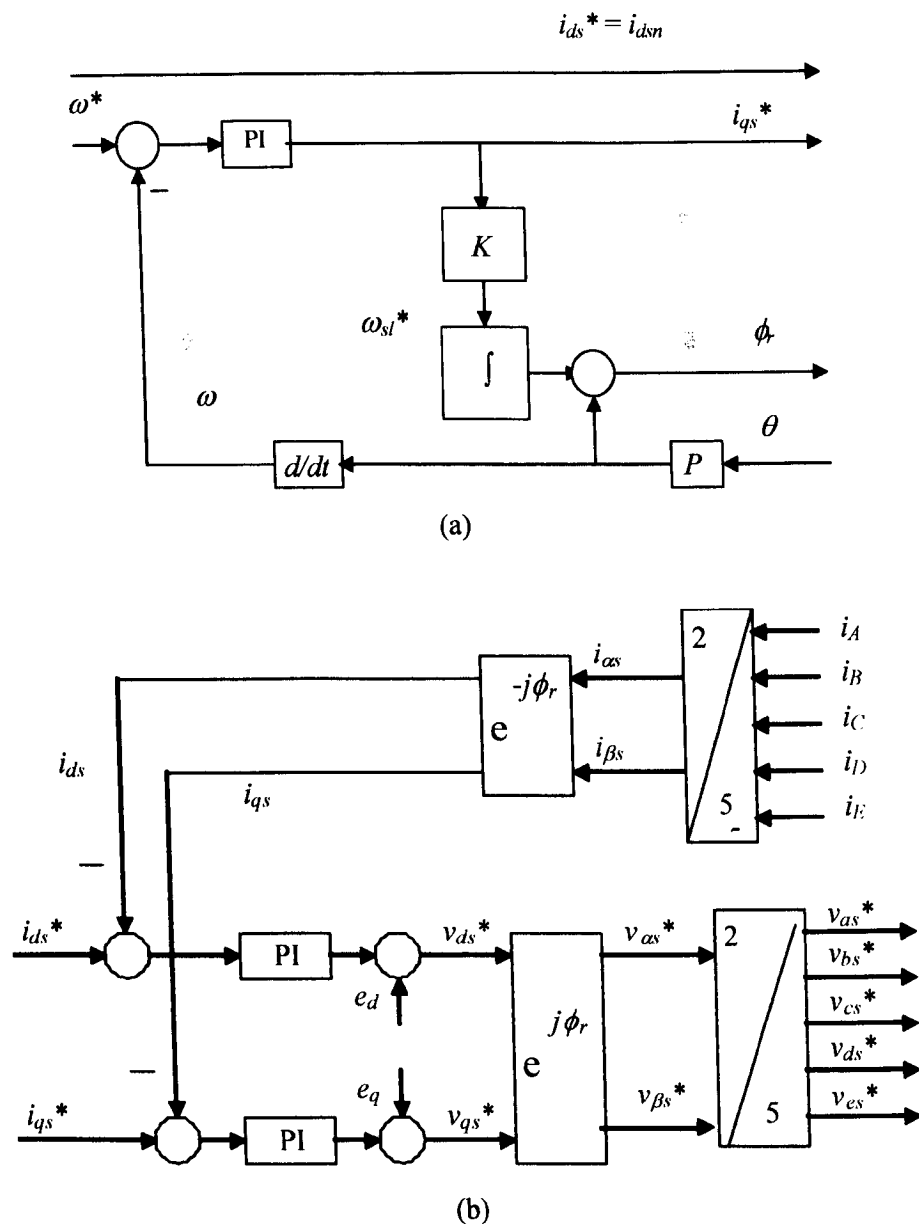


Fig. 8.1: Vector control of a five-phase induction machine: indirect rotor flux oriented controller (a) and synchronous current controllers with decoupling voltages of (8.47a) (b).

8.4.1 *Tuning of the PI current controllers*

Current PI controllers were tuned using an empirical method. A detailed description of this method used can be found in Iqbal (2003). The current controller gains were kept deliberately low in-order to approximate the low bandwidth typically found in high power applications, where it is envisaged that the multi-phase multi-motor drive will have the most benefit. In such applications the switching frequency is restricted by semiconductor capability in-order to prevent excessive switching losses [Xu and Ye (1995)]. PI current controller gains were therefore set as follows $K_p = 300$ and $T_i = 0.01$, giving a bandwidth of approximately 960 Hz.

8.4.2 *Simulation of a five-phase vector controlled induction machine with current control in the synchronous reference frame*

The five-phase vector controlled induction machine with current control in the synchronous reference frame is investigated via simulation. A single five-phase induction machine is modelled in the phase domain by setting all matrices with subscript '2' to zero in equation (8.16). The five-phase machine is initially magnetised by applying a rated rotor flux command (d-axis current) in ramped manner. Once rated rotor flux is established in the machine a speed command of 299 rad/s (1427 rpm) is applied at $t = 0.4$ seconds in a ramped manner over time interval of 0.01 seconds. Torque limit is set to twice the rated torque of the machine (16.67 Nm). Operation is in the base speed region under no-load conditions. The PWM inverter is treated as ideal and therefore the inverter phase voltage references equal the inverter output phase voltages.

Torque and speed responses of the five-phase machine are illustrated in Fig. 8.2, where it can be seen that torque developed by the machine very quickly reaches the maximum allowed value after the speed command has been applied. The torque stays at the maximum allowed value until the machine has reached the required speed. The acceleration of the machine is therefore the fastest possible. As can be seen from Fig. 8.2 the rotor flux remains completely unaffected by the change in torque and decoupled flux and torque control has been achieved. It is evident from the stator d and q-axis currents that the transformation to the synchronous reference frame is performing as expected as the currents are DC in steady-state (these currents are compared to the

reference currents generated by the vector controller). The stator phase “a” and “b” voltage and current are shown in Fig. 8.2d and Fig. 8.2e, where it can be seen that the current very quickly steps to the maximum value and stays at the maximum value until the machine has reached the required speed. Fig. 8.2f shows the stator d and q-axis voltage references generated by the summation of the decoupling voltages given by (8.47) and the current controller outputs, as shown in Fig. 8.1.

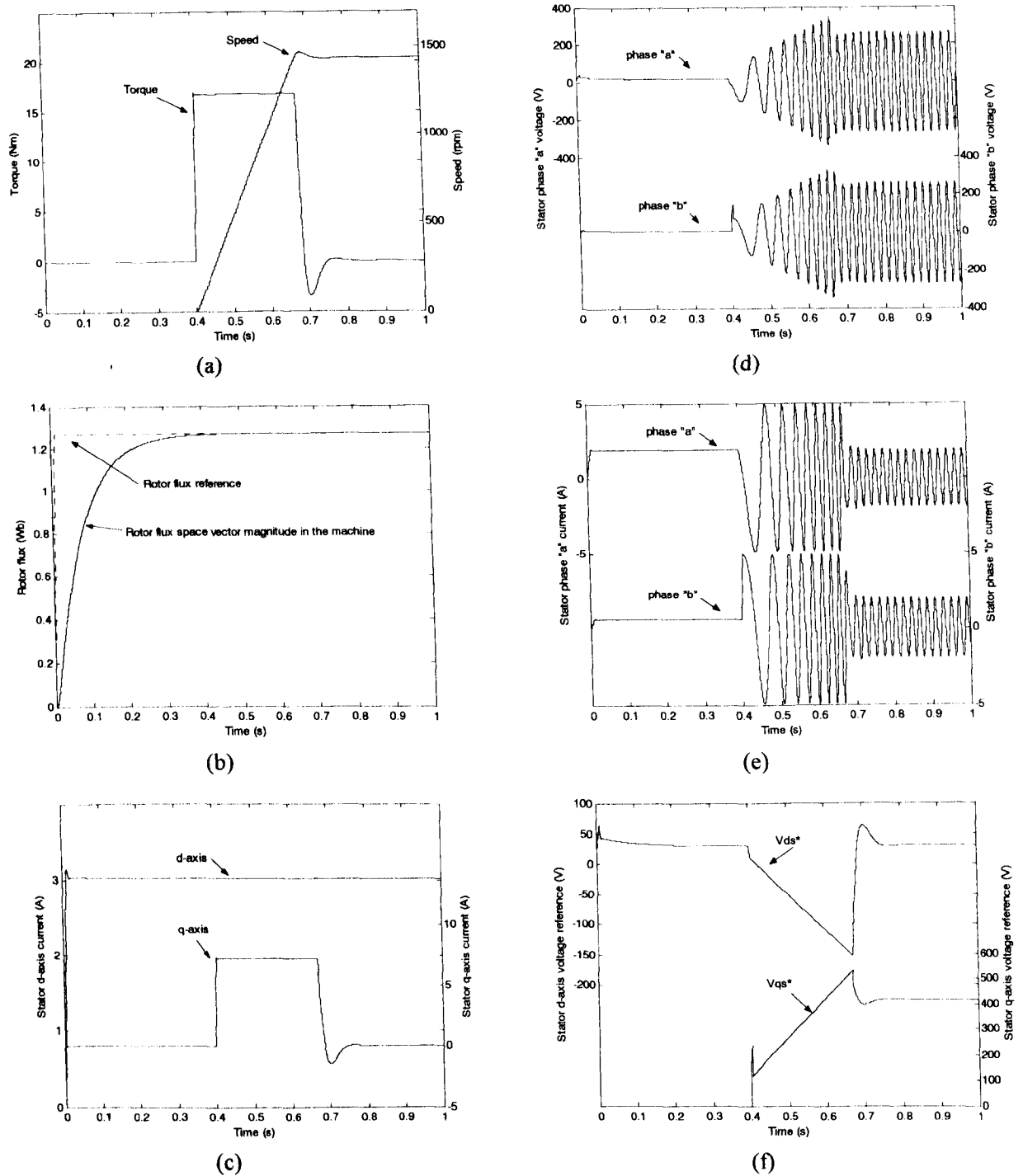


Fig. 8.2: Rotor flux oriented control of a five-phase induction machine with current control in the synchronous reference frame. Torque and speed response (a), rotor flux (b), stator d-q axis currents (c), stator phase “a” and “b” voltage (d), stator phase “a” and “b” current (e) and stator d-q axis voltage references.

8.5 Series-connected five-phase two-motor drive with current control in the synchronous reference frame

The suitability of the control scheme considered in section 8.4 is next examined for the five-phase series-connected two-motor drive. The connection diagram is the one shown in Fig. 4.1. The relationship between phase currents of the two machines and the inverter output currents is, from Fig. 4.1, governed with (8.2). The corresponding correlation between inverter phase voltages and phase voltages of the two series-connected machines is, again from Fig. 4.1, determined with (8.1). Since current control will be performed in the rotating reference frame, inverter phase voltage references have to be created using the following expressions, which are a direct consequence of the relationships given in (8.1):

$$\begin{aligned} v_A^* &= v_{as1}^* + v_{as2}^* & v_B^* &= v_{bs1}^* + v_{bs2}^* & v_C^* &= v_{cs1}^* + v_{cs2}^* \\ v_D^* &= v_{ds1}^* + v_{ds2}^* & v_E^* &= v_{es1}^* + v_{es2}^* \end{aligned} \quad (8.50)$$

Vector control for each five-phase machine and generation of machine voltage references will be performed in an identical manner to that shown in Fig. 8.1 with the exception that measured current ordering for machine 2, required for calculation of stator d-q axis current components, is, according to (8.2), i_A, i_C, i_E, i_B, i_D . Decoupling voltages, for constant rotor flux operation, are given with:

$$\begin{aligned} e_{d1} &= -\omega_{r1} \sigma_1 L_{s1} i_{qs1}^* & e_{d2} &= -\omega_{r2} \sigma_2 L_{s2} i_{qs2}^* \\ e_{q1} &= \omega_{r1} (L_{s1} / L_{m1}) \psi_{r1}^* = \omega_{r1} L_{s1} i_{ds1}^* & e_{q2} &= \omega_{r2} (L_{s2} / L_{m2}) \psi_{r2}^* = \omega_{r2} L_{s2} i_{ds2}^* \end{aligned} \quad (8.51)$$

where it is assumed that reference rather than estimated stator current d-q axis components are utilised. Stator d-q axis voltage references for the two machines are obtained using (8.48). Machine phase voltage references are generated next as:

$$\begin{aligned} v_{asj}^* &= \sqrt{\frac{2}{5}} [v_{dsj}^* \cos \phi_{rj} - v_{qsj}^* \sin \phi_{rj}] \\ v_{bsj}^* &= \sqrt{\frac{2}{5}} [v_{dsj}^* \cos(\phi_{rj} - \alpha) - v_{qsj}^* \sin(\phi_{rj} - \alpha)] \\ &----- \\ v_{esj}^* &= \sqrt{\frac{2}{5}} [v_{dsj}^* \cos(\phi_{rj} - 4\alpha) - v_{qsj}^* \sin(\phi_{rj} - 4\alpha)] \end{aligned} \quad (8.52)$$

where $j = 1$ or 2 and $\alpha = 2\pi/5$. The voltages of (8.50) are then created and impressed using a method of PWM.

8.5.1 Simulation of a vector controlled five-phase two-motor series-connected drive with current control in the synchronous reference frame

It is shown in this section that generation of inverter voltage references according to the described algorithm does not produce satisfactory dynamic performance of the two-motor drive. In particular, cross-coupling between the control of the two machines takes place in transients. For simulation purposes the two series-connected five-phase induction machines are represented with the phase domain model of section 8.2. The PWM inverter is treated as ideal, so that the inverter output voltages (8.1) equal the inverter voltage references of (8.50). Speed mode of operation is considered and the torque limit of each machine is set to twice the rated value (i.e., 16.67 Nm). The machines are at first excited using a rotor flux command of rated value. Once the rotor flux has reached steady-state, a rated speed command (299 rad/s) is applied to IM1 at $t = 0.4$ s. At $t = 0.5$ s a speed command equal to 50% of the rated speed (149 rad/s) is applied to IM2. Torque, speed and rotor flux responses of the two machines are shown in Fig. 8.3. Stator phase “a” voltage reference for each machine is shown in Fig. 8.3f where it can be seen that the voltage for machine 1 is identical to that shown in Fig 8.2d where one five-phase machine was considered.

After the initial excitation, a sudden disturbance can be observed in the rotor flux trace of both machines. This disturbance is not evidenced in the torque and speed responses since speed mode of operation is simulated, and since the reduction in rotor flux is rather small. Nevertheless, the disturbance in the rotor flux indicates a temporary loss of the decoupled and independent control of the two machines. It appears during application of torque and during sudden torque reduction to zero, when the speeds of the two machines are around the set values. The latter disturbance is of larger amplitude in the machine running at higher frequency (IM1). In general, higher the stator supply frequency is, larger the second drop in the rotor flux will be. The deterioration in the dynamics is likely to be much more pronounced in an actual realisation, where inverter switching frequency and the sampling frequency are finite. However if the current

controllers are sufficiently fast (high bandwidth) then the disturbance in the rotor flux can be significantly reduced or possibly even eliminated.

A physical explanation of the reasons behind the loss of decoupled control is given next. In order to facilitate the explanation simulation results for vector control of a five-phase induction machine are taken into consideration, particularly d-q axis voltage references for the single five-phase machine (Fig. 8.2e). Figures 8.3c-d illustrates d-q axis voltage references within the two-motor drive system of Fig. 4.1, generated by means of (8.50) with decoupling voltages of (8.48). If only one five-phase motor is required to operate under identical operating conditions, using a five-phase voltage source inverter and the same vector controller, the stator d-q axis voltage references differ substantially, as illustrated in Fig. 8.2e. Although the operating conditions of the machine are identical in Figs. 8.2e and 8.3, it is obvious that series connection of the two machines leads to significantly higher values of d-q axis voltage references in both transient and steady-state operation. The values read from graphs of Figs. 8.2e and 8.3c as well as corresponding values for 50% speed reference setting, are summarised in Table 8.1. It can be seen that the difference in maximum transient values is substantially larger than the difference in steady-state values. There is practically no difference in steady-state for v_{ds}^* due to no-load operating conditions.

Each of the two machines in Fig. 4.1 carries, apart from its own flux/torque producing currents, flux/torque producing currents of the other machine. This second set of currents does not produce flux and torque in the machine and it therefore leads to the flow of x-y current components in the machine. However, it does produce a certain amount of voltage drop, called x-y voltage drop. This voltage drop appears on impedance comprising a series connection of the stator resistance and the stator leakage reactance (at the stator frequency of the other machine). When two (or more) multi-phase machines are connected in series and inverter current control is performed in the stationary reference frame, the inverter produces automatically output voltages of an appropriate waveform that compensate for the x-y voltage drops in the two machines. However if the inverter current control is performed using synchronous current controllers, the outputs of the control system are voltage references rather than current references. This means that the control system must generate voltages that will compensate in advance for the x-y voltage drops in the two machines. The algorithm described so far does not account for the additional x-y voltage drops. Since the role of the current PI controllers is to impose desired d-q axis current references, the PI

controllers ultimately provide a compensation for the x-y voltage drops. This explains the origin of the difference between the stator d-q voltage references shown in Figs. 8.2e and 8.3, and summarized in Table 8.1. However, since the compensation takes place through PI control, it is inadequate during rapid transients, especially at higher operating frequencies with high stator current values.

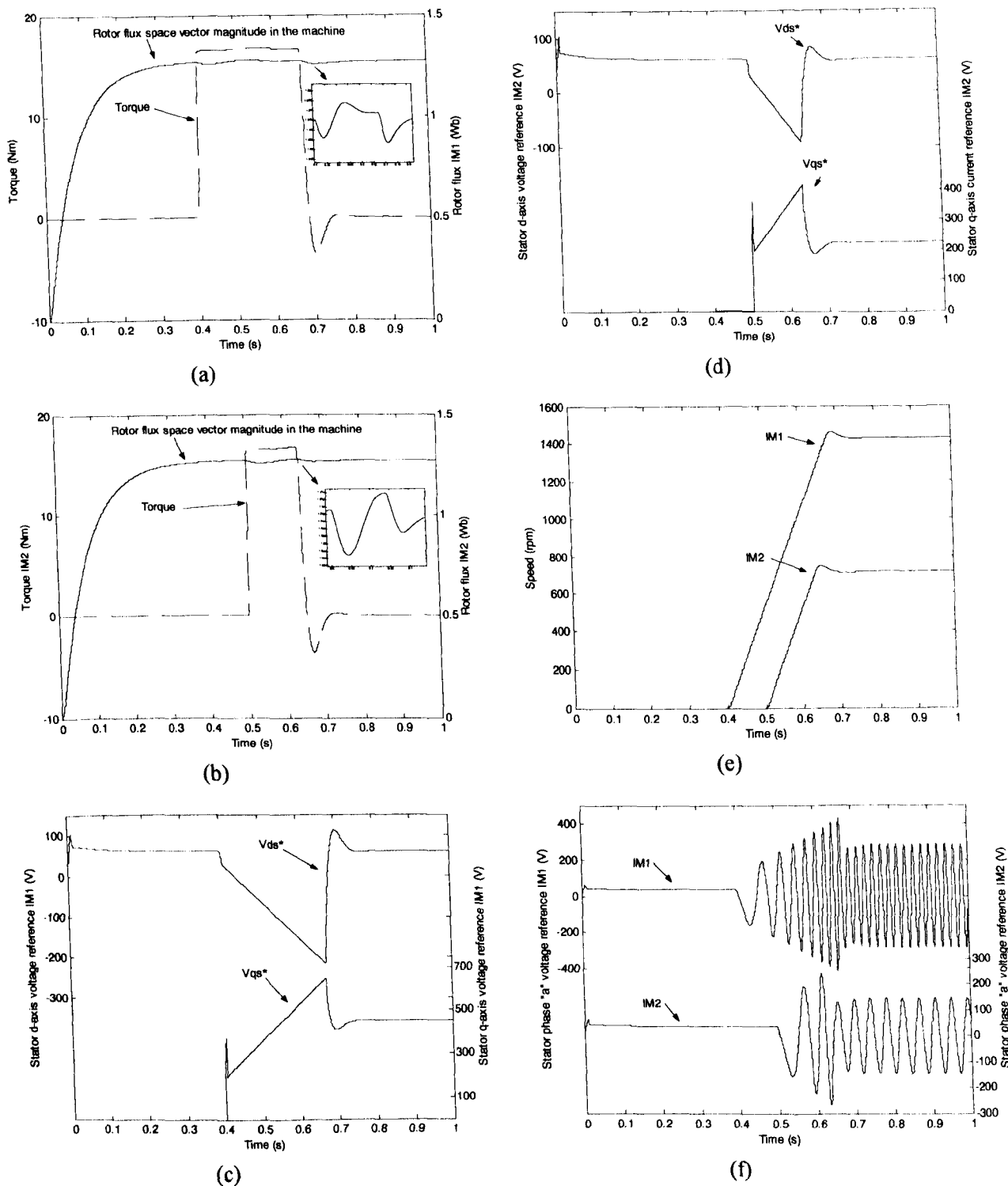


Fig. 8.3: Vector control of two five-phase induction machines connected in series, with phase transposition: Rotor flux and torque response of IM1 (a), rotor flux and torque response of IM2 (b), stator d-q axis voltage references of IM1 (c), stator d-q axis voltage references of IM2 (d), speed response of each machine (e) and stator phase "a" voltage reference of each machine (f).

A disturbance in the rotor flux therefore results when x-y voltage drops rapidly change, as shown in Figs. 8.3a-b. In simple terms, the control system of Fig. 8.1 is unaware of the need to create in advance the additional x-y voltages that will be dropped on each machine. A modification of the basic control scheme of Fig. 8.1 is therefore required and it is developed in the next two sections.

Table 8.1: Comparison of d-q axis voltage references for single machine and two-machine cases.

Single machine case, Fig. 8.2f (149 rad/s not shown)				
Speed (rad/s)	v_{ds}^* , peak (V)		v_{qs}^* , peak (V)	
	Max. value	Steady-state value	Max. value	Steady-state value
299	-152.5	30.25	534.6	417.5
149	-70	30	325.8	208.7
Two-machine case, Fig.8.3				
Machine	v_{ds}^* , peak (V)		v_{qs}^* , peak (V)	
	Max. value	Steady-state value	Max. value	Steady-state value
IM1 (299 rad/s)	-216	60.5	645	452.16
IM2 (149 rad/s)	-90.9	60.5	418.6	225.38

8.6 Feed-forward compensation of x-y voltage drops in the stationary reference frame

It has been shown in section 8.5.1 that the control system must generate such voltage references that will include the demand for the x-y voltage drops created in the multi-phase multi-motor drive system. As can be seen in Fig 8.1b the individual phase voltage references for the two machines are created by their respective vector control systems. The formation of these phase voltage references must account for the need to have in both machines, apart from the d-q voltages, an appropriate set of values for the x-y voltage references. Hence it is not sufficient to have only d-q current controllers in the rotating reference frame, which create d-q axis voltage components. In addition, it is also required to create appropriate x-y voltage components as well. This section considers a method of creating the required x-y voltage components in a feed-forward manner in the stationary reference frame. This method will further be referred to as the feed-forward method. It compensates for the x-y voltage drops based on the knowledge of the x-y current references that will flow through the machines. According to (8.24) α - β axis currents (in stationary reference frame) of one machine appear as x-y currents in the other machine, and vice versa. This means that x-y stator current references of one machine can be obtained by applying the co-ordinate transformation on d-q axis

current references of the other machine, and vice versa. In the case of a five-phase series-connected two-motor drive the required stator voltage x-y component references are then created in a feed-forward manner. In the case of a six-phase two-motor drive x-y voltage components exist for only the six-phase machine because the flux/torque producing currents of the six-phase machine cancel when entering the three-phase machine. Thus the feed-forward x-y voltage calculation is only required for the six-phase machine. Feed-forward x-y voltage reference calculation is governed, for the five-phase two-motor drive, with:

$$\begin{aligned} v_{xs1}^* &= R_{s1} i_{xs1}^* + L_{ls1} di_{xs1}^*/dt \\ v_{ys1}^* &= R_{s1} i_{ys1}^* + L_{ls1} di_{ys1}^*/dt \end{aligned} \quad (8.53a)$$

$$\begin{aligned} v_{xs2}^* &= R_{s2} i_{xs2}^* + L_{ls2} di_{xs2}^*/dt \\ v_{ys2}^* &= R_{s2} i_{ys2}^* + L_{ls2} di_{ys2}^*/dt \end{aligned} \quad (8.53b)$$

where x-y current references are:

$$\begin{aligned} \underline{i}_{xy(M1)}^* &= \underline{i}_{dq(M2)}^* \exp(j\phi_{r2}) \\ [\underline{i}_{xy(M2)}^*]^{cc} &= \underline{i}_{dq(M1)}^* \exp(j\phi_{r1}) \end{aligned} \quad (8.54)$$

Superscript *cc* stands for complex conjugate and accounts for the relationship given in (8.24). For the six-phase two-motor drive x-y voltage references are required for the six-phase machine only and are obtained using (8.53a) with:

$$\underline{i}_{xy(M1)}^* = (1/\sqrt{2}) \underline{i}_{dq(M2)}^* \exp(j\phi_{r2}) \quad (8.55)$$

this accounts for the relationship given in (8.44). Phase voltage references are further calculated for the five-phase case using:

$$\begin{aligned} v_{asj}^* &= \sqrt{\frac{2}{5}} [v_{dsj}^* \cos \phi_{rj} - v_{qsj}^* \sin \phi_{rj} + v_{xsj}^*] \\ v_{bsj}^* &= \sqrt{\frac{2}{5}} [v_{dsj}^* \cos(\phi_{rj} - \alpha) - v_{qsj}^* \sin(\phi_{rj} - \alpha) + v_{xsj}^* \cos 2\alpha + v_{ysj}^* \sin 2\alpha] \\ v_{csj}^* &= \sqrt{\frac{2}{5}} [v_{dsj}^* \cos(\phi_{rj} - 2\alpha) - v_{qsj}^* \sin(\phi_{rj} - 2\alpha) + v_{xsj}^* \cos 4\alpha + v_{ysj}^* \sin 4\alpha] \\ v_{dsj}^* &= \sqrt{\frac{2}{5}} [v_{dsj}^* \cos(\phi_{rj} - 3\alpha) - v_{qsj}^* \sin(\phi_{rj} - 3\alpha) + v_{xsj}^* \cos 4\alpha - v_{ysj}^* \sin 4\alpha] \\ v_{esj}^* &= \sqrt{\frac{2}{5}} [v_{dsj}^* \cos(\phi_{rj} - 4\alpha) - v_{qsj}^* \sin(\phi_{rj} - 4\alpha) + v_{xsj}^* \cos 2\alpha - v_{ysj}^* \sin 2\alpha] \end{aligned} \quad (8.56)$$

where $\alpha = 2\pi/5$ and $j = 1, 2$. The inverter voltage reference generation for the five-phase case remains as in (8.50). The vector control scheme of the five-phase two-motor

system with feed-forward x-y voltage drop compensation is illustrated in Fig. 8.4. For the sake of simplicity decoupling voltages are not shown but are still given with (8.51). Similarly, phase voltage references are calculated for the six-phase machine using:

$$\begin{aligned}
 v_{as1}^* &= \sqrt{\frac{2}{6}} [v_{ds1}^* \cos \phi_{r1} - v_{qs1}^* \sin \phi_{r1} + v_{xs1}^*] \\
 v_{bs1}^* &= \sqrt{\frac{2}{6}} [v_{ds1}^* \cos(\phi_{r1} - \alpha) - v_{qs1}^* \sin(\phi_{r1} - \alpha) + v_{xs1}^* \cos 2\alpha + v_{ys1}^* \sin 2\alpha] \\
 v_{cs1}^* &= \sqrt{\frac{2}{6}} [v_{ds1}^* \cos(\phi_{r1} - 2\alpha) - v_{qs1}^* \sin(\phi_{r1} - 2\alpha) + v_{xs1}^* \cos 4\alpha + v_{ys1}^* \sin 4\alpha] \\
 v_{ds1}^* &= \sqrt{\frac{2}{6}} [v_{ds1}^* \cos(\phi_{r1} - 3\alpha) - v_{qs1}^* \sin(\phi_{r1} - 3\alpha) + v_{xs1}^* \cos 6\alpha - v_{ys1}^* \sin 6\alpha] \\
 v_{es1}^* &= \sqrt{\frac{2}{6}} [v_{ds1}^* \cos(\phi_{r1} - 4\alpha) - v_{qs1}^* \sin(\phi_{r1} - 4\alpha) + v_{xs1}^* \cos 8\alpha - v_{ys1}^* \sin 8\alpha] \\
 v_{fs1}^* &= \sqrt{\frac{2}{6}} [v_{ds1}^* \cos(\phi_{r1} - 5\alpha) - v_{qs1}^* \sin(\phi_{r1} - 5\alpha) + v_{xs1}^* \cos 10\alpha - v_{ys1}^* \sin 10\alpha]
 \end{aligned} \tag{8.57}$$

where $\alpha = 2\pi/6$. The inverter voltage reference generation for the six-phase case is, on the basis of (8.28), governed with:

$$\begin{aligned}
 v_A^* &= v_{as1}^* + v_{bs2}^* & v_B^* &= v_{bs1}^* + v_{cs2}^* & v_C^* &= v_{cs1}^* + v_{ds2}^* \\
 v_D^* &= v_{ds1}^* + v_{as2}^* & v_E^* &= v_{es1}^* + v_{bs2}^* & v_F^* &= v_{fs1}^* + v_{cs2}^*
 \end{aligned} \tag{8.58}$$

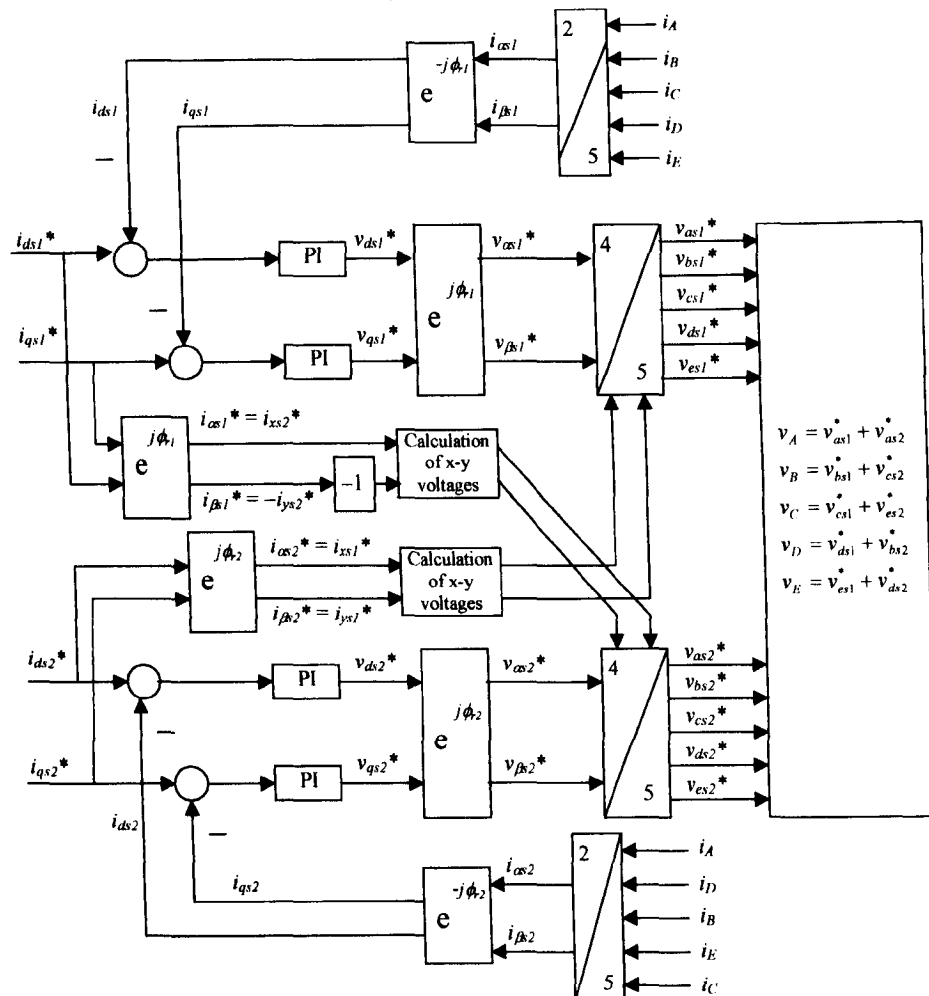


Fig. 8.4. Vector control of two series-connected five-phase machines: current control in the rotating frame and feed-forward reference x-y voltage calculation.

The vector control scheme of the six-phase two-motor drive with current control in the rotating reference frame and feed-forward reference x-y voltage calculation is illustrated in Fig. 8.5.

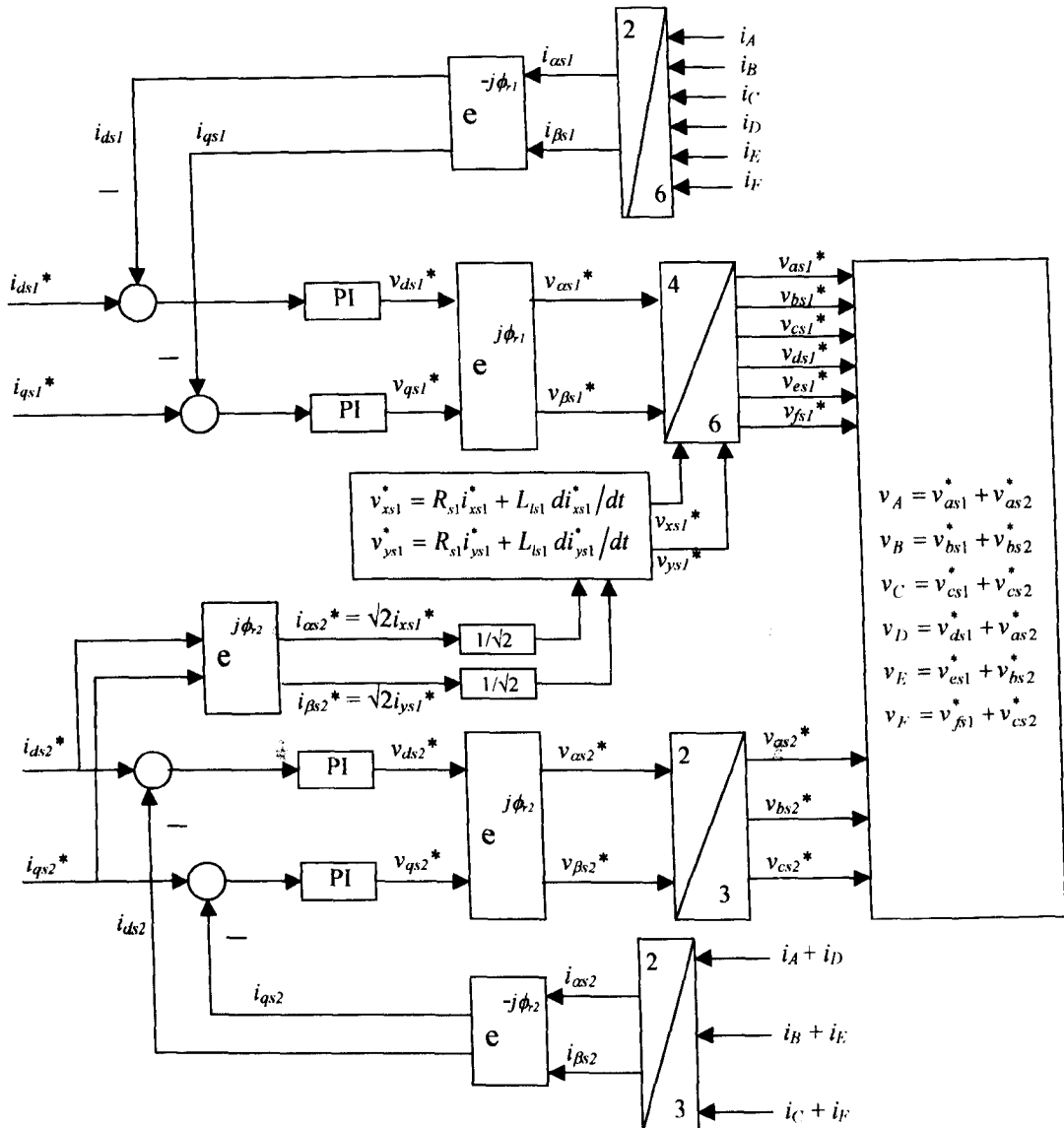


Fig. 8.5: Vector control of series-connected six-phase and three-phase induction machine: current control in the rotating frame and feed-forward reference x-y voltage calculation.

8.6.1 Simulation verification of the feed-forward method of x-y voltage drop compensation in the stationary reference frame for the five-phase and six-phase two-motor drives

Verification of the proposed feed-forward method of x-y voltage drop compensation is performed by simulation of both the five-phase two-motor drive and the six-phase two-motor drive in this section. In the case of a five-phase two-motor drive a simulation is performed in an identical manner as in section 8.5.1. The simulation results shown in Fig. 8.6a depict the rotor flux responses of each machine. It

is evident from Fig. 8.6a that the disturbance in the rotor flux response, previously seen in Fig. 8.3a and Fig. 8.3b when no x-y voltage compensation is used, has been completely eliminated. This means that a complete decoupling between the control of the two machines has been achieved. Speed and torque response of each machine remain as shown in Fig. 8.3 and so are not repeated here. The improvement is a result of the calculation of the stator phase voltage references according to (8.56). These contain now in steady-state two sinusoidal components at two different frequencies, corresponding to operating frequencies of the two machines. This is due to the nature of (8.56), which combines d-q axis voltage components corresponding to the operating frequency of one machine, with x-y axis voltage components that correspond to the operating frequency of the other machine. The stator phase “a” voltage reference of each machine is shown in Fig. 8.6b, where it can be seen that the phase “a” voltage reference of machine 1 in steady-state is the summation of two sinusoidal components at two different frequencies. This is less obvious for machine 2 because machine 2 operates at a much lower frequency than machine 1. However it can be seen that the

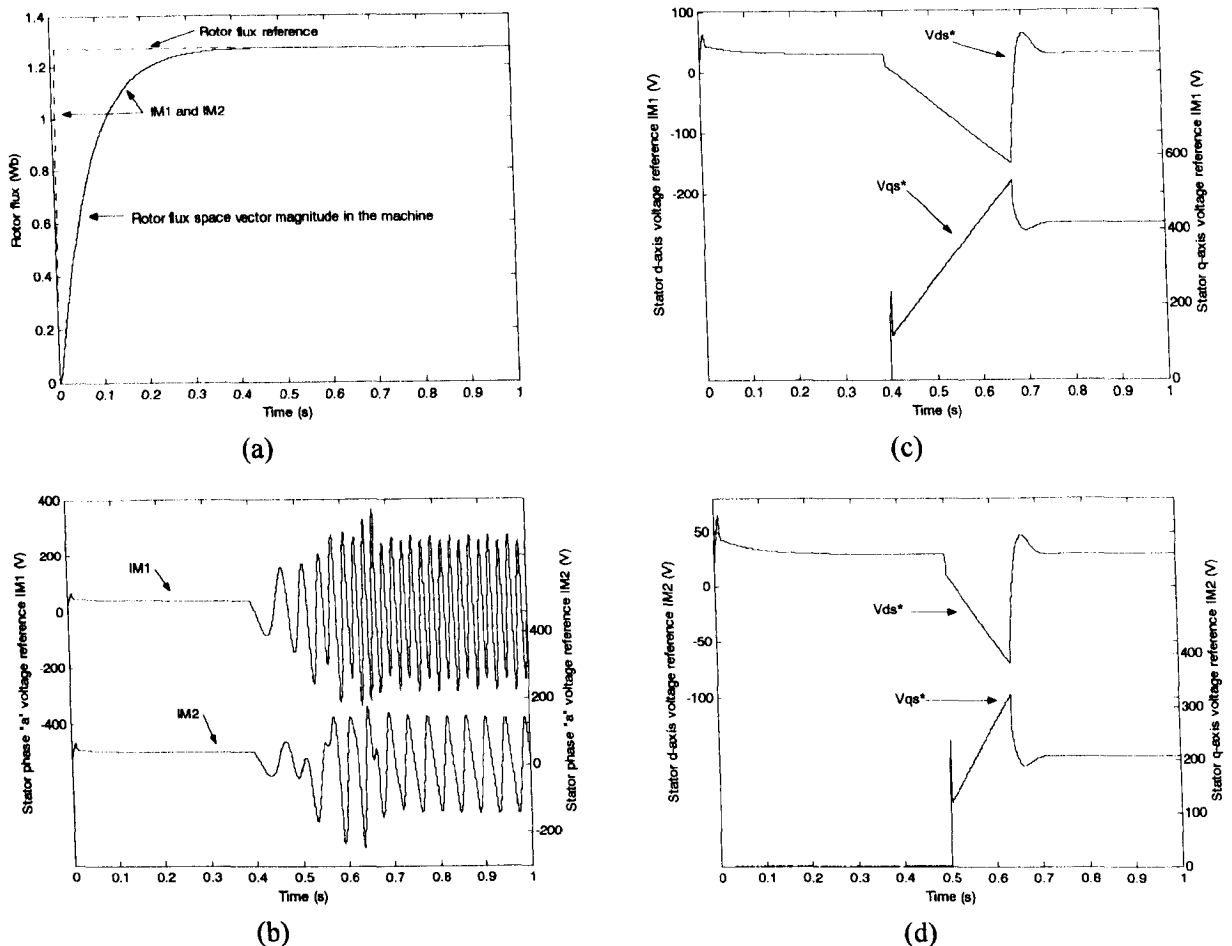


Fig. 8.6: Vector control of two five-phase induction machines connected in series, with phase transposition (feed-forward method): Rotor flux response (a), stator phase “a” voltage reference IM1 and IM2 (b), stator d-q axis voltage references IM1 (c) and stator d-q axis voltage references IM2 (d).

phase “a” voltage reference for machine 2 starts changing at 0.4s, which is when the speed command is applied to machine 1. This contrasts with Fig. 8.3f where the machine 2 phase “a” voltage reference starts changing at $t = 0.5s$, when the speed command is applied to machine 2. Next Fig. 8.7 depicts simulation results for the six-phase two-motor drive. Initially a rated rotor flux command (d-axis current) is applied to each machine (six-phase = 1.379 Wb, three-phase = 0.975 Wb). Once rated flux has been

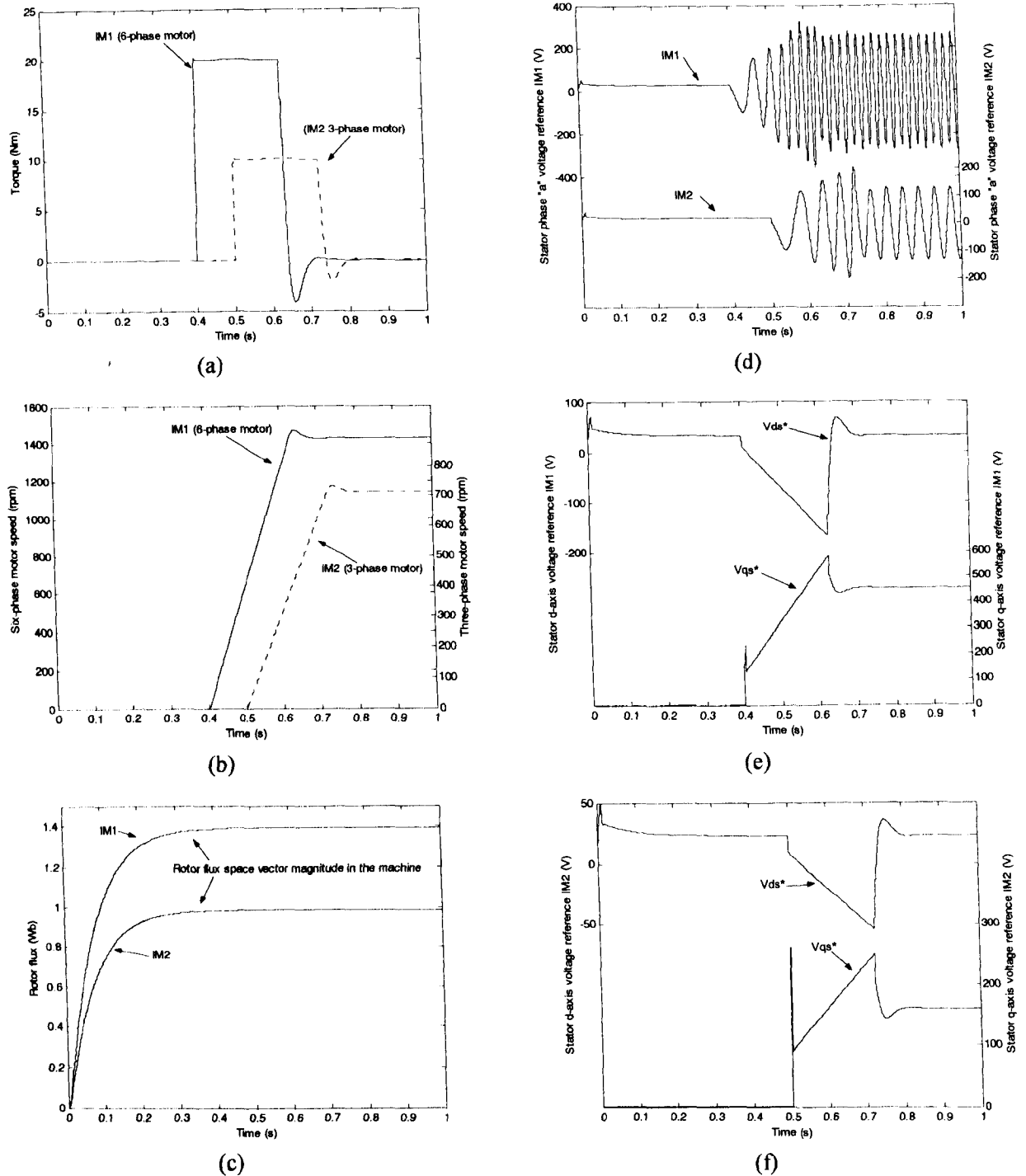


Fig. 8.7: Vector control of series connection of six-phase and three-phase induction machines with current control in the synchronous reference frame (feed-forward method): Torque response of IM1 and IM2 (a), speed response of IM1 and IM2 (b), rotor flux response of IM1 and IM2 (c), stator phase “a” voltage reference of IM1 and IM2 (d), stator d-q axis voltage references of IM1 (e) and stator d-q axis voltage references of IM2 (f).

established in both machines a speed command of 299 rad/s is applied to the six-phase motor (IM1) at $t = 0.4$ s and a speed command of 149 rad/s is applied to the three-phase motor (IM2) at $t = 0.5$ s. The torque limit is set to twice rated value for each machine (six-phase = 20 Nm, three-phase = 10 Nm). The torque, speed and rotor flux response of the machines can be seen in Figs. 8.7a – 8.7c, respectively. These figures show that completely decoupled control has been achieved. It is shown that the dynamic response of the six-phase machine is not affected by the flow of x-y current components through the stator of the machine. This is because the x-y voltage drops are compensated for using the stator voltage reference calculation (Fig. 8.5) according to (8.57). As can be seen in Fig. 8.5, x-y voltage compensation is only required for the six-phase machine. This is due to cancellation of the torque/flux producing currents of the six-phase machine at the point of connection with the three-phase machine. In other words, there are no x-y voltage drops created by the six-phase machine, hence the control of the three-phase machine does not need to compensate for them. Fig. 8.7d shows the stator phase “a” voltage reference of each machine. It is evident that the stator phase “a” voltage reference of the six-phase machine is in steady-state the summation of two sinusoidal signals at two different frequencies. Stator d-q axis voltage references for both machines are also shown in Fig. 8.7e and Fig. 8.7f.

The simulation results presented in this section have shown that the additional voltage drops created by the flow of x-y currents through the stator windings can be compensated for using the proposed feed-forward method. Although the feed-forward method achieves excellent results it significantly adds to the complexity of the drive and so a simpler method is therefore proposed in the next section.

8.7 Feed-forward compensation of x-y voltage drops in the synchronous reference frame

As mentioned previously, the feed-forward method of compensating for x-y voltage drops in the stationary reference frame achieves excellent results. However, it requires two additional co-ordinate transformations (for the five-phase case) and differentiation in the process of x-y voltage calculation. On the other hand, it is not possible to simply add x-y current controllers since there are $n-1$ independent currents in any n -phase system with an isolated neutral point and that is the number of currents that are already controlled (two pairs of d-q currents in both two-motor drives). A simpler

solution is therefore required.

It is shown in this section that the required x-y voltage compensation can be performed in the synchronous reference frame by modifying the decoupling voltage calculation (8.47). This method will further be referred to as the modified decoupling circuit method. In all the cases presented so far it was assumed that the decoupling d-q voltages are calculated in the same way as for a three-phase induction machine. However, it is shown in Jones et al (2004b) that the inverter equations in the rotor flux oriented reference frame are:

$$\begin{aligned} \underline{v}_{dq}^{INV(1)} &= (R_{s1} + R_{s2})\underline{i}_{dq}^{INV(1)} + (L_{s1} + L_{ls2})\frac{d\underline{i}_{dq}^{INV(1)}}{dt} + L_{m1}\frac{d\underline{i}_{r1}^{(1)}}{dt} + j\omega_{r1}[(L_{s1} + L_{ls2})\underline{i}_{dq}^{INV(1)} + L_{m1}\underline{i}_{r1}^{(1)}] \\ \underline{v}_{xy}^{INV(2)} &= (R_{s1} + R_{s2})\underline{i}_{xy}^{INV(2)} + (L_{s1} + L_{s2})\frac{d\underline{i}_{xy}^{INV(2)}}{dt} + L_{m2}\frac{d\underline{i}_{r2}^{(2)}}{dt} + j\omega_{r2}[(L_{ls1} + L_{s2})\underline{i}_{xy}^{INV(2)} + L_{m2}\underline{i}_{r2}^{(2)}] \end{aligned} \quad (8.59)$$

where (1) denotes quantities in the reference frame attached to rotor flux of machine 1, while (2) stands for quantities in the reference frame attached to rotor flux of machine 2. Equations (8.59) can be further written as:

$$\begin{aligned} \underline{v}_{dq}^{INV(1)} &= (R_{s1} + R_{s2})\underline{i}_{dq}^{INV(1)} + L_{ls2}\frac{d\underline{i}_{dq}^{INV(1)}}{dt} + \frac{d\underline{\psi}_{s1}^{(1)}}{dt} + j\omega_{r1}[L_{ls2}\underline{i}_{dq}^{INV(1)} + \underline{\psi}_{s1}^{(1)}] \\ \underline{v}_{xy}^{INV(2)} &= (R_{s1} + R_{s2})\underline{i}_{xy}^{INV(2)} + L_{ls1}\frac{d\underline{i}_{xy}^{INV(2)}}{dt} + \frac{d\underline{\psi}_{s2}^{(2)}}{dt} + j\omega_{r2}[L_{ls1}\underline{i}_{xy}^{INV(2)} + \underline{\psi}_{s2}^{(2)}] \end{aligned} \quad (8.60)$$

Since under the condition of rotor flux oriented control

$$\begin{aligned} \underline{\psi}_{s1}^{(1)} &= (L_{m1}/L_{r1})\underline{\psi}_{r1}^{(1)} + \sigma_1 L_{s1}\underline{i}_{dq}^{INV(1)} \\ \underline{\psi}_{s2}^{(2)} &= (L_{m2}/L_{r2})\underline{\psi}_{r2}^{(2)} + \sigma_2 L_{s2}\underline{i}_{xy}^{INV(2)} \end{aligned} \quad (8.61)$$

hold true, one has from (8.60) and (8.61):

$$\begin{aligned} \underline{v}_{dq}^{INV(1)} &= (R_{s1} + R_{s2})\underline{i}_{dq}^{INV(1)} + (\sigma_1 L_{s1} + L_{ls2})\frac{d\underline{i}_{dq}^{INV(1)}}{dt} + \frac{L_{m1}}{L_{r1}}\frac{d\underline{\psi}_{r1}^{(1)}}{dt} + j\omega_{r1}[(L_{ls2} + \sigma_1 L_{s1})\underline{i}_{dq}^{INV(1)} + \frac{L_{m1}}{L_{r1}}\underline{\psi}_{r1}^{(1)}] \\ \underline{v}_{xy}^{INV(2)} &= (R_{s1} + R_{s2})\underline{i}_{xy}^{INV(2)} + (\sigma_2 L_{s2} + L_{ls1})\frac{d\underline{i}_{xy}^{INV(2)}}{dt} + \frac{L_{m2}}{L_{r2}}\frac{d\underline{\psi}_{r2}^{(2)}}{dt} + j\omega_{r2}[(L_{ls1} + \sigma_2 L_{s2})\underline{i}_{xy}^{INV(2)} + \frac{L_{m2}}{L_{r2}}\underline{\psi}_{r2}^{(2)}] \end{aligned} \quad (8.62)$$

Since the two equations in (8.62) are of identical form, it is sufficient to consider only the first one further on. By defining the time constant T as:

$$T = (\sigma_1 L_{s1} + L_{ls2}) / (R_{s1} + R_{s2}) \quad (8.63)$$

the outputs of the PI current controllers can be written as:

$$\begin{aligned} v_d' &= (R_{s1} + R_{s2}) \left(i_d^{INV(1)} + T \frac{di_d^{INV(1)}}{dt} \right) \\ v_q' &= (R_{s1} + R_{s2}) \left(i_q^{INV(1)} + T \frac{di_q^{INV(1)}}{dt} \right) \end{aligned} \quad (8.64)$$

Inverter d-q voltage references are obtained as:

$$\begin{aligned} v_d^{INV(1)*} &= v_d' + e_d \\ v_q^{INV(1)*} &= v_q' + e_q \end{aligned} \quad (8.65)$$

Comparison of (8.64)-(8.65) with the first equation of (8.62) yields decoupling circuit voltages as:

$$\begin{aligned} e_d &= -\omega_{r1} (\sigma_1 L_{s1} + L_{ls2}) i_q^{INV(1)} \\ e_q &= \omega_{r1} \left(\frac{L_{s1}}{L_{m1}} \psi_{r1}^{(1)} + L_{ls2} i_d^{INV(1)} \right) \end{aligned} \quad (8.66a)$$

Here of course d-q currents are identically equal to the d-q axis stator current references of machine 1. That is:

$$\begin{aligned} e_{d1} &= -\omega_{r1} (\sigma_1 L_{s1} + L_{ls2}) i_{qs1}^* \\ e_{q1} &= \omega_{r1} \left(\frac{L_{s1}}{L_{m1}} \psi_{r1}^* + L_{ls2} i_{ds1}^* \right) \end{aligned} \quad (8.66b)$$

Identical result is obtained for the second machine, with an appropriate change of indices. Equations (8.66a) show that truly decoupled control requires compensation of additional voltage drops on leakage reactance of the machine, caused by the flow of x-y currents. Since the terms are frequency dependent, their omission from the decoupling voltages will have a more pronounced effect at higher speeds of rotation.

In the case of the six-phase drive, there is a need to modify only the decoupling circuit of the three-phase machine. This will follow from inverter x-y equations. Equations are in principle the same as (8.66), except that only half of the total three-phase machine current flows through one phase of the six-phase machine. Let the six-phase machine be machine 1 and the three-phase machine be machine 2. Then:

$$\begin{aligned} e_{d2} &= -\omega_{r2} (\sigma_2 L_{s2} + 0.5 L_{ls1}) i_{qs2}^* \\ e_{q2} &= \omega_{r2} \left(\frac{L_{s2}}{L_{m2}} \psi_{r2}^* + 0.5 L_{ls1} i_{ds2}^* \right) \end{aligned} \quad (8.67)$$

8.7.1 Simulation verification of the modified decoupling circuit method for the five-phase and six-phase two-motor drives

In order to verify the proposed modification of the decoupling circuit a simulation is performed for the five-phase drive in an identical manner to section 8.5.1, using vector control scheme shown in Fig. 8.1. Decoupling voltage calculation is performed according to (8.66) rather than (8.51). Stator phase voltage references remain to be determined with (8.49) and inverter phase voltage references are still governed by (8.50).

Rotor flux response of the two machines is shown in Fig. 8.8, where it can be seen that the disturbance seen in Fig. 8.3 has been completely eliminated. This means that complete decoupling of the control of the two machines results. Hence the proposed modification of the decoupling circuit enables full compensation of the cross-coupling introduced by the series connection of the two machines. The d-q axis voltage references are shown in Fig. 8.8 and have significantly higher values, when compared to those obtained using the feed-forward method (Fig. 8.6c and Fig. 8.6d). The d-q voltage references now have to cater for the x-y stator voltage drops, which are covered by the x-y voltage references in the feed-forward method. Stator phase “a” voltage references for each machine are depicted in Fig 8.8 where it can be seen that both voltage references are sinusoidal in steady-state due to the fact that x-y voltages are not used in their calculation.

A simulation of the six-phase two-motor drive is performed in order to verify the proposed modification to the decoupling voltages calculation given by (8.67). As previously mentioned there is only the need to modify the decoupling circuit of the three-phase machine and so the six-phase machine decoupling calculation remains that given by (8.47). Each machine is controlled using vector control scheme similar to that presented in Fig 8.1, respecting the phase number of the machine under consideration (i.e. six-phase or three-phase machine). Stator phase voltage references are determined in a similar fashion to (8.48). Inverter phase voltage references are calculated according to (8.58).

Simulation results for the six-phase case are depicted in Fig. 8.9 where once again it can be seen that completely decoupled control has been achieved. The speed, torque and rotor flux response of each machine (Fig. 8.9) are unchanged from those achieved using the feed-forward method (Fig. 8.7). However, the d-q voltage references of the

three-phase machine (Fig. 8.9) are higher than in the configuration using the feed-forward method (Fig. 8.7f). This is again due to the d-q axis voltages having to compensate for the x-y voltage drops. The d-q axis voltage references of the six-phase machine (Fig. 8.9) however remain the same as those obtained using the feed-forward method (Fig. 8.7e). The stator phase “a” voltage references are shown in Fig. 8.9 and are sinusoidal waveforms in steady-state.

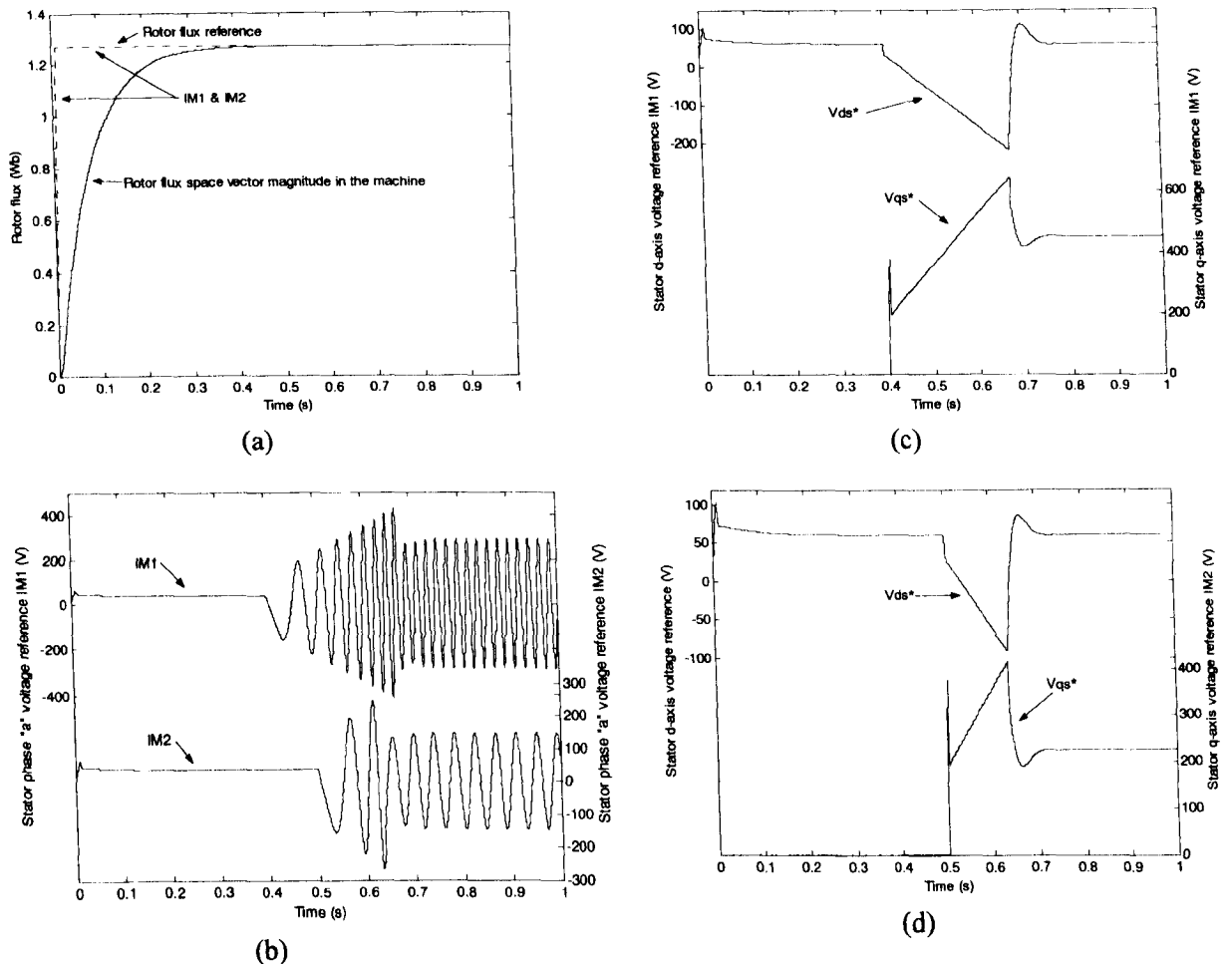


Fig. 8.8: Vector control of two five-phase induction machines connected in series, with phase transposition (modified decoupling circuit): Rotor flux response (a), stator phase “a” voltage reference IM1 and IM2 (b), stator d-q axis voltage references IM1 (c) and stator d-q axis voltage references IM2 (d).

8.8 Summary

This chapter has considered the possibility of performing current control in the rotating reference frame with regard to the series-connected multi-phase multi-machine drive system. In order to achieve this, induction machines under consideration need to be modelled as voltage fed. It is shown that the model of the voltage fed induction machine is much more involved because stator dynamics have to be taken into

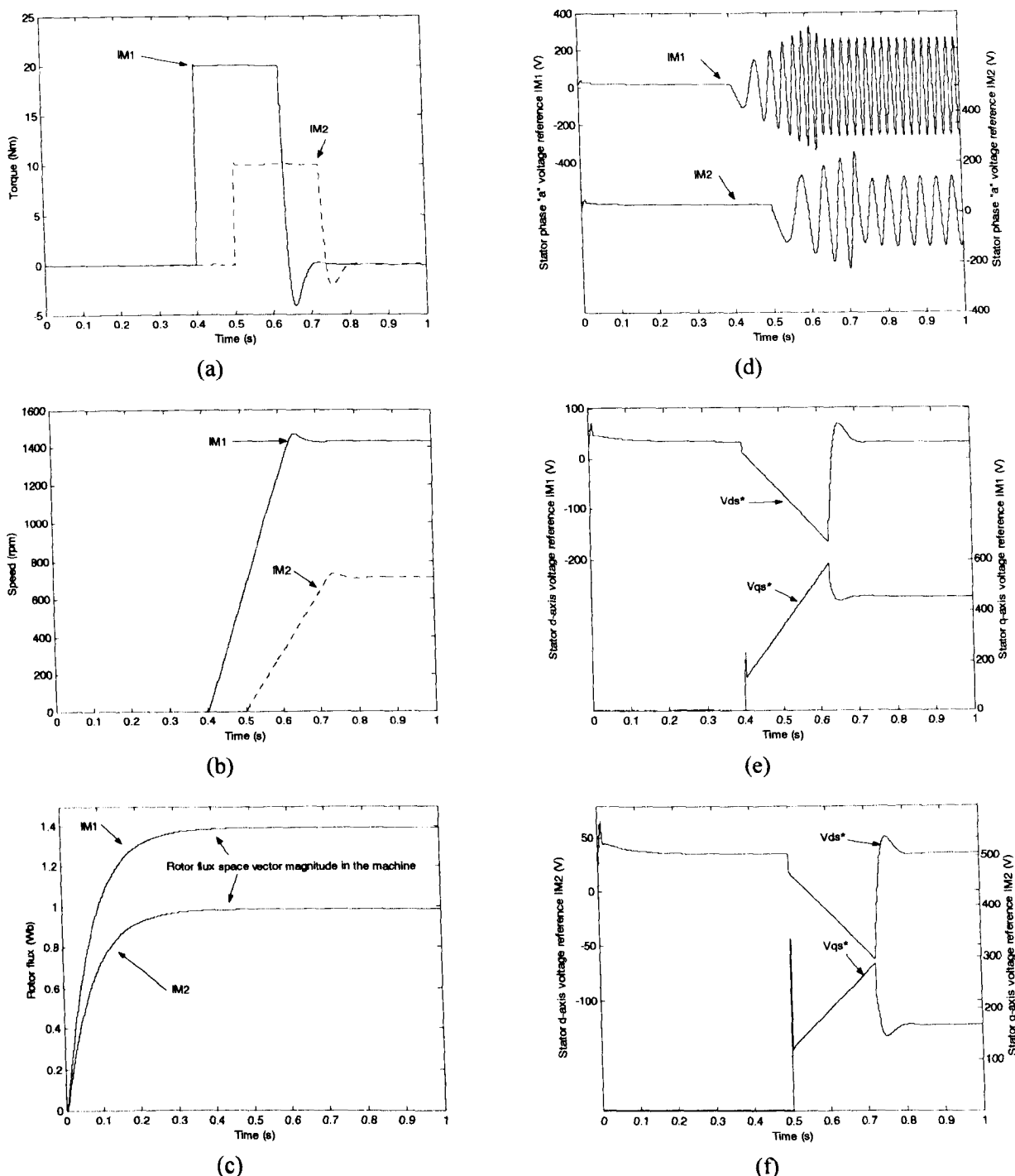


Fig. 8.9: Vector control of series connection of six-phase and three-phase induction machines with current control in the synchronous reference frame (modified decoupling circuit): Torque response of IM1 and IM2 (a), speed response of IM1 and IM2 (b), rotor flux response of IM1 and IM2 (c), stator phase "a" voltage reference of IM1 and IM2 (d), stator d-q axis voltage reference of IM1 (e) and stator d-q axis voltage reference of IM2 (f).

consideration. Initially a five-phase induction machine is simulated with current control in the rotating reference frame. This allows a comparison to be drawn with a series-connected five-phase two-motor drive with current control performed in the rotating reference frame. Simulation results for the five-phase two-motor drive show a disturbance in the rotor flux of each machine. It is shown that this disturbance is due to

the flow of x-y currents through the stator of both machines. These x-y currents produce a certain amount of voltage drop (termed x-y voltage drop), which the control is unaware of. This voltage drop appears on impedance comprising a series connection of the stator resistance and stator leakage reactance (at the frequency of the other machine). Therefore when current control is performed in the rotating reference frame the control system must generate voltages that will compensate for the x-y voltage drops in each machine. It should be noted that rotor flux disturbance can be significantly reduced if the current controllers are sufficiently fast, however in high power applications, where the inverter switching frequency is low, the PI current controllers cannot compensate for the x-y voltage drops. Hence two methods of compensating for the x-y voltage drops are proposed in the chapter: a method in the stationary reference frame, termed the feed-forward method, and a method in the synchronous reference frame, termed the modified decoupling circuit method. Both methods are verified via simulation of the five-phase and six-phase two-motor drive. It is shown that both methods perform very well and completely decoupled control of the two machines is achieved. However, the modified decoupling circuit method is preferred because it offers the simplest realisation.

Both methods require knowledge of machine parameters. This means that the potential problems with parameter variation effects are amplified, since accuracy of the parameter determination of one machine affects the control of the other machine, and vice versa. The situation worsens as the number of machines increases. For example, in the case of the three-motor seven-phase drive decoupling voltage calculation would involve parameters of all three machines. It therefore appears as advantageous to utilise current control in the stationary reference frame in conjunction with series-connected multi-phase multi-motor drives, since the accuracy of control and performance of one machine are then independent of the parameters of the other machines in the group.

CHAPTER 9

QUASI SIX-PHASE CONFIGURATIONS

9.1 Introduction

Multi-phase AC machines are particularly suitable for high power applications where reduction of the inverter per-phase rating is required. By far the most popular choice of multi-phase machine is a quasi six-phase induction or synchronous machine with two three-phase windings on the stator, spatially displaced by 30° (often referred to as dual three-phase or split phase machine). A quasi six-phase machine can be constructed by splitting the individual stator phase belts of a three-phase motor in half with an angular separation of 30° between the two halves. The main reason for selecting the asymmetrical six-phase winding instead of a true six-phase winding (60° displacement between any two consecutive phases) has been discussed in detail in Nelson and Krause (1979) and is in essence the possibility of reducing the torque ripple, caused by low order stator current harmonics. The torque ripples' dominant frequency is shifted from six to twelve times the fundamental frequency and the magnitude is significantly attenuated. This advantage of a quasi six-phase machine arrangement was of great importance in pre-PWM era of VSI control, when six-step VSIs were used. However, with modern inverter current control techniques and operation of the VSI in PWM mode, this property of quasi six-phase machines becomes somewhat irrelevant, since the low frequency harmonics can be easily suppressed from the inverter output currents for low to medium power machines.

The improvement of the pulsating torque is a result of the cancellation of harmonic flux components of the order $6n \pm 1$ ($n = 1,3,5 \dots$ etc.,) in the air gap. However, the stator windings can carry large amplitude currents in the x-y (uncoupled) equivalent circuits. These harmonics, when they exist, contribute significantly to the stator current since the impedance of the x-y equivalent circuits is low (it consists entirely of stator resistance and leakage inductance). The generation of these harmonic currents in the stator phases can be limited using large costly harmonic filters, Klingshirn (1985). Another possibility is to remove all the $6n \pm 1$ ($n = 1,3,5 \dots$) order harmonics from the phase voltage using an open end winding configuration as described

in Mohapatra et al (2003).

This chapter considers a series-connected two-motor drive consisting of either two quasi six-phase machines or a quasi six-phase machine and a two-phase machine. Once more each machine can be controlled independently provided that the stator windings are connected in an appropriate way. These configurations allow the x-y currents to be used to control the other machine in the group and so avoid the need for the previously mentioned harmonic current reduction methods. This is so since active impedance of one machine serves as a filter for the x-y current harmonics of the other machine, and vice versa.

The chapter begins with a description of a quasi six-phase induction machine. Connectivity matrices and connection diagrams for both configurations, which allow independent control of two machines, are further presented. In order to verify the proposed configurations simulations are undertaken, using the phase domain models of the two-motor quasi six-phase and two-motor quasi six-phase/two-phase drives. Current control, performed in the stationary reference frame or the rotating reference frame using the decoupling circuit method of section 8.7, is considered.

9.2 Two-motor drive with two quasi six-phase machines

Stator winding of a quasi six-phase machine consists of two three-phase windings, mutually displaced in space by 30° , as illustrated in Fig. 9.1. The phases of the first three-phase winding are identified with symbols a, b, c , while symbols d, e, f stand for the second three-phase winding displaced by 30° with respect to the first one. The neutral points of the two windings are normally kept isolated to prevent the stator current harmonics of the order divisible by three from flowing. The decoupling transformation matrix for such a six-phase machine is given with:

$$\underline{C} = \sqrt{\frac{2}{6}} \begin{bmatrix} 1 & \cos 2\pi/3 & \cos 4\pi/3 & \cos \pi/6 & \cos 5\pi/6 & \cos 9\pi/6 \\ 0 & \sin 2\pi/3 & \sin 4\pi/3 & \sin \pi/6 & \sin 5\pi/6 & \sin 9\pi/6 \\ 1 & \cos 4\pi/3 & \cos 8\pi/3 & \cos 5\pi/6 & \cos \pi/6 & \cos 9\pi/6 \\ 0 & \sin 4\pi/3 & \sin 8\pi/3 & \sin 5\pi/6 & \sin \pi/6 & \sin 9\pi/6 \\ 1 & 1 & 1 & 0 & 0 & 0 \\ 0 & 0 & 0 & 1 & 1 & 1 \end{bmatrix} \quad (9.1a)$$

where the phase ordering is a, b, c, d, e, f . As explained in chapter 4, inspection of the

transformation matrix (9.1a) leads to the connectivity matrix shown in Table 9.1 and the resulting connection diagram (Fig. 9.2). It is assumed that both machines operate in steady-state and that the required phase currents for flux and torque production in the two machines are given with sinusoidal functions of the form ($\alpha = \pi/6$):

$$\begin{aligned}
 i_{a1}^* &= \sqrt{2}I_1 \sin(\omega_1 t) & i_{a2}^* &= \sqrt{2}I_2 \sin(\omega_2 t) \\
 i_{b1}^* &= \sqrt{2}I_1 \sin(\omega_1 t - 4\alpha) & i_{b2}^* &= \sqrt{2}I_2 \sin(\omega_2 t - 4\alpha) \\
 i_{c1}^* &= \sqrt{2}I_1 \sin(\omega_1 t - 8\alpha) & i_{c2}^* &= \sqrt{2}I_2 \sin(\omega_2 t - 8\alpha) \\
 i_{d1}^* &= \sqrt{2}I_1 \sin(\omega_1 t - \alpha) & i_{d2}^* &= \sqrt{2}I_2 \sin(\omega_2 t - \alpha) \\
 i_{e1}^* &= \sqrt{2}I_1 \sin(\omega_1 t - 5\alpha) & i_{e2}^* &= \sqrt{2}I_2 \sin(\omega_2 t - 5\alpha) \\
 i_{f1}^* &= \sqrt{2}I_1 \sin(\omega_1 t - 9\alpha) & i_{f2}^* &= \sqrt{2}I_2 \sin(\omega_2 t - 9\alpha)
 \end{aligned} \tag{9.2}$$

Let the inverter current references be created according to Fig. 9.2,

$$\begin{aligned}
 i_A^* &= i_{a1}^* + i_{a2}^* & i_B^* &= i_{b1}^* + i_{c2}^* \\
 i_C^* &= i_{c1}^* + i_{b2}^* & i_D^* &= i_{d1}^* + i_{e2}^* \\
 i_E^* &= i_{e1}^* + i_{d2}^* & i_F^* &= i_{f1}^* + i_{f2}^*
 \end{aligned} \tag{9.3}$$

and let the current control be ideal, so that the inverter output currents may be taken as equal to the inverter current references of (9.3). The inverter phase currents are identically equal to the phase currents flowing through machine 1. However, for the second machine, due to the phase transposition introduced in (9.3) the following holds true:

$$\begin{aligned}
 i_{a2} &= i_A^* & i_{b2} &= i_C^* \\
 i_{c2} &= i_B^* & i_{d2} &= i_E^* \\
 i_{e2} &= i_D^* & i_{f2} &= i_F^*
 \end{aligned} \tag{9.4}$$

Application of the decoupling transformation matrix (9.1a) on inverter currents of (9.3) produces two pairs of inverter current components, which are simultaneously corresponding current components of machine 1. Let the first pair be denoted with symbols α , β and let the second pair have indices x , y , then:

$$\begin{aligned}
 i_\alpha^{INV} + j i_\beta^{INV} &= i_{\alpha s}^{M1} + j i_{\beta s}^{M1} = \sqrt{6}I_1 (\sin \omega_1 t - j \cos \omega_1 t) \\
 i_x^{INV} + j i_y^{INV} &= i_{x s}^{M1} + j i_{y s}^{M1} = \sqrt{6}I_2 (\sin \omega_2 t - j \cos \omega_2 t)
 \end{aligned} \tag{9.5}$$

Similarly, application of (9.1) in conjunction with (9.4) produces:

$$\begin{aligned}
 i_{as}^{M2} + ji_{\beta s}^{M2} &= \sqrt{6}I_2(\sin \omega_2 t - j \cos \omega_2 t) \equiv i_x^{INV} + ji_y^{INV} \\
 i_{xs}^{M2} + ji_{ys}^{M2} &= \sqrt{6}I_1(\sin \omega_1 t - j \cos \omega_1 t) \equiv i_\alpha^{INV} + ji_\beta^{INV}
 \end{aligned}
 \tag{9.6}$$

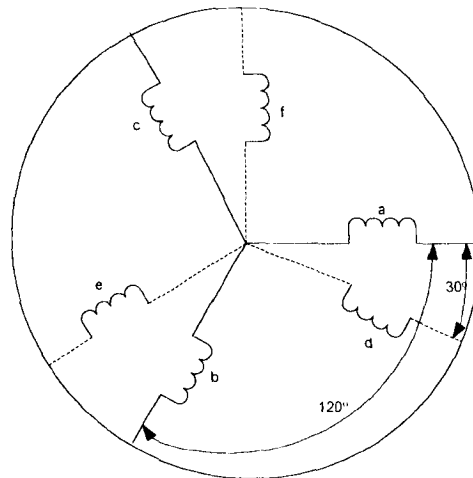


Fig. 9.1: Schematic representation of a quasi six-phase (split phase, dual three-phase) machine's stator winding.

Table 9.1. Connectivity matrix for the quasi six-phase drive.

	A	B	C	D	E	F
M1	1	2	3	4	5	6
M2	1	3	2	5	4	6

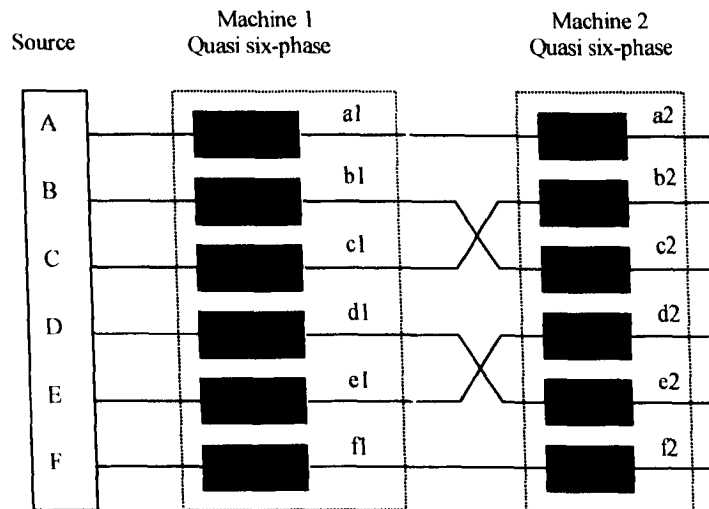


Fig. 9.2. Series-connection of two quasi six-phase machines.

Expressions (9.5)-(9.6) show that the flux/torque producing stator current α , β components of machine 1 appear as non flux/torque producing currents for machine 2, and vice versa. Hence the formation of the inverter current references according to (9.3) leads to the possibility of independent vector control of the two series-connected quasi six-phase machines. It should be noted that, due to the isolated neutral points, zero

sequence stator current components (described with the last two rows of the transformation matrix (9.1)) cannot exist.

It is interesting to note that the same result is possible with an alternative series-connection of stator windings, illustrated in Fig. 9.3. While in Fig. 9.2 series-connection with an appropriate phase transposition involves interfacing of “a”, “b”, “c” three-phase windings of the two machines and interfacing of “d”, “e”, “f” three-phase windings, connection diagram of Fig. 9.3 involves connection of “a”, “b”, “c” windings of one machine with “d”, “e”, “f” windings of the other machine. Inverter reference current generation for the scheme of Fig. 9.3 is governed with:

$$\begin{aligned}
 i_A^* &= i_{a1}^* + i_{e2}^* & i_B^* &= i_{b1}^* + i_{f2}^* \\
 i_C^* &= i_{c1}^* + i_{d2}^* & i_D^* &= i_{d1}^* + i_{a2}^* \\
 i_E^* &= i_{e1}^* + i_{b2}^* & i_F^* &= i_{f1}^* + i_{c2}^*
 \end{aligned}
 \tag{9.7}$$

The phase currents of machine 2 are now:

$$\begin{aligned}
 i_{a2} &= i_D^* & i_{b2} &= i_E^* \\
 i_{c2} &= i_F^* & i_{d2} &= i_C^* \\
 i_{e2} &= i_A^* & i_{f2} &= i_B^*
 \end{aligned}
 \tag{9.8}$$

It can be easily verified, by application of (9.1) in conjunction with (9.7) and (9.8), that the same result as in (9.5)-(9.6) is obtained again (with some additional phase shifts).

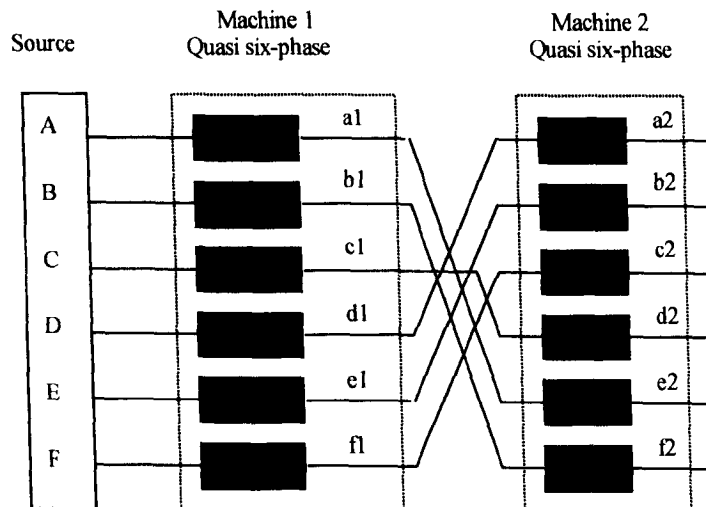


Fig. 9.3. An alternative series-connection of two quasi six-phase machines.

Due to the nature of the quasi six-phase machine, an alternative configuration of the quasi six-phase two-motor drive is possible, which enables series-connection of a two-

phase machine to the quasi six-phase machine. This scheme is discussed in the following section.

9.3 Two-motor drive with a quasi six-phase machine and a two-phase machine

If one considers that the quasi six-phase machine consists of two three-phase windings displaced by 30° from each other and that a balanced three-phase system of currents will sum to zero, then it becomes obvious that a two-phase machine can be connected in series with the quasi six-phase machine and the torque/flux producing currents of the quasi six-phase machine will cancel at the point of connection with the two-phase machine. The proposed connectivity matrix and connection diagram can be seen in Table 9.2 and Fig. 9.4 respectively.

Table 9.2. Connectivity matrix for the quasi six-phase drive.

	A	B	C	D	E	F
M1	1	2	3	4	5	6
M2	1	1	1	2	2	2

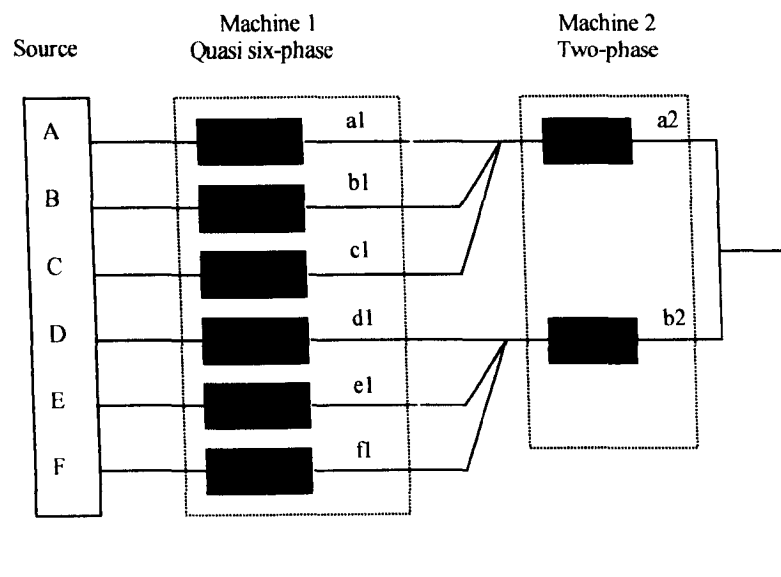


Fig. 9.4. Series-connection of a quasi six-phase machine and a two-phase machine

It is important to note that for the configuration of Fig. 9.4 the quasi six-phase machine has essentially connected star points. Hence for this configuration, modified

form of the transformation matrix (9.1) holds true:

$$\underline{C} = \sqrt{\frac{2}{6}} \begin{bmatrix} 1 & \cos 2\pi/3 & \cos 4\pi/3 & \cos \pi/6 & \cos 5\pi/6 & \cos 9\pi/6 \\ 0 & \sin 2\pi/3 & \sin 4\pi/3 & \sin \pi/6 & \sin 5\pi/6 & \sin 9\pi/6 \\ 1 & \cos 4\pi/3 & \cos 8\pi/3 & \cos 5\pi/6 & \cos \pi/6 & \cos 9\pi/6 \\ 0 & \sin 4\pi/3 & \sin 8\pi/3 & \sin 5\pi/6 & \sin \pi/6 & \sin 9\pi/6 \\ 1 & 1 & 1 & 1 & 1 & 1 \\ 1 & -1 & 1 & -1 & 1 & -1 \end{bmatrix} \quad (9.1b)$$

The possibility of achieving completely decoupled control for each machine in the proposed configuration shown in Fig. 9.4 is investigated next. For that purpose it is assumed that both machines operate in steady-state and that the required phase currents for flux\torque production in the quasi six-phase machine are:

$$\begin{aligned} i_{a1}^* &= \sqrt{2}I_1 \sin(\omega_1 t) \\ i_{b1}^* &= \sqrt{2}I_1 \sin(\omega_1 t - 4\alpha) \\ i_{c1}^* &= \sqrt{2}I_1 \sin(\omega_1 t - 8\alpha) \\ i_{d1}^* &= \sqrt{2}I_1 \sin(\omega_1 t - \alpha) \\ i_{e1}^* &= \sqrt{2}I_1 \sin(\omega_1 t - 5\alpha) \\ i_{f1}^* &= \sqrt{2}I_1 \sin(\omega_1 t - 9\alpha) \end{aligned} \quad (9.9)$$

Let the torque\flux producing currents of the two-phase machine be:

$$\begin{aligned} i_{a2} &= \sqrt{2}I_2 \sin \omega_2 t \\ i_{b2} &= \sqrt{2}I_2 \sin(\omega_2 t - \pi/2) = -\sqrt{2}I_2 \cos \omega_2 t \end{aligned} \quad (9.10)$$

Assume that there are two indirect vector controllers for the two machines, which generate the references according to (9.9) and (9.10). Suppose further that the inverter current references are again obtained by summation, but using this time:

$$\begin{aligned} i_A^* &= i_{a1}^* + (1/3)i_{a2}^* \\ i_B^* &= i_{b1}^* + (1/3)i_{a2}^* \\ i_C^* &= i_{c1}^* + (1/3)i_{a2}^* \\ i_D^* &= i_{d1}^* + (1/3)i_{b2}^* \\ i_E^* &= i_{e1}^* + (1/3)i_{b2}^* \\ i_F^* &= i_{f1}^* + (1/3)i_{b2}^* \end{aligned} \quad (9.11)$$

It follows from (9.9)-(9.11) that:

$$\begin{aligned} i_A^* + i_B^* + i_C^* &= i_{a2}^* \\ i_D^* + i_E^* + i_F^* &= i_{b2}^* \end{aligned} \quad (9.12)$$

Application of (9.1b) in conjunction with (9.11) and taking into account (9.9)-(9.10) yields:

$$\begin{aligned} i_\alpha^{INV} &= \sqrt{6}I_1 \sin \omega_1 t \\ i_\beta^{INV} &= -\sqrt{6}I_1 \cos \omega_1 t \\ i_x^{INV} &= 0 \\ i_y^{INV} &= 0 \\ i_{0+}^{INV} &= \sqrt{\frac{2}{6}}i_{a2}^* = \sqrt{\frac{2}{3}}I_2 \sin \omega_2 t \\ i_{0-}^{INV} &= \sqrt{\frac{2}{6}}i_{b2}^* = -\sqrt{\frac{2}{3}}I_2 \cos \omega_2 t \end{aligned} \quad (9.13)$$

Obviously, machine 2 flux/torque producing currents of (9.10) will be producing zero-sequence currents in each of the two three-phase winding sets of machine 1. According to (9.11)-(9.12), inverter currents of the first three phases sum to the current of phase “a” of machine 2; similarly inverter currents of the last three phases sum to the current of phase “b” of machine 2. These will form zero sequence currents of the same value in two three-phase winding sets of machine 1. Since the neutral point of the complete drive will always carry current the issue of where to connect it needs to be addressed. One possibility is to use split series capacitors in the DC link and connect the neutral to the mid-point of the DC link. Another possibility is to use a separate inverter leg (phase) for the connection of the neutral. This issue is beyond the scope of this thesis but would have to be explored in detail for any implementation related considerations. It is possible to enhance the torque developed by the six-phase machine by injection of 3rd harmonic current as described in Lyra et al (2001). If $\omega_2 = 3\omega_1$ then the two-phase motor currents will give torque enhancement for the six-phase machine.

9.4 Phase domain model of voltage fed series-connected two-motor drive with two quasi six-phase machines

In order to simulate the proposed series connected two-motor drive shown in Fig. 9.2 it is necessary to first model the complete drive system. Due to the series-

connection of two stator windings according to Fig. 9.2 the following holds true:

$$\begin{aligned} v_A &= v_{a1} + v_{a2} & v_B &= v_{b1} + v_{c2} \\ v_C &= v_{c1} + v_{b2} & v_D &= v_{d1} + v_{e2} \\ v_E &= v_{e1} + v_{d2} & v_F &= v_{f1} + v_{f2} \end{aligned} \quad (9.14)$$

$$\begin{aligned} i_A &= i_{a1} = i_{a2} & i_B &= i_{b1} = i_{c2} \\ i_C &= i_{c1} = i_{b2} & i_D &= i_{d1} = i_{e2} \\ i_E &= i_{e1} = i_{d2} & i_F &= i_{f1} = i_{f2} \end{aligned} \quad (9.15)$$

Capital letters stand for inverter phase-to-neutral voltages and inverter currents in equations (9.14)-(9.15). Index '1' denotes induction machine directly connected to the six-phase inverter and index '2' denotes the second induction machine which is connected to the first induction machine through phase transposition. Voltage equations for the complete system can be written in compact matrix form as:

$$\underline{v} = \underline{R}\underline{i} + \frac{d(\underline{L}\underline{i})}{dt} \quad (9.16)$$

where the system is of the 18th order and:

$$\underline{v} = \begin{bmatrix} \underline{v}^{INV} \\ \underline{0} \\ \underline{0} \end{bmatrix} \quad \underline{i} = \begin{bmatrix} \underline{i}^{INV} \\ \underline{i}_{r1} \\ \underline{i}_{r2} \end{bmatrix} \quad (9.17)$$

$$\begin{aligned} \underline{v}^{INV} &= [v_A \quad v_B \quad v_C \quad v_D \quad v_E \quad v_F]^T \\ \underline{i}^{INV} &= [i_A \quad i_B \quad i_C \quad i_D \quad i_E \quad i_F]^T \end{aligned} \quad (9.18)$$

$$\begin{aligned} \underline{i}_{r1} &= [i_{ar1} \quad i_{br1} \quad i_{cr1} \quad i_{dr1} \quad i_{er1} \quad i_{fr1}]^T \\ \underline{i}_{r2} &= [i_{ar2} \quad i_{br2} \quad i_{cr2} \quad i_{dr2} \quad i_{er2} \quad i_{fr2}]^T \end{aligned} \quad (9.19)$$

The resistance and inductance matrices of (9.16) can be written as:

$$\underline{R} = \begin{bmatrix} \underline{R}_{s1} + \underline{R}_{s2} & & \\ & \underline{R}_{r1} & \\ & & \underline{R}_{r2} \end{bmatrix} \quad (9.20)$$

$$\underline{L} = \begin{bmatrix} \underline{L}_{s1} + \underline{L}_{s2}' & \underline{L}_{sr1} & \underline{L}_{sr2}' \\ \underline{L}_{rs1} & \underline{L}_{r1} & \underline{0} \\ \underline{L}_{rs2}' & \underline{0} & \underline{L}_{r2} \end{bmatrix} \quad (9.21)$$

Superscript ' in (9.21) denotes once more sub-matrices of machine 2 that have been modified through the phase transposition operation. The sub-matrices of (9.20)-(9.21) are all six by six matrices and are given with the following expressions:

$$\begin{aligned} \underline{R}_{s1} &= \text{diag}(R_{s1} \ R_{s1} \ R_{s1} \ R_{s1} \ R_{s1} \ R_{s1}) \\ \underline{R}_{r1} &= \text{diag}(R_{r1} \ R_{r1} \ R_{r1} \ R_{r1} \ R_{r1} \ R_{r1}) \end{aligned} \quad (9.22a)$$

$$\begin{aligned} \underline{R}_{s2} &= \text{diag}(R_{s2} \ R_{s2} \ R_{s2} \ R_{s2} \ R_{s2} \ R_{s2}) \\ \underline{R}_{r2} &= \text{diag}(R_{r2} \ R_{r2} \ R_{r2} \ R_{r2} \ R_{r2} \ R_{r2}) \end{aligned} \quad (9.22b)$$

$$\underline{L}_{s1} = \begin{bmatrix} L_{ls1} + M_1 & M_1 \cos 4\alpha & M_1 \cos 8\alpha & M_1 \cos \alpha & M_1 \cos 5\alpha & M_1 \cos 9\alpha \\ M_1 \cos 8\alpha & L_{ls1} + M_1 & M_1 \cos 4\alpha & M_1 \cos 9\alpha & M_1 \cos \alpha & M_1 \cos 5\alpha \\ M_1 \cos 4\alpha & M_1 \cos 8\alpha & L_{ls1} + M_1 & M_1 \cos 5\alpha & M_1 \cos 9\alpha & M_1 \cos \alpha \\ M_1 \cos 11\alpha & M_1 \cos 3\alpha & M_1 \cos 7\alpha & L_{ls1} + M_1 & M_1 \cos 4\alpha & M_1 \cos 8\alpha \\ M_1 \cos 7\alpha & M_1 \cos 11\alpha & M_1 \cos 3\alpha & M_1 \cos 8\alpha & L_{ls1} + M_1 & M_1 \cos 4\alpha \\ M_1 \cos 3\alpha & M_1 \cos 7\alpha & M_1 \cos 11\alpha & M_1 \cos 4\alpha & M_1 \cos 8\alpha & L_{ls1} + M_1 \end{bmatrix} \quad (9.23)$$

$$\underline{L}_{r1} = \begin{bmatrix} L_{lr1} + M_1 & M_1 \cos 4\alpha & M_1 \cos 8\alpha & M_1 \cos \alpha & M_1 \cos 5\alpha & M_1 \cos 9\alpha \\ M_1 \cos 8\alpha & L_{lr1} + M_1 & M_1 \cos 4\alpha & M_1 \cos 9\alpha & M_1 \cos \alpha & M_1 \cos 5\alpha \\ M_1 \cos 4\alpha & M_1 \cos 8\alpha & L_{lr1} + M_1 & M_1 \cos 5\alpha & M_1 \cos 9\alpha & M_1 \cos \alpha \\ M_1 \cos 11\alpha & M_1 \cos 3\alpha & M_1 \cos 7\alpha & L_{lr1} + M_1 & M_1 \cos 4\alpha & M_1 \cos 8\alpha \\ M_1 \cos 7\alpha & M_1 \cos 11\alpha & M_1 \cos 3\alpha & M_1 \cos 8\alpha & L_{lr1} + M_1 & M_1 \cos 4\alpha \\ M_1 \cos 3\alpha & M_1 \cos 7\alpha & M_1 \cos 11\alpha & M_1 \cos 4\alpha & M_1 \cos 8\alpha & L_{lr1} + M_1 \end{bmatrix} \quad (9.24)$$

$$\underline{L}_{s2} = \begin{bmatrix} L_{ls2} + M_2 & M_2 \cos 8\alpha & M_2 \cos 4\alpha & M_2 \cos 5\alpha & M_2 \cos \alpha & M_2 \cos 9\alpha \\ M_2 \cos 4\alpha & L_{ls2} + M_2 & M_2 \cos 8\alpha & M_2 \cos 9\alpha & M_2 \cos 5\alpha & M_2 \cos \alpha \\ M_2 \cos 8\alpha & M_2 \cos 4\alpha & L_{ls2} + M_2 & M_2 \cos \alpha & M_2 \cos 9\alpha & M_2 \cos 5\alpha \\ M_2 \cos 7\alpha & M_2 \cos 3\alpha & M_2 \cos 11\alpha & L_{ls2} + M_2 & M_2 \cos 8\alpha & M_2 \cos 4\alpha \\ M_2 \cos 11\alpha & M_2 \cos 7\alpha & M_2 \cos 3\alpha & M_2 \cos 4\alpha & L_{ls2} + M_2 & M_2 \cos 8\alpha \\ M_2 \cos 3\alpha & M_2 \cos 11\alpha & M_2 \cos 7\alpha & M_2 \cos 8\alpha & M_2 \cos 4\alpha & L_{ls2} + M_2 \end{bmatrix} \quad (9.25)$$

$$\underline{L}_{r2} = \begin{bmatrix} L_{lr2} + M_2 & M_2 \cos 4\alpha & M_2 \cos 8\alpha & M_2 \cos \alpha & M_2 \cos 5\alpha & M_2 \cos 9\alpha \\ M_2 \cos 8\alpha & L_{lr2} + M_2 & M_2 \cos 4\alpha & M_2 \cos 9\alpha & M_2 \cos \alpha & M_2 \cos 5\alpha \\ M_2 \cos 4\alpha & M_2 \cos 8\alpha & L_{lr2} + M_2 & M_2 \cos 5\alpha & M_2 \cos 9\alpha & M_2 \cos \alpha \\ M_2 \cos 11\alpha & M_2 \cos 3\alpha & M_2 \cos 7\alpha & L_{lr2} + M_2 & M_2 \cos 4\alpha & M_2 \cos 8\alpha \\ M_2 \cos 7\alpha & M_2 \cos 11\alpha & M_2 \cos 3\alpha & M_2 \cos 8\alpha & L_{lr2} + M_2 & M_2 \cos 4\alpha \\ M_2 \cos 3\alpha & M_2 \cos 7\alpha & M_2 \cos 11\alpha & M_2 \cos 4\alpha & M_2 \cos 8\alpha & L_{lr2} + M_2 \end{bmatrix} \quad (9.26)$$

$$\underline{L}_{sr1} = M_1 \begin{bmatrix} \cos \theta_1 & \cos(\theta_1 + 4\alpha) & \cos(\theta_1 + 8\alpha) & \cos(\theta_1 + \alpha) & \cos(\theta_1 + 5\alpha) & \cos(\theta_1 + 9\alpha) \\ \cos(\theta_1 + 8\alpha) & \cos \theta_1 & \cos(\theta_1 + 4\alpha) & \cos(\theta_1 + 9\alpha) & \cos(\theta_1 + \alpha) & \cos(\theta_1 + 5\alpha) \\ \cos(\theta_1 + 4\alpha) & \cos(\theta_1 + 8\alpha) & \cos \theta_1 & \cos(\theta_1 + 5\alpha) & \cos(\theta_1 + 9\alpha) & \cos(\theta_1 + \alpha) \\ \cos(\theta_1 + 11\alpha) & \cos(\theta_1 + 3\alpha) & \cos(\theta_1 + 7\alpha) & \cos \theta_1 & \cos(\theta_1 + 4\alpha) & \cos(\theta_1 + 8\alpha) \\ \cos(\theta_1 + 7\alpha) & \cos(\theta_1 + 11\alpha) & \cos(\theta_1 + 3\alpha) & \cos(\theta_1 + 8\alpha) & \cos \theta_1 & \cos(\theta_1 + 4\alpha) \\ \cos(\theta_1 + 3\alpha) & \cos(\theta_1 + 7\alpha) & \cos(\theta_1 + 11\alpha) & \cos(\theta_1 + 4\alpha) & \cos(\theta_1 + 8\alpha) & \cos \theta_1 \end{bmatrix}$$

$$\underline{L}_{rs1} = \underline{L}_{sr1}^T \quad (9.27)$$

$$\underline{L}_{sr2} = M_2 \begin{bmatrix} \cos \theta_2 & \cos(\theta_2 + 4\alpha) & \cos(\theta_2 + 8\alpha) & \cos(\theta_2 + \alpha) & \cos(\theta_2 + 5\alpha) & \cos(\theta_2 + 9\alpha) \\ \cos(\theta_2 + 4\alpha) & \cos(\theta_2 + 8\alpha) & \cos \theta_2 & \cos(\theta_2 + 5\alpha) & \cos(\theta_2 + 9\alpha) & \cos(\theta_2 + \alpha) \\ \cos(\theta_2 + 8\alpha) & \cos \theta_2 & \cos(\theta_2 + 4\alpha) & \cos(\theta_2 + 9\alpha) & \cos(\theta_2 + \alpha) & \cos(\theta_2 + 5\alpha) \\ \cos(\theta_2 + 7\alpha) & \cos(\theta_2 + 11\alpha) & \cos(\theta_2 + 3\alpha) & \cos(\theta_2 + 8\alpha) & \cos \theta_2 & \cos(\theta_2 + 4\alpha) \\ \cos(\theta_2 + 11\alpha) & \cos(\theta_2 + 3\alpha) & \cos(\theta_2 + 7\alpha) & \cos \theta_2 & \cos(\theta_2 + 4\alpha) & \cos(\theta_2 + 8\alpha) \\ \cos(\theta_2 + 3\alpha) & \cos(\theta_2 + 7\alpha) & \cos(\theta_2 + 11\alpha) & \cos(\theta_2 + 4\alpha) & \cos(\theta_2 + 8\alpha) & \cos \theta_2 \end{bmatrix}$$

$$\underline{L}_{rs2} = \underline{L}_{sr2}^T \quad (9.28)$$

Expansion of (9.16) yields:

$$\underline{v} = \begin{bmatrix} \underline{v}^{INV} \\ \underline{0} \\ \underline{0} \end{bmatrix} = \begin{bmatrix} \underline{R}_{s1} + \underline{R}_{s2} & & \\ & \underline{R}_{r1} & \\ & & \underline{R}_{r2} \end{bmatrix} \begin{bmatrix} \underline{i}^{INV} \\ \underline{i}_{r1} \\ \underline{i}_{r2} \end{bmatrix} + \begin{bmatrix} \underline{L}_{s1} + \underline{L}_{s2}' & \underline{L}_{sr1} & \underline{L}_{sr2}' \\ \underline{L}_{rs1} & \underline{L}_{r1} & \underline{0} \\ \underline{L}_{rs2}' & \underline{0} & \underline{L}_{r2} \end{bmatrix} \frac{d}{dt} \begin{bmatrix} \underline{i}^{INV} \\ \underline{i}_{r1} \\ \underline{i}_{r2} \end{bmatrix} +$$

$$\begin{bmatrix} \underline{0} & \frac{d}{dt} \underline{L}_{sr1} & \frac{d}{dt} \underline{L}_{sr2}' \\ \frac{d}{dt} \underline{L}_{rs1} & \underline{0} & \underline{0} \\ \frac{d}{dt} \underline{L}_{rs2}' & \underline{0} & \underline{0} \end{bmatrix} \begin{bmatrix} \underline{i}^{INV} \\ \underline{i}_{r1} \\ \underline{i}_{r2} \end{bmatrix} \quad (9.29)$$

Torque equations of the two machines in terms of inverter currents of (9.3) are:

$$T_{el} = -P_1 M_1 \left\{ \begin{array}{l} (i_A i_{ar} + i_B i_{br} + i_C i_{cr} + i_D i_{dr} + i_E i_{er} + i_F i_{fr}) \sin \theta_1 + \\ (i_C i_{ar} + i_A i_{br} + i_B i_{cr} + i_F i_{dr} + i_D i_{er} + i_E i_{fr}) \sin(\theta_1 + 4\alpha) + \\ (i_B i_{ar} + i_C i_{br} + i_A i_{cr} + i_E i_{dr} + i_F i_{er} + i_D i_{fr}) \sin(\theta_1 + 8\alpha) + \\ (-i_E i_{ar} - i_F i_{br} - i_D i_{cr} + i_A i_{dr} + i_B i_{er} + i_C i_{fr}) \sin(\theta_1 + \alpha) + \\ (-i_D i_{ar} - i_E i_{br} - i_F i_{cr} + i_C i_{dr} + i_A i_{er} + i_B i_{fr}) \sin(\theta_1 + 5\alpha) + \\ (-i_F i_{ar} - i_D i_{br} - i_E i_{cr} + i_B i_{dr} + i_C i_{er} + i_A i_{fr}) \sin(\theta_1 + 9\alpha) \end{array} \right\} \quad (9.30)$$

$$T_{e2} = -P_2 M_2 \left\{ \begin{array}{l} (i_A i_{ar} + i_C i_{br} + i_B i_{cr} + i_E i_{dr} + i_D i_{er} + i_F i_{fr}) \sin \theta_2 + \\ (i_B i_{ar} + i_A i_{br} + i_C i_{cr} + i_F i_{dr} + i_E i_{er} + i_D i_{fr}) \sin(\theta_2 + 4\alpha) + \\ (i_C i_{ar} + i_B i_{br} + i_A i_{cr} + i_D i_{dr} + i_F i_{er} + i_E i_{fr}) \sin(\theta_2 + 8\alpha) + \\ (-i_D i_{ar} - i_F i_{br} - i_E i_{cr} + i_A i_{dr} + i_C i_{er} + i_B i_{fr}) \sin(\theta_2 + \alpha) + \\ (-i_E i_{ar} - i_D i_{br} - i_F i_{cr} + i_B i_{dr} + i_A i_{er} + i_C i_{fr}) \sin(\theta_2 + 5\alpha) + \\ (-i_F i_{ar} - i_E i_{br} - i_D i_{cr} + i_C i_{dr} + i_B i_{er} + i_A i_{fr}) \sin(\theta_2 + 9\alpha) \end{array} \right\} \quad (9.31)$$

9.5 Phase domain model of voltage fed series connected two-motor drive with a quasi six-phase machine and a two-phase machine

This section considers the phase domain model of the series connected quasi six-phase/two-phase multi-motor drive configuration shown in Fig. 9.4. Due to the series-connection of the two machines in the manner shown in Fig. 9.4 the following holds true:

$$\begin{array}{ll} v_A = v_{a1} + v_{a2} & v_B = v_{b1} + v_{a2} \\ v_C = v_{c1} + v_{a2} & v_D = v_{d1} + v_{b2} \\ v_E = v_{e1} + v_{b2} & v_F = v_{f1} + v_{b2} \end{array} \quad (9.32)$$

$$\begin{array}{ll} i_A = i_{a1} & i_B = i_{b1} \\ i_C = i_{c1} & i_D = i_{d1} \\ i_E = i_{e1} & i_F = i_{f1} \end{array} \quad (9.33a)$$

$$\begin{array}{l} i_{a2} = i_A + i_B + i_C \\ i_{b2} = i_D + i_B + i_F \end{array} \quad (9.33b)$$

Voltage equations for the complete system remain to be given in compact matrix form with equations (9.16)-(9.18). However the system is of the 14th order because the drive incorporates a quasi six-phase machine and a two-phase machine, therefore:

$$\begin{array}{l} \underline{i}_{r1} = [i_{ar1} \quad i_{br1} \quad i_{cr1} \quad i_{dr1} \quad i_{er1} \quad i_{fr1}]^T \\ \underline{i}_{r2} = [i_{ar2} \quad i_{br2}]^T \end{array} \quad (9.34)$$

The resistance and inductance matrices of (9.16) are governed once more by once more (9.29). The sub-matrices of (9.29) are six by six matrices for the quasi six-phase machine and remain equal to those given by equations (9.22a), (9.23), (9.24) and (9.27). Due to series-connection of the two machines the remaining sub-matrices of (9.29) are:

$$\begin{aligned} \underline{R}_{s2} &= \text{diag}(R_{s2} \ R_{s2} \ R_{s2} \ R_{s2} \ R_{s2} \ R_{s2}) \\ \underline{R}_{r2} &= \text{diag}(R_{r2} \ R_{r2}) \end{aligned} \quad (9.35)$$

$$\underline{L}_{s2} = \begin{bmatrix} L_{ls2} + M_2 & L_{ls2} + M_2 & L_{ls2} + M_2 & M_2 \cos 3\alpha & M_2 \cos 3\alpha & M_2 \cos 3\alpha \\ L_{ls2} + M_2 & L_{ls2} + M_2 & L_{ls2} + M_2 & M_2 \cos 3\alpha & M_2 \cos 3\alpha & M_2 \cos 3\alpha \\ L_{ls2} + M_2 & L_{ls2} + M_2 & L_{ls2} + M_2 & M_2 \cos 3\alpha & M_2 \cos 3\alpha & M_2 \cos 3\alpha \\ M_2 \cos 3\alpha & M_2 \cos 3\alpha & M_2 \cos 3\alpha & L_{ls2} + M_2 & L_{ls2} + M_2 & L_{ls2} + M_2 \\ M_2 \cos 3\alpha & M_2 \cos 3\alpha & M_2 \cos 3\alpha & L_{ls2} + M_2 & L_{ls2} + M_2 & L_{ls2} + M_2 \\ M_2 \cos 3\alpha & M_2 \cos 3\alpha & M_2 \cos 3\alpha & L_{ls2} + M_2 & L_{ls2} + M_2 & L_{ls2} + M_2 \end{bmatrix} \quad (9.36)$$

$$\underline{L}_{r2} = M_2 \begin{bmatrix} \cos(\theta_2) & -\sin(\theta_2) \\ \sin(\theta_2) & \cos(\theta_2) \end{bmatrix} \quad (9.37)$$

$$\underline{L}_{sr2} = M_2 \begin{bmatrix} \cos(\theta_2) & \cos(\theta_2) & \cos(\theta_2) & -\sin(\theta_2) & -\sin(\theta_2) & -\sin(\theta_2) \\ \sin(\theta_2) & \sin(\theta_2) & \sin(\theta_2) & \cos(\theta_2) & \cos(\theta_2) & \cos(\theta_2) \end{bmatrix}^T \quad (9.38)$$

$$\underline{L}_{rs2} = \underline{L}_{sr2}^T$$

The torque developed by the two-phase machine in terms of inverter currents is:

$$T_{e2} = -P_2 M_2 \left\{ \begin{aligned} &((i_A + i_B + i_C) i_{ar2} + (i_D + i_E + i_F) i_{br2}) \sin(\theta_2) \\ &((i_A + i_B + i_C) i_{br2} - (i_D + i_E + i_F) i_{ar2}) \cos(\theta_2) \end{aligned} \right\} \quad (9.39)$$

The equation (9.30) still describes the torque developed by the quasi six-phase machine.

9.6 Current control techniques

Current control may be performed in either stationary reference frame or the synchronous (rotating) reference frame. This section considers both types of current control methods with respect to the quasi six-phase multi-machine drive for both the two quasi six-phase motor drive and the quasi six-phase/two-phase motor drive. Current control in the rotating reference frame allows voltage drops created by the flow of non-torque/flux producing currents through the stator of each machine to cause a perturbation in the dynamic performance of the drive. Two different methods of compensating for the x-y voltage drops associated with the multi-phase multi-motor drive were presented in chapter 8 for symmetrical multi-phase machines. It was concluded that, the modified decoupling circuit method offered by far the simplest realisation of the two types of x-y voltage drop compensation considered. It is for this reason that only this method will be considered for the quasi six-phase configurations in this chapter.

9.6.1 Current control in the stationary reference frame

A standard method of achieving indirect rotor flux oriented control for operation in the base speed region, shown in Fig. 5.25 ($n = 6$ or $n = 2$), is considered. Individual phase current references of the two quasi six-phase machines are given with:

$$\begin{aligned}
 i_{a(1)}^* &= \sqrt{2/6}[i_{ds1}^* \cos \phi_{r1} - i_{qs1}^* \sin \phi_{r1}] \\
 i_{b(1)}^* &= \sqrt{2/6}[i_{ds1}^* \cos(\phi_{r1} - 4\alpha) - i_{qs1}^* \sin(\phi_{r1} - 4\alpha)] \\
 \text{-----} \\
 i_{f(1)}^* &= \sqrt{2/6}[i_{ds2}^* \cos(\phi_{r2} - 9\alpha) - i_{qs2}^* \sin(\phi_{r2} - 9\alpha)] \\
 & \hspace{15em} (9.40) \\
 i_{a(2)}^* &= \sqrt{2/6}[i_{ds2}^* \cos \phi_{r2} - i_{qs2}^* \sin \phi_{r2}] \\
 i_{b(2)}^* &= \sqrt{2/6}[i_{ds2}^* \cos(\phi_{r2} - 4\alpha) - i_{qs2}^* \sin(\phi_{r2} - 4\alpha)] \\
 \text{-----} \\
 i_{f(2)}^* &= \sqrt{2/6}[i_{ds2}^* \cos(\phi_{r2} - 9\alpha) - i_{qs2}^* \sin(\phi_{r2} - 9\alpha)]
 \end{aligned}$$

For the quasi six-phase/two-phase configuration individual phase current references are given with:

$$\begin{aligned}
 i_{a(6-phase)}^* &= \sqrt{2/6}[i_{ds1}^* \cos \phi_{r1} - i_{qs1}^* \sin \phi_{r1}] \\
 i_{b(6-phase)}^* &= \sqrt{2/6}[i_{ds1}^* \cos(\phi_{r1} - 4\alpha) - i_{qs1}^* \sin(\phi_{r1} - 4\alpha)] \\
 \text{-----} \\
 i_{f(6-phase)}^* &= \sqrt{2/6}[i_{ds1}^* \cos(\phi_{r1} - 9\alpha) - i_{qs1}^* \sin(\phi_{r1} - 9\alpha)] \\
 & \hspace{15em} (9.41) \\
 i_{a(2-phase)}^* &= [i_{ds2}^* \cos \phi_{r2} - i_{qs2}^* \sin \phi_{r2}] \\
 i_{b(2-phase)}^* &= [i_{ds2}^* \cos(\phi_{r2} - 3\alpha) - i_{qs2}^* \sin(\phi_{r2} - 3\alpha)]
 \end{aligned}$$

Phase current references are further summed according to the connection diagrams of Figs. 9.2 or 9.4 in order to yield the inverter current references of (9.7) or (9.11).

9.6.2 Current control in the synchronous reference frame

Individual vector control scheme for the two machines is in principal the same. The vector controller for each machine is similar to the scheme shown in Fig.8.1. for the five-phase machine. Machine phase voltage references are created for the two quasi six-phase motor drive using:

$$\begin{aligned}
 v_{a(1)}^* &= \sqrt{2/6}[v_{ds1}^* \cos \phi_{r1} - v_{qs1}^* \sin \phi_{r1}] \\
 v_{b(1)}^* &= \sqrt{2/6}[v_{ds1}^* \cos(\phi_{r1} - 4\alpha) - v_{qs1}^* \sin(\phi_{r1} - 4\alpha)] \\
 \text{-----} \\
 v_{f(1)}^* &= \sqrt{2/6}[v_{ds2}^* \cos(\phi_{r2} - 9\alpha) - v_{qs2}^* \sin(\phi_{r2} - 9\alpha)]
 \end{aligned} \tag{9.42}$$

$$\begin{aligned}
 v_{a(2)}^* &= \sqrt{2/6}[v_{ds2}^* \cos \phi_{r2} - v_{qs1}^* \sin \phi_{r2}] \\
 v_{b(2)}^* &= \sqrt{2/6}[v_{ds2}^* \cos(\phi_{r2} - 4\alpha) - v_{qs2}^* \sin(\phi_{r2} - 4\alpha)] \\
 \text{-----} \\
 v_{f(2)}^* &= \sqrt{2/6}[v_{ds2}^* \cos(\phi_{r2} - 9\alpha) - v_{qs2}^* \sin(\phi_{r2} - 9\alpha)]
 \end{aligned}$$

and for the quasi six-phase/two-phase drive using:

$$\begin{aligned}
 v_{a(1)}^* &= \sqrt{2/6}[v_{ds1}^* \cos \phi_{r1} - v_{qs1}^* \sin \phi_{r1}] \\
 v_{b(1)}^* &= \sqrt{2/6}[v_{ds1}^* \cos(\phi_{r1} - 4\alpha) - v_{qs1}^* \sin(\phi_{r1} - 4\alpha)] \\
 \text{-----} \\
 v_{f(1)}^* &= \sqrt{2/6}[v_{ds1}^* \cos(\phi_{r1} - 9\alpha) - v_{qs1}^* \sin(\phi_{r1} - 9\alpha)]
 \end{aligned} \tag{9.43}$$

$$\begin{aligned}
 v_{a(1)}^* &= [v_{ds2}^* \cos \phi_{r2} - v_{qs2}^* \sin \phi_{r2}] \\
 v_{b(1)}^* &= [v_{ds2}^* \cos(\phi_{r2} - 3\alpha) - v_{qs2}^* \sin(\phi_{r2} - 3\alpha)]
 \end{aligned}$$

The overall inverter phase voltage references for the two quasi six-phase machine configuration of Fig. 9.2 are obtained as:

$$\begin{aligned}
 v_A^* &= v_{a1}^* + v_{a2}^* & v_B^* &= v_{b1}^* + v_{c2}^* \\
 v_C^* &= v_{c1}^* + v_{b2}^* & v_D^* &= v_{d1}^* + v_{e2}^* \\
 v_E^* &= v_{e1}^* + v_{d2}^* & v_F^* &= v_{f1}^* + v_{f2}^*
 \end{aligned} \tag{9.44}$$

Similarly, for the quasi six-phase/two-phase scheme:

$$\begin{aligned}
 v_A^* &= v_{a1}^* + v_{a2}^* & v_B^* &= v_{b1}^* + v_{a2}^* \\
 v_C^* &= v_{c1}^* + v_{a2}^* & v_D^* &= v_{d1}^* + v_{b2}^* \\
 v_E^* &= v_{e1}^* + v_{b2}^* & v_F^* &= v_{f1}^* + v_{b2}^*
 \end{aligned} \tag{9.45}$$

It is shown in chapter 8 that a problem arises when current control is performed in the rotating reference frame, due to the flow of x-y currents through the stators of each machine. This is due to the voltage reference generation described above, which does not recognise in advance the existence of these additional voltage drops. The consequence is a degradation of the dynamic performance of the system, due to the appearance of unwanted transients in the rotor flux. However, a simple solution to the problem exists and it follows the same reasoning employed in chapter 8 in the case of

true (symmetrical) series-connected multi-phase motor drives. The solution involves a modified decoupling voltage calculation. Using analogy, for the two quasi six-phase machine configuration the decoupling voltages need to be calculated as:

$$\begin{aligned} e_{d1} &= -\omega_{r1}(\sigma_1 L_{s1} + L_{ls2})i_{qs1}^* & e_{d2} &= -\omega_{r2}(\sigma_2 L_{s2} + L_{ls1})i_{qs2}^* \\ e_{q1} &= \omega_{r1}\left(\left(L_{s1}/L_{m1}\right)\psi_{r1}^* + L_{ls2}i_{ds1}^*\right) & e_{q2} &= \omega_{r2}\left(\left(L_{s2}/L_{m2}\right)\psi_{r2}^* + L_{ls1}i_{ds2}^*\right) \end{aligned} \quad (9.46)$$

Similarly, for the quasi six-phase/two-phase scheme:

$$\begin{aligned} e_{d1} &= -\omega_{r1}\sigma_1 L_{s1}i_{qs1}^* & e_{d2} &= -\omega_{r2}(\sigma_2 L_{s2} + 1/3 L_{ls1})i_{qs2}^* \\ e_{q1} &= \omega_{r1}(L_{s1}/L_{m1})\psi_{r1}^* & e_{q2} &= \omega_{r2}\left(\left(L_{s2}/L_{m2}\right)\psi_{r2}^* + 1/3 L_{ls1}i_{ds2}^*\right) \end{aligned} \quad (9.47)$$

The decoupling voltage calculation for the quasi six-phase machine in (9.47) does not include the stator leakage reactance term of the two-phase machine. This is so since the torque/flux producing currents of the quasi six-phase machine cancel at the point of connection to the two-phase machine. Therefore no x-y currents flow through the stator of the two-phase machine and there are no x-y voltage drops. Coefficient 1/3 takes into account that only 33.3% of the two-phase machine current flows through any of the phases of the quasi six-phase machine.

9.7 Simulation verification

In order to verify the developed concepts, both configurations were simulated. Once more the PWM inverter is treated as ideal. Thus the inverter output phase currents equal the inverter phase current references for current control in the stationary reference frame, and inverter output phase voltages equal inverter phase voltage references for current control in the rotating reference frame. Speed mode of operation (PI speed control) is analysed, with torque limit of the two-phase machine set to twice the rated value (6.67 Nm) and to rated value for the quasi six-phase machine (10 Nm). Excitation is initiated first by applying forced excitation to both machines. Acceleration transient under no-load condition is studied next. Quasi six-phase machine IM1 is accelerated to the rated speed (299 rads/s elec.), while IM2 is accelerated to one half of the rated speed (149 rad/s elec.) for the configuration with two quasi six-phase machines. In the quasi six-phase/two-phase configuration IM2 (two-phase machine) is accelerated to 100 rad/s elec. Simulation results for the two quasi six-phase machine configuration with current control in the stationary reference frame are shown in Fig. 9.5, while the quasi six-

phase/two-phase configuration performance is illustrated in Fig. 9.6. As can be seen from Figs. 9.5a-c and 9.6a-c, completely decoupled control of each machine has been achieved, since changes in rotor flux or torque in one machine in no way affect the other

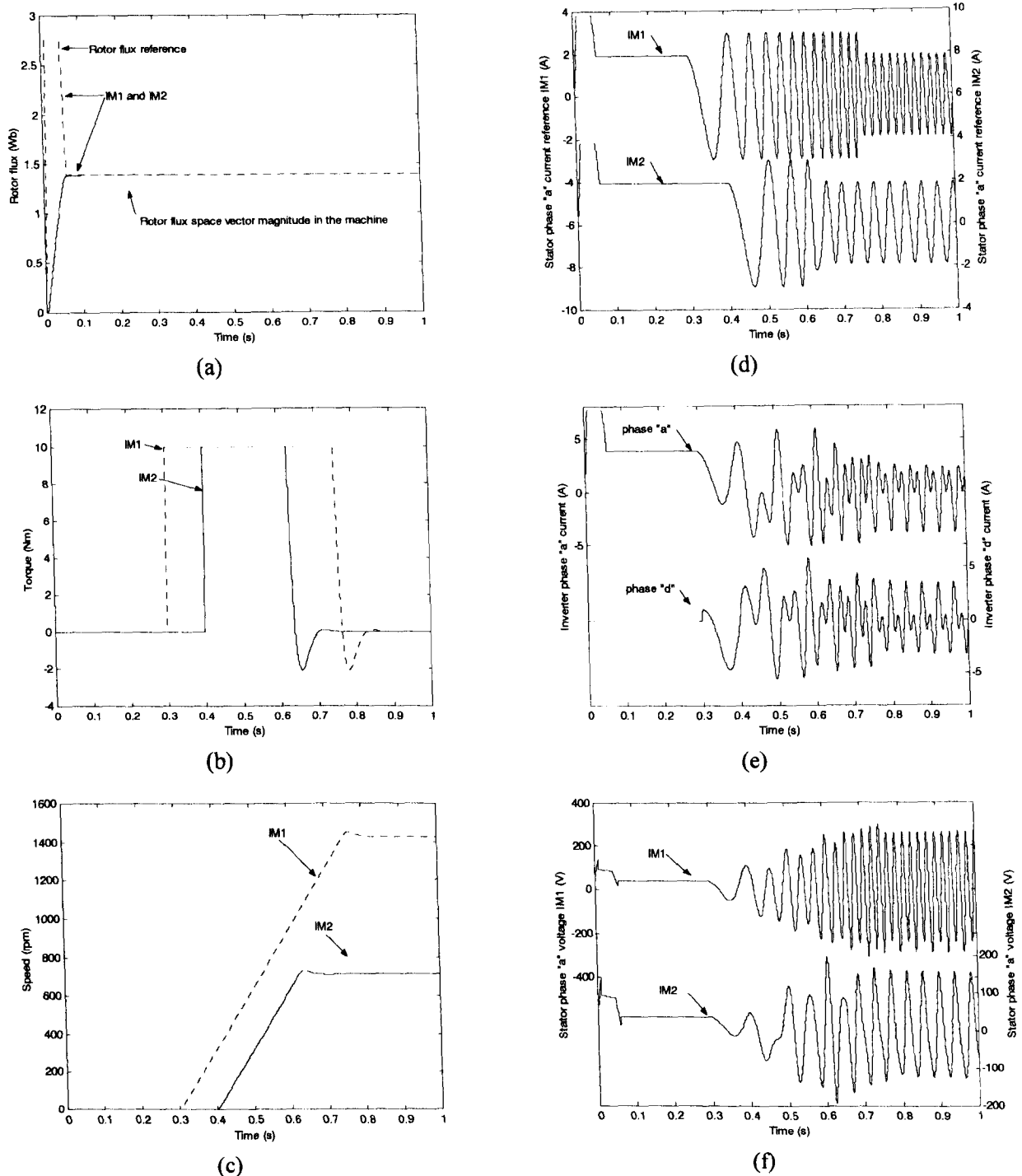


Fig. 9.5. Two quasi six-phase motors connected in series current control in the stationary reference frame: Rotor flux response (a), torque response (b), speed response (c), phase “a” current references (d), source phase “a” and “d” currents (e) and stator phase “a” voltage of each machine (f).

machine. Stator phase “a” current reference created by the vector controller of Fig. 3.1 for each machine is shown in Figs. 9.5d and 9.6b. Inverter current references for phases “a” and “d” (Figs. 9.5e and 9.6b) are highly distorted due to the summations described

by (9.3) and (9.11). Stator phase “a” voltages for each machine are obtained by reconstruction and are shown in Figs. 9.5f and 9.6b. In each case the voltage of the quasi six-phase machine exhibits a small level of distortion caused by the flow of x-y current components. However the two-phase machine is not affected by the series-connection because no x-y currents flow through the machine and so the steady-state stator voltages of the two-phase machine remain undistorted.

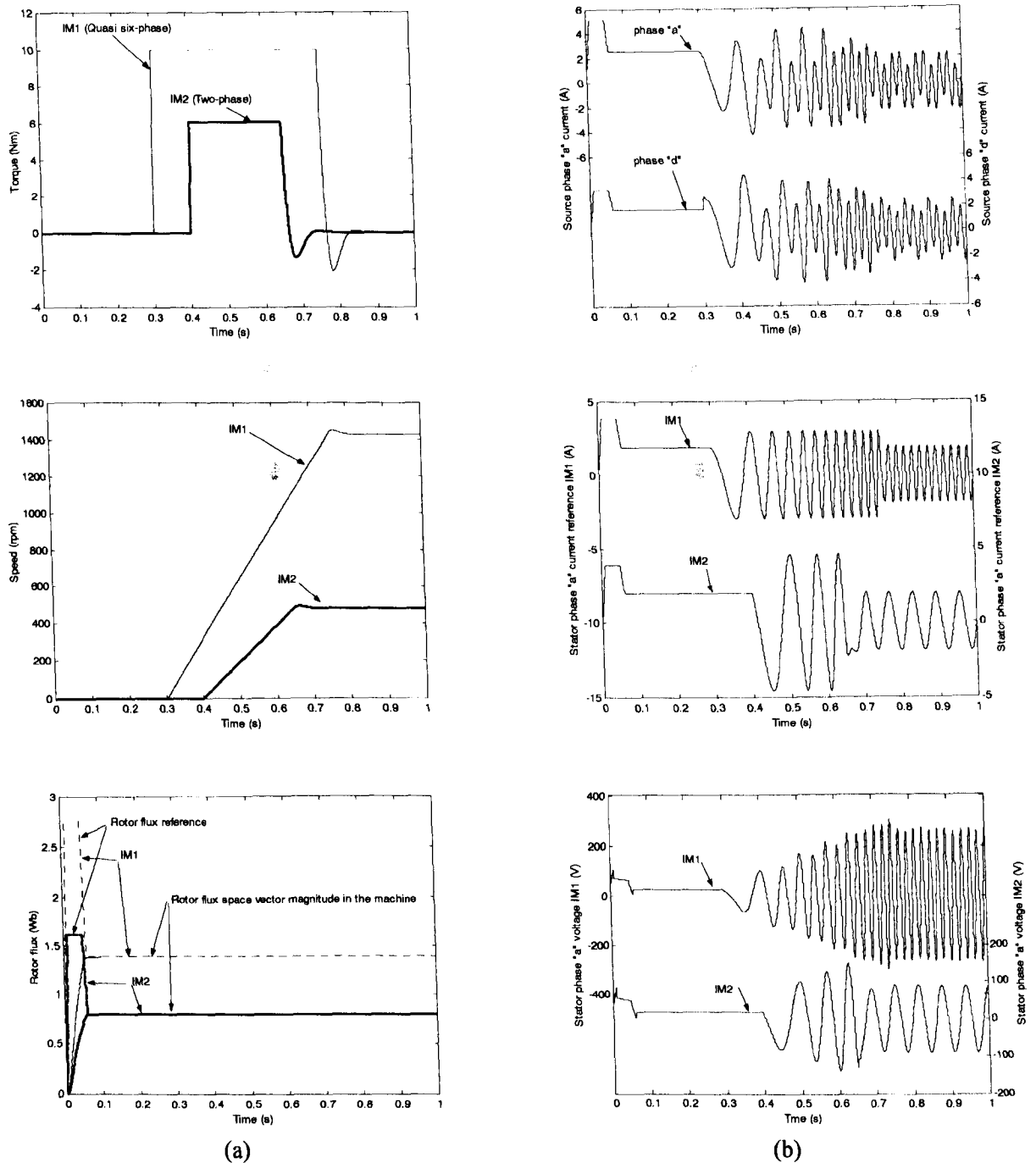


Fig. 9.6. Dynamics of the series-connected two-motor drive with a quasi six-phase machine and a two-phase machine, current control in the stationary reference frame: torque, speed and rotor flux response (a) and inverter phase “a, d” currents, stator phase “a” current references and stator phase “a” voltages (b).

Current control in the rotating reference frame is considered next. Figs. 9.7a and

9.7b show dynamic responses for the two quasi six-phase machine configuration and quasi six-phase/two-phase machine configuration, respectively. In principal torque and speed responses are very much the same as in Figs. 9.5a and 9.6a (and are therefore not shown), where current control in the stationary reference frame was used. Stator phase “a” voltage references, generated by the vector controller of each machine, are shown in

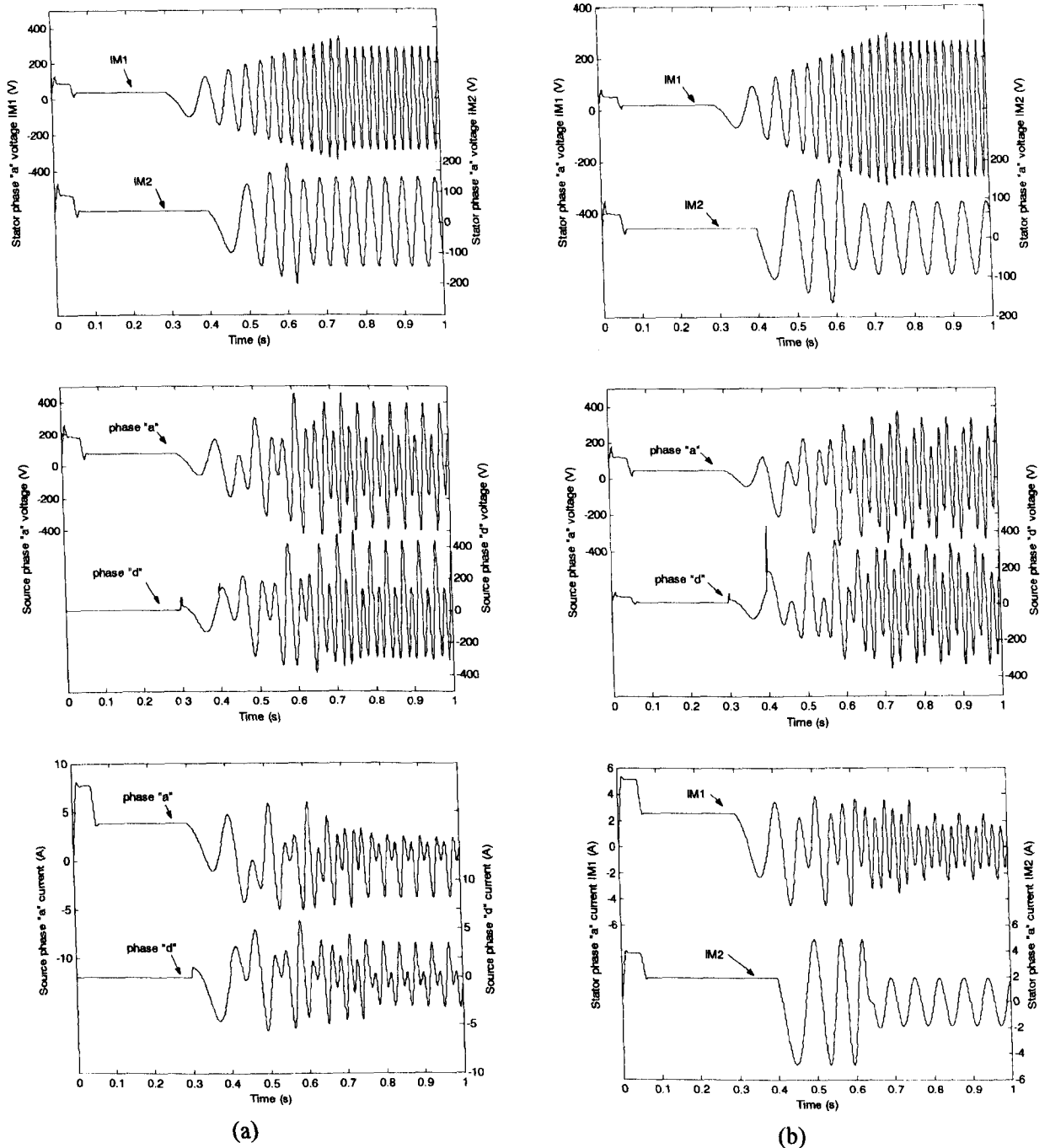


Fig. 9.7: Two quasi six-phase motor drive (a) and quasi six-phase/two-phase motor drive (b) behaviour, using current control in the rotating reference frame.

Figs. 9.7a and 9.7b and have a familiar waveform to that of a traditional three-phase vector controlled drive. Inverter phase “a” voltages are highly distorted as are the stator phase “a” currents references of the quasi six-phase machine due to the flow of x-y

currents. As expected, the two-phase machine stator phase “a” current is sinusoidal as this machine remains unaffected by the series-connection to the quasi six-phase machine.

9.8 Current cancellation

The nature of the quasi six-phase series connected multi-motor drive makes it possible for the phase current or voltage references (depending on the method of current control) generated by individual vector controllers to cancel when summed according to the phase transposition, in a similar manner to that shown in section 5.6 and 6.4 for symmetrical multi-phase multi-motor drives. The two configurations of the quasi six-phase multi-motor drive are considered in this section and it is shown both analytically and with the aid of simulation results that the performance of the proposed configurations is not affected by the phase current reference cancellation.

9.8.1 Two quasi six-phase machines configuration

This section considers cancellation of the phase current references in the configuration where two quasi six-phase machines are connected in series using the appropriate phase transposition (Fig. 9.2). In the example considered here both machines are given a speed command of 314 rad/s (which corresponds to a stator current frequency of 50 Hz). It is assumed that both machines are identical and operating under identical conditions. If a speed command is applied to the second machine (IM2) 10ms after the first machine and both machines accelerate to the commanded speed in an identical manner, then the steady-state inverter current references, generated according to (9.3), can be written for final steady-state as ($I_1 = I_2 = I$, $\omega_1 = \omega_2 = \omega_s$):

$$\begin{aligned}
 i_A^* &= 0 \\
 i_B^* &= \underline{\underline{\sqrt{2}I_1 \sin(\omega_1 t - 4\alpha)}} - \underline{\underline{\sqrt{2}I_2 \sin(\omega_2 t - 8\alpha)}} \\
 i_C^* &= \underline{\underline{\sqrt{2}I_1 \sin(\omega_1 t - 8\alpha)}} - \underline{\underline{\sqrt{2}I_2 \sin(\omega_2 t - 4\alpha)}} \\
 i_D^* &= \underline{\underline{\sqrt{2}I_1 \sin(\omega_1 t - \alpha)}} - \underline{\underline{\sqrt{2}I_2 \sin(\omega_2 t - 5\alpha)}} \\
 i_E^* &= \underline{\underline{\sqrt{2}I_1 \sin(\omega_1 t - 5\alpha)}} - \underline{\underline{\sqrt{2}I_2 \sin(\omega_2 t - \alpha)}} \\
 i_F^* &= 0
 \end{aligned} \tag{9.48}$$

Note that, in contrast to sections 5.6 and 6.4, here two inverter current references become zero. The spatial mmf distribution in the quasi six-phase machine is given by:

$$\begin{aligned}
 F_a &= Ni_A \cos(\varepsilon) \\
 F_b &= Ni_B \cos(\varepsilon - 4\alpha) \\
 F_c &= Ni_C \cos(\varepsilon - 8\alpha) \\
 F_d &= Ni_D \cos(\varepsilon - \alpha) \\
 F_e &= Ni_E \cos(\varepsilon - 5\alpha) \\
 F_f &= Ni_F \cos(\varepsilon - 9\alpha)
 \end{aligned} \tag{9.49}$$

Consider current references (single-underlined terms in equation (9.48)) created by the vector controller of machine 1. They produce in machine 1 mmfs of (9.50):

$$\begin{aligned}
 F_b &= 0.5\sqrt{2}NI_1 (\sin(\omega_1 t + \varepsilon - 8\alpha) + \sin(\omega_1 t - \varepsilon_f)) \\
 F_c &= 0.5\sqrt{2}NI_1 (\sin(\omega_1 t + \varepsilon - 16\alpha) + \sin(\omega_1 t - \varepsilon)) \\
 F_d &= 0.5\sqrt{2}NI_1 (\sin(\omega_1 t + \varepsilon - 2\alpha) + \sin(\omega_1 t - \varepsilon)) \\
 F_e &= 0.5\sqrt{2}NI_1 (\sin(\omega_1 t + \varepsilon - 10\alpha) + \sin(\omega_1 t - \varepsilon))
 \end{aligned} \tag{9.50}$$

Therefore the total mmf produced in machine 1 by the current components belonging to machine 1 is:

$$2\sqrt{2}NI_1 \sin(\omega_1 t - \varepsilon) \tag{9.51}$$

Consider current references (double-underlined terms in equation (9.48)), created by the vector controller of machine 2. These currents produce in machine 1:

$$\begin{aligned}
 F_b &= -0.5\sqrt{2}NI_2 (\sin(\omega_2 t + \varepsilon - 12\alpha) + \sin(\omega_2 t - \varepsilon - 4\alpha)) \\
 F_c &= -0.5\sqrt{2}NI_2 (\sin(\omega_2 t + \varepsilon - 12\alpha) + \sin(\omega_2 t - \varepsilon + 4\alpha)) \\
 F_d &= -0.5\sqrt{2}NI_2 (\sin(\omega_2 t + \varepsilon - 6\alpha) + \sin(\omega_2 t - \varepsilon - 4\alpha)) \\
 F_e &= -0.5\sqrt{2}NI_2 (\sin(\omega_2 t + \varepsilon - 6\alpha) + \sin(\omega_2 t - \varepsilon + 4\alpha))
 \end{aligned} \tag{9.52}$$

Therefore the total mmf produced in machine 1 by the current components belonging to machine 2 is:

$$N\sqrt{2}I_2 \sin(\omega_2 t - \varepsilon) \tag{9.53}$$

As mentioned previously both machines are identical and therefore have phase current references of identical magnitudes and frequencies. Thus (9.51) and (9.53) sum to give the total mmf generated in machine 1 as:

$$3\sqrt{2}NI \sin(\omega_s t - \varepsilon) \quad (9.54)$$

This is what one would expect to see in a six-phase machine operating under normal conditions. Thus the performance of the machine is not affected by the phase current reference cancellation. In effect, the remaining stator current references generated by the vector controller of each machine reinforce each other in the air gap and maintain the rotating mmf normally found in quasi six-phase machines. However the currents in the remaining phases will increase in order to deliver the required power to the machine. The same logic can be applied to machine 2 and the same conclusion can be drawn.

A simulation is performed in order to verify that the machines will perform as expected if inverter phase current cancellation occurs. The torque generated by the machines is limited to 10Nm (rated value). Both machines are magnetised as in section 9.7. Next a speed command of 314 rad/s is applied to machine 1 and 0.01 seconds later to machine 2. Torque, speed and rotor flux response (Fig. 9.8) show that the dynamic performance of the machines is not affected and that the rotor flux remains undisturbed by the cancellation of the inverter current references. The cancellation of the inverter phase “a” and “f” current references can clearly be seen in Figs. 9.8d-e. Stator phase “a” current references created by the vector controller of each machine can be seen in Fig. 9.8f. These current references eventually sum to zero as shown in Fig 9.8d.

9.8.2 Two quasi six-phase machines alternative configuration

This section considers cancellation of the phase current references in the configuration where two quasi six-phase machines are connected in series using the alternative phase transposition shown in Fig. 9.3. In the example considered here both machines are again given a speed command of 314 rad/s. The machines are identical and operate under identical conditions. If a speed command is applied to the second machine (IM2) 1.67ms after the first machine and both machines accelerate to the commanded speed in an identical manner, then the steady-state inverter current references generated according to (9.7) can be written as ($I_1 = I_2 = I$, $\omega_1 = \omega_2 = \omega_s$):

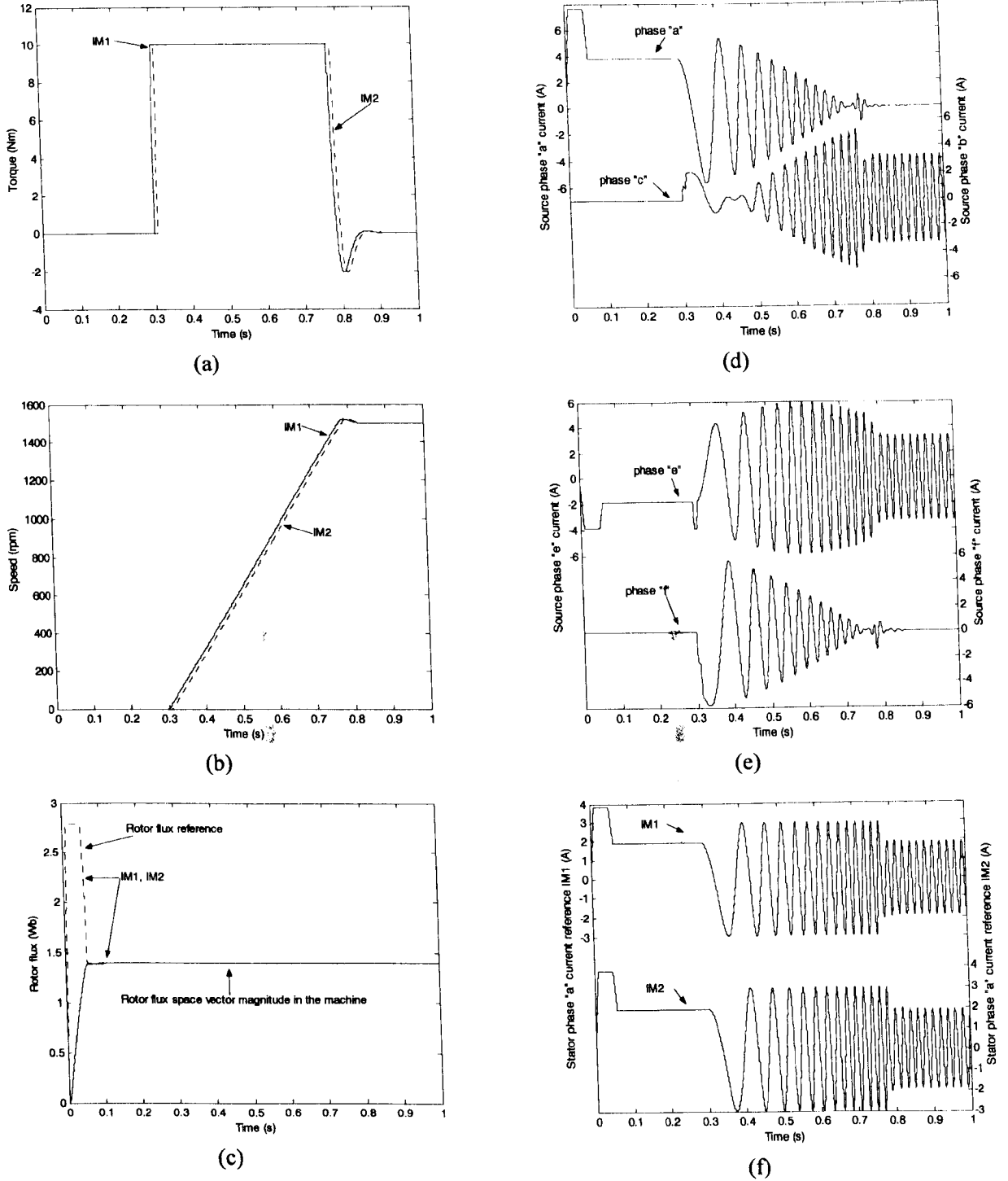


Fig. 9.8: Two quasi six-phase induction machines connected in series with phase transposition (current control in the stationary reference frame). Torque (a), speed (b), and rotor flux (c) developed by each machine. Source phase “a-c” (d), “e-f” (e) currents and stator phase “a” current references for each machine (f).

$$\begin{aligned}
 i_A^* &= \sqrt{2}I_1 \sin(\omega_1 t) + \sqrt{2}I_2 \sin(\omega_2 t - 6\alpha) \\
 i_B^* &= \sqrt{2}I_1 \sin(\omega_1 t - 4\alpha) + \sqrt{2}I_2 \sin(\omega_2 t - 10\alpha) \\
 i_C^* &= \sqrt{2}I_1 \sin(\omega_1 t - 8\alpha) + \sqrt{2}I_2 \sin(\omega_2 t - 2\alpha) \\
 i_D^* &= \sqrt{2}I_1 \sin(\omega_1 t - \alpha) + \sqrt{2}I_2 \sin(\omega_2 t - \alpha) \\
 i_E^* &= \sqrt{2}I_1 \sin(\omega_1 t - 5\alpha) + \sqrt{2}I_2 \sin(\omega_2 t - 5\alpha) \\
 i_F^* &= \sqrt{2}I_1 \sin(\omega_1 t - 9\alpha) + \sqrt{2}I_2 \sin(\omega_2 t - 9\alpha)
 \end{aligned} \tag{9.55}$$

This can be written as:

$$\begin{aligned}
 i_A^* &= 0 \\
 i_B^* &= 0 \\
 i_C^* &= 0 \\
 i_D^* &= 2 * \sqrt{2} I \sin(\omega_s t - \alpha) \\
 i_E^* &= 2 * \sqrt{2} I \sin(\omega_s t - 5\alpha) \\
 i_F^* &= 2 * \sqrt{2} I \sin(\omega_s t - 9\alpha)
 \end{aligned} \tag{9.56}$$

In this situation current cancellation takes place in all three phases of one of the two three-phase windings. Close inspection of (9.56) reveals that both quasi six-phase machines will now run as equivalent three-phase machines. Twice as much current will flow through the remaining phases in order to develop the same torque. Simulation results presented in Fig 9.9 show the performance of the two quasi six-phase machines in terms of torque, speed and rotor flux response. The response is identical to those one would see under normal operating conditions. Figs. 9.9e-f show the inverter current references generated by the summation given in (9.7), where it can be seen that phase “a” to “c” source currents become zero in steady-state.

9.8.3 Quasi six-phase/two-phase configuration

This section considers the response of the configuration consisting of a quasi six-phase machine and a two-phase machine (Fig. 9.4) when inverter phase “a” current reference becomes zero. It is assumed that both machines have steady-state reference currents of exactly the same frequency while $I_2 = 3I_1$. If both machines are given a speed command of 314 rad/s with 0.01 seconds between speed command application, then inverter current references are given by: ($I_1 = I$, $I_2 = 3I_1$, $\omega_1 = \omega_2 = \omega_s$):

$$\begin{aligned}
 i_A^* &= 0 \\
 i_B^* &= \sqrt{2} I \sin(\omega_1 t - 4\alpha) - \sqrt{2} I \sin(\omega_2 t) \\
 i_C^* &= \sqrt{2} I \sin(\omega_1 t - 8\alpha) - \sqrt{2} I \sin(\omega_2 t) \\
 i_D^* &= \sqrt{2} I \sin(\omega_1 t - \alpha) - \sqrt{2} I \sin(\omega_2 t - 3\alpha) \\
 i_E^* &= \sqrt{2} I \sin(\omega_1 t - 5\alpha) - \sqrt{2} I \sin(\omega_2 t - 3\alpha) \\
 i_F^* &= \sqrt{2} I \sin(\omega_1 t - 9\alpha) - \sqrt{2} I \sin(\omega_2 t - 3\alpha)
 \end{aligned} \tag{9.57}$$

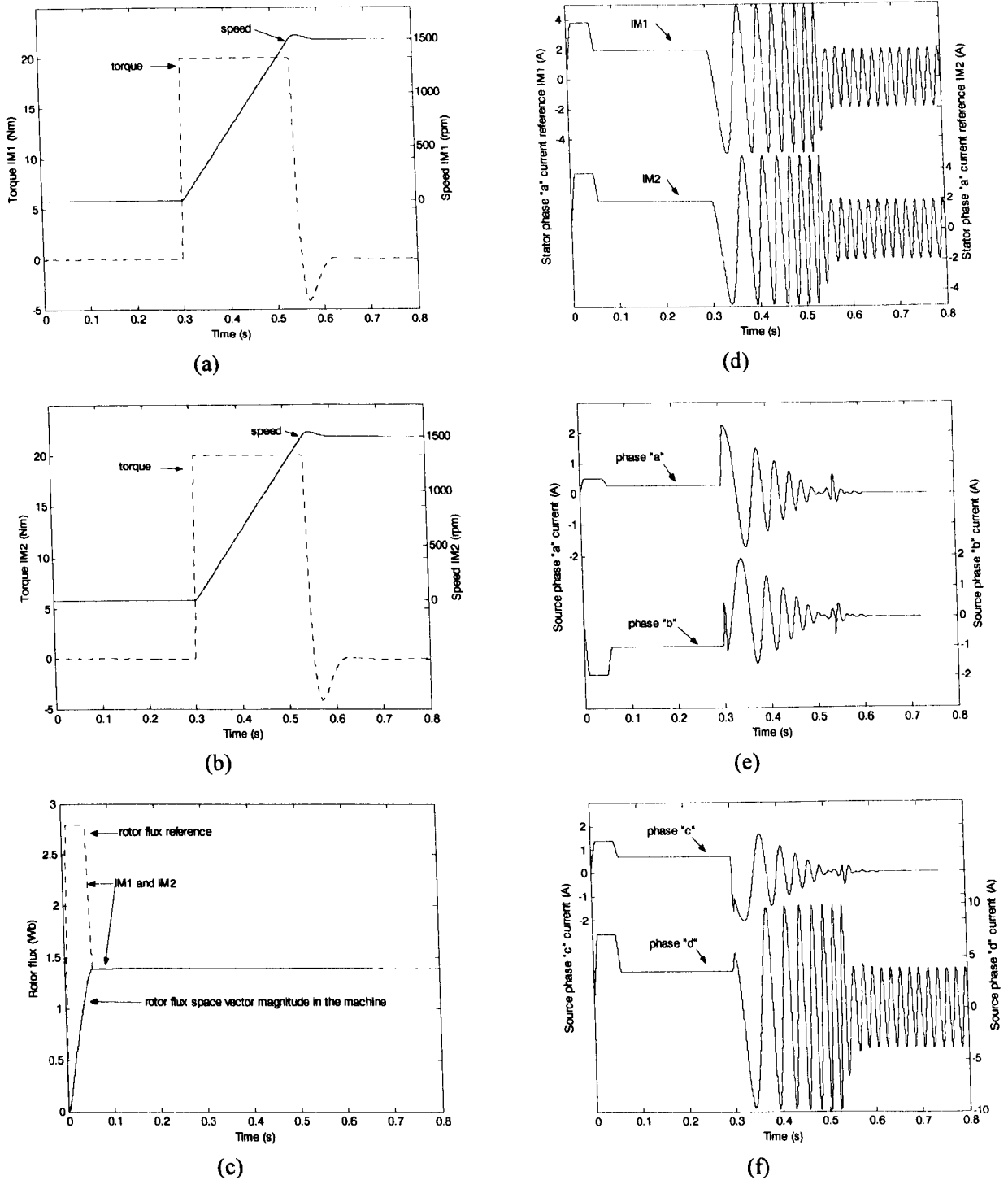


Fig. 9.9: Two quasi six-phase induction machines connected in series with phase transposition (current control in the stationary reference frame: Torque (a), speed (b), and rotor flux (c) developed by each machine. Stator phase “a” current references for each machine (d) and source phase “a-c” (e), “e-f” (f) currents.

Consider current references (single-underlined terms in equation (9.57)) created by the vector controller of machine 1. These currents cause in machine 1 the following mmfs:

$$\begin{aligned}
 F_b &= 0.5\sqrt{2}NI(\sin(\omega_1 t + \varepsilon - 8\alpha) + \sin(\omega_1 t - \varepsilon)) \\
 F_c^b &= 0.5\sqrt{2}NI(\sin(\omega_1 t + \varepsilon - 16\alpha) + \sin(\omega_1 t - \varepsilon)) \\
 F_d &= 0.5\sqrt{2}NI(\sin(\omega_1 t + \varepsilon - 2\alpha) + \sin(\omega_1 t - \varepsilon)) \\
 F_e &= 0.5\sqrt{2}NI(\sin(\omega_1 t + \varepsilon - 10\alpha) + \sin(\omega_1 t - \varepsilon)) \\
 F_f &= 0.5\sqrt{2}NI(\sin(\omega_1 t + \varepsilon - 18\alpha) + \sin(\omega_1 t - \varepsilon))
 \end{aligned} \tag{9.58}$$

Therefore the total mmf produced in machine 1 by the current components belonging to machine 1 is:

$$2.5\sqrt{2}NI \sin(\omega_1 t - \varepsilon) - 0.5NI \sin(\omega_1 t + \varepsilon) \tag{9.59}$$

Consider current references (double-underlined terms in equation 9.57) created by the vector controller of machine 2. These currents cause in machine 1:

$$\begin{aligned}
 F_b &= -0.5\sqrt{2}NI(\sin(\omega_2 t + \varepsilon - 4\alpha) + \sin(\omega_2 t - \varepsilon + 4\alpha)) \\
 F_c &= -0.5\sqrt{2}NI(\sin(\omega_2 t + \varepsilon - 8\alpha) + \sin(\omega_2 t - \varepsilon + 8\alpha)) \\
 F_d &= -0.5\sqrt{2}NI(\sin(\omega_2 t + \varepsilon - 4\alpha) + \sin(\omega_2 t - \varepsilon + 2\alpha)) \\
 F_e &= -0.5\sqrt{2}NI(\sin(\omega_2 t + \varepsilon - 8\alpha) + \sin(\omega_2 t - \varepsilon + 2\alpha)) \\
 F_f &= -0.5\sqrt{2}NI(\sin(\omega_2 t + \varepsilon - 12\alpha) + \sin(\omega_2 t - \varepsilon + 6\alpha))
 \end{aligned} \tag{9.60}$$

Therefore the total mmf produced in machine 1 by the current components belonging to machine 2 is:

$$0.5\sqrt{2}NI \sin(\omega_2 t - \varepsilon) + 0.5NI \sin(\omega_2 t + \varepsilon) \tag{9.61}$$

Equations (9.59) and (9.61) sum to give the total mmf generated in machine 1 as:

$$3\sqrt{2}NI \sin(\omega_s t - \varepsilon) \tag{9.62}$$

Thus the required revolving field is maintained in the quasi six-phase machine, because the phase currents of two machines create rotating fields which reinforce each other in the air gap of the quasi six-phase machine. The two-phase machine is supplied in this case with:

$$\begin{aligned}
 i_{a2}^* &= 3\sqrt{2}I \sin(\omega_s t) \\
 i_{a2}^* &= 3\sqrt{2}I \sin(\omega_s t + 3\alpha)
 \end{aligned} \tag{9.63}$$

Thus the two-phase machine will also operate as normal.

9.9 Summary

This chapter has considered the situation when a quasi six-phase machine is utilised in the series connected multi-phase multi-machine drive. It has been shown that the quasi six-phase machine configuration enables independent control of two quasi six-phase machines connected in series or series-connection of a quasi six-phase machine and a two-phase machine. Two possible configurations exist for the case when two quasi six-phase machines are connected in series. The first configuration involves interfacing of “a”, “b”, “c” three-phase windings of the two machines and interfacing of “d”, “e”, “f” three phase windings, whereas the alternative configuration involves connection of “a”, “b”, “c” windings of one machine with “d”, “e”, “f” windings of the other machine. In both configurations the two star points are isolated. This contrasts with quasi six-phase/two-phase configuration where there is a single star point and the neutral conductor has to be utilised.

Simulation studies are presented for the two quasi six-phase machine configuration and the quasi six-phase/two-phase configuration with current control performed in the stationary reference frame and the rotating reference frame. Inverter current reference cancellation is considered and it is shown both by simulation and analytically that the performance of is not affected in terms of speed, torque, and flux response.

CHAPTER 10

EXPERIMENTAL INVESTIGATION

10.1 Introduction

This chapter contains an extract of the experiments conducted within the research project. The chapter begins with a description of a laboratory rig designed on the basis of four commercially available three-phase inverters. The mains inputs of the diode bridge rectifiers and the DC links are paralleled and the rig can therefore be used for any supply phase numbers from five to twelve. For the purposes of the work undertaken in this chapter two three-phase inverters are configured as a six-phase supply.

An experimental investigation into the dynamic performance of a symmetrical six-phase induction machine under rotor flux oriented control is undertaken at first. Acceleration, deceleration and reversing performance of the drive is investigated and the corresponding results are presented. Behaviour of the drive for application of step loading and un-loading is also tested.

Once testing of the single six-phase machine is completed, performance of a six-phase two-motor drive consisting of the same six-phase induction machine and a three-phase induction machine connected in series is investigated experimentally. Acceleration, deceleration and reversing performance of each motor is investigated, while the other motor is held at a constant speed. Disturbance rejection capability during step loading and un-loading is also tested. These experiments are done in order to prove the existence of completely decoupled control between the two machines. The six-phase machine is operated under similar conditions in both the single motor drive and two-motor drive experiments. This enables a comparison to be made between its performance as a single drive and as part of the two-motor drive.

Next, a two-motor drive, comprising a symmetrical six-phase induction machine and a three-phase PMSM, connected in series, is experimentally investigated in order to prove that the concept is independent of the type of AC machine employed.

Finally, steady-state current waveforms and spectra are presented for the single six-phase motor drive. In order to allow a comparison, steady-state voltage and current

waveforms, along with their corresponding spectra, are also presented for the two-motor drive, consisting of two induction machines. Various results presented in this chapter can be found in Jones et al (2004a), Jones et al (2004c), and Levi et al (2004d).

10.2 Description of the experimental rig

A six-phase inverter is constructed using two commercially available industrial, MOOG DS2000, drives as shown schematically in Fig. 10.1. The two drives are a part of the twelve-phase rig, obtained by using four three-phase inverters (Fig. 10.2). Only the left-hand half of the complete power electronic system of Fig. 10.2 is used for the work described in this chapter. Each drive comprises a 6-pack IGBT bridge (three-phase inverter) and 3-phase diode rectifier with its own DC link circuit. The power connections of the DC-bus ('+AT' for the positive rail and '-AT' for the negative rail) are connected so that the DC-links of the inverters are in parallel. This results in an inverter with a total of 12 IGBT power switches and six output phases. The first three-phase inverter supplies phases A, C and E, while the second inverter supplies phases B, D and F. Each DS2000 has an internal dynamic braking IGBT and control circuit, which allows the excessive DC voltage that occurs during braking to be suppressed by an external braking resistor.

The purpose of the six-phase inverter is to control the phase currents and it behaves as a current source. The current-controlled VSI operates at 10 kHz switching frequency. Each inverter phase has a dedicated HALL-effect sensor (LEM) for measuring the output phase current. For this purpose, an additional LEM sensor has been added to each DS2000 drive (the reason is that a standard DS2000 drive is aimed for a three-phase servomotor and is therefore equipped with only two current sensors). Hence all the six phase currents are measured and made controllable. The measured inverter currents are sampled in such a way as to filter out the PWM current ripple. A total of 2^n equidistant samples of the current are taken and averaged in each switching period. By doing so, the over-sampled values are FIR filtered. Each inverter has its own DSP (TM320F240), which performs closed loop current control in the stationary reference frame. Current control is performed using digital form of the ramp comparison PWM, with PI controllers in the most basic form [Brod and Novotny (1985)]. The structure of the current controller used in the first three-phase inverter is shown in Fig. 10.3. If current control is performed in the manner shown in figure 10.3,

the current error cannot be driven to zero. Not even the integral action within the controller can achieve this goal as the reference phase currents are exhibiting sinusoidal changes even in steady-state. This results in steady-state amplitude and phase errors, which vary as function of the operating frequency [Nagase et al (1984)]. Hence the problem of deviation of the actual motor phase current with respect to its reference will be experienced at higher operating frequencies [Brod and Novotny (1985)]. Several solutions to this problem have been put forward in the literature. These include varying the gain of the current controller in proportion to the fundamental frequency [Nagase et

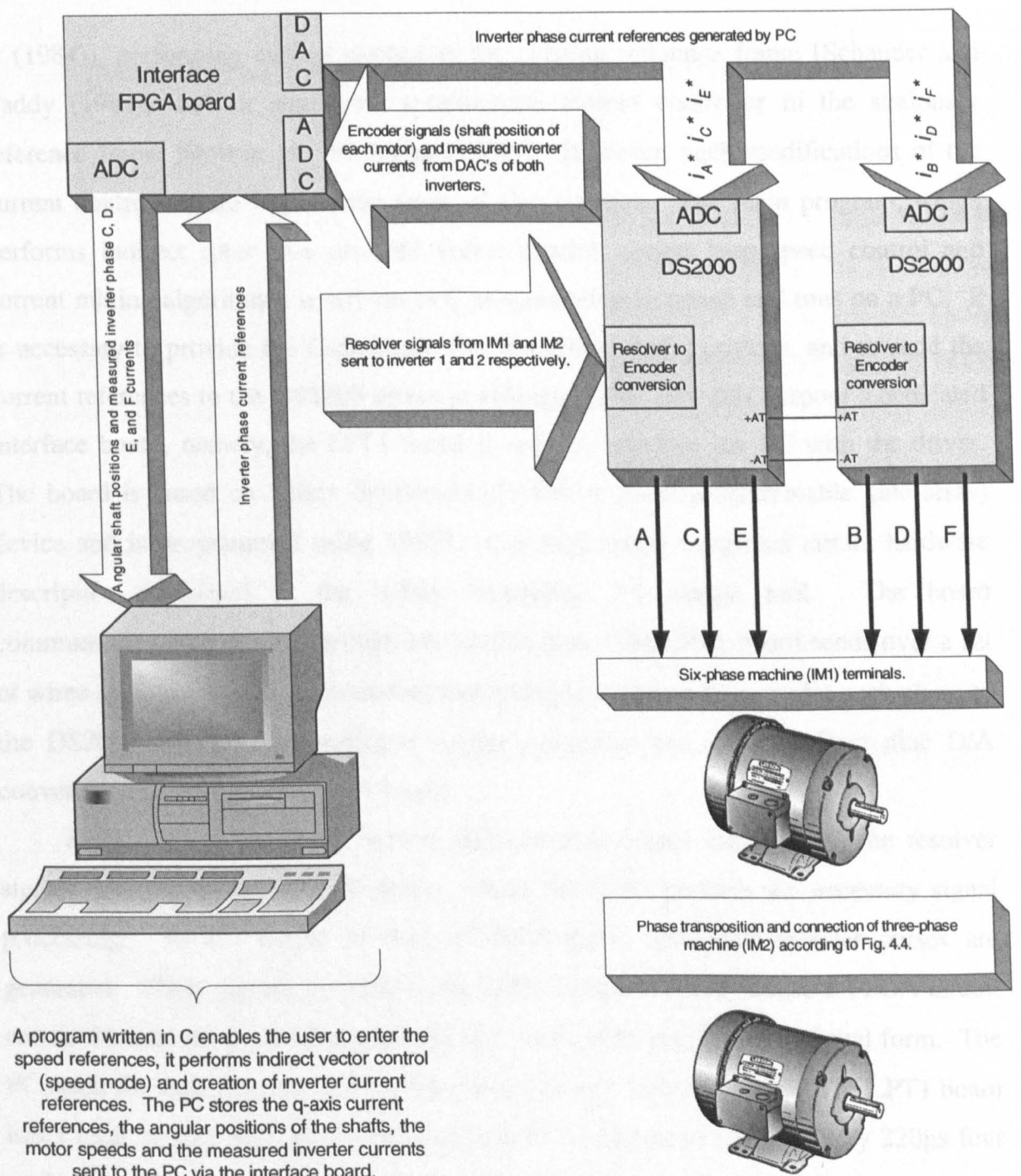


Fig. 10.1: Six-phase experimental rig.

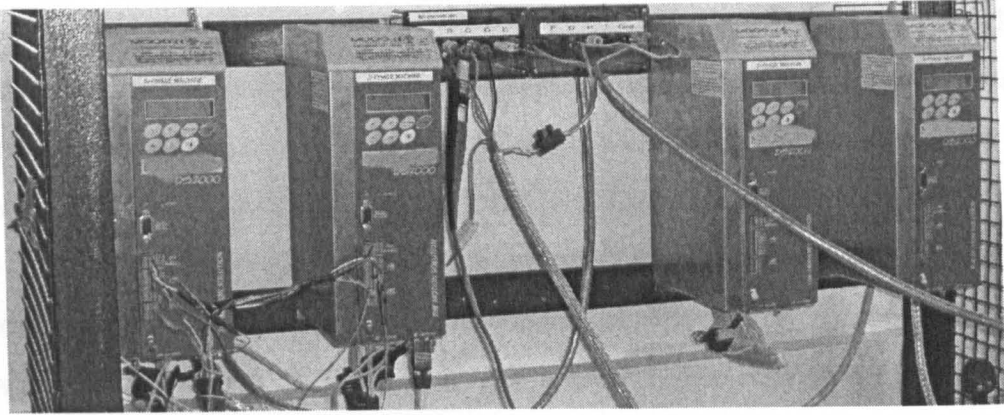


Fig. 10.2: Experimental 12-phase rig, capable of driving up to four series-connected motors in sensed mode (up to five if at least one machine operates in speed sensorless mode).

al (1984)], performing current control in the rotating reference frame [Schauder and Caddy (1982)] and an equivalent synchronous current controller in the stationary reference frame [Rowan and Kerkman (1986)]. However, such modifications of the current controllers are beyond the scope of this research. The main program, which performs indirect rotor flux oriented vector control, closed loop speed control and current mixing algorithms, is written in C programming language and runs on a PC. It is necessary to provide the C-program with the motor shaft positions, and to send the current references to the DS2000 drives in analogue form. For this purpose a dedicated interface board, namely, the LPT1 board is used to interface the PC with the drives. The board is based on Xilinx Spartan-family FPGA (field programmable gate array) device and is programmed using VHDL (very high speed integrated circuit hardware description language) in the Xilinx foundation 3.1 design tool. The board communicates with the PC through the parallel port. The LPT1 board sends over a set of wires analogue signals, representing the analogue current references for each phase to the DS2000 drives. The analogue current references are obtained from nine D/A converters, mounted on the LPT1 board.

Each motor is equipped with a shaft position sensor (resolver). The resolver signals are sent to the DS2000 drives, where the DSPs perform the necessary signal processing. At the output of each DS2000 drive, simulated encoder pulses are generated. These signals are sent to the LPT1 interface board, where a FPGA circuit counts the encoder pulses and generates the motor shaft position in a digital form. The PC reads the shaft position and provides the necessary control actions. The LPT1 board has a total of four A/D inputs, which are used for data acquisition. Every 220 μ s four analogue inputs are sampled. These A/D inputs are used to record the measured

inverter phase currents, C, D, E and F and send them to the PC through the parallel port, where they are stored along with the rotor speeds, q-axis current references and d-q transformation angles.

At the end of each experimental run the data stored on the PC is processed using a Matlab m-file. This allows plotting of inverter current references, motor current references, actual inverter currents (phases B, C, E, F), q-axis current references and motor speeds.

10.3 Details of the motors used in the experiments

The symmetrical six-phase motor with 60 degrees spatial displacement between any two consecutive phases was obtained by rewinding a commercially available three-phase induction machine (Sever 1ZK100-8). The original three-phase induction machine was 8-pole, 0.75 kW, 50 Hz, 220 V (phase to neutral) with a rated speed of 675 rpm. The six-phase induction machine is 6-pole, 1.1 kW, 50 Hz, 110 V (phase to neutral) with a rated speed of 900 rpm. Details of the six-phase winding can be found in Appendix B. The three-phase induction machine used in the experiments is a commercially available servo-motor MOOG FAS Y-090-V-030, which is 4-pole, 1 kW, 100 Hz, 187 V (phase to neutral) with the rated synchronous speed of 3000 rpm when used with a 8/22 DS2000 drive.

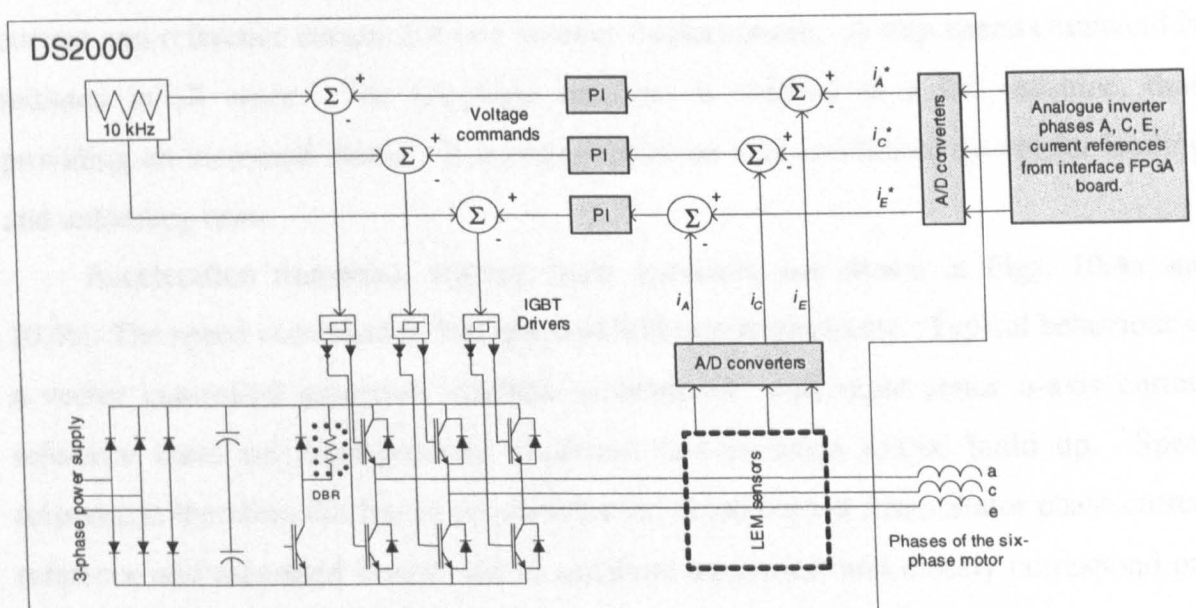


Fig. 10.3: Current controller structure, for the first three-phase inverter.

The three-phase PMSM used in the experiments is a commercially available MOOG servo-motor FAE N7-V4-030, which is 6-pole, 1.1 kW, 150Hz, 216 V (phase to neutral) with the rated speed of 3000 rpm. Detailed data for both three-phase machines can be found in Appendix A. A permanent magnet DC motor is used as a DC generator, in order to provide a load to the machine under investigation. The DC motor is rated at 1.5 kW when the form factor is 1.05 and the maximum armature current is 9 A. It is rated at 1.1 kW when the form factor is 1.4 and the maximum armature current is 7 A. The rated armature DC voltage of the motor is 180V, and the rated speed is 1800 rpm. A resistor bank is connected to the armature terminals of the DC motor for loading purpose. The load resistance is set depending on the operating speed of the driving motor.

10.4 Transient performance of a symmetrical six-phase induction motor

A series of experimental tests are performed in order to examine the dynamic performance of the true six-phase induction motor operating under indirect rotor flux oriented control. The drive is operated in the base speed region (constant flux) with constant stator d-axis current reference. The six-phase motor is fitted with a resolver and operates in sensed mode. The results of the experimental study are illustrated for all transients by displaying the speed response, stator q-axis current reference, actual current and reference current for one inverter (stator) phase. A step speed command is initiated in all cases. The six-phase machine is coupled to a DC machine, thus providing an increased inertia. It operates under no-load conditions except for loading and unloading tests.

Acceleration transients, starting from standstill, are shown in Figs. 10.4a and 10.4b. The speed command is 500 rpm and 600 rpm respectively. Typical behaviour of a vector controlled induction machine is observed, with rapid stator q-axis current reference build up corresponding to almost instantaneous torque build up. Speed response is therefore the fastest possible for the given current limit. Stator phase current reference and measured current are in excellent agreement and closely correspond one to the other in final steady-state.

The second test is a deceleration transient illustrated in Figs 10.4c and 10.4d. The machine is decelerated from -800 rpm (40Hz) and -500 rpm, respectively, down to zero

speed. The same quality of performance as for the acceleration transient is obtained. However, at -800 rpm there is some discrepancy between the inverter current reference and the actual current. This is a consequence of the applied simplest method of digital ramp comparison current control [Brod and Novotny (1985)].

Next, reversing performance of the drive is investigated. Transition from -300 rpm to 300 rpm is illustrated in Fig. 10.5a, while Fig. 10.5b shows speed reversal from 500 rpm to -500 rpm. Prolonged operation in the stator current limit results in both cases, leading to rapid change of direction of rotation. Measured phase current and reference phase current are in excellent agreement. It is important to note that the actual current in all steady-states at non-zero frequency contains essentially only the fundamental harmonic (PWM ripple is filtered out using FIR filters). Low order harmonics practically do not appear in the actual current. Therefore, problems caused by low order harmonics of the order $6n\pm 1$ ($n = 1, 3, 5, \dots$), reported in Gopakumar et al (1993) and Mohapatra et al (2003), are successfully eliminated by the current control method applied here. Finally, the drive behaviour during step loading and step unloading is illustrated in Figs 10.5c and 10.5d respectively. Fig. 10.5c applies to step loading (40% of the rated) at 300 rpm, while step unloading (51% of the rated) in Fig. 10.5d takes place at 500 rpm. It can be seen that the drive disturbance rejection capability is excellent and commensurate with expected performance of a vector controlled drive.

Presented experimental results indicate existence of a certain ripple in the stator q-axis current (caused by slight fluctuation of the rotor speed), in addition to the measurement noise, observable at medium and higher speeds of rotation. It has been established by an experiment that the six-phase machine used in this work is characterised with a certain level of asymmetry between phases. The two neutral points were disconnected and the two three-phase windings (as, cs, es and ds, fs, bs) were supplied with the same set of three-phase currents. In an ideal symmetrical six-phase machine this would produce zero net air-gap flux and zero torque and the machine would stay at standstill. However, the machine did rotate, indicating the existence of some parasitic torque caused by a certain level of asymmetry between the phases. This is believed to be the cause of the ripples, which can be eliminated by a better machine design.

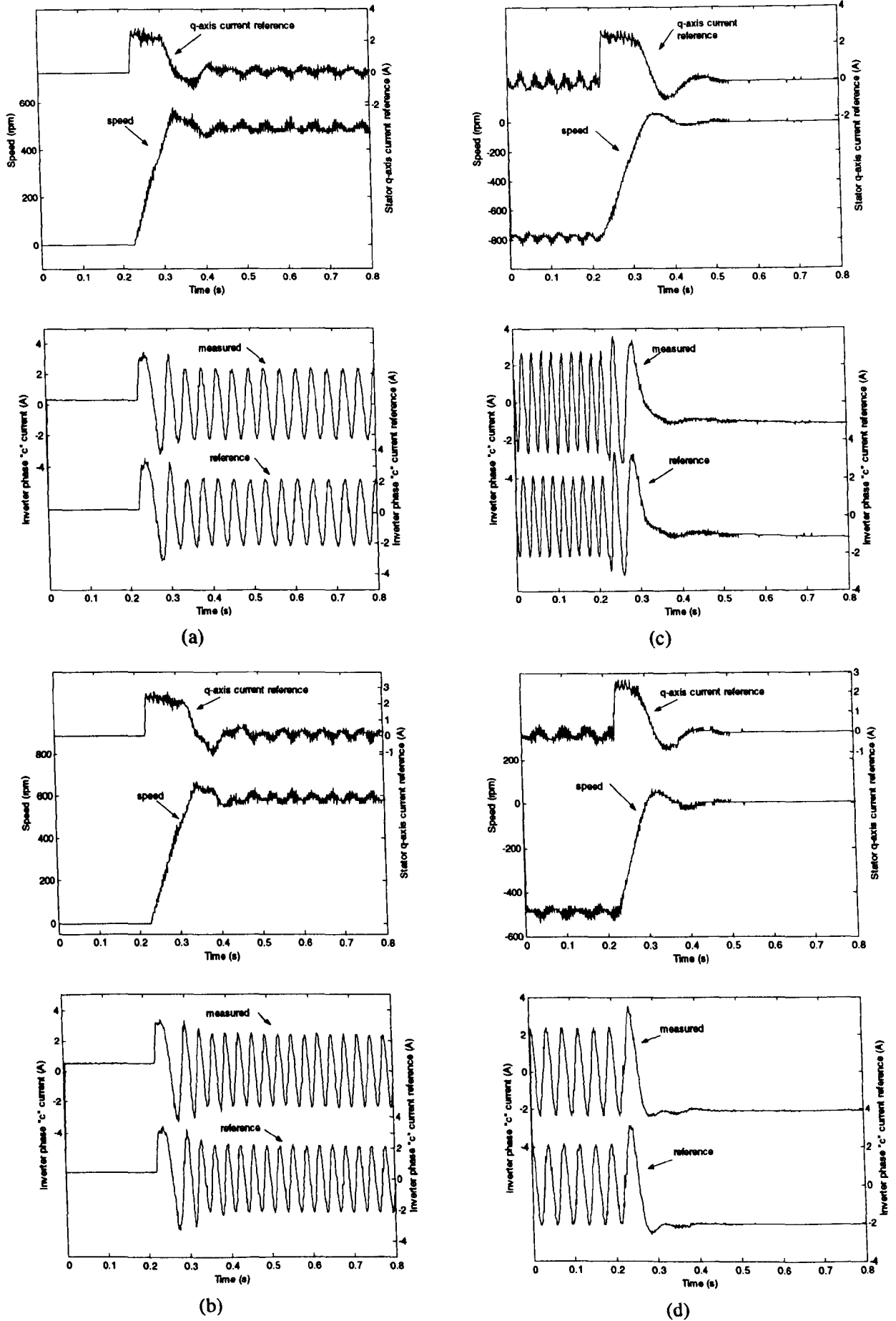


Fig. 10.4: Transient performance of the symmetrical six-phase induction motor: acceleration transient, 0 rpm to 500 rpm (a), 0 rpm to 600 rpm (b), deceleration transient, -800 rpm to 0 rpm (c) and -500 rpm to 0 rpm (d).

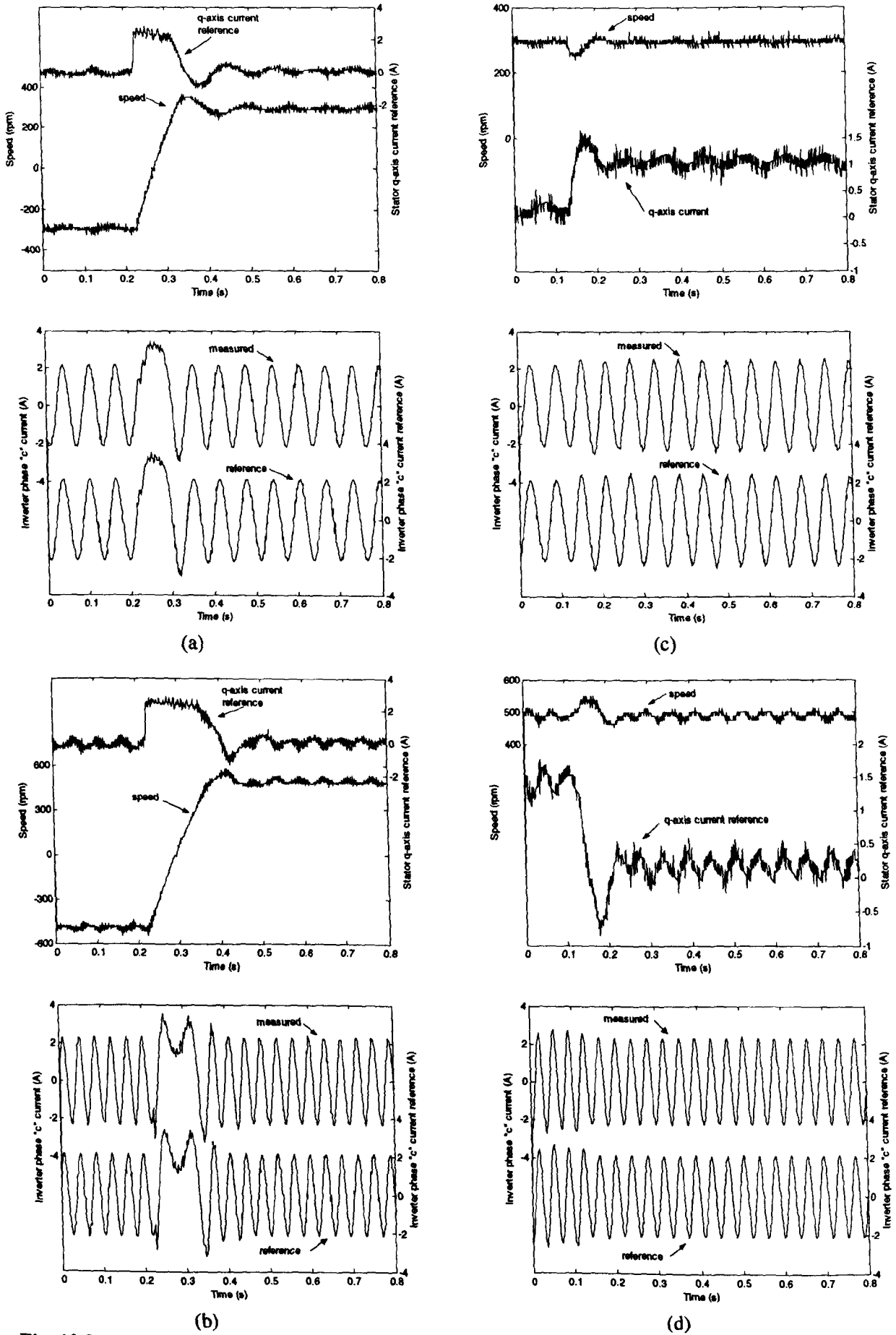


Fig. 10.5: Transient performance of a symmetrical six-phase induction motor: speed reversal from -300 rpm to 300 rpm (a), -500 rpm to 500 rpm (b), step loading at 300 rpm (c) and step unloading at 500 rpm.

10.5 Experimental investigation of a series-connected two-motor six-phase drive system dynamics

Various experimental tests are performed in order to prove the existence of decoupled dynamic control in the six-phase series-connected two-motor drive, described in section 6.2. The drive incorporates the six-phase motor described in section 10.3 and used in the previous investigations, and a three-phase induction machine, described in section 10.3. Both machines are equipped with resolvers and operate in speed-sensored mode. Operation in the base speed region only is considered and the stator d-axis current references of both machines are constant at all times. Additional inertia is mounted on the six-phase motor shaft (Fig. 10.6). Both machines are running under no-load conditions, except for the loading transients, when they are coupled to the permanent magnet DC machine. The C-code running on the PC performs closed loop speed control and indirect rotor flux oriented control according to Fig. 3.1, in parallel for the two machines. Individual stator current references of the two machines are calculated according to (6.3) and summed according to (6.4) to form inverter phase current references.

The approach adopted in the experimental investigation is the following. Both machines are excited and brought to a certain steady-state operating speed. A speed transient is then initiated for one of the two machines, while the speed reference of the

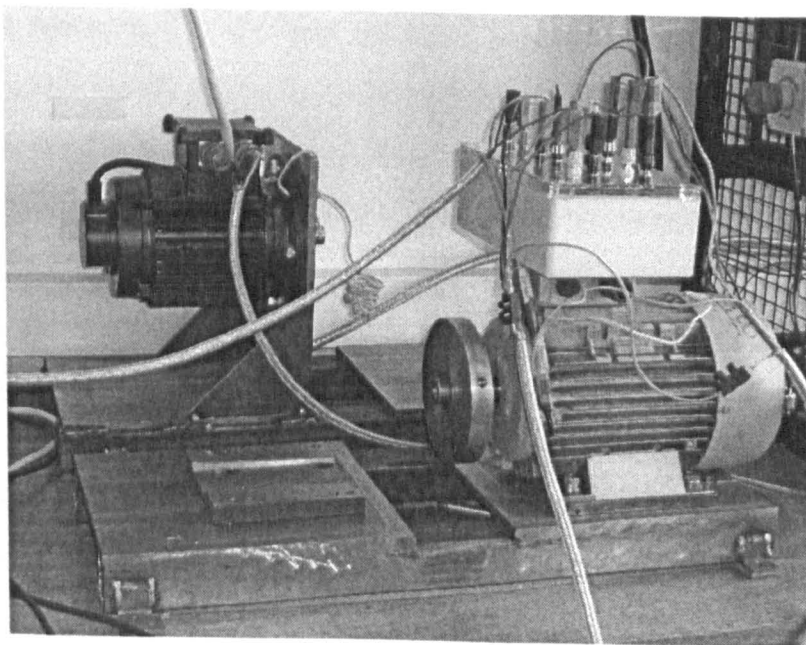


Fig. 10.6: Experimental rig: six-phase induction motor (front) and three-phase induction motor (back).

other remains constant. If the control is truly decoupled, operating speed of the machine running at constant speed should not change when a transient is initiated for the other machine. However, due to the fast action of the speed controller, some small variation of the speed could be unobservable. The ultimate proof of the truly decoupled control is therefore the absence of variation in the stator q-axis current command of the machine running at constant speed, since this indicates absence of any speed error at the input of the speed controller. Experimentally obtained traces include in all cases speeds, stator q-axis current references, stator phase current references (one phase only) for both machines, as well as the measured and reference current for one inverter phase. Some experimental results from this section can be found in Levi et al (2004d) and Jones et al (2004c).

10.5.1 Six-phase motor transients

At first, acceleration transients of the six-phase machine are investigated. The three-phase machine runs at 800 rpm and the six-phase motor is accelerated from 0 rpm to 500 rpm. Next, the three-phase machine runs at 600 rpm and the six-phase machine accelerates from 0 rpm to 800 rpm. Deceleration performance of the six-phase machine is considered next. The three-phase machine runs at 1200 rpm, while the six-phase machine is decelerated from -500 rpm to 0 rpm. The second deceleration test involves the three-phase motor held at 600 rpm and the six-phase motor decelerated from -800 rpm to 0 rpm. The results of the four tests are shown in Figs. 10.7a, 10.7b, 10.8a and 10.8b, respectively. As can be seen from the traces of the stator q-axis current references, initiation of the acceleration transient for the six-phase machine does not impact on dynamics of the three-phase machine at all. This is confirmed with the corresponding speed traces as well. Stator phase current references for the three-phase machine do not change either. Inverter current references, being determined with (6.5), are complex functions, which contain two sinusoidal components of two different frequencies in any steady-state. As is evident from Figs 10.7a and 10.8a reference and measured inverter currents are in very good agreement. However, at the higher speed of 800 rpm (Figs. 10.7b and 10.8b) there is some discrepancy, due to the current control method used.

The next two tests, illustrated in Figs. 10.9a and 10.9b, involve reversing

transients. Initially the three-phase machine is kept at standstill while the six-phase machine is reversed from -300 rpm to 300 rpm (Fig.10.9a). Next, the three-phase machine is kept again at 0 rpm while the six-phase machine is reversed from 500 rpm to -500 rpm (Fig. 10.9b). Figs. 10.9a to 10.9b show that initiation of the reversing transient for the six-phase machine has very little impact on the three-phase machine since stator q-axis current remains basically unchanged. Further proof can be seen in Figs 10.9a and 10.9b, where phase current references of the three-phase motor do not change. Measured inverter phase currents and inverter phase current references are in good agreement and show that current control performs well at these speeds.

Finally, step loading (40% of the rated torque) and unloading (51% of the rated torque) of the six-phase machine are illustrated in Figs 10.10a and 10.10b, respectively. Step loading takes place with the six-phase motor operating at 300 rpm, while the three-phase machine is held at 600 rpm. Step unloading takes place with the six-phase machine operating at 500 rpm and the three-phase motor at 800 rpm. As can be seen in Fig.10.10a, the three-phase machine is undisturbed during the loading transient, while the six-phase machine's speed recovers to the reference speed in a very short time interval with a very small dip, due to the rapid build-up of the stator q-axis current reference. Similar conclusions can be drawn from the unloading transient (Fig. 10.10b). Phase current references of the two machines and the inverter and measured current are included again and these confirm the undisturbed operation of the three-phase machine. All the six-phase motor transients were chosen to be the same as those used in the single six-phase motor investigation (section 10.4), with the exception of the acceleration transient 0 rpm to 800 rpm (Fig. 10.7b). This approach enables a comparison of the performance of the six-phase motor when operated as a single drive with its performance in a two-motor drive. In each case the q-axis current and the speed responses of the six-phase motor correspond very closely, during both transients and steady-state. Some ripple in speed and stator q-axis current reference observable in Figs. 10.7 to 10.10, is essentially the consequence of the imperfections of the six-phase machine (as explained in section 10.4) and is not a consequence of the control coupling within the two-motor drive system. This proves that the dynamic and steady-state performance of the six-phase motor is basically not affected by its connection to the three-phase motor.

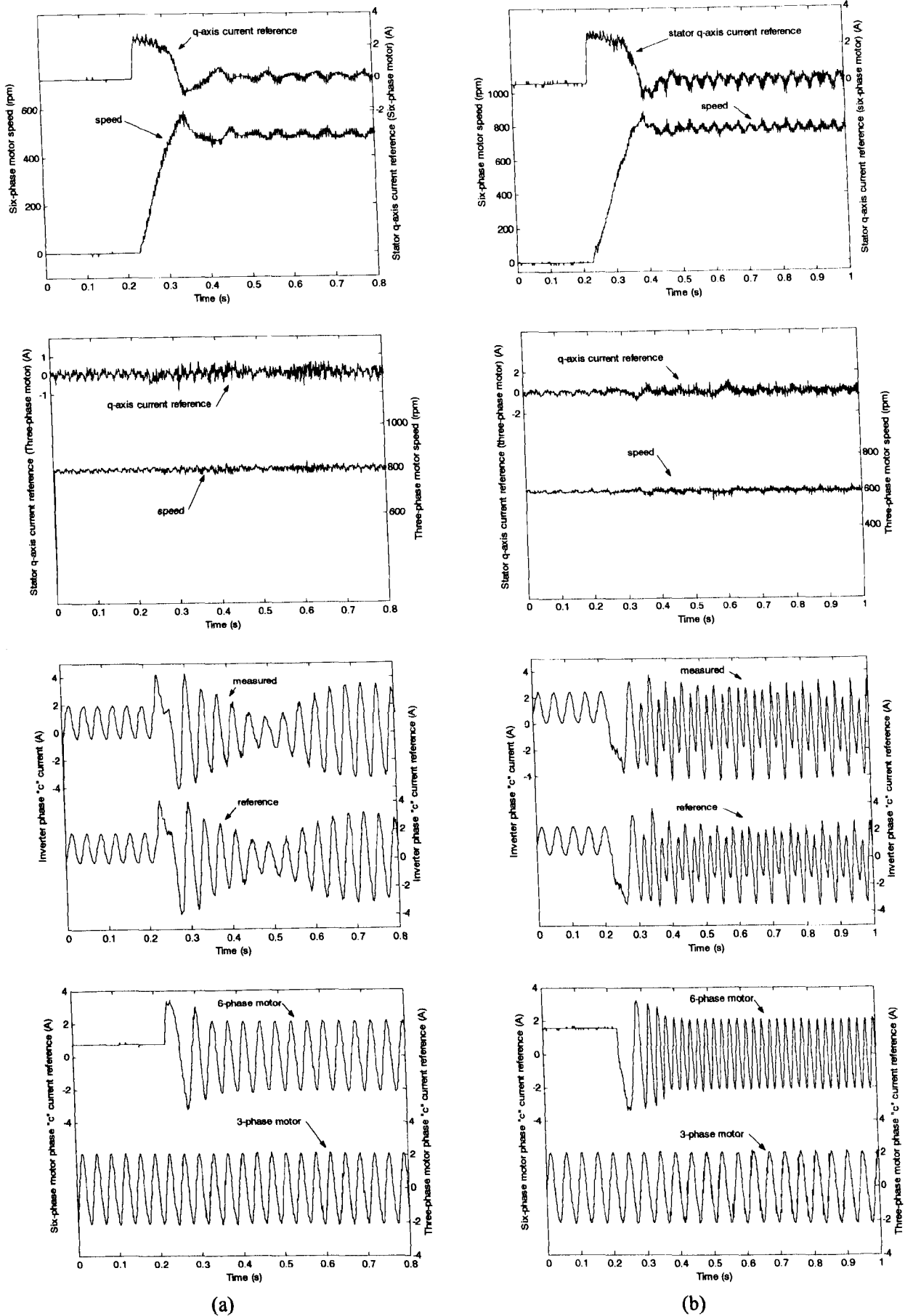


Fig. 10.7: Transient performance of the six-phase two-motor drive: six-phase motor acceleration transients, 0 rpm to 500 rpm (a) and 0 rpm to 800 rpm (b).

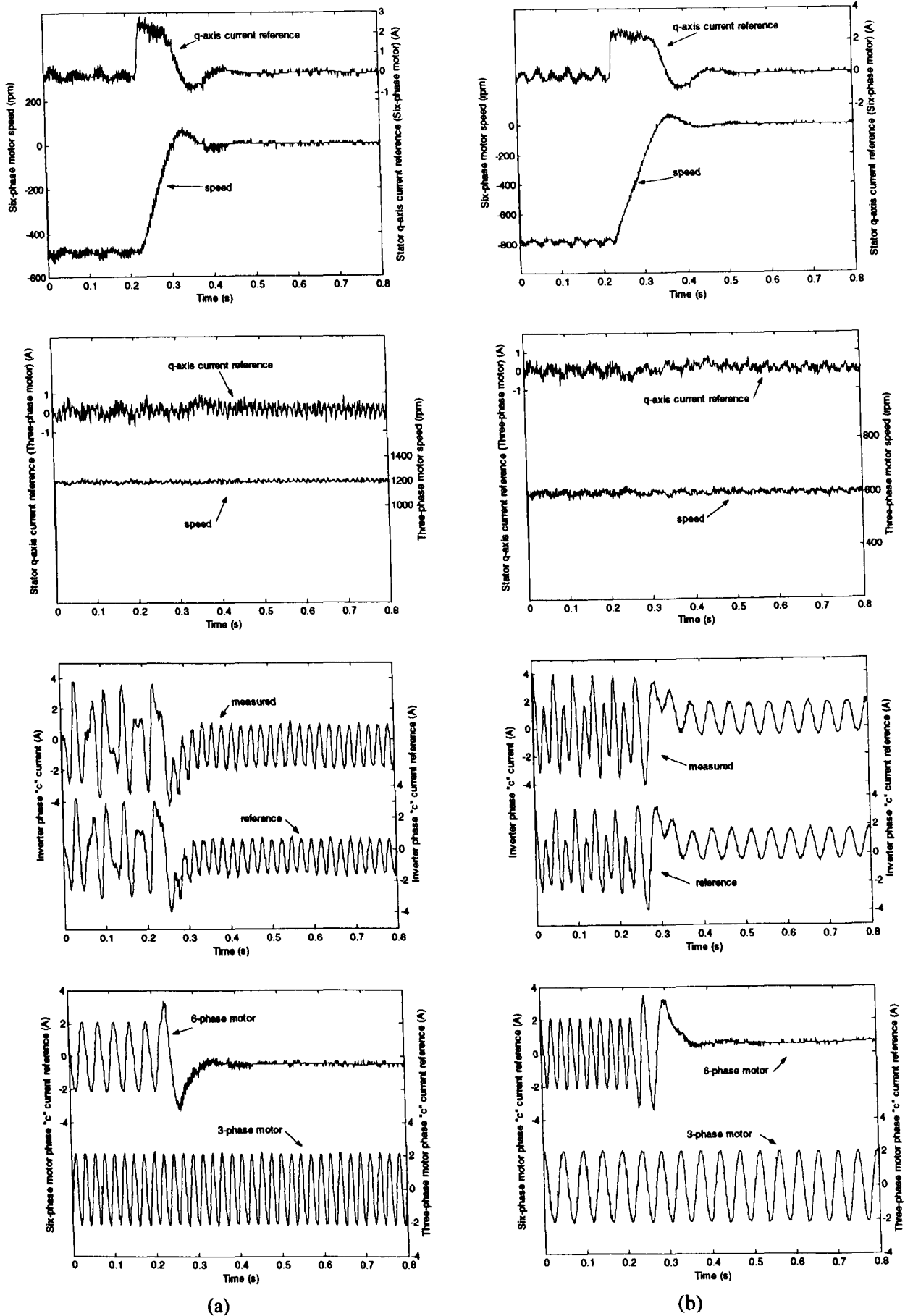


Fig. 10.8: Transient performance of the six-phase two-motor drive: six-phase motor deceleration transients, -500 rpm to 0 rpm (a) and -800 rpm to 0 rpm (b).

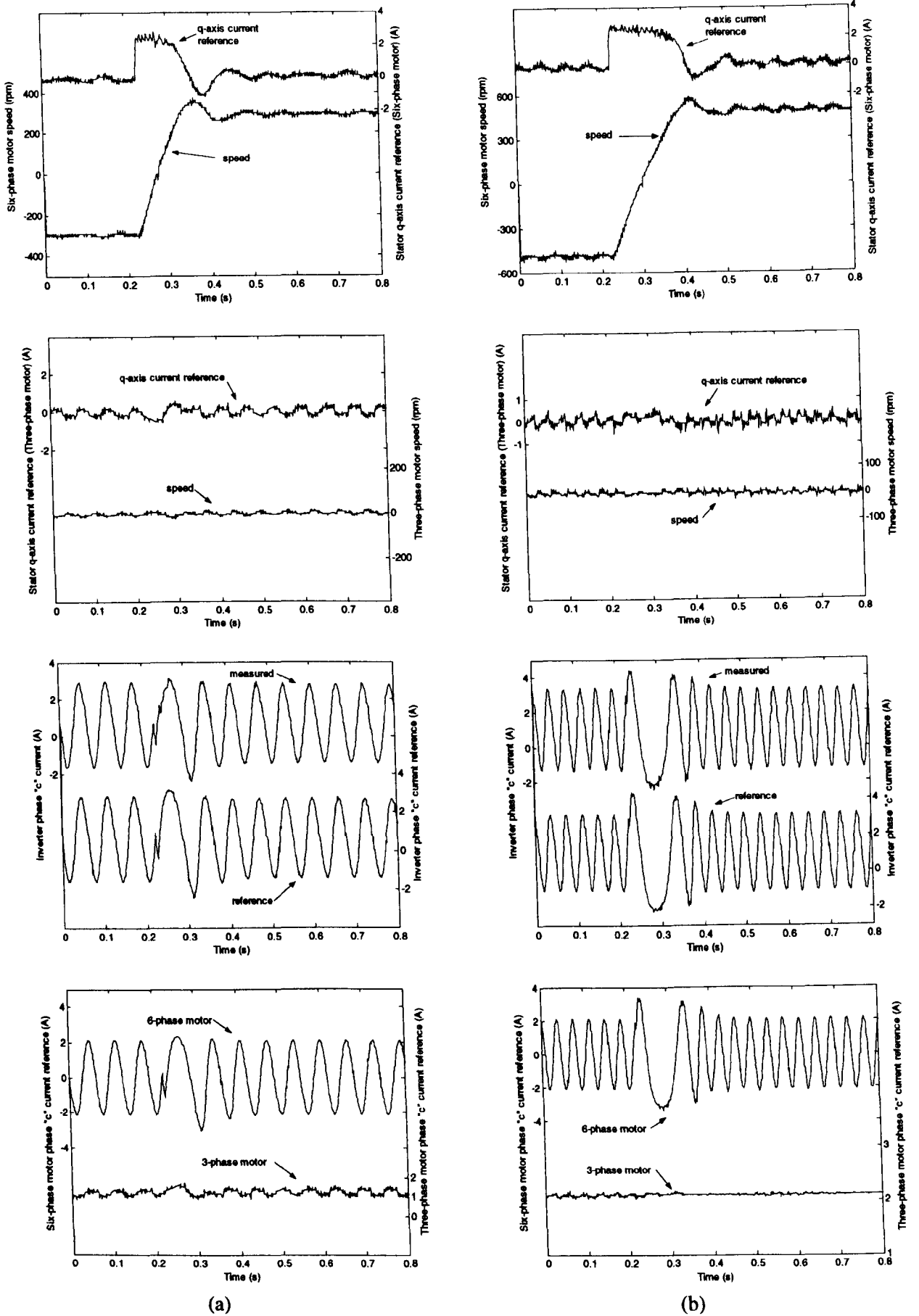


Fig. 10.9: Transient performance of the six-phase two-motor drive: six-phase motor speed reversal: -300 rpm to 300 rpm (a) and -500 rpm to 500 rpm (b).

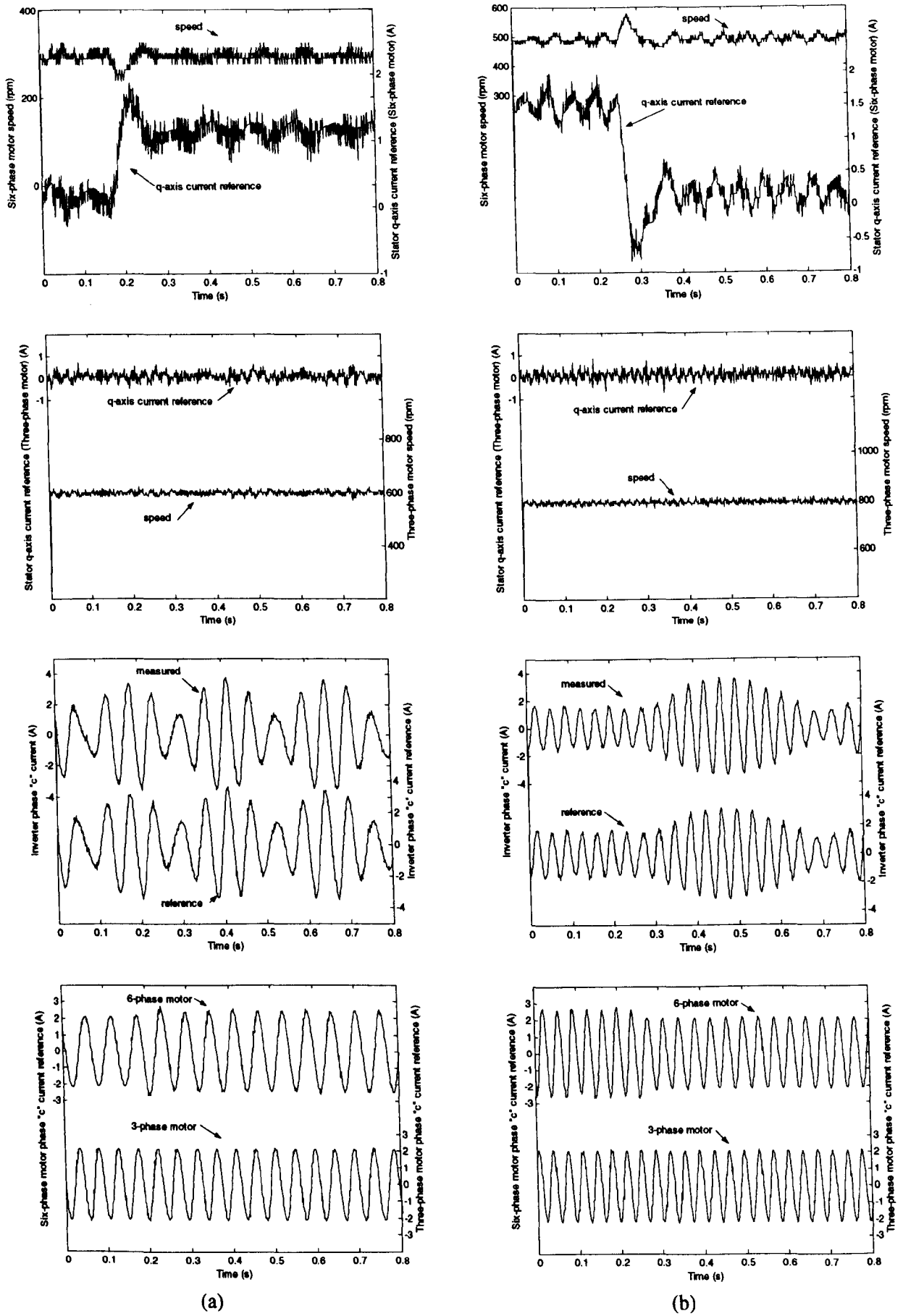


Fig. 10.10: Transient performance of the six-phase two-motor drive: step loading at 300 rpm (a) and step unloading at 500 rpm (b) of the six-phase motor.

10.5.2 Three-phase motor transients

In this section dynamic performance of the three-phase induction machine is investigated. Acceleration transient is considered first. The six-phase machine is held at -500 rpm, while the three-phase motor is accelerated from 0 rpm to 300 rpm. Next, the six-phase motor is held at -500 rpm, while the three-phase motor is accelerated from 0 rpm to 1200 rpm. Deceleration of the three-phase machine is investigated by holding the six-phase machine at 500 rpm, while the three-phase motor is decelerated from 300 rpm to standstill and from 1200 rpm to standstill. The results of these four tests are illustrated in Figs. 10.11a, 10.11b, 10.12a and 10.12b, respectively. The results show that initiation of a speed transient for the three-phase motor has no impact on the behaviour of the six-phase motor, since neither the speed nor the stator q-axis current reference change. This is further confirmed by inspection of the phase current references of the six-phase machine, which do not exhibit any change whatsoever during the transient of the three-phase machine. Measured and reference inverter current are in very good agreement.

The next two tests, illustrated in Figs. 10.13a and 10.13b, investigate reversing transients. Initially the six-phase machine speed is maintained at a constant -600 rpm, while the three-phase machine is reversed from -300 rpm to 300 rpm (Fig. 10.13a). During the next test, the six-phase machine is held at 0 rpm while the three-phase machine is reversed from 600 rpm to -600 rpm (Fig. 10.13b). The same conclusions can be made here as in the acceleration/deceleration tests.

Step load application to the three-phase machine, which runs at 600 rpm while the six-phase machine runs at 400 rpm, is illustrated in Fig. 10.14a. The applied load is app. 53% of the rated three-phase motor torque. Step load removal is illustrated in Fig. 10.14b and takes place with the three-phase machine operating at 800 rpm and the six-phase motor running at 600 rpm. The load removed from the three-phase machine is 51% of the rated value. It can be seen that loading and unloading of the three-phase motor does not affect the speed and q-axis current reference of the six-phase motor. Upon application of the load the speed of the three-phase machine dips and then quickly recovers to the reference speed. Likewise upon removal of the load the three-phase motor speed overshoots the reference speed, but quickly recovers in a very short time interval. Phase current reference of the two motors confirms decoupled control. Once again, inverter current references and measured inverter currents match very well.

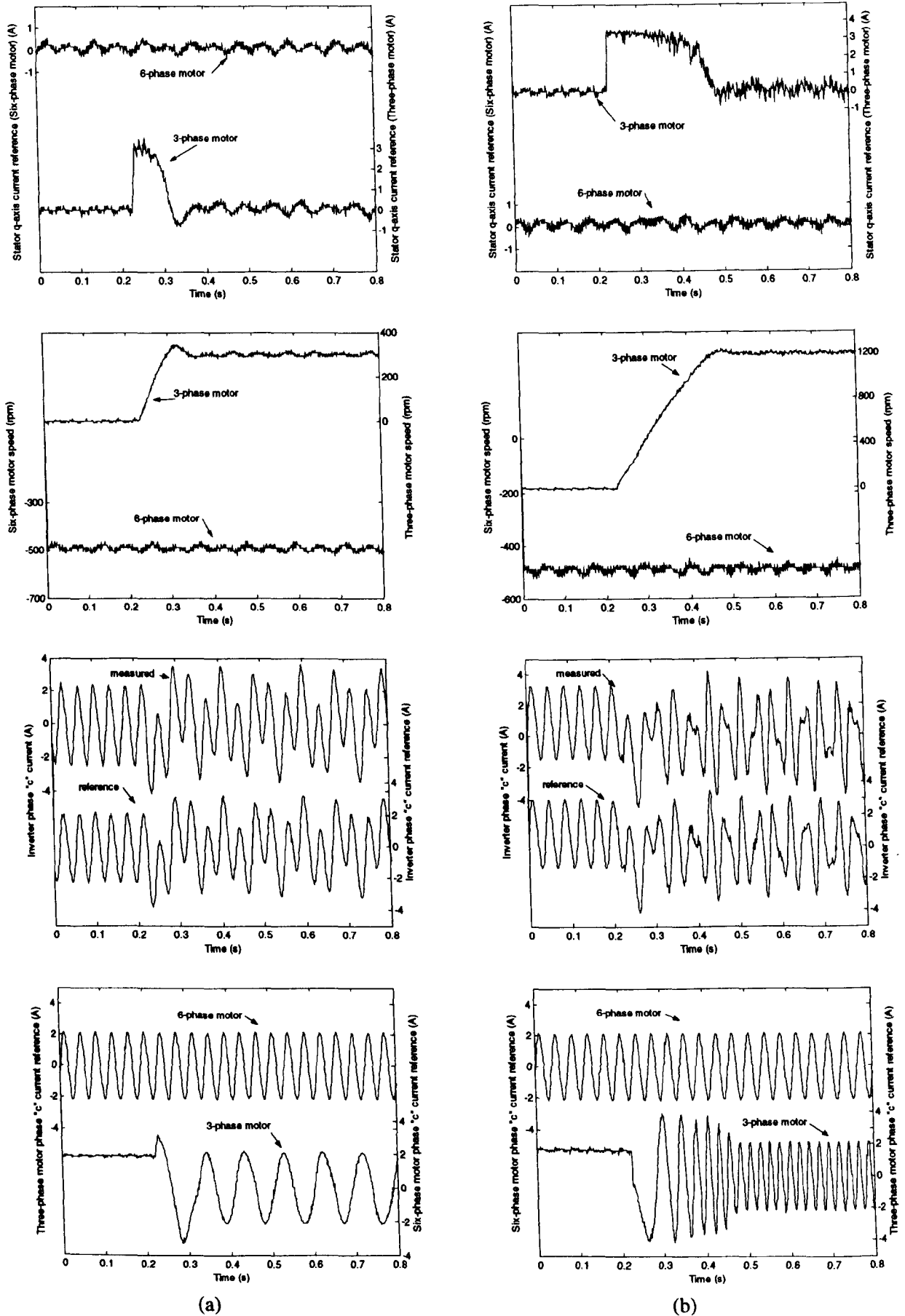


Fig. 10.11: Transient performance of the six-phase two-motor drive: three-phase motor acceleration transients, 0 rpm to 300 rpm (a) and 0 rpm to 1200 rpm (b).

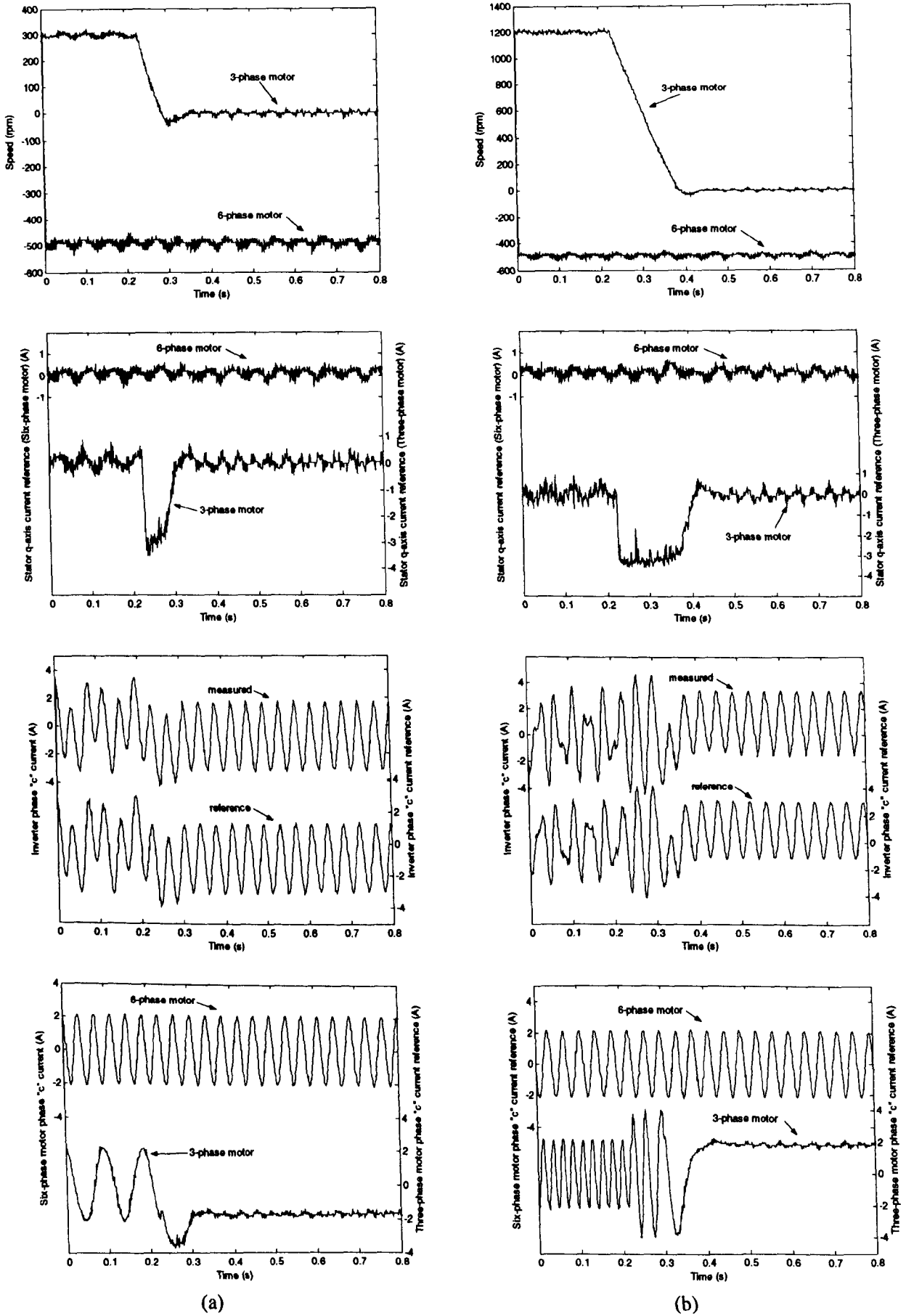


Fig. 10.12: Transient performance of the six-phase two-motor drive: three-phase motor deceleration transients, 300 rpm to 0 rpm (a) and 1200 rpm to 0 rpm (b).

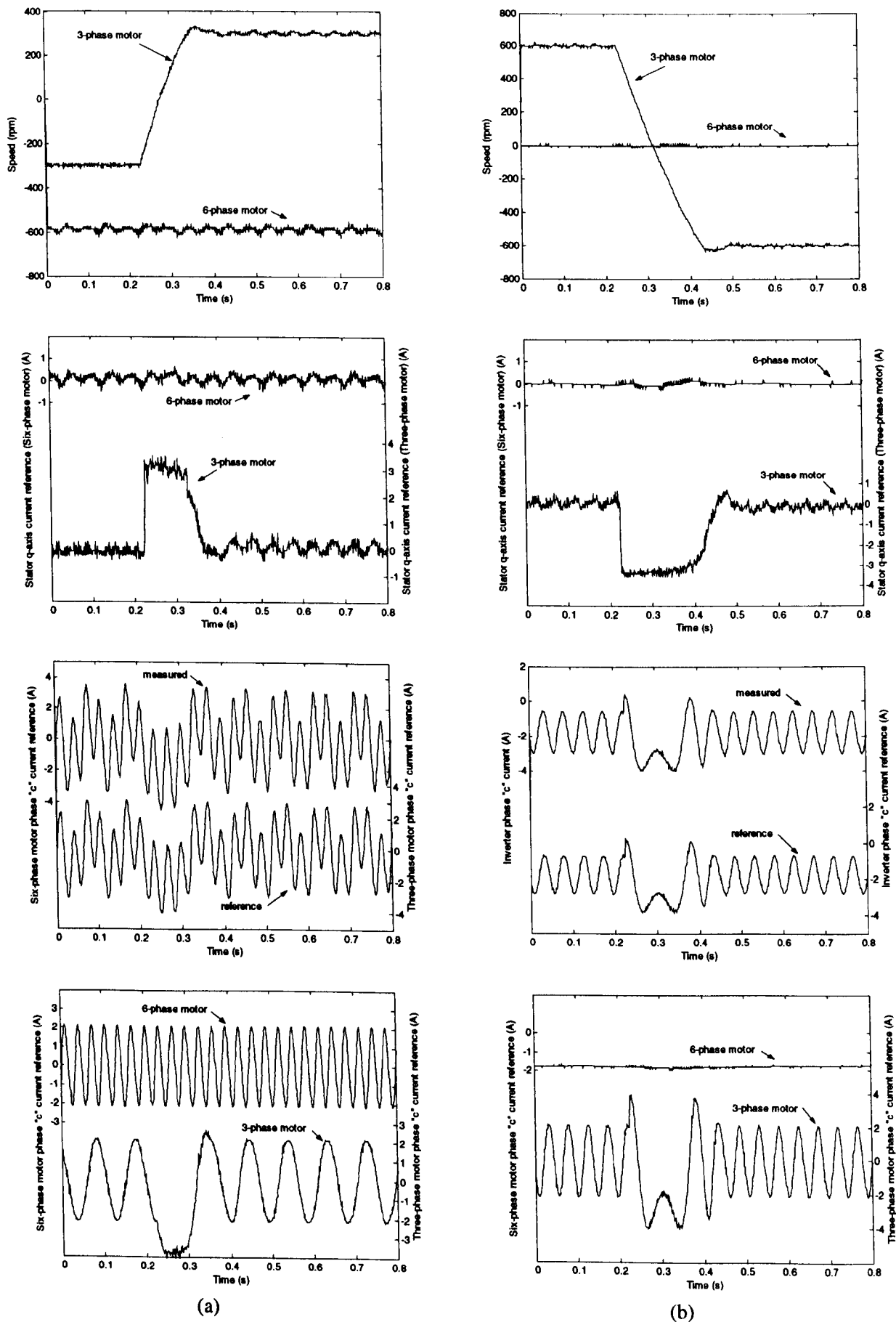


Fig. 10.13: Transient performance of the six-phase two-motor drive: three-phase motor speed reversal -300 rpm to 300 rpm (a) and 600 rpm to -600 rpm (b).

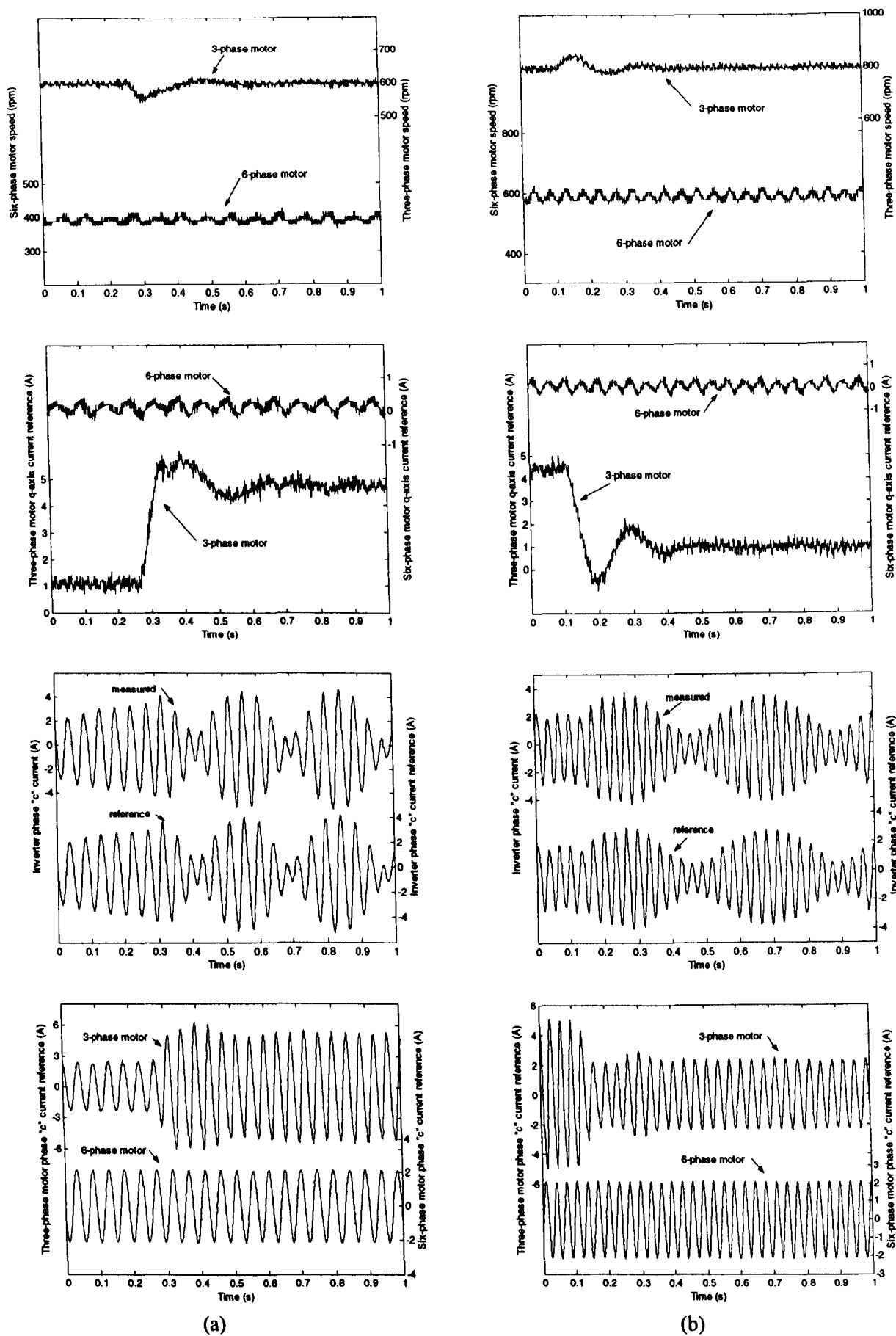


Fig. 10.14: Transient performance of the six-phase two-motor drive: step loading at 400 rpm (a) and step unloading at 800 rpm (b) of three-phase motor.

10.6 Experimental investigation of dynamics of a two-motor drive, using a three-phase permanent magnet synchronous machine

The possibility of using different types of AC machines in the multi-phase multi-machine drive has been discussed in chapter 7 and Jones et al (2004). A seven-phase three-motor configuration, comprising an induction machine, a PMSM and a Syn-Rel machine, has been considered. It was concluded that the construction of the rotor is of no importance as long as the multi-phase stator windings are sinusoidally distributed. An experimental investigation is performed in this section in order to further corroborate this conclusion. A six-phase two-motor rig is constructed, which consists of the six-phase induction machine used in the previous experiments and the PMSM described in section 10.3. C-code, performs speed control and indirect rotor flux oriented control for the six-phase IM and the three-phase PMSM according to Figs. 3.1 and 7.1, respectively. The stator d-axis current is held at zero for the PMSM as the machine will only be operated in the base speed region. Control of the six-phase motor is performed in an identical manner as in the previous experiments.

The approach adopted in the experimental investigation is the same as that described in section 10.5. Both machines are initially brought to a certain steady-state operating speed. A speed transient is then initiated for one of the two machines, while the speed reference of the other remains constant. Both machines operate under no-load conditions unless otherwise stated. Additional inertia is mounted on the PMSM. The six-phase machine is coupled to a DC machine, thus providing an increased inertia (Fig. 10.15).

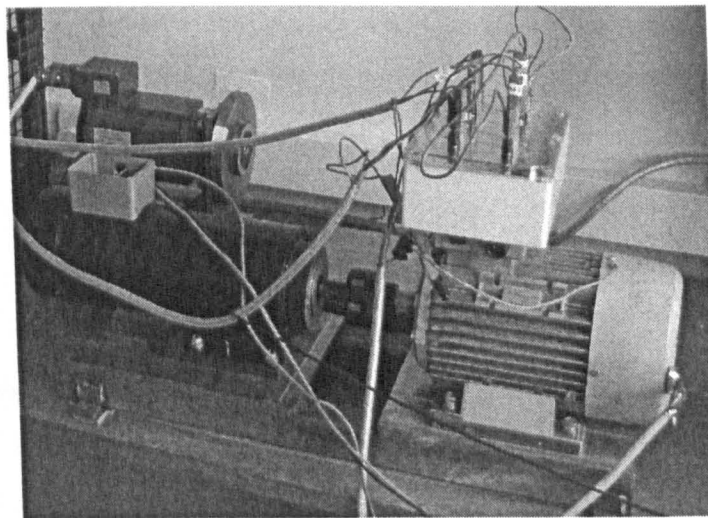


Fig. 10.15: Experimental rig: six-phase induction motor coupled to a DC generator (front) and three-phase PMSM (back).

10.6.1 Experimental results

The first set of experiments involves acceleration transients of the two machines. The PMSM is accelerated from standstill to 800 rpm, while the six-phase motor is held at 500 rpm. Next, the six-phase machine is accelerated from standstill to 600 rpm, while the PMSM is held at 300 rpm. The second set of experiments consists of deceleration transients. The PMSM is decelerated from 900 rpm to 0 rpm, with the six-phase motor running at a constant 500 rpm. Next, the PMSM is held at 600 rpm, while the six-phase motor decelerates to 0 rpm from 500 rpm. Experimental results are shown in Figs. 10.16a, 10.16b, 10.17a and 10.17b, respectively. These include stator q-axis current reference of both machines, measured speed response of both machines, inverter current references and actual inverter currents for one of the six phases as well as individual phase current references of the two machines. The results show that neither machine is affected by the application of a speed command to the other motor. This is evident from the speed response and the q-axis current reference of the six-phase motor, which does not change when a speed command is applied to the PMSM. There is a very small change in the stator q-axis current reference of the PMSM when a speed command is applied to the six-phase motor. This is believed to be due to incomplete six-phase motor current cancellation at the point of connection to the PMSM (as discussed in section 10.7). This phenomenon is also visible in the phase current references of the PMSM. In all the cases under consideration inverter phase references and measured inverter currents are in good agreement. Steady-state phase current references of the six-phase machine closely match measured inverter phase currents. This is so since the PMSM operates under no-load conditions and requires no magnetising current ($I_{ds}^* = 0$), thus the steady-state phase currents of the machine are very small.

The next two tests illustrate reversing transients. Transition from -300 rpm to 300 rpm is illustrated in Fig. 10.18a for the PMSM, while the six-phase machine is held at 600 rpm. Speed reversal of the six-phase machine is shown in Fig. 10.18b, where the six-phase machine is reversed from -500 rpm to 500 rpm, while the three-phase machine is kept at standstill. The same observations as made for the previous tests apply, thus proving that fully decoupled control is maintained during reversal of each machine.

The last two tests involve step loading and unloading of the six-phase motor.

Loading (54% of the rated torque) takes place at 600 rpm, with the PMSM held at 500 rpm and is illustrated in Fig. 10.19a. Unloading (51% of the rated torque) takes place at 500 rpm, while the PMSM runs at 800 rpm and is shown in Fig. 10.19b. As can be seen in 10.19a the three-phase machine is undisturbed during loading transient, while the six-phase machine's speed recovers to the reference speed in a very short time interval with a very small dip, due to the rapid build-up of the stator q-axis current reference. Similar conclusions can be drawn from the unloading transient (Fig. 10.19b). Phase current references of the two machines and the inverter reference and measured current are included again. These also confirm the undisturbed operation of the three-phase machine.

10.7 Experimental investigation of steady-state operation

This section considers the steady-state performance of the single six-phase motor drive discussed in section 10.4 and the six-phase two-motor drive discussed in section 10.5. Steady-state stator current measurements are made for both configurations and the resulting current waveforms and spectra are presented. Additionally steady-state voltage measurements are also made and recorded for the two-motor six-phase drive. The resulting voltage waveforms and spectra are presented. Operating conditions are chosen to coincide with some of those considered in sections 10.4 and 10.5 respectively.

The motor phase current is recorded using the Tektronic AM6203 Hall-effect probe and Tektronic AM503 amplifier. This system can accurately record currents of up to 20A with frequencies from 0Hz to 20MHz. The amplifier is connected to an oscilloscope to which it provides analogue signals of up to $\pm 50\text{mV}$. The Hewlett-Packard HP3566SA dynamic signal analyser is used for recording the current waveforms and/or spectra.

For recording the PWM voltages a potential divider is used in conjunction with oscilloscope probes with attenuation of 10. Additionally, a low-pass filter is included in order to eliminate the high-frequency components (PWM ripple). Line voltage is recorded by connecting two oscilloscope probes to two attenuated and filtered phase voltage signals. The two signals are recorded by the HP35665A analyser and consequently processed, in order to obtain the voltage waveform and spectra.

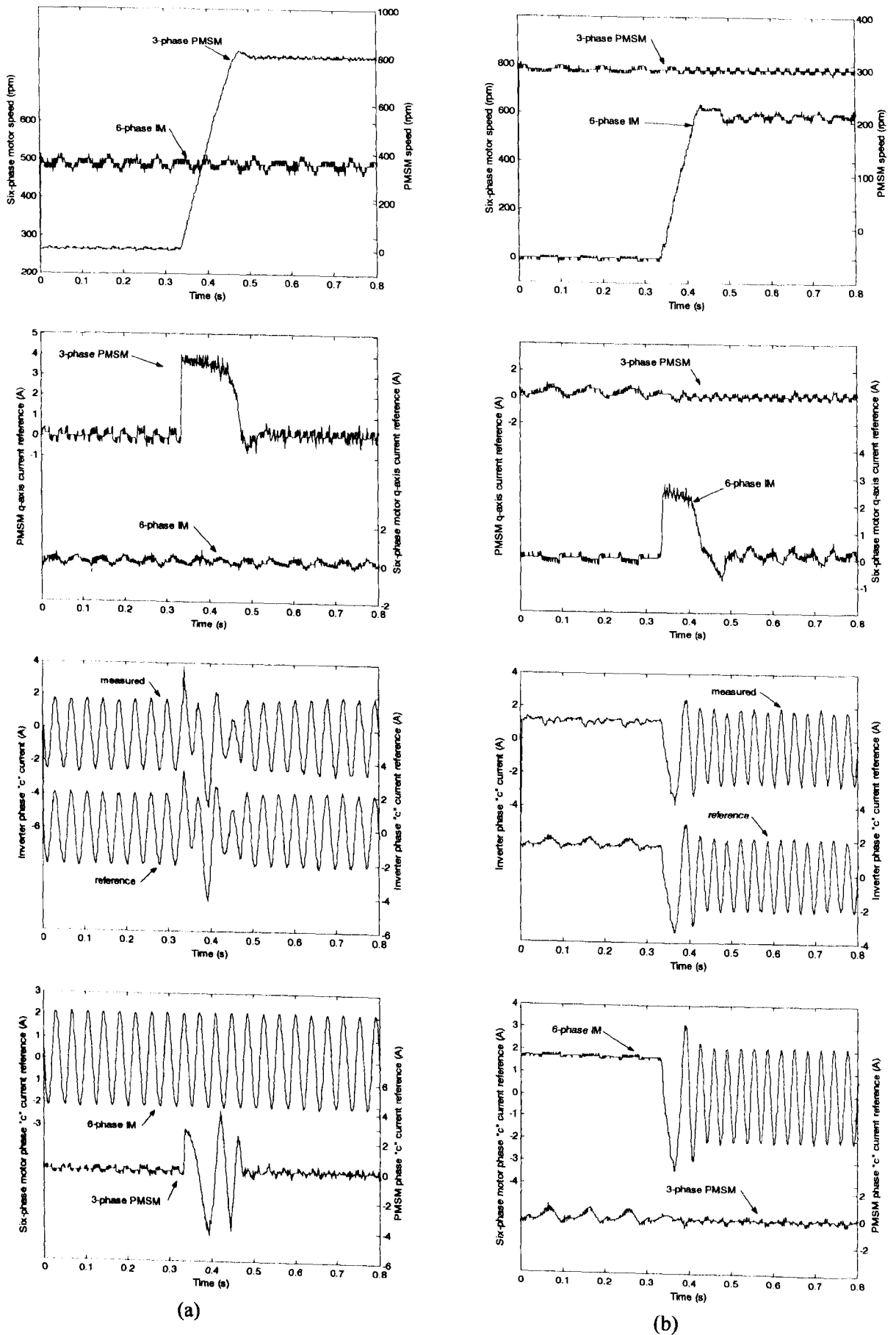


Fig. 10.16: Transient performance of the six-phase two-motor drive: PMSM acceleration transient, 0 rpm to 800 rpm (a) and six-phase induction motor acceleration transient, 0 rpm to 600 rpm (b).

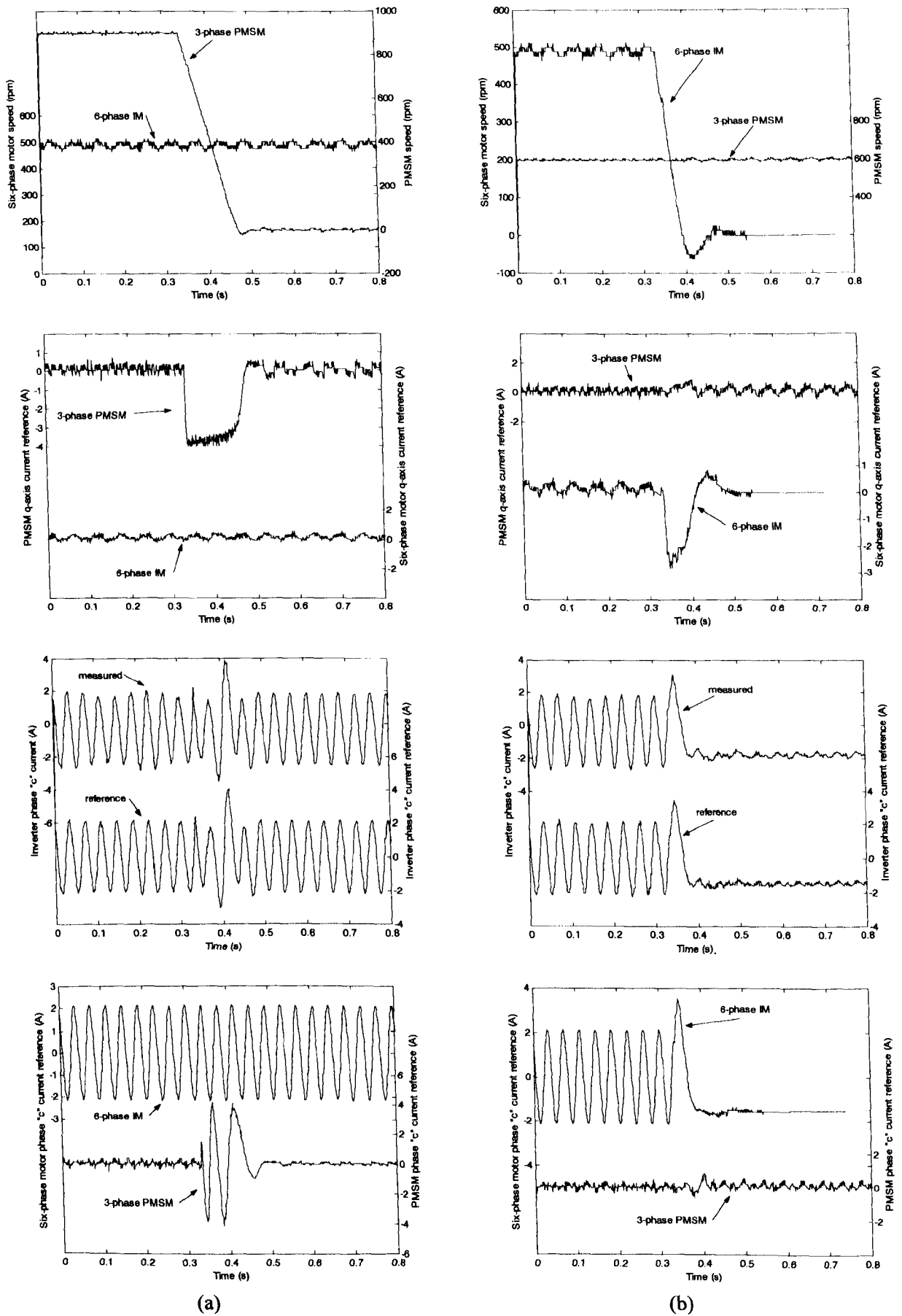


Fig. 10.17: Transient performance of the six-phase two-motor drive: PMSM deceleration transient, 900 rpm to 0 rpm (a) and six-phase induction motor deceleration transient, 500 rpm to 0 rpm (b).

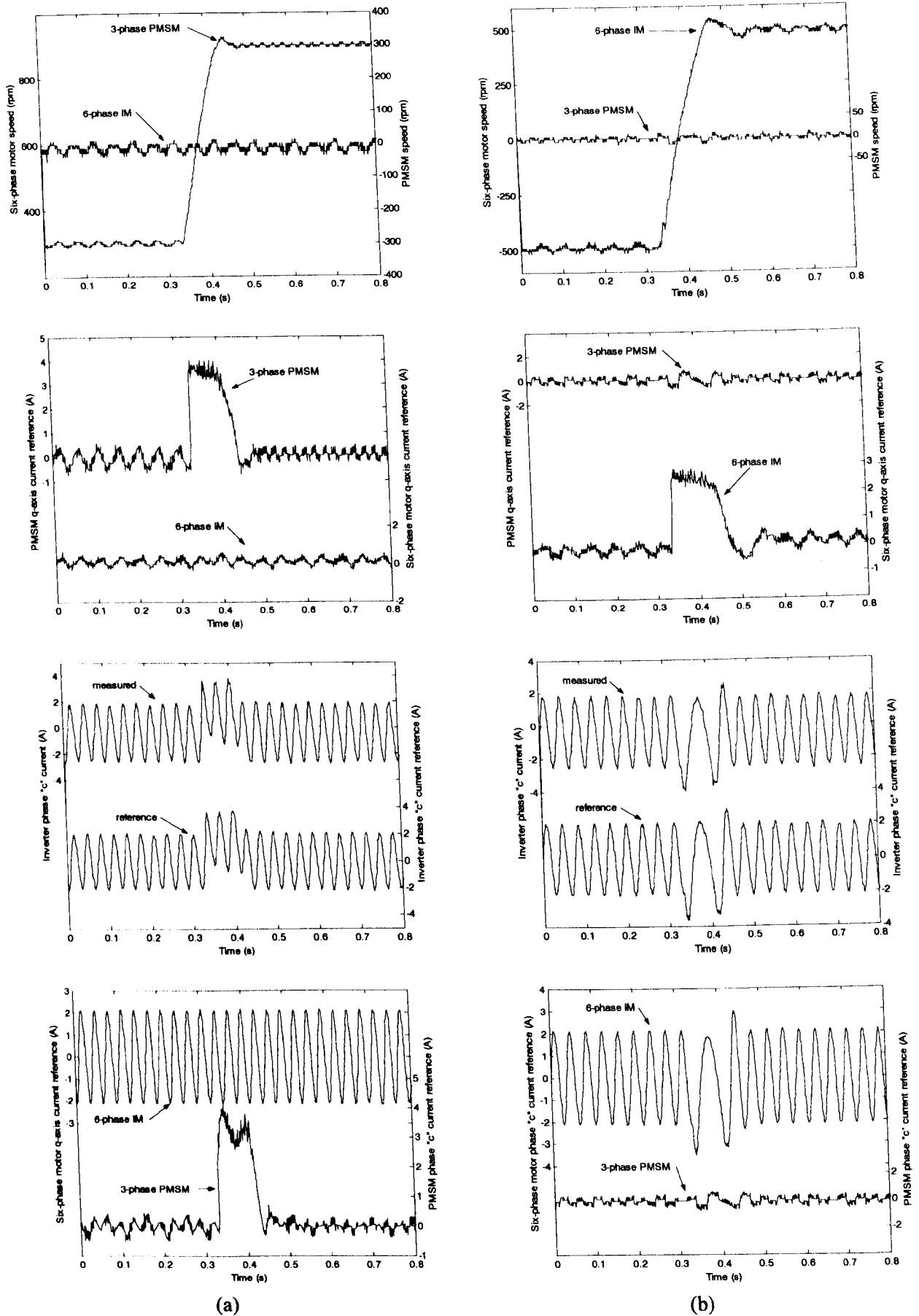


Fig. 10.18: Transient performance of the six-phase two-motor drive: PMSM speed reversal, -300 rpm to 300 rpm (a) and six-phase IM speed reversal, -500 rpm to 500 rpm (b).

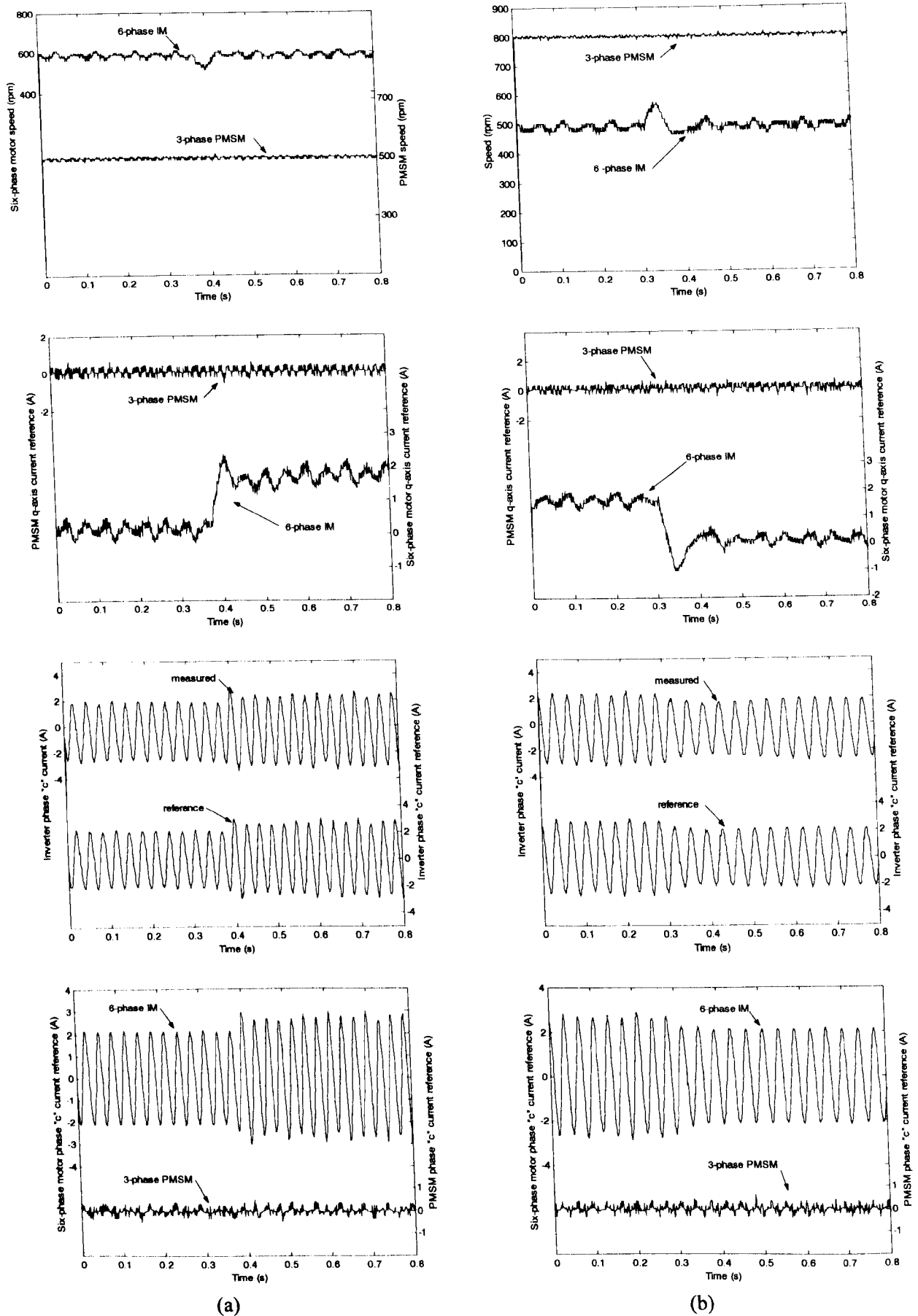


Fig. 10.19: Transient performance of the six-phase two-motor drive: step loading at 600 rpm (a) and step unloading at 500 rpm (b) of the six-phase motor.

10.7.1 Steady-state performance of symmetrical six-phase induction machine

In this section steady-state current measurements are undertaken for the single six-phase motor drive. The machine runs under no-load conditions and the stator d-axis current reference setting is 1.5A rms. Time domain current waveforms and spectra are presented for various operating speeds.

Time domain current waveforms and associated low frequency parts of the spectra are displayed in Figs. 10.20a to 10.20c for operation at 15Hz, 25Hz and 40Hz, respectively. As can be seen from Figs. 10.20a-b, low order current harmonics are practically non-existent at low to medium operating frequencies, confirming the ability of the adopted current control scheme to eliminate unwanted x-y and zero sequence harmonics. Some lower order harmonics can be observed at higher operating frequencies (Fig. 10.20c). However, these are of negligibly small amplitudes. It should be noted that the fundamental current component at 15Hz and 25Hz closely corresponds to the stator d-axis current reference of 1.5A rms, while at 40Hz it is slightly higher due to the ramp-comparison current control method used.

10.7.2 Steady-state performance of a two-motor six-phase drive

An experimental investigation into the steady-state performance of a two-motor six-phase drive is undertaken in order to further prove that each motor is operating independently. Steady-state phase current measurements are taken at the point of connection to the six-phase motor (inverter phase currents) and the three-phase motor using the already mentioned equipment. Line to line voltage at the inverter input (A to C) and at the three-phase motor terminals (a to b) is measured as well. Initially the six-phase machine operates at 500 rpm (25Hz), while the three-phase machine runs at 1200 rpm (40Hz). Next, the six-phase machine operates at 800 rpm (40 Hz), while the three-phase machine runs at 600 rpm (20Hz). Resulting current waveforms and spectra are illustrated in Figs. 10.21a and 10.21b, respectively. The stator current of the six-phase motor (inverter current) is essentially a sum of two sinusoidal components at two frequencies, as can be clearly seen from the spectrum of the current. The fundamental six-phase motor current component at 25Hz closely corresponds to the stator d-axis

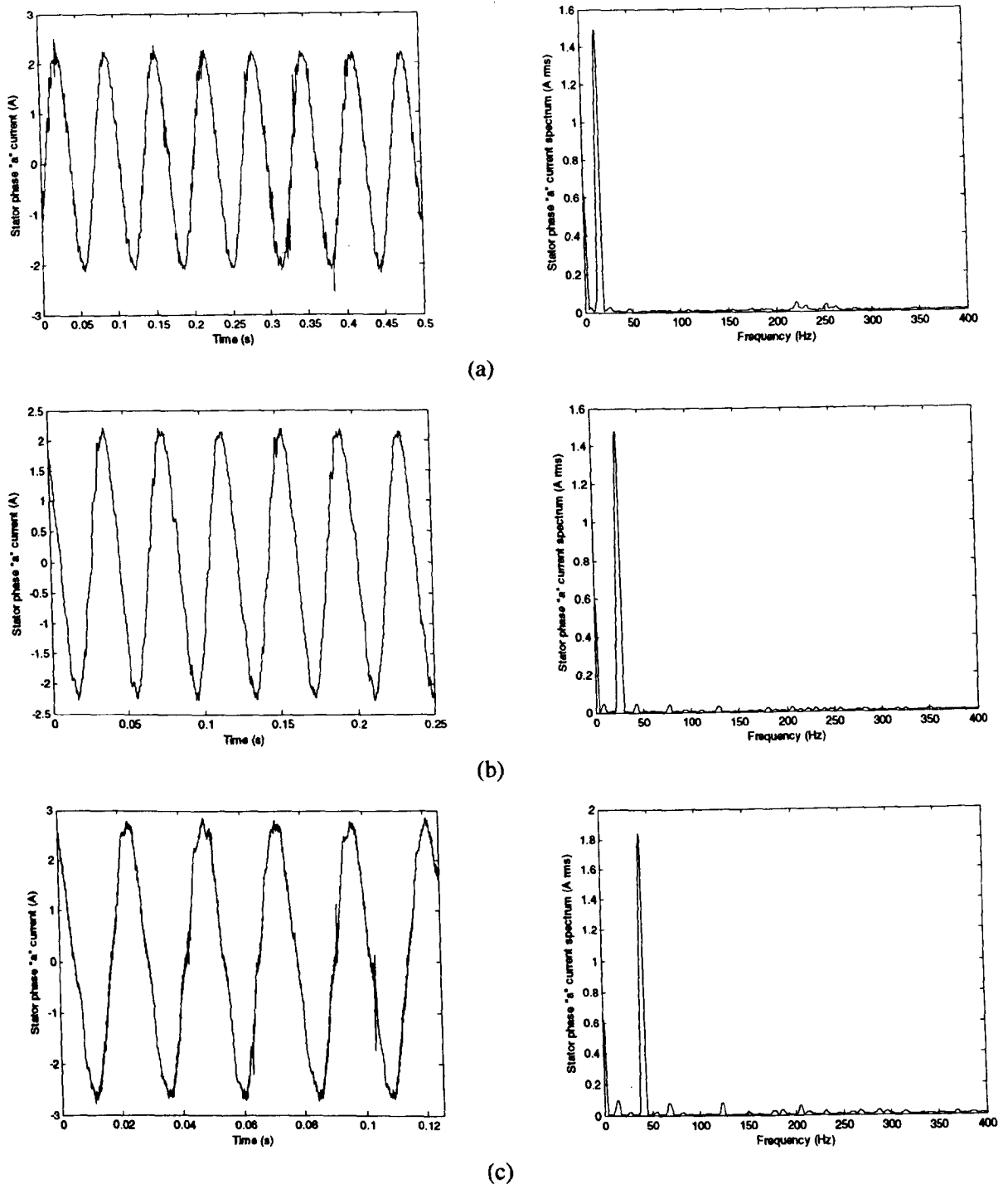


Fig. 10.20: Rotor flux oriented control of a six-phase IM: steady-state phase current and its spectrum at 300 rpm (15 Hz) (a), 500 rpm (25 Hz) (b) and 800 rpm (40 Hz) (c).

current reference of 1.5A rms, while at 40Hz it is slightly higher. In both tests the three-phase motor current spectrum shows that the component at the three-phase motor's operating frequency is close to twice the value of the harmonic at the same frequency in the inverter current, as it should be according to the presented theory. It should be noted that there is a small harmonic component at the operating frequency of the six-phase motor, which according to the theory, should not exist at all in the three-

phase motor current. This means that the cancellation of the flux/torque producing currents of the six-phase machine is not ideal at the point of connection with the three-phase machine. This phenomenon is believed to be associated with some asymmetry between the two three-phase inverters. The unwanted harmonic was found to be of a more or less constant rms value (between 0.2 and 0.3 A) regardless of the operating frequency of the six-phase motor. The cause of existence of this current harmonic is left here unresolved and it represents one of the directions for further work.

Voltage waveforms and spectra recorded under the same conditions can be seen in Figs 10.22a and 10.22b. It is clear that the inverter voltage spectrum contains two components, one at the operating frequency of the six-phase machine and another at the operating frequency of the three-phase machine. Three-phase motor voltages clearly show the component at the operating frequency of the three-phase machine, which is very close to the value recorded at the inverter side. Once again, there is a small negligible harmonic component at the operating frequency of the six-phase motor. There is also a voltage component at 50Hz present in all the voltage results. This is believed to be a consequence of the measuring method, as no such component can be seen in the current spectra.

10.8 Summary

An experimental laboratory rig has been described in this chapter. The rig is capable of supplying up to twelve phases. The rig is constructed of four commercially available MOOG DS2000 three-phase VSIs. For the purpose of the work carried out during this research one half of the rig was configured as a six-phase supply. This enables an experimental investigation of the performance of a symmetrical six-phase induction machine under indirect rotor flux oriented control, as well as experimentation on the series-connected two-motor drive systems.

Experiments are at first performed in order to determine both the transient and steady-state performance of the six-phase motor. These include acceleration, deceleration, reversing and step loading/unloading transients. Excellent dynamics, commensurate with vector control algorithm, are demonstrated, thus proving that the method of achieving rotor flux oriented control described in chapter 4 is indeed valid.

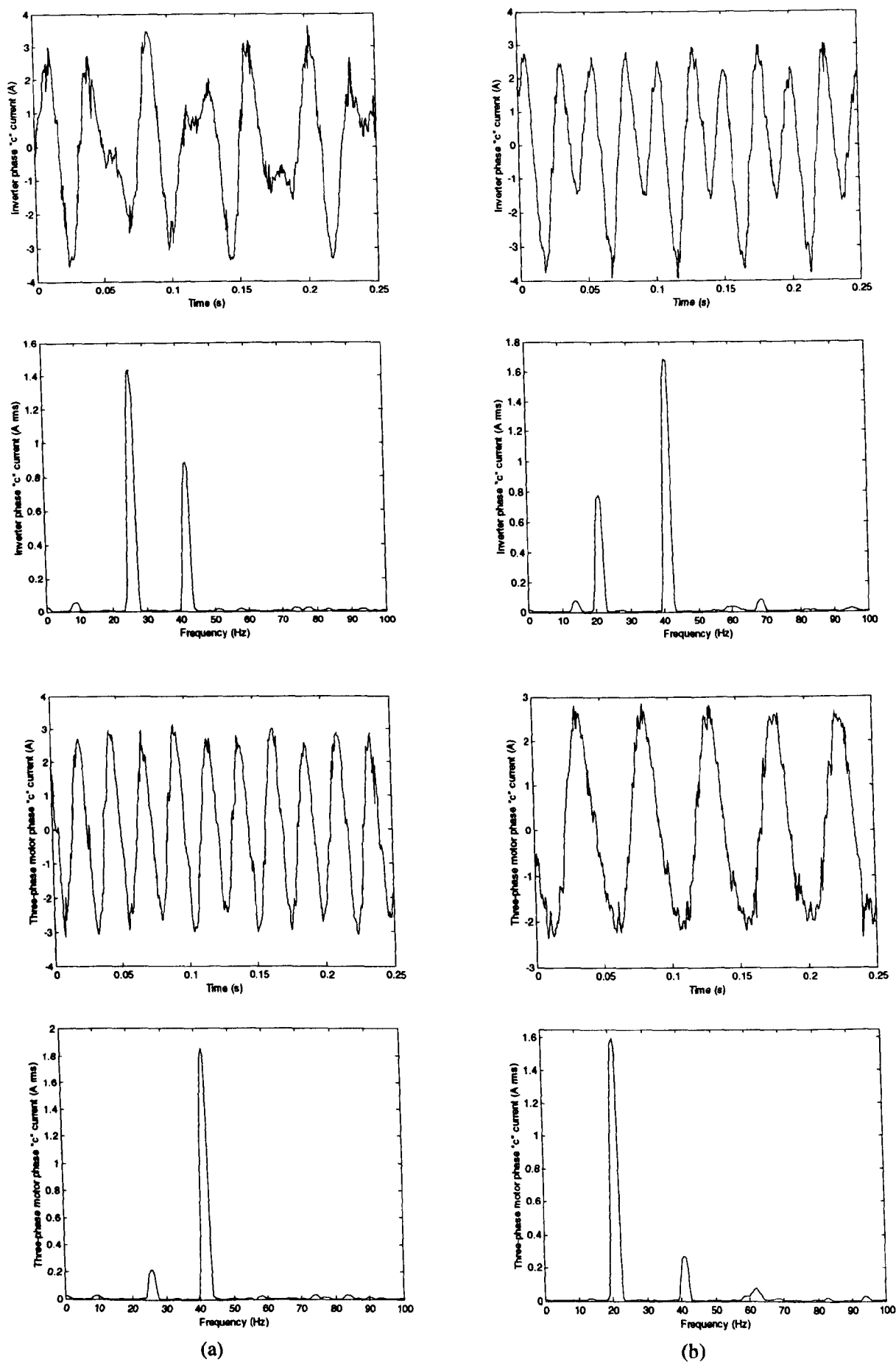


Fig. 10.21: Steady-state performance of the six-phase two-motor drive: six-phase motor (n_6) and three-phase motor (n_3) stator phase currents and spectra, conditions: $n_6 = 500$ rpm, $n_3 = 1200$ rpm (a) and $n_6 = 800$ rpm, $n_3 = 600$ rpm (b).

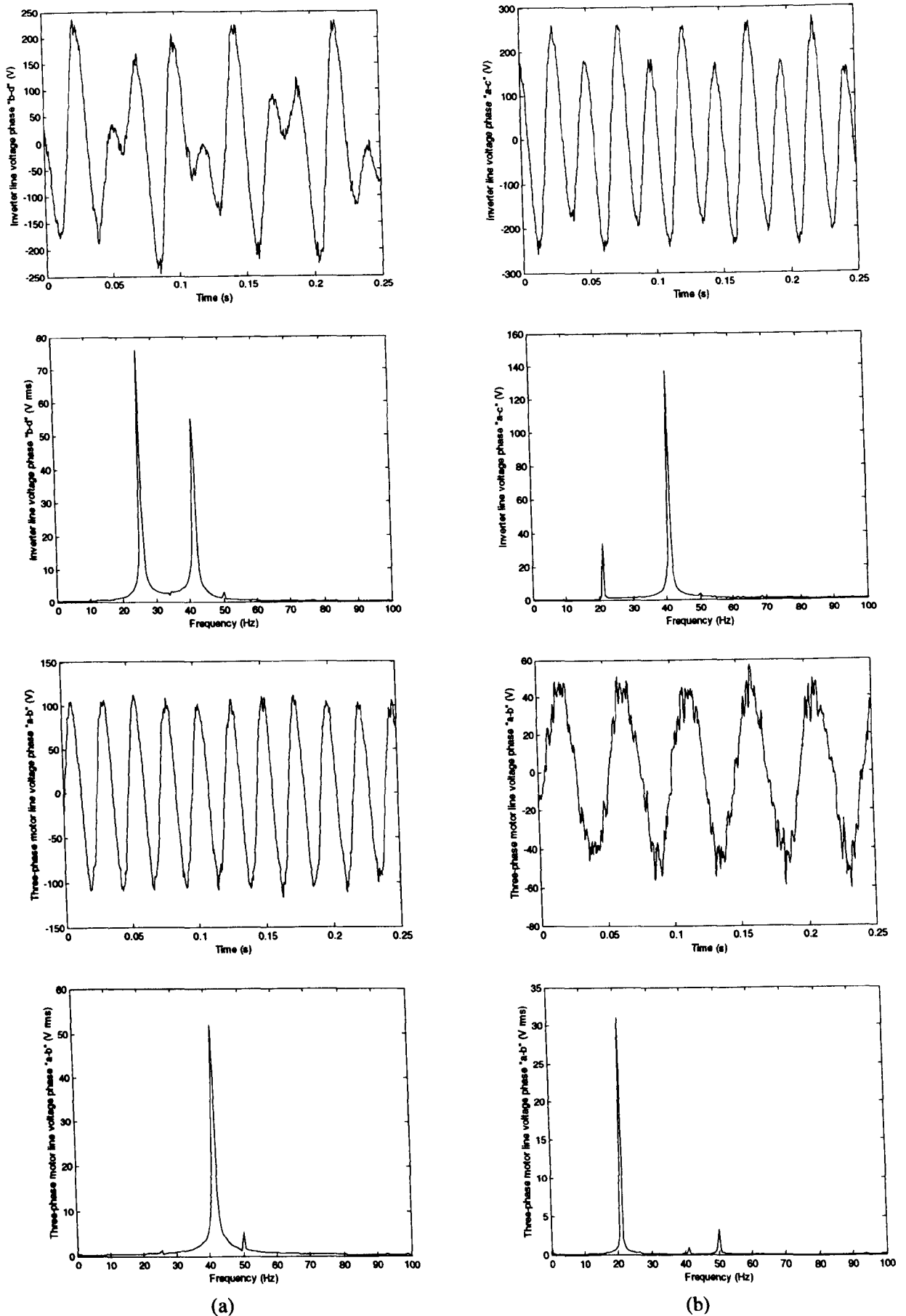


Fig. 10.22: Steady-state performance of the six-phase two-motor drive: Six-phase motor (n6) and three-phase motor (n3) stator line voltages and spectra, conditions: n6 = 500 rpm, n3 = 1200 rpm (a) and 800 rpm, n3 = 600 rpm (b).

Hence an indirect vector control algorithm can be applied to achieve independent rotor flux and torque control in the same manner as it is done for a three-phase machine. It is shown that unwanted harmonics, which can flow in x-y circuits, can be easily suppressed by implementing current control exercised upon phase currents. It is shown as well that a certain ripple, in addition to measurement noise appears in both stator q-axis current reference and speed response. The existence of these ripples is assigned to imperfections in the machine design, which lead to some level of asymmetry between two three-phase windings. This is regarded as important, since by and large the ripples observed later on in the studies of two-motor drives in six-phase machine variables are very much the same and are therefore not a consequence of the coupling of control of the two machines.

The chapter continues on to consider dynamics of the six-phase two-motor drive consisting of a six-phase induction motor and a three-phase induction motor connected in series. Performance of each machine is investigated experimentally with the other machine running at constant speed in order to determine if decoupled control has been achieved in accordance with the presented theory. Presentation of acceleration, deceleration, reversing and loading/unloading transients clearly shows that both machines operate independent of the other and that high performance control of each motor is achieved.

Next, the three-phase induction motor is replaced with a three-phase PMSM in order to prove that the multi-phase multi-motor concept is independent of the type of AC machine employed. Once again the transient performance of the drive is experimentally evaluated in the same manner as previously mentioned. It is shown that decoupled control of two machines is achieved.

Finally, steady-state performance is examined experimentally. The resulting current waveforms and spectra for a single six-phase induction motor drive demonstrate that unwanted harmonics are suppressed by the current control method employed. Presentation of steady-state currents and voltages of the six-phase two-motor drive shows two components at two different frequencies, corresponding to the two operating frequencies of the two machines. This is found to be in complete agreement with the presented theory, except for the presence of a small harmonic in the three-phase motor current at the operating frequency of the six-phase machine.

CHAPTER 11

CONCLUSION

11.1 Summary and conclusions

This research project develops a novel concept for a multi-machine drive system, which allows independent control of a set of AC machines supplied from a single current-controlled voltage source inverter. In order to achieve independent control of individual AC machines it is necessary to construct the multi-machine drive using multi-phase machines. Mathematical modelling of multi-phase machines using the general theory of electrical machines and assuming sinusoidal mmf distribution, is undertaken and it is shown that there are only two components (d-q) for stator and rotor which contribute to the torque developed by the machine (stator/rotor coupling) and $[(n - 3)/2]$ pairs (odd phase number machine) or $[(n-4)/2]$ pairs (even phase number machine) of components (x-y) which do not. Since only one pair of stator d-q current components is needed for the flux and torque control in one machine, there is a possibility of using the existing degrees of freedom (x-y components) for control of other machines that would be connected in series with the first machine. Therefore, if the supply has an odd number of phases it is possible to connect at most the stator windings of $(n - 1)/2$ machines in series and independently control each machine. Whereas, if the supply has an even number of phases it is possible to connect at most $(n - 2)/2$ machines in series and control them independently.

In order to enable independent control of each multi-phase motor within the multi-motor drive, series connection needs to be done in such a way that what one motor sees as the d-q axis stator current components the other motors see as x-y current components, and vice versa. This is achieved by introducing a phase transposition between the stator connections of the motors within the multi-motor drive. The necessary phase transposition between the stator windings of the machines is established by analysing the properties of the transformation matrix, allowing the so-called connectivity matrix and a corresponding connection diagram to be formed for an arbitrary supply phase number.

The major advantage of the series-connected multi-phase multi-machine drive over the more traditional three-phase system (with individual three-phase VSIs paralleled to the same DC link) is that the overall number of inverter legs is reduced. For example, in the five-phase case it is possible to connect two five-phase machines in series, requiring a total of five inverter legs. This represents a saving of one inverter leg over the traditional three-phase two-motor configuration. Higher the number of phases is, larger the reduction in the number of inverter legs is. A reduction in the number of inverter legs translates into a reduction in the protection and firing circuit components. It is expected that this will in turn lead to improved reliability and reduced inverter costs. Multi-machine drives comprising an inverter with an even number of phases do not offer savings in the number of inverter legs unless the phase number is greater than or equal to eight.

The number of connectable machines and the phase number of individual machines within the multi-motor drive are dependent upon the properties of the supply phase number. For both odd and even supply numbers there are three possible situations that may arise. These are detailed in Chapter 4. Of particular interest are the configurations that arise when the supply has an even phase number. In all such cases the multi-machine drive comprises machines with different phase numbers. Only supply phase numbers that allow the maximum number of connectable machines are of any potential importance because these configurations allow saving of the maximum number of inverter legs, when compared with an equivalent three-phase system. The viable multi-phase multi-motor drive systems are therefore those for which the number of supply phases is either a prime number or power of the prime number (for odd phase number supplies) or n is such that $n/2$ is a prime number or is a power of two (for the even number case).

A second advantage of the proposed multi-motor drives is the easiness of the implementation of the vector control algorithm for all the machines of the group within a single DSP. If there are k series-connected machines the DSP needs to execute k individual vector control algorithms in parallel, giving at the output, after appropriate summation, the references for the inverter phase currents. This will positively reflect on both the reliability and cost of the drive compared to its three-phase counterpart.

The third advantage of the multi-phase series-connected drive systems is the possibility of direct utilisation of the braking energy, developed by some of the machines in the group, by the other machines that are operating in motoring. This

means that the braking energy does not have to be returned to the DC link and therefore it does not circulate through the inverter. In other words, the system provides full regenerative braking as long as the total braking energy, developed by some of the machines in the system, is smaller than the total motoring energy, required by the other machines in the system. Only once when the braking energy exceeds the required motoring energy, power is returned to the DC link and dynamic braking becomes necessary.

The major drawback of the concept is an increase in the stator winding losses (and a considerably smaller increase in the stator iron losses) due to the flow of flux/torque producing currents of all the machines through stator windings of all the machines. As x-y currents do not flow in the rotor the rotor winding losses are not affected. This will inevitably decrease the efficiency of individual machines in the multi-motor drive and will yield an overall reduction in the total efficiency of the drive system, when compared to an equivalent three-phase drive system.

Although the six-phase two-motor drive offers no advantage in terms of inverter leg saving, the fact that no x-y currents flow through the three-phase motor windings makes this configuration extremely appealing for some applications. A six-phase single-motor drive is often employed due to high power requirements. In many such situations there is a need for a low power auxiliary motor drive, which has to be controlled independently. In such cases the series-connected two-motor drive enables control of the second machine at no extra cost, since the existing inverter can be utilised. The three-phase machine is not adversely affected by its series connection to the six-phase machine and the three-phase machine (of low power) will have negligible impact on efficiency of the six-phase machine (high power).

It has been shown further that the concept is completely independent of the type of rotor the AC machines have as long as the multi-phase machines have a sinusoidal field distribution. This means that different types of AC machine can be employed within the multi-motor drive system. This fact is of particular importance for machine tool applications, where an induction machine is often used for positioning of the work piece, while a PMSM is used to drive the cutting tool. This makes the six-phase two-motor drive a potentially viable solution for such applications, especially because no magnetising currents are required for the PMSM and therefore they do not flow through the six-phase machine.

If the five-phase two-motor drive is constructed using induction machines then the

flow of x-y currents through the stator of both machines will create a significant increase in stator losses. Each machine will have to be de-rated in order to cope with the increased stator currents and thermal load. However the five-phase two-motor drive may prove advantageous in winding applications, if two PMSMs are employed. In winding applications one machine typically operates at low speed (low voltage) with high torque (high current) while the other machine operates at high speed (high voltage) with low torque (low current). This means that the total stator rms current of each machine may actually stay below or up to rated during the whole operating cycle, thus eliminating the need for de-rating. Efficiency would however still be worse than with two traditional three-phase drives. However, total inverter installed power may be close to 5/6 of the installed power for two three-phase motor drives.

The basic concept of series-connected multi-phase multi-motor drive systems has been developed assuming that current control is executed in the stationary reference frame (i.e. inverter phase currents are directly controlled). A detailed study of the applicability of the current control in the rotating reference frame is studied at a later stage in the thesis.

The research has shown that application of current control in the synchronous reference frame requires x-y voltage drop compensation. Otherwise the dynamic performance of the drive is negatively affected. Two possible methods of x-y voltage drop compensation are suggested in the research. The first method involves compensating for the x-y voltage drops in a feed-forward manner. It is based on the knowledge of the x-y current references, which are governed by d-q current references of a different machine in the group. The second method involves modification of the decoupling circuit to compensate for x-y voltage drops across the leakage reactances of the other machines. It is shown via simulation that both methods perform very well. However, the modified decoupling circuit method is preferred because it offers the simpler realisation. Both methods require knowledge of machine parameters. This means that the potential problems with parameter variation effects are amplified. It is therefore concluded that current control in the stationary reference frame is advantageous for series-connected drives because the accuracy of control and performance of one machine is then independent of the parameters of the other machines in the group.

Most of the theoretical work in the thesis concentrates on symmetrical multi-phase machines, with spatial displacement between any two consecutive phases equal to $2\pi/n$.

However, as already emphasised, multi-phase AC machines are particularly suitable for high power applications, with the most popular choice being a quasi six-phase AC machine with two three-phase windings on the stator, spatially displaced by 30° . Series-connected two-motor drives, based on application of this machine, are therefore considered as well. It is shown that a quasi six-phase supply enables two different configurations of the multi-motor drive. Both configurations permit independent control of two machines connected in series. The first configuration comprises two quasi six-phase motors, while the second configuration employs a quasi six-phase motor and a two-phase motor. The quasi six-phase/two-phase configuration offers a greater benefit because the two-phase machine does not suffer in any adverse way due its connection to the quasi six-phase machine. It should be noted that the issue of where to connect the neutral point of such a system requires further investigation. Both configurations utilise the additional degrees of freedom to control the second machine in the group and therefore avoid the need for special harmonic current reduction methods. This is so since active impedance of one machine serves as a filter for the x-y current harmonics of the other machine, and vice versa.

The novel multi-phase multi-motor drive system analysed in this research has been verified by simulation for the five, six, seven, nine, ten and fifteen phase configurations. These simulations rely on machine models, which make certain simplifying assumptions, the most important of which is that the machines have perfect sinusoidally distributed windings and therefore perfect sinusoidal mmf distribution. This is not the case in reality. Therefore, definitive proof of the concept is provided by means of an experimental rig. Initially, performance of a true six-phase induction machine is examined during both transient and steady state conditions for both loaded and unloaded operation (base speed region only). It is shown that the machine suffers from some torque pulsations, which are believed to be due to a certain level of asymmetry between the two three-phase windings. However dynamic performance of the machine is still excellent. Performance of a six-phase two-motor drive is further qualitatively examined, using two induction machines, for both loaded and unloaded operation. It is shown that the dynamic and steady state performance of the six-phase motor is practically not affected by its connection to the three-phase motor, and vice versa. The dynamic performance of each machine is commensurate with that of a three-phase high performance drive. Steady state current spectra show that current cancellation at the point of connection to the three-phase motor is not entirely perfect as

a small current at the operating frequency of the six-phase machine flows into the three-phase motor. Finally, the six-phase two-motor configuration comprising a six-phase induction machine and a three-phase PMSM is examined experimentally. Once again the results show that decoupled control of each machine is achieved thus proving that the concept is independent of the type of AC machine employed.

Torque and speed pulsations, observed in the waveforms for the six-phase machine, are by and large those that exist when the six-phase machine is operated on its own. It is however fair to say that the experimental results do show some evidence of additional pulsations, in both machines, which are rather small and are believed to be a consequence of parasitic torque components produced by higher spatial harmonics of the mmf.

11.2 Future work

The research undertaken so far has examined the possibility of achieving decoupled control of a number of n -phase AC machines connected in series and supplied by a single n -phase VSI. Although the research has proven that the concept is valid and feasible, a great deal more work still remains. The main directions are believed to be:

- Detailed modelling of multi-phase VSIs and development of suitable PWM control strategies, applicable in conjunction with current control in the rotating reference frame. This essentially means development of suitable space vector modulation techniques for multi-phase VSIs, an area where very little research has been done so far.
- The possibility of connecting the multi-phase machines in parallel should be investigated and compared to the situation when the motors are connected in series. On the basis of the analogy between series and parallel electric circuits, it is believed that parallel connection should be realisable for a least some supply phase numbers.
- Further investigation into the five-phase two-motor drive with regard to winder applications and a comparison with the current three-phase system is another direction for further research.

- Connection of neutral point in the quasi six-phase/two-phase configuration requires further consideration, particularly because the quasi six-phase machine is by far the most popular multi-phase motor used in high power applications. Injection of third harmonic current into the quasi six-phase machine windings in order to boost the torque developed by the machine should also be investigated for this configuration.
- Fault tolerance ability of the proposed multi-motor drives should be further considered with regard to loss of an inverter phase. Although fault tolerance has stayed outside the scope of research here, it has been shown that the two-motor five-phase and six-phase drives can operate with current cancellation in one inverter phase (i.e., without one inverter phase).
- An evaluation of the required inverter rating in terms of switch voltage and current rating and DC bus voltage for series-connected two-motor drives. DC bus voltage can be quite arbitrarily doubled for two-motor drives, compared to the one needed for a single-motor-drive. However, it is believed that actual required DC bus voltage is smaller than this value.
- Total efficiency of the multi-phase multi-motor drive compared to the equivalent three-phase multi-motor drive (including inverter losses) requires investigation in order to establish the practicality of the proposed system.
- Investigation into the amount of machine de-rating required due to the heating effects of increased stator losses related to the flow of x - y currents. This needs to be done for certain types of applications, such as for example the one in winders.
- The reason for appearance of the current harmonics at the operating frequency of the six-phase machine in the current spectrum of the three-phase machine requires further attention. No satisfactory explanation for this phenomenon has been provided in this thesis.
- Practical implementation of current control performed in the synchronous reference frame using modified decoupling circuit scheme developed in chapter 8 and implementation of synchronous current controller in the stationary reference frame should be considered in order to remove dependence of the current controller performance on the speed of the machines.
- Last but not least, multi-phase machines are highly unlikely to have an

mmf distribution which is very close to sinusoidal. Hence an investigation of theoretical/simulation nature should be conducted, which would be based on enhanced machine models that account for at least some of the special harmonics of the mmf. Such a study should be conducted for the five-phase and six-phase two-motor drive systems, since these hold the best prospect for industrial applications.

REFERENCES

- Abbas, M.A., Christen, R. (1984), Characteristics of a high-power density six-phase induction motor, *Proc. IEEE Ind. Appl. Soc. Annu. Meeting IAS*, Chicago, IL, pp. 494-502.
- Abbas, M.A., Christen, R., Jahns, T.M. (1984), Six-phase voltage source inverter driven induction motor, *IEEE Trans. on Industry Applications*, vol. IA-20, no. 5, pp. 1251-1259.
- Andresen, E., Bieniek, K. (1980), On the performance of inverter fed induction motors with six phase, *Proc. Int. Conf. on Electrical Machines ICEM*, Athens, Greece, pp. 909-917.
- Andresen, E., Bieniek, K. (1981), 6-phase induction motors for current-source inverter drives, *Proc. IEEE Ind. Appl. Soc. Annual Meeting IAS*, New York, NY, pp. 607-618.
- Belhadj, J., Belkhodja, I., Fornel, B., Pietrzak-David, M. (2001), DTC strategy for multi-machine multi-inverter industrial system, *Proc. Eur. Power Elect. and Appl. Conf. EPE*, Graz, Austria, CD-ROM, Paper no. pp. 01002.
- Brod, D. M., Novotny, D. W., (1985), current control of VSI_PWM inverters, *IEEE Trans. on Industry Applications*, vol. IA-21, no. 4, 1985, pp. 562-570.
- Camillis, L.De., Matuonto, M., Monti, A., Vignati, A. (2001), Optimizing current control performance in double winding asynchronous motors in large power inverter drives, *IEEE Trans on Power Electronics*, vol.16, no.5, pp. 676-685.
- Chan, C.C., Jiang, J.Z., Chen, G.H., Wang, X.Y., Chau, K.T. (1994), A novel polyphase multipole square-wave permanent magnet motor drive for electric vehicles, *IEEE Trans. on Industry Applications*, vol. 30, no. 5, pp. 1258-1266.
- Coates, C.E., Platt, D., Gosbell, V.J. (2001), Performance evaluation of a nine-phase synchronous reluctance drive; *Proc. IEEE Ind. Appl. Soc. Annual Meeting IAS*, Chicago, IL, p.2041-2047.
- Favre, E., Jufer, M., Fleury, C. (1993), Five-phase permanent magnet synchronous motor, *Proc. Power Conversion and Intelligent Motion PCIM Conf.*, Nuremberg, Germany, pp. 475-487.

- Ferraris, P., Lazzari, M. (1983), Phase numbers and their related effects on the characteristics of inverter fed induction motor drives, *Proc. IEEE Ind. Appl. Soc. Annu. Meeting IAS*, Mexico City, Mexico, pp. 494-502.
- Fortuna, S., Palazzoli, N. (1999), ASM double star system instability in DC line, *Proc. Eur. Power Elec. and Appl. Conf. EPE*, Lausanne, Switzerland, CD-ROM Paper no. 384.
- Fu, J.R., Lipo, T.A. (1994), Disturbance-free operation of a multiphase current-regulated motor drive with an opened phase, *IEEE Trans. on Industry Applications*, vol. 30, no. 5, pp. 1267-1274.
- Gataric, S. (2000), A polyphase Cartesian vector approach to control of polyphase AC machines, *Proc. IEEE Ind. Appl. Soc. Annual Meeting IAS*, Rome, Italy, CD-ROM Paper no. 38_02.
- Golubev, A.N., Ignatenko, S.V. (2000), Influence of number of stator winding phases on the noise characteristics of an asynchronous motor, *Russian Electrical Engineering*, vol. 71, no. 6, pp. 41-46.
- Gopakumar, K., Ranganathan, V.T., Bhat, S.R. (1993), Split-phase induction motor operation from PWM voltage source inverter, *IEEE Trans. on Industry Applications*, vol. 29, no. 5, pp. 927-932.
- Gopakumar, K., Sathiakumar, S., Biswas, S.K., Vithayathil, J. (1984), Modified current source inverter fed induction motor drive with reduced torque pulsations, *IEE Proceedings, Pt. B*, vol. 131, no. 4, pp. 159-164.
- Grochowalski, J. (2000), Mmf of high phase order induction motors with different angles between stator windings and supply voltages, *Proc. Int. Conf. Power Electronics and Motion Control PEMC*, Kosice, Slovakia, pp. 5.28-5.32.
- Hadiouche, D., Razik, H., Rezzoug, A. (2000), Modelling of a double-star induction motor with an arbitrary shift angle between its three phase windings, *Proc. Int. Conf. Power Electronics and Motion Control PEMC*, Kosice, Slovakia, pp. 5.125-5.130.
- Hodge, C., Williamson S., Smith, S. (2002), Direct drive propulsion motors, *Proc. Int. Conf. on Electrical Machines ICEM*, Bruges, Belgium, CD-ROM Paper no. 087.
- Ibrahim, Z. (1999), Fuzzy logic control of PWM inverter-fed sinusoidal permanent magnet synchronous motor drives, PhD Thesis, Liverpool John Moores University, UK.

- Iqbal, A, (2003), Series and parallel connected multi-phase multi-motor drive systems with single inverter supply. MPhil/PhD Transfer report' Liverpool John Moores University, UK.
- Iqbal, A, Levi, E, (2004), Modelling of a six-phase series-connected two-motor drive system, *Proc. Int. Conf. on Electrical Machines ICEM*, Krakow Poland, CD ROM paper no. 98.
- Jacobina, C.B., Oliveira, T.M., Correa, M.B., Lima, A.M.N., Silva, E.R.C. (2002), Component minimized drive system for multi-machine applications, *Proc. IEEE Power Elec. Spec. Conf. PESC*, Cairns, Australia, Paper no. 10028.
- Jahns, T.M. (1980), Improved reliability in solid-state AC drives by means of multiple independent phase-drive units, *IEEE Trans. on Industry Applications*, vol. IA-16, no. 3, pp. 321-331.
- Javanovic, M.G., (1996), Sensorless control of synchronous reluctance machines, PhD Thesis, The University of Newcastle, Australia, pp. 171-188.
- Jones, M., Levi, E. (2002), A literature survey of the state-of-the-art in multiphase AC drives, *36th Universities Power Engineering Conference UPEC*, Stafford, UK, pp. 505-510.
- Jones, M., Levi, E., Vukosavic, S. N., Toliyat, H. A. (2003a), A novel nine-phase four-motor drive system with completely decoupled dynamic control, *Proc. IEEE Ind. Elec. Society Annual Meeting IECON*, Roanoke, Virginia, pp. 208-213.
- Jones, M., Levi, E., Vukosavic, S. N., Toliyat, H. A. (2003b), Independent vector control of a seven-phase three-motor drive system supplied from a single voltage source inverter, *Proc. IEEE Power Elec. Spec. Conf. PESC*, Acapulco, Mexico, pp. 1865-1870.
- Jones, M., Levi, E. (2004), Combining induction and synchronous machines in a seven-phase series-connected three-motor drive, *Proc. European Conf. on Power Electronics and Motion Control, EPE-PEMC*, Riga, Latvia, CD-ROM paper no. A71123.
- Jones, M., Vukosavic, S. N, Levi, E. (2004a), Independent vector control of a six-phase series-connected two-motor drive, *Second International IEE Conference on Power Electronics, Machines and Drives PEMD*, Edinburgh, UK, vol. 2, pp. 879-884.

- Jones, M., Levi, E., Iqbal, A. (2004b), A five-phase series-connected two-motor drive with current control in the rotating reference frame, *Proc. IEEE Power Electronics Specialists Conf. PESC*, Aachen, Germany, pp. 3278-3284.
- Jones, M., Vukosavic, S.N., Levi, E., Iqbal, A. (2004c), A novel six-phase series-connected drive with decoupled dynamic control, *Proc. IEEE Ind. Appl. Soc. Annual Meeting IAS*, Seattle, WA, pp. 639-646 CD-ROM 04IAS17p6.
- Jones, M., Levi, E., Iqbal, A. (2005), Vector control of a five-phase series connected two-motor drive using synchronous current controllers, *Electric-Power-Components and Systems*, vol. 33, no. 4. (accepted for publication).
- Kawai, H., Kouno, Y., Matsuse, K. (2002), Characteristics of speed sensorless vector control of parallel connected dual induction motor fed by a single inverter. *Proc. IEEE Power Conversion Conf. PCC*, Osaka, Japan, pp. 522-526.
- Kestelyn, X., Semail, E., Hautier, J.P. (2002), Vectorial multi-machine modelling for a five-phase machine, *Proc. Int. Conf. on Electrical Machines ICEM*, Bruges, Belgium, CD-ROM Paper no. 394.
- Klingshirn, E.A. (1983), High phase order induction motors - Part I - Description and theoretical considerations, *IEEE Trans. on Power Apparatus and Systems*, vol. PAS-102, no. 1, pp. 47-53.
- Klingshirn, E. A., (1985), Harmonic filters for six-phase and other multi phase motors on voltage source inverter, *IEEE Trans. on Industry Applications*, vol. IA-21, no. 4, pp. 588-593.
- Klumper, C., Blaabjerg, F. (2002), A direct power electronic conversion topology for multi-drive applications, *Proc. Int. Conf. Power Electronics and Motion Control EPE-PEMC*, Cavat, Croatia, CD-ROM Paper no. ssjwk-05.
- Krishnan, R. (2001), *Electric motor drives*, Prentice Hall, New Jersey.
- Kouno, Y., Kawai, H., Yokomizo, S., Matsuse, K. (2001), A speed sensorless vector control method of parallel connected dual induction motor fed by a single inverter, *Proc. IEEE Ind. Appl. Soc. Annual Meeting IAS*, Chicago, IL, CD-ROM Paper No.29_04.
- Ledezma, E., McGrath, B., Muoz, A., Lipo, T.A. (2001), Dual ac-drive system with a reduced switch count, *IEEE Trans. on Industry Applications*, vol. 37, no. 5, pp. 1325-1333.

- Lee, B.K., Fahimi, B., Ehsani, M. (2001), Overview of reduced parts converter topologies for ac motor drives, *Proc. IEEE Power Elec. Spec. Conf. PESC*, Vancouver, Canada, pp. 2019-2024.
- Levi, E., Jones, M., Vukosavic, S.N. (2003a), Even-phase multi-motor vector controlled drive with single inverter supply and series connection of stator windings," *IEE Proc. – Electric Power Applications*, vol. 150, no. 5, pp. 580-590.
- Levi, E., Jones, M., Vukosavic, S.N. Toliyat, H.A, (2003b), A five-phase two-machine vector controlled induction motor drive supplied from a single inverter, *Proc. European Conf. on Power Electronics and Applications EPE*, Toulouse, France, CD-ROM paper no. 0001.
- Levi, E., Iqbal, I., Vukosavic, S.N., Toliyat, H. A. (2003c), Modeling and control of a five-phase series connected two-motor drive, *Proc. IEEE Ind. Elec. Society Annual Meeting IECON*, Roanoke, Virginia, USA, pp. 208-213.
- Levi, E., Jones, M., Vukosavic, S.N., Toliyat, H.A, (2004a), Operating principles of a novel multi-phase multi-motor vector controlled drive, *IEEE Trans. on Energy Conversion*, vol. 19, no. 3. pp. 508-517.
- Levi, E., Jones, M., Vukosavic, S.N., Toliyat, H.A. (2004b), A five-phase two-machine vector controlled induction motor drive supplied from a single inverter, *EPE Journal – European Power Electronics and Drives*, vol. 14, no. 3. pp. 38-48.
- Levi, E., Jones, M., Vukosavic, S.N., H.A. Toliyat, H.A. (2004c) A novel concept of a multi-phase, multi-motor vector controlled drive system supplied from a single voltage source inverter, *IEEE Trans. on Power Electronics*, vol. 19, no. 2, pp. 320-335.
- Levi, E., Vukosavic, S. N., Jones, M. (2004d), Vector control schemes for series-connected six-phase two-motor drive systems, *IEE Proc. – Electric Power Applications*, (accepted for publication)
- Lipo, T.A. (1980), A d-q model for six phase induction machines, *Proc. Int. Conf. on Electrical Machines ICEM*, Athens, Greece, pp. 860-867.
- Lipo, T.A. (1984), A Cartesian vector approach to reference frame theory of AC machines, *Proc. Int. Conf. on Electrical Machines ICEM*, Lausanne, Switzerland, pp. 239-242.
- Lyra, R.O.C., Lipo, T.A. (2001), Torque density improvements in a six-phase induction motor with third harmonic current injection. *Proc. IEEE Ind. Appl. Soc. Annu. Meeting IAS*, Chicago, IL, CD-ROM Paper no. IL p.43_02.

- Ma, J.D., Wu, B., Zargari, N.R., Rizzo, S.C. (2001), A space vector modulated CSI-based AC drive for multimotor applications, *IEEE Trans. on Power Electronics*, vol. 16, no. 4, pp. 535-544.
- Mantero, S., Paola, E.De., Marina, G. (1999), An optimised control strategy for double star motors configuration in redundancy operation mode, *Proc. Eur. Power Elec. and Appl. Conf. EPE*, Lausanne, Switzerland, CD-ROM Paper no. 013.
- Matsumoto, Y., Ozaki, S., Kawamura A. (2001), A novel vector control of single-inverter multiple induction motor drives for Shinkansen traction system, *Proc. IEEE Applied Power Elec. Conf. APEC*, Anaheim, CA, pp. 608-614.
- Miller, J. M., Stefanovic, V., Ostovic, V, (2001), Design considerations for an automotive integrated starter-generator with pole-phase modulation, *IEEE Proc. Ind. Appl. Soc. Annual Meeting IAS*, Chicago, IL, pp 56-06.
- Mitcham, A, Cullen, J.J.A. (2002), Permanent magnet generator options for the more electric aircraft, *Proc. IEE Power Electronics, Machines and Drives Conf. PEMD*, Bath, UK, pp. 241-245.
- Mohapatra, K. K., Gopakumar, K, Somasekhar, V. T., Umanand, L, (2003), A harmonic elimination scheme for an open-end winding induction motor drive, *IEEE Trans. on Industrial Electronics*, vol. 50, no. 4, pp. 1187-1198.
- Monti, A., Morando, A.P., Resta, L., Riva, M. (1995), Comparing two level GTO-inverter feeding a double star asynchronous motor with a three level GTO-inverter feeding a single star asynchronous motor, *Proc. Eur. Power Elec. and Appl. Conf. EPE*, Seville, Spain, pp. 2419-2425.
- Nagase, H., Matsusa, Y., Ohnishi, K., Ninomiya, H., Koike, T. (1984), High performance induction motor drive system using a PWM inverter, *IEEE Trans. Ind. Appl.*, vol IA-20, no. 6pp,1482-1489.
- Nelson, R.H., Krause, P.C. (1974) Induction machine analysis for arbitrary displacement between multiple winding sets, *IEEE Trans. on Power Apparatus and Systems*, vol. PAS-93, no. 3, pp. 841-848.
- Novotny, D.W., Lipo, T.A, (1996), Vector control and dynamics of AC drives, *Oxford Clarendon press*. ISBN 0198564392.
- Pavithran, K.N., Parimelalagan, R., Krishnamurthy, M.R. (1988), Studies on inverter-fed five-phase induction motor drive, *IEEE Trans. on Power Electronics*, vol. 3, no. 2, pp. 224-235.

- Pena-Eguiluz, R., Pietrzak-David, M., Fornel, B. (2001), Observation strategy in a mean control structure for parallel connected dual induction motors in a railway traction drive system, *Proc. Eur. Power Elec. and Appl. Conf. EPE*, Graz, Austria, CD-ROM Paper no. PP01016.
- Pena-Eguiluz, R., Pietrzak-David, M., Fornel, B. (2002), Comparison of several control strategies for parallel connected dual induction motors, *Proc. Int. Conf. Power Electronics and Motion Control. EPE-PEMC*, Cavat, Croatia, CD-ROM Paper no. T11-010.
- Petrov, G.P. (1998), Mathematical model of a six-phase squirrel-cage induction motor, *Elektrichestvo*, no. 9, pp. 33-39.
- Rowan, T. M., Kerkman, R. J., (1986), A new synchronous current regulator and an analysis of current-regulated PWM inverters, *IEEE Trans. on Industry Applications*, vol. IA-22, no. 4, pp. 678-690.
- Schauder, C. D., Caddy, R., (1982), Current control of voltage-source inverters for fast four-quadrant drive performance, *IEEE Trans. Ind. Appl.*, vol. IA-18, pp 163-171.
- Shi, R., Toliyat, H.A., El-Antably A. (2001a), Field oriented control of five-phase synchronous reluctance motor drive with flexible 3rd harmonic current injection for high specific torque, *Proc. IEEE Ind. Appl. Soc. Annual Meeting IAS*, Chicago, IL, pp. 2097-103.
- Shi, R., Toliyat, H.A., El-Antably, A. (2001b), A DSP-based direct torque control of five-phase synchronous reluctance motor, *Proc. IEEE Applied Power Elec. Conf. APEC*, Anaheim, CA, pp 1077-1082.
- Singh, G.K. (2002), Multi-phase induction machine drive research- a survey, *Electric Power Systems Research*, vol. 61, pp. 139-147.
- Smith, S. (2002), Developments in power electronics, machines and drives, *Power Engineering Journal*, February, pp. 13-17.
- Steiner, M., Deplazes, R., Stemmler, H. (2000), A new transformerless topology for AC-fed traction vehicles using multi-star induction motors, *EPE Journal*, vol. 10, no. 3-4, pp. 45-53.
- Toliyat, H.A. (1998), Analysis and simulation of five-phase variable-speed induction motor drives under asymmetrical connections, *IEEE Trans. on Power Electronics*, vol. 13, no. 4, pp. 748-756.

- Toliyat, H.A., Lipo, T.A., Coleman, J. (1991), Analysis of a concentrated winding induction machine for adjustable speed drive applications Part 1 (Motor analysis), *IEEE Trans. on Energy Conversion*, vol. 6, no. 4, pp. 679-683.
- Toliyat, H.A., Lipo, T.A. (1994), Analysis of concentrated winding induction machines for adjustable speed drive applications - Experimental results, *IEEE Trans. on Energy Conversion*, vol. 9, no. 4, pp. 695-700.
- Toliyat, H.A., Rahimian, M.M., Lipo, T.A. (1993), Analysis and modeling of five phase converters for adjustable speed drive applications, *Proc. Eur. Conf. on Power Elec and Appl EPE*, Brighton, UK, pp. 194-199.
- Toliyat, H.A., Shi, R., Xu, H. (2000), A DSP-based vector control of five-phase synchronous reluctance motor, *Proc. IEEE Ind. Appl. Soc. Annual Meeting IAS*, Rome, Italy, CD-ROM Paper no. 40_05.
- Toliyat, H.A., Waikar, S.P., Lipo, T.A. (1998), Analysis and simulation of five-phase synchronous reluctance machines including third harmonic of airgap mmf, *IEEE Trans. on Industry Applications*, vol. 34, no. 2, pp. 332-339.
- Toliyat, H.A., Xu, H. (2000), A novel direct torque control (DTC) method for five-phase induction machines, *Proc. IEEE Applied Power Elec. Conf. APEC*, New Orleans, LA, pp. 162-168.
- Toliyat, H.A., Xu, L., Lipo, T.A. (1992), A five-phase reluctance motor with high specific torque, *IEEE Trans. on Industry Applications*, vol. 28, no. 3, pp. 659-667.
- Veen, J.L.F. van der., Offringa, L.J.J., Vandenput, A.J.A. (1997), Minimising rotor losses in high-speed high-power permanent magnet synchronous generators with rectifier loads, *IEE Proc. - Electr. Power Appl.*, vol. 144, no. 5, pp. 331-337.
- Ward, E.E., Härer, H. (1969), Preliminary investigation of an inverter-fed 5-phase induction motor, *Proc. IEE*, vol. 116, no. 6, pp. 980-984.
- Watanabe, T., Yamashita, M. (2002), Basic study of anti-slip control without speed sensor for multiple motor drive of electric railway vehicles, *Proc. IEEE Power Conversion Conf. PCC*, Osaka, Japan, pp. 1026-1032.
- Weh, H., Schroder, U. (1985), Static inverter concepts for multiphase machines with square-wave current-field distribution, *Proc. Eur. Power Elec. and Appl. Conf EPE*, Brussels, Belgium, pp. 1.147-1.152.
- White, D.C., Woodson, H.H. (1959), *Electromechanical Energy Conversion*, John Wiley and Sons, New York, NY.

- Williamson, S., Smith, S. (2001), Pulsating torques and losses in multiphase induction machines, *Proc. IEEE Ind. Appl. Soc. Annual Meeting IAS*, Chicago, IL, CD-ROM Paper No. 27_07.
- Xu, L., Fu, W. (2002), Evaluation of third harmonic component effects in five-phase synchronous reluctance motor drives using time-stepping finite-element method, *IEEE Trans. on Industry Applications*, vol. 38 no. pp. 638-644.
- Xu, H., Toliyat H.A., Petersen, L.J. (2001), Rotor field oriented control of five-phase induction motor with the combined fundamental and third harmonic currents, *Proc. IEEE Applied Power Elec. Conf. APEC*, Anaheim, CA, pp 392-398.
- Xu, L., Ye, L. (1995), Analysis of a novel stator winding structure minimising harmonic current and torque ripple for dual six-step converter-fed high power AC machines, *IEEE Trans. on Industry Applications*, vol. 31, no. 1, pp. 84-90.
- Zdenek, D. (1986), 25 MW high-speed electric drive with thyristor speed control, *Czechoslovak Heavy Industry*, no. 4, pp. 5-9.
- Zhao, Y., Lipo, T.A. (1995), Space vector PWM control of dual three-phase induction machine using vector space decomposition, *IEEE Trans. on Industry Applications*, vol. 31, no. pp. 1100-1109.

APPENDIX A

Three-phase machine data

Table A.1: Three-phase permanent magnet synchronous motor data

Type	FAE N7 V4 030
Nominal speed	3000 rpm
Number of pole pairs	3
Rated frequency	150 Hz
Rated torque, at rated speed	3.5 Nm
Nominal power, continuous cycle at rated speed	1.1 kW
Maximum torque at rated speed with DS2000 drive (8/22 drive)	20 Nm
Inertia	0.075 kgm ²
Stator winding per-phase resistance at 20 degrees C	1.93 Ohms
Electrical time constant (L/R)	6.35 ms
Winding per-phase inductance (data sheet)	12.25 mH
Winding per-phase inductance (test sheet, average value)	10.97 mH
Nominal current, rated speed, rated load	1.9444 A
Torque constant	1.8 Nm/A (rms)
Mechanical time constant	1.55 ms
Measured back emf at 1000 rpm (line to line)	109.6 V
Back emf constant	0.2V/(rad/s)

Table A.2 Three-phase induction motor data

Type	FAS Y 090-V-030
Nominal speed	3000 rpm
Number of pole pairs	2
Nominal frequency	100 Hz
Nominal torque, continuous duty at rated speed	3.18 Nm
Nominal power, continuous at rated speed	1 kW
Maximum torque at rated speed with DS2000 drive (8/22)	20 Nm
Inertia	0.275 kgm ²
Nominal current, locked rotor	5.5 A
Nominal torque, continuous cycle with locked rotor	6 Nm
Winding (stator) phase-to-phase resistance at 20 degrees C	1.4 Ohms
Stator per-phase resistance, hot (Ohms)	0.88
Rotor per-phase resistance, hot (Ohms)	0.758
Stator leakage inductance (mH)	2.75
Rotor leakage inductance (mH)	2.56
Magnetising inductance (mH)	81.72
Equivalent iron loss resistance at 120 Hz (kOhms)	2.53

APPENDIX B

Six-phase induction motor data

Table B.1: Original three-phase motor data

Type	Sever 1ZK100-8
Power	0.75 kW
Frequency	50 Hz
Rated speed	675 rpm
Voltage	220 V (phase to neutral)
Rated slip	10%
Number of pole pairs	8
Stator slots	36
Rotor slots	44

The motor was rewound into six-phase star configuration (true, six-phase, 60 degrees spatial displacement between any two consecutive phases).

Table B.2: Six-phase motor data

Type	1ZK100-6
Power	1.1 kW
Frequency	50 Hz
Rated speed	900 rpm
Voltage	110 V (phase to neutral)
Number of pole pairs	6
Rated current	3.5 A
Rated slip	10%
Stator slots	36
Rotor slots	44

The lap winding is distributed into 36 stator slots. The winding type is double-layer, integral slot winding. It is a short-pitched winding, with the pitch equal to five slots. Pole-pitch is six slots, since there are 36 slots and six poles ($36/6=6$). In each slot there are two conductors, the upper and the lower, belonging to two different phases. Each of the six phases has its conductors in the upper slot layer in six slots, and the returning conductors (in the second layer) in another six slots.

Note that the machine was originally three-phase with eight poles. Since number of slots divided by the product of the number of poles and number of phases is not an integer ($36/(3 \times 8)=1.5$), the original winding was fractional slot winding.

Table B.3 lists the numbers of slots in which conductors of individual phases are. The first number is always the conductor in the top layer and the second number is the conductor in the lower layer. In each row, there are two slots for upper and two for lower conductors, denoting a phase belt for each phase under one pole-pair. Since there are three pole-pairs, there are three rows in the table.

Table B.3: Six-phase machine winding data

A	B	C	D	E	F
1-6, 2-7	3-8, 4-9	5-10, 6-11	7-12, 8-13	9-14, 10-15	11-16, 12-17
13-18, 14-19	15-20, 16-21	17-22, 18-23	19-24, 20-25	21-26, 22-27	23-28, 24-29
25-30, 26-31	27-32, 28-33	29-34, 30-35	31-36, 32-1	33-2, 33-3	35-4, 36-5
Start (1) and end (2) of each phase winding					
A1=1 A2=31	B1=27 B2=9	C1=5 C2=35	D1=31 D2=13	E1=9 E2=3	F1=35 F2=17

Since there are 12 slots per one pole pair, and each phase occupies two slots out of 12, the winding is six-phase. Since the phases follow each other in consecutive order (i.e. phase A is in top layer of 1,2, phase B in 3,4, phase C in 5,6 etc., while A', B', C' etc. are in lower layer), this means that the spatial displacement between any two consecutive phases is 60 degrees.

Detailed schematic of the winding, as it is distributed in the 36 slots, is shown in Table B.4. For each slot it is indicated which phases have a conductor in that slot. Phase notation a,b,c,d,e,f applies to conductors in the upper layer; while phase notation a',b',c',d',e',f' applies to conductors in the lower layer. As can be seen from Table B.4, winding pitch is five slots, while the pole-pitch is six slots.

When windings are distributed in the slots (rather than concentrated), total induced emf (which is a phasor sum) is less than the algebraic sum of the induced emfs in individual conductors. This is taken into account through so-called breadth factor. If the winding is not with the full pole pitch, there is additionally the effect of chording, which is taken into account through the so-called pitch factor. Product of the breadth factor and pitch factor is

called winding factor. Hence $k_w = k_b k_p$, where indices w, b, and p stand for winding, breadth and pitch factors. Breadth factor and pitch factor can be calculated according to:

$$\begin{aligned} k_b &= \frac{\sin(n\gamma/2)}{n \sin(\gamma/2)} \\ k_p &= \cos \frac{\pi - \rho}{2} \end{aligned} \tag{B1}$$

Here n is the number of slots per phase belt (two in the case of this winding), γ is obtained by dividing 180 degrees with the number of slots per pole (here $180/6=30$ degrees, since there are six slots per pole) and ρ is the distance between two conductors of the same phase under two opposite poles in electrical radians (here distance from slot 1 to slot 6, which is 150 electrical degrees). Using these numbers one gets the breadth factor as equal to 0.9659 and the pitch factor as equal to 0.9659. Hence the winding factor is 0.93301.

APPENDIX C

Simulation data

The basis for all n -phase induction machine simulations is a three-phase induction machine, with magnetising inductance of 0.42 H and rated torque of 5 Nm. Rated rotor flux (rms) is for this benchmark three-phase machine equal to 0.5683 Wb, rated rms d-q axis currents are $I_{dsn} = 1.35$ A and $I_{qsn} = 1.6$ A. Hence in the case of an n -phase machine:

$$\begin{aligned}
 M &= 0.42/(n/2) \\
 |\underline{\psi}_r^*| &= \sqrt{n}(0.5683) \\
 T_{en} &= 5(n/3) \\
 i_{dsn} &= \sqrt{n}I_{dsn} \\
 i_{qsn} &= \sqrt{n}I_{qsn}
 \end{aligned} \tag{C.1}$$

Rated phase voltage and current are for all cases 220 V (rms) and 2.1 A (rms). Table C.1 lists the rotor flux, rated torque, rated d-q axis currents and the phase current reference (taking into account the torque command magnitude) for all the simulations mentioned within this thesis.

Table C.1: Simulation data

Phase number	Rated torque- T_{en} (Nm)	Commanded torque- T_e^* (Nm)	Rated d-axis current i_{dsn} (A)	Rated q-axis current i_{qsn} (A)	Peak phase current ($\sqrt{2}$ rms) (A)	Rotor flux ref. $ \underline{\psi}_r^* $ (Wb)
2ph	3.33	3.33	1.91	2.26	2.97	0.8036
3ph	5	10	2.34	2.78	4.93	0.9853
3ph	5	5	2.34	2.78	2.97	0.9853
3ph	5	4	2.34	2.78	2.64	0.9853
5ph	8.33	16.67	3.03	3.59	4.93	1.2707
5ph	8.33	8.33	3.03	3.59	2.97	1.2707
6ph	10	20	3.31	3.93	4.93	1.392
6ph	10	15	3.31	3.93	3.91	1.392
6ph	10	10	3.31	3.93	2.97	1.392
7ph	11.67	23.34	3.58	4.25	4.93	1.503
9ph	15	15	4.06	4.82	2.97	1.7049
9ph	15	10	4.06	4.82	2.44	1.7049
9ph	15	5	4.06	4.82	2.06	1.7049
10ph	16.67	16.67	4.28	5.08	2.97	1.797
10ph	16.67	11.11	4.28	5.08	2.44	1.797
15ph	25	25	5.24	6.22	2.97	2.201
15ph	25	18.75	5.24	6.22	2.56	2.201
15ph	25	12.5	5.24	6.22	2.22	2.201
15ph	25	6.25	5.24	6.22	1.99	2.201

APPENDIX D

Publications from the thesis

D.1 Journal papers

- Levi, E., Jones, M., Vukosavic, S.N. (2003), Even-phase multi-motor vector controlled drive with single inverter supply and series connection of stator windings," *IEE Proc. – Electric Power Applications*, vol. 150, no. 5, pp. 580-590.
- Levi, E., Jones, M., Vukosavic, S.N., Toliyat, H.A. (2004), Operating principles of a novel multi-phase multi-motor vector controlled drive, *IEEE Trans. on Energy Conversion*, vol. 19, no. 3. pp. 508-517.
- Levi, E., Jones, M., Vukosavic, S.N., Toliyat, H.A. (2004), A five-phase two-machine vector controlled induction motor drive supplied from a single inverter, *EPE Journal – European Power Electronics and Drives*, vol. 14, no. 3. pp. 38-48.
- Levi, E., Jones, M., Vukosavic, S.N., H.A. Toliyat, H.A. (2004) A novel concept of a multi-phase, multi-motor vector controlled drive system supplied from a single voltage source inverter, *IEEE Trans. on Power Electronics*, vol. 19, no. 2, pp 320-335.
- Levi, E., Vukosavic, S. N., Jones, M. (2004), Vector control schemes for series-connected six-phase two-motor drive systems, *IEE Proc. – Electric Power Applications*, (accepted for publication)
- Jones, M., Levi, E., Iqbal, A. (2005), Vector control of a five-phase series connected two-motor drive using synchronous current controllers, *Electric-Power-Components and Systems*, vol. 33 no. 4. (accepted for publication).

D.2 Conference papers

- Jones, M., Levi, E. (2002), A literature survey of the state-of-the-art in multiphase AC drives, *36th Universities Power Engineering Conference UPEC*, Stafford, UK, pp. 505-510.
- Jones, M., Levi, E., Vukosavic, S. N., Toliyat, H. A. (2003), A novel nine-phase four-motor drive system with completely decoupled dynamic control, *Proc. IEEE Ind. Elec. Society Annual Meeting IECON*, Roanoke, Virginia, pp. 208-213.
- Jones, M., Levi, E., Vukosavic, S. N., Toliyat, H. A. (2003), Independent vector control of a seven-phase three-motor drive system supplied from a single voltage source inverter, *Proc. IEEE Power Elec. Spec. Conf. PESC*, Acapulco, Mexico, pp. 1865-1870.
- Levi, E., Jones, M., Vukosavic, S.N. Toliyat, H.A, (2003), A five-phase two-machine vector controlled induction motor drive supplied from a single inverter, *Proc. European Conf. on Power Electronics and Applications EPE*, Toulouse, France, CD-ROM paper no. 0001.
- Jones, M., Levi, E. (2004), Combining induction and synchronous machines in a seven-phase series-connected three-motor drive, *Proc. European Conf. on Power Electronics and Motion Control, EPE-PEMC*, Riga, Latvia, CD-ROM paper no. A71123.
- Jones, M., Vukosavic, S. N., Levi, E. (2004), Independent vector control of a six-phase series-connected two-motor drive, *Second International IEE Conference on Power Electronics, Machines and Drives PEMD*, Edinburgh, UK, vol. 2, pp. 879-884.
- Jones, M., Levi, E., Iqbal, A. (2004), A five-phase series-connected two-motor drive with current control in the rotating reference frame, *Proc, IEEE Power Electronics Specialists Conf. PESC*, Aachen, Germany, pp. 3278-3284.

Jones, M., Vukosavic, S.N., Levi, E., Iqbal, A. (2004), A novel six-phase series-connected drive with decoupled dynamic control, *Proc. IEEE Ind. Appl. Soc. Annual Meeting IAS*, Seattle, WA, pp. 639-646 CD-ROM 04IAS17p6.